

**INVESTIGATIONS ON THE CLIMATIC TRENDS AND SHIFTS IN
THE SPATIAL DISTRIBUTION OF MARINE FISH SPECIES OF
NORTHERN INDIAN OCEAN**

by

**SWATHY S.
(2015 - 20 - 021)**

THESIS

**Submitted in partial fulfilment of the requirements for the
degree of**

B.Sc. – M.Sc. (Integrated) Climate Change Adaptation

Faculty of Agriculture

Kerala Agricultural University



ACADEMY OF CLIMATE CHANGE EDUCATION AND RESEARCH

VELLANIKKARA, THRISSUR – 680 656 KERALA,

INDIA

2020

DECLARATION

I, Swathy S., (2015 - 20 - 021) hereby declare that this thesis entitled “**Investigations on the climatic trends and shifts in the spatial distribution of marine fish species of Northern Indian Ocean**” is a bonafide record of research work done by me during the course of research and the thesis has not previously formed the basis for the award to me of any degree, diploma, associateship, fellowship or other similar titles, of any other University or Society.

Vellanikkara

Date:

Swathy S.

(2015 - 20 - 021)

CERTIFICATE

Certified that this thesis entitled “**Investigations on the climatic trends and shifts in the spatial distribution of marine fish species of Northern Indian Ocean**” is a record of research work done independently by **Ms Swathy S.**, under my guidance and supervision and that it has not previously formed the basis for the award of any degree, diploma, fellowship or associateship to her.

Kochi

Dr. Sreenath K. R.

Date:

Scientist,
Marine Biodiversity Division
Central Marine Fisheries Research Institute
Ernakulam North P.O., Kochi-18

CERTIFICATE

We, the undersigned members of the advisory committee of Ms Swathy S., a candidate for the degree of **B.Sc.-M.Sc. (Integrated) Climate Change Adaptation**, agree that the thesis entitled “**Investigations on the climatic trends and shifts in the spatial distribution of marine fish species of Northern Indian Ocean**” may be submitted by **Ms Swathy S., (2015 - 20 - 021)** in partial fulfilment of the requirements for the degree.

Dr. Sreenath K. R.

(Chairman, Advisory Committee)

Scientist

Marine Biodiversity Division

ICAR-Central Marine Fisheries Research

Institute, Kochi, Kerala.

Dr. P. O. Nameer

(Member, Advisory Committee)

Special Officer

Academy of Climate Change Education and

Research, Kerala Agricultural University

Vellanikkara, Thrissur

Dr. Joshi K. K.,

(Member, Advisory
Committee)

Principal Scientist & Head,
Marine Biodiversity Division,

Central Marine Fisheries

Research Institute, Kochi,

Kerala.

Dr. Grinson George,

(Member, Advisory
Committee)

Senior Scientist,

Fisheries Resource

Assessment Division,

ICAR - Central Marine

Fisheries Research

Institute, Kochi, Kerala.

Dr. Eldho Varghese

(Member, Advisory
Committee)

Scientist,

Fisheries Resource

Assessment Division,

ICAR - Central Marine

Fisheries Research

Institute, Kochi, Kerala.

(EXTERNAL EXAMINER)

ACKNOWLEDGMENT

At the very outset of this dissertation work, I would like to extend my heartfelt obligation towards all the personage who has helped me in this endeavour. Without their active cooperation, help & encouragement, I would not have made headway in this work.

*I am extremely privileged to express my deepest sense of gratitude to my major advisor **Dr. Sreenath K.R.**, Scientist, Marine Biodiversity Division, CMFRI for his ample instructions, ineffable support, and patience. Many thanks for his selfless efforts to uplift, edify, and guide my way throughout this journey.*

*I am immensely grateful to **Dr. P.O. Nameer**, Special officer, ACCER, and my advisory committee member for his encouragement and motivation, which helped me in the timely completion of my thesis.*

*I cannot begin to express my indebtedness to Principal Scientist and Head, MBD, and my advisory committee member **Dr. Joshi, K.K.** for his insightful comments, generous attitude, and guardianship towards me. I also thank him for considering me as a member of the MBD family.*

*I had the great pleasure of having a collaboration with **Dr. Annette Samuelsen**, NERSC, Norway. Special thanks for her invaluable contributions and expeditious responses. I also thank **Dr. N. Nandini Menon**, NERCI for her kind help.*

*I would like to acknowledge my gratefulness to **Dr. Grinson George**, Senior Scientist, FRAD, and **Dr. Eldho Varghese**, Scientist, FRAD, members of the advisory committee, for their suggestions and queries, which helped me a lot to polish my work.*

*I thank all the **Scientists and staffs of MBD** and my fellow lab mates particularly **Mr. Alvin Anto**, **Mr. Aju K Raju**, **Ms. Krishnaveny**, **Ms. Twinkle Sebastain**, **Mrs. Reshma B.**, **Ms. Reenu Antony**, **Ms. Sheeba K.B.**, **Ms. Treasa A.S.A.**, and **Ms. Sandra** for their cooperation, encouragement, and companionship throughout the period.*

*I humbly extend my sincere thanks to **Dr. A. Gopalakrishnan**, Director, Central Marine Fisheries Research Institute and Academy of Climate Change Education and Research for providing all provisions for accomplishing my dissertation work.*

*Special thanks to my batchmates **Exemiers 2015**, my seniors, especially **Mrs. Anakha Mohan**, my juniors, **Ms. Shana S. S.** and **Ms. Vimuktha V.** for their paramount support and amity throughout my academic track. I thank all **faculties and staff of ACCER** who directly or indirectly helped me in this venture.*

*With all sincerity, I bow before the Almighty for bestowing his blessing of strength upon me to carry out this work. I cannot forget to thank my **parents and family** for all the unconditional support in this very intense academic year.*

Any omission in this brief acknowledgment doesn't mean a lack of gratitude.

Swathy S.

TABLE OF CONTENTS

1. INTRODUCTION	1
2. REVIEW OF LITERATURE	3
2.1. ENSO	3
2.2. Indian Ocean Dipole (IOD)	4
2.3. Indian Ocean Warming	5
2.4. Climate Change and its influence on the distribution of different species	7
2.5. Distribution of Marine fish species	8
2.5.1. Global Distribution	8
2.5.2. Indian Context	9
2.6. Ecological Forecasting Methods	10
2.6.1. Population Models	10
2.6.2. Species Distribution Models (SDMs)	11
2.6.2.1. Correlative SDMs	11
2.6.2.2. Mechanistic SDMs	12
2.6.3. Methods used in the Species Distribution Modelling	12
2.6.4. Generalized Dissimilarity Models (GDM)	13
2.6.5. GLM and GAM models	13
2.6.6. Multivariate Adaptive Regression Splines (MARS)	13
2.6.7. Genetic Algorithm for Rule-set Prediction (GARP)	14
2.6.8. Boosted Regression Trees (BRT)	14
2.6.9. Maximum Entropy Modelling (MaxEnt)	14
2.6.10. SDM in marine organisms	15
2.6.11. Species Distribution Modelling of marine fishes	17
3. MATERIAL AND METHODS	19
3.1. Study area	19
3.2. Data Sources	20
3.2.1. EOF Data Source	20
3.2.2. Species Occurrence Data	20
3.2.3. Selection of environmental layers	24
3.3. Data Analysis	24

3.3.1.	Climatology maps	24
3.3.2.	Trend maps	24
3.3.3.	EOF	25
3.3.4.	Correlation	25
3.3.5.	Predicting Marine fish Distribution	25
3.3.6.	Prediction of Future Distribution	26
4.	RESULTS	27
4.1.	Climate Variability	27
4.1.1.	Empirical Orthogonal Formula (EOF)	27
4.1.2.	Time Series	28
4.2.	Species distributions models	29
4.2.1.	<i>Alepisaurus ferox</i> Lowe, 1833	29
4.2.1.1.	Model Evaluation	29
4.2.1.2.	Predicted distribution	31
4.2.2.	<i>Spratelloides delicatulus</i> (Bennett, 1832)	31
4.2.2.1.	Model Evaluation	31
4.2.2.2.	Predicted distribution	33
4.2.3.	<i>Sardinella longiceps</i> Valenciennes, 1847	34
4.2.3.1.	Model Evaluation	34
4.2.3.2.	Predicted distribution	35
4.2.4.	<i>Stolephorus indicus</i> (van Hasselt, 1823)	36
4.2.4.1.	Model Evaluation	36
4.2.4.2.	Predicted distribution	37
4.2.5.	<i>Uraspis secunda</i> (Poey, 1860)	38
4.2.5.1.	Model Evaluation	38
4.2.5.2.	Predicted distribution	39
4.2.6.	<i>Seriola rivoliana</i> Valenciennes, 1833	40
4.2.6.1.	Model Evaluation	40
4.2.6.2.	Predicted distribution	41
4.2.7.	<i>Megalaspis cordyla</i> (Linnaeus, 1758)	42
4.2.7.1.	Model Evaluation	42
4.2.7.2.	Predicted distribution	43
4.2.8.	<i>Elagatis bipinnulata</i> (Quoy & Gaimard, 1825)	44

4.2.8.1.	Model Evaluation	44
4.2.8.2.	Predicted distribution	45
4.2.9.	<i>Decapterus macarellus</i> (Cuvier, 1833)	46
4.2.9.1.	Model Evaluation	46
4.2.9.2.	Predicted distribution	47
4.2.10.	<i>Caranx sexfasciatus</i> Quoy & Gaimard, 1825	48
4.2.10.1.	Model Evaluation	48
4.2.10.2.	Predicted distribution	49
4.2.11.	<i>Coryphaena hippurus</i> Linnaeus, 1758	50
4.2.11.1.	Model Evaluation	50
4.2.12.	<i>Gempylus serpens</i> Cuvier, 1829	52
4.2.12.1.	Model Evaluation	52
4.2.12.2.	Predicted distribution	53
4.2.13.	<i>Istiophorus platypterus</i> (Shaw, 1792)	54
4.2.13.1.	Model Evaluation	54
4.2.13.2.	Predicted distribution	55
4.2.14.	<i>Makaira nigricans</i> Lacepède, 1802	56
4.2.14.1.	Model Evaluation	56
4.2.14.2.	Predicted distribution	57
4.2.15.	<i>Kajikia albida</i> (Poey, 1860)	58
4.2.15.1.	Model Evaluation	58
4.2.15.2.	Predicted distribution	59
4.2.16.	<i>Istiompax indica</i> (Cuvier, 1832)	60
4.2.16.1.	Model Evaluation	60
4.2.16.2.	Predicted distribution	61
4.2.17.	<i>Thunnus obesus</i> (Lowe, 1839)	62
4.2.17.1.	Model Evaluation	62
4.2.17.2.	Predicted distribution	63
4.2.18.	<i>Thunnus albacares</i> (Bonnaterre, 1788)	64
4.2.18.1.	Model Evaluation	64
4.2.19.	<i>Thunnus alalunga</i> (Bonnaterre, 1788)	67
4.2.19.1.	Model Evaluation	67
4.2.19.2.	Predicted distribution	68

4.2.20.	<i>Rastrelliger kanagurta</i> (Cuvier, 1816)	69
4.2.20.1.	Model Evaluation	69
4.2.20.2.	Predicted distribution	70
4.2.21.	<i>Katsuwonus pelamis</i> (Linnaeus, 1758)	71
4.2.21.1.	Model Evaluation	71
4.2.22.	<i>Scomberomorus commerson</i> (Lacepède, 1800)	73
4.2.22.1.	Model Evaluation	73
4.2.22.2.	Predicted distribution	74
4.2.23.	<i>Sphyræna barracuda</i> (Edwards, 1771)	75
4.2.23.1.	Model Evaluation	75
4.2.23.2.	Predicted distribution	76
4.2.24.	<i>Canthidermis maculata</i> (Bloch, 1786)	77
4.2.24.1.	Model Evaluation	77
4.2.24.2.	Predicted distribution	78
4.2.25.	<i>Carcharhinus falciformis</i> (Müller & Henle, 1839)	79
4.2.25.1.	Model Evaluation	79
4.2.25.2.	Predicted distribution	80
4.2.26.	<i>Carcharhinus plumbeus</i> (Nardo, 1827)	81
4.2.26.1.	Model Evaluation	81
4.2.26.2.	Predicted distribution	82
4.2.27.	<i>Carcharhinus limbatus</i> (Müller & Henle, 1839)	83
4.2.27.1.	Model Evaluation	83
4.2.27.2.	Predicted distribution	84
4.2.28.	<i>Carcharhinus brevipinna</i> (Müller & Henle, 1839)	85
4.2.28.1.	Model Evaluation	85
4.2.29.	<i>Carcharhinus longimanus</i> (Poey, 1861)	87
4.2.29.1.	Model Evaluation	87
4.2.29.2.	Predicted distribution	88
4.2.30.	<i>Sphyrna mokarran</i> (Rüppell, 1837)	90
4.2.30.1.	Model Evaluation	90
4.2.30.2.	Predicted distribution	91
4.2.31.	<i>Sphyrna zygaena</i> (Linnaeus, 1758)	92
4.2.31.1.	Model Evaluation	92

4.2.31.2. Predicted distribution	93
4.2.32. <i>Alopias vulpinus</i> (Bonnaterre, 1788)	94
4.2.32.1. Model Evaluation	94
4.2.32.2. Predicted distribution	95
4.2.33. <i>Rhincodon typus</i> Smith, 1828	96
4.2.33.1. Model Evaluation	96
4.2.34. <i>Galeocerdo cuvier</i> Smith, 1828	98
4.2.34.1. Model Evaluation	98
5. DISCUSSION	168
6. SUMMARY	173
7. REFERENCES	175

LIST OF TABLES

Table 1 Table showing the percentage contribution and permutation importance of each environmental variable for the predicted current distribution of <i>Alepisaurus ferox</i>	30
Table 2 Table showing the percentage contribution and permutation importance of each environmental variable for the predicted current distribution of <i>Spratelloides delicatulus</i>	32
Table 3 Table showing the percentage contribution and permutation importance of each environmental variable for the predicted current distribution of <i>Sardinella longiceps</i>	34
Table 4 Table showing the percentage contribution and permutation importance of each environmental variable for the predicted current distribution of <i>Stolephorus indicus</i>	37
Table 5 Table showing the percentage contribution and permutation importance of each environmental variable for the predicted current distribution of <i>Uraspis secunda</i>	39
Table 6 Table showing the percentage contribution and permutation importance of each environmental variable for the predicted current distribution of <i>Seriola rivoliana</i>	41
Table 7 Table showing the percentage contribution and permutation importance of each environmental variable for the predicted current distribution of <i>Megalaspis cordyla</i>	43
Table 8 Table showing the percentage contribution and permutation importance of each environmental variable for the predicted current distribution of <i>Elagatis bipinnulata</i>	45
Table 9 Table showing the percentage contribution and permutation importance of each environmental variable for the predicted current distribution of <i>Caranx sexfasciatus</i>	49
Table 10 Table showing the percentage contribution and permutation importance of each environmental variable for the predicted current distribution of <i>Coryphaena hippurus</i>	51
Table 11 Table showing the percentage contribution and permutation importance of each environmental variable for the predicted current distribution of <i>Gempylus serpens</i>	53
Table 12 Table showing the percentage contribution and permutation importance of each environmental variable for the predicted current distribution of <i>Istiophorus platypterus</i>	55
Table 13 Table showing the percentage contribution and permutation importance of each environmental variable for the predicted current distribution of <i>Makaira nigricans</i>	57
Table 14 Table showing the percentage contribution and permutation importance of each environmental variable for the predicted current distribution of <i>Kajikia albida</i>	59
Table 15 Table showing the percentage contribution and permutation importance of each environmental variable for the predicted current distribution of <i>Istiompax indica</i>	61
Table 16 Table showing the percentage contribution and permutation importance of each environmental variable for the predicted current distribution of <i>Thunnus obesus</i>	63
Table 17 Table showing the percentage contribution and permutation importance of each environmental variable for the predicted current distribution of <i>Thunnus albacares</i>	65
Table 18 Table showing the percentage contribution and permutation importance of each environmental variable for the predicted current distribution of <i>Thunnus alalunga</i>	67
Table 19 Table showing the percentage contribution and permutation importance of each environmental variable for the predicted current distribution of <i>Rastrelliger kanagurta</i>	69
Table 20 Table showing the percentage contribution and permutation importance of each environmental variable for the predicted current distribution of <i>Katsuwonus pelamis</i>	71
Table 21 Table showing the percentage contribution and permutation importance of each environmental variable for the predicted current distribution of <i>Scomberomorus commerson</i>	73

Table 22	Table showing the percentage contribution and permutation importance of each environmental variable for the predicted current distribution of <i>Sphyrna barracuda</i> ..	75
Table 23	Table showing the percentage contribution and permutation importance of each environmental variable for the predicted current distribution of <i>Canthidermis maculata</i>	77
Table 24	Table showing the percentage contribution and permutation importance of each environmental variable for the predicted current distribution of <i>Carcharhinus falciformis</i>	79
Table 25	Table showing the percentage contribution and permutation importance of each environmental variable for the predicted current distribution <i>Carcharhinus plumbeus</i>	81
Table 26	Table showing the percentage contribution and permutation importance of each environmental variable for the predicted current distribution of <i>Carcharhinus limbatus</i>	84
Table 27	Table showing the percentage contribution and permutation importance of each environmental variable for the predicted current distribution of <i>Carcharhinus brevipinna</i>	86
Table 28	Table showing the percentage contribution and permutation importance of each environmental variable for the predicted current distribution of <i>Carcharhinus longimanus</i>	88
Table 29	Table showing the percentage contribution and permutation importance of each environmental variable for the predicted current distribution of <i>Sphyrna mokarran</i>	90
Table 30	Table showing the percentage contribution and permutation importance of each environmental variable for the predicted current distribution of <i>Sphyrna zygaena</i>	92
Table 31	Table showing the percentage contribution and permutation importance of each environmental variable for the predicted current distribution of <i>Alopias vulpinus</i>	94
Table 32	Table showing the percentage contribution and permutation importance of each environmental variable for the predicted current distribution of <i>Rhincodon typus</i>	96
Table 33	Table showing the percentage contribution and permutation importance of each environmental variable for the predicted current distribution	98

LIST OF FIGURES

Fig. 1 Satellite Map of Study Area.....	19
Fig. 2 Empirical Orthogonal Maps (EOF1, EOF2, EOF3, EOF4) maps of SST data in the NIO region	27
Fig. 3 Trend lines PC1, PC2, PC3 and PC4 of SST data from the NIO region	28
Fig. 4 Jackknife test showing the AUC values when a variable is used in isolation or the variable is excluded from the model.....	30
Fig. 5 Jackknife test showing the AUC values when a variable is used in isolation or the variable is excluded from the model.....	32
Fig. 6 Jackknife test showing the AUC values for <i>S. longiceps</i> when a variable is used in isolation or the variable is excluded from the model.....	35
Fig. 7 Jackknife test showing the AUC values of <i>S. indicus</i> when a variable is used in isolation or the variable is excluded from the model.....	37
Fig. 8 Jackknife test showing the AUC values of <i>U. secunda</i> when a variable is used in isolation or the variable is excluded from the model.....	39
Fig. 9 Jackknife test showing the AUC values of <i>Seriola rivoliana</i> when a variable is used in isolation or the variable is excluded from the model.....	41
Fig. 10 Jackknife test showing the AUC values of <i>Megalaspis cordyla</i> when a variable is used in isolation or the variable is excluded from the model	43
Fig. 11 Jackknife test showing the AUC values of <i>Elagatis bipinnulata</i> when a variable is used in isolation or the variable is excluded from the model	45
Fig. 12 Jackknife test showing the AUC values of <i>Decapterus macarellus</i> when a variable is used in isolation or the variable is excluded from the model.....	47
Fig. 13 Jackknife test showing the AUC values of <i>Caranx sexfasciatus</i> when a variable is used in isolation or the variable is excluded from the model.....	49
Fig. 14 Jackknife test showing the AUC values of <i>Coryphaena hippurus</i> when a variable is used in isolation or the variable is excluded from the model.....	51
Fig. 15 Jackknife test showing the AUC values of <i>Gempylus serpens</i> when a variable is used in isolation or the variable is excluded from the model	53
Fig. 16 Jackknife test showing the AUC values of <i>Istiophorus platypterus</i> when a variable is used in isolation or the variable is excluded from the model.....	55
Fig. 17 Jackknife test showing the AUC values of <i>Makaira nigricans</i> when a variable is used in isolation or the variable is excluded from the model	57
Fig. 18 Jackknife test showing the AUC values of <i>Kajikia albida</i> when a variable is used in isolation or the variable is excluded from the model.....	59
Fig. 19 Jackknife test showing the AUC values of <i>Istiompax indica</i> when a variable is used in isolation or the variable is excluded from the model.....	61
Fig. 20 Jackknife test showing the AUC values of <i>Thunnus obesus</i> when a variable is used in isolation or the variable is excluded from the model.....	63
Fig. 21 Jackknife test showing the AUC values of <i>Thunnus albacares</i> when a variable is used in isolation or the variable is excluded from the model	65

Fig. 22 Jackknife test showing the AUC values of <i>Thunnus alalunga</i> when a variable is used in isolation or the variable is excluded from the model	68
Fig. 23 Jackknife test showing the AUC values of <i>Rastrelliger kanagurta</i> when a variable is used in isolation or the variable is excluded from the model.....	70
Fig. 24 Jackknife test showing the AUC values of <i>Katsuwonus pelamis</i> when a variable is used in isolation or the variable is excluded from the model.....	72
Fig. 25 Jackknife test showing the AUC values of <i>Scomberomorus commerson</i> when a variable is used in isolation or the variable is excluded from the model.....	74
Fig. 26 Jackknife test showing the AUC values of <i>Sphyræna barracuda</i> when a variable is used in isolation or the variable is excluded from the model.....	76
Fig. 27 Jackknife test showing the AUC values of <i>Canthidermis maculata</i> when a variable is used in isolation or the variable is excluded from the model.....	78
Fig. 28 Jackknife test showing the AUC values of <i>Carcharhinus falciformis</i> when a variable is used in isolation or the variable is excluded from the model.....	80
Fig. 29 Jackknife test showing the AUC values of <i>Carcharhinus plumbeus</i> when a variable is used in isolation or the variable is excluded from the model.....	82
Fig. 30 Jackknife test showing the AUC values of <i>Carcharhinus limbatus</i> when a variable is used in isolation or the variable is excluded from the model.....	84
Fig. 31 Jackknife test showing the AUC values of <i>Carcharhinus brevipinna</i> when a variable is used in isolation or the variable is excluded from the model.....	86
Fig. 32 Jackknife test showing the AUC values of <i>Carcharhinus longimanus</i> when a variable is used in isolation or the variable is excluded from the model	88
Fig. 33 Jackknife test showing the AUC values of <i>Sphyrna mokarran</i> when a variable is used in isolation or the variable is excluded from the model	91
Fig. 34 Jackknife test showing the AUC values of <i>Sphyrna zygaena</i> when a variable is used in isolation or the variable is excluded from the model	93
Fig. 35 Jackknife test showing the AUC values of <i>Alopias vulpinus</i> when a variable is used in isolation or the variable is excluded from the model.....	95
Fig. 36 Jackknife test showing the AUC values of <i>Rhincodon typus</i> when a variable is used in isolation or the variable is excluded from the model.....	97
Fig. 37 Jackknife test showing the AUC values of <i>Galeocerdo cuvier</i> when a variable is used in isolation or the variable is excluded from the model	99
Fig. 38 The average sensitivity vs. 1- specificity graph for <i>A. ferox</i> showing the mean Area Under the Curve (AUC) and standard deviation for the predicted current distribution the predicted future distributions	100
Fig. 39 Map showing the predicted current and future distributions of <i>A. ferox</i>	101
Fig. 40 The average sensitivity vs. 1- specificity graph for <i>Spratelloides delicatulus</i> showing the mean Area Under the Curve (AUC) and standard deviation for the predicted current distribution the predicted future distributions	102
Fig. 41 Map showing the predicted current and future distributions of <i>Spratelloides delicatulus</i>	103
Fig. 42 The average sensitivity vs. 1- specificity graph for <i>Sardinella longiceps</i> showing the mean Area Under the Curve (AUC) and standard deviation for the predicted current distribution the predicted future distributions	104

Fig. 43 Map showing the predicted current and future distributions of <i>Sardinella longiceps</i>	105
Fig. 44 The average sensitivity vs. 1- specificity graph for <i>Stolephorus indicus</i> showing the mean Area Under the Curve (AUC) and standard deviation for the predicted current distribution the predicted future distributions	106
Fig. 45 Map showing the predicted current and future distributions of <i>Stolephorus indicus</i> .	107
Fig. 46 The average sensitivity vs. 1- specificity graph for <i>Uraspis secunda</i> showing the mean Area Under the Curve (AUC) and standard deviation for the predicted current distribution the predicted future distributions	108
Fig. 47 Map showing the predicted current and future distributions of <i>Uraspis secunda</i>	109
Fig. 48 The average sensitivity vs. 1- specificity graph for <i>Seriola rivoliana</i> showing the mean Area Under the Curve (AUC) and standard deviation for the predicted current distribution the predicted future distributions	110
Fig. 49 Map showing the predicted current and future distributions of <i>Seriola rivoliana</i>	111
Fig. 50 The average sensitivity vs. 1- specificity graph for <i>Megalaspis cordyla</i> showing the mean Area Under the Curve (AUC) and standard deviation for the predicted current distribution the predicted future distributions.	112
Fig. 51 Map showing the predicted current and future distributions of <i>Megalaspis cordyla</i> ..	113
Fig. 52 The average sensitivity vs. 1- specificity graph for <i>Elagatis bipinnulata</i> showing the mean Area Under the Curve (AUC) and standard deviation for the predicted current distribution the predicted future distributions	114
Fig. 53 Map showing the predicted current and future distributions of <i>Elagatis bipinnulata</i> .	115
Fig. 54 The average sensitivity vs. 1- specificity graph for <i>Decapterus macarellus</i> showing the mean Area Under the Curve (AUC) and standard deviation for the predicted current distribution the predicted future distributions	116
Fig. 55 Map showing the predicted current and future distributions of <i>Decapterus macarellus</i>	117
Fig. 56 The average sensitivity vs. 1- specificity graph for <i>Caranx sexfasciatus</i> showing the mean Area Under the Curve (AUC) and standard deviation for the predicted current distribution the predicted future distributions	118
Fig. 57 Map showing the predicted current and future distributions of <i>C. sexfasciatus</i>	119
Fig. 58 The average sensitivity vs. 1- specificity graph for <i>Coryphaena hippurus</i> showing the mean Area Under the Curve (AUC) and standard deviation for the predicted current distribution the predicted future distributions	120
Fig. 59 Map showing the predicted current and future distributions of <i>Coryphaena hippurus</i>	121
Fig. 60 The average sensitivity vs. 1- specificity graph for <i>Gempylus serpens</i> showing the mean Area Under the Curve (AUC) and standard deviation for the predicted current distribution the predicted future distributions	122
Fig. 61 Map showing the predicted current and future distributions of <i>Gempylus serpens</i> ..	123
Fig. 62 The average sensitivity vs. 1- specificity graph for <i>Istiophorus platypterus</i> showing the mean Area Under the Curve (AUC) and standard deviation for the predicted current distribution the predicted future distributions	124
Fig. 63 Map showing the predicted current and future distributions of <i>Istiophorus platypterus</i>	125

Fig. 64 The average sensitivity vs. 1- specificity graph for <i>Makaira nigricans</i> showing the mean Area Under the Curve (AUC) and standard deviation for the predicted current distribution the predicted future distributions	126
Fig. 65 Map showing the predicted current and future distributions of <i>Makaira nigricans</i>	127
Fig. 66 The average sensitivity vs. 1- specificity graph for <i>Kajikia albida</i> showing the mean Area Under the Curve (AUC) and standard deviation for the predicted current distribution the predicted future distributions	128
Fig. 67 Map showing the predicted current and future distributions of <i>Kajikia albida</i>	129
Fig. 68 The average sensitivity vs. 1- specificity graph for <i>Istiompax indica</i> showing the mean Area Under the Curve (AUC) and standard deviation for the predicted current distribution the predicted future distributions	130
Fig. 69 Map showing the predicted current and future distributions of <i>Istiompax indica</i>	131
Fig. 70 The average sensitivity vs. 1- specificity graph for <i>Thunnus obesus</i> showing the mean Area Under the Curve (AUC) and standard deviation for the predicted current distribution the predicted future distributions	132
Fig. 71 Map showing the predicted current and future distributions of <i>Thunnus obesus</i>	133
Fig. 72 The average sensitivity vs. 1- specificity graph for <i>Thunnus albacares</i> showing the mean Area Under the Curve (AUC) and standard deviation for the predicted current distribution the predicted future distributions	134
Fig. 73 Map showing the predicted current and future distributions of <i>Thunnus albacares</i> ..	135
Fig. 74 Map showing the predicted current and future distributions of <i>T. alalunga</i>	137
Fig. 75 The average sensitivity vs. 1- specificity graph for <i>R. kanagurta</i> showing the mean Area Under the Curve (AUC) and standard deviation for the predicted current distribution the predicted future distributions	138
Fig. 76 Map showing the predicted current and future distributions of <i>R. kanagurta</i>	139
Fig. 77 The average sensitivity vs. 1- specificity graph for <i>Katsuwonus pelamis</i> showing the mean Area Under the Curve (AUC) and standard deviation for the predicted current distribution the predicted future distributions	140
Fig. 78 Map showing the predicted current and future distributions <i>K. pelamis</i>	141
Fig. 79 The average sensitivity vs. 1- specificity graph for <i>Scomberomorus commerson</i> showing the mean Area Under the Curve (AUC) and standard deviation for the predicted current distribution the predicted future distributions	142
Fig. 80 Map showing the predicted current and future distributions of <i>S. commerson</i>	143
Fig. 81 The average sensitivity vs. 1- specificity graph for <i>Sphyraena barracuda</i> showing the mean Area Under the Curve (AUC) and standard deviation for the predicted current distribution the predicted future distributions	144
Fig. 82 Map showing the predicted current and future distributions of <i>Sphyraena barracuda</i>	145
Fig. 83 The average sensitivity vs. 1- specificity graph for <i>Canthidermis maculata</i> showing the mean Area Under the Curve (AUC) and standard deviation for the predicted current distribution the predicted future distributions	146
Fig. 84 Map showing the predicted current and future distributions of <i>Canthidermis maculata</i>	147

Fig. 85 The average sensitivity vs. 1- specificity graph for <i>Carcharhinus falciformis</i> showing the mean Area Under the Curve (AUC) and standard deviation for the predicted current distribution the predicted future distributions	148
Fig. 86 Map showing the predicted current and future distributions of <i>Carcharhinus falciformis</i>	149
Fig. 87 The average sensitivity vs. 1- specificity graph for <i>Carcharhinus plumbeus</i> showing the mean Area Under the Curve (AUC) and standard deviation for the predicted current distribution the predicted future distributions	150
Fig. 88 Map showing the predicted current and future distributions of <i>Carcharhinus plumbeus</i>	151
Fig. 89 The average sensitivity vs. 1- specificity graph for <i>Carcharhinus limbatus</i> showing the mean Area Under the Curve (AUC) and standard deviation for the predicted current distribution the predicted future distributions	152
Fig. 90 Map showing the predicted current and future distributions of <i>Carcharhinus limbatus</i>	153
Fig. 91 The average sensitivity vs. 1- specificity graph for <i>Carcharhinus brevipinna</i> showing the mean Area Under the Curve (AUC) and standard deviation for the predicted current distribution the predicted future distributions	154
Fig. 92 Map showing the predicted current and future distributions of <i>Carcharhinus brevipinna</i>	155
Fig. 93 The average sensitivity vs. 1- specificity graph for <i>Carcharhinus longimanus</i> showing the mean Area Under the Curve (AUC) and standard deviation for the predicted current distribution the predicted future distributions	156
Fig. 94 Map showing the predicted current and future distributions of <i>Carcharhinus longimanus</i>	157
Fig. 95 The average sensitivity vs. 1- specificity graph for <i>Sphyrna mokarran</i> showing the mean Area Under the Curve (AUC) and standard deviation for the predicted current distribution the predicted future distributions	158
Fig. 96 Map showing the predicted current and future distributions of <i>Sphyrna mokarran</i> ...	159
Fig. 97 The average sensitivity vs. 1- specificity graph for <i>Sphyrna zygaena</i> showing the mean Area Under the Curve (AUC) and standard deviation for the predicted current distribution the predicted future distributions	160
Fig. 98 Map showing the predicted current and future distributions of <i>Sphyrna zygaena</i>	161
Fig. 99 The average sensitivity vs. 1- specificity graph for <i>Alopias vulpinus</i> showing the mean Area Under the Curve (AUC) and standard deviation for the predicted current distribution the predicted future distributions	162
Fig. 100 Map showing the predicted current and future distributions of <i>Alopias vulpinus</i>	163
Fig. 102 Map showing the predicted current and future distributions of <i>Rhincodon typus</i>	165
Fig. 103 The average sensitivity vs. 1- specificity graph for <i>Galeocerdo cuvier</i> showing the mean Area Under the Curve (AUC) and standard deviation for the predicted current distribution the predicted future distributions	166
Fig. 104 Map showing the predicted current and future distributions of <i>Galeocerdo cuvier</i> .	167

ABBREVIATIONS

ASCII	American Standard Code for Information Interchange
AUC	Area Under the Curve
BEST	Bivariate El Niño Southern Oscillation Index
BIOCLIM	Bioclimatic variables
BRT	Boosted Regression Tree
CART	Classification and Regression Trees
CDO	Climate Data Operator
CITES	Convention on International Trade in Endangered Species
CMEMS	Copernicus Marine Environment Monitoring Services
CMFRI	Central Marine Fisheries Research Institute
CMIP	Coupled Model Intercomparison Project
CP	Central Pacific
CT	Classification Trees
DMI	Dipole Mode Index
ENM	Environmental Niche Modelling
ENSO	El Niño Southern Oscillation
EOF	Empirical Orthogonal Function
EP	Eastern Pacific
EU	European Union
FAO	Food and Agricultural Organization
GAM	Generalized Additive Model
GARP	Genetic Algorithm for Rule-Set Prediction
GBIF	Global Biodiversity Information Facility
GCS	Geographic coordinate system
GDM	Generalized Dissimilarity Model
GEBCO	General Bathymetric Chart of Ocean
GIS	Geographic Information System
GLM	Generalized Linear Model
IDW	Inverse Distance Weight
IOD	Indian Ocean Dipole
IODZM	Indian Ocean Dipole/Zonal Mode
IPCC	Intergovernmental Panel on Climate Change
IUCN	International Union for Conservation of Nature
LHF	Latent Heat Flux
MARS	Multivariate Adaptive Regression Splines
MaxEnt	Maximum Entropy Model
MEI	Multivariate Enso Index
NHF	Net Heat Flux

NIO	Northern Indian Ocean
NOAA	National Oceanic and Atmospheric Administration
OBIS	Ocean Biodiversity Information System
PC	Principal Component
PCA	Principal Component Analysis
RCP	Representative Concentration Pathway
RES	Relative Environmental Suitability
RF	Random Forest
ROC	Receiver Operating Curve
SDM	Species Distribution Model
SOI	Southern Oscillation Index
SSS	Sea Surface Salinity
SST	Sea Surface Temperature
SWIO	South West Indian Ocean
TED	Turtle Exclusion Device
TIO	Tropical Indian Ocean
WGS	World Geodetic System

CHAPTER 1

INTRODUCTION

The global climate is a complex system, which is being subjected to various evolutions from the time of origin of the earth and it continues. The alterations in the system can be due to natural fluctuations but the unforeseen abrupt changes are owing to the anthropogenic effects. The global temperature is estimated to have risen 1°C more than the pre-industrialized period due to human activities (IPCC, 2018). Future warming substantially exceeds the threshold of 2°C and the trends are most likely leading towards the higher end of IPCC projections (New *et al.*, 2011). As climate change and warming are uneven throughout the world, the increasing trend in global average temperature brings out that regions of warming are more than cooling (Lindsey and Dahlman, 2020). The manifestations of climate change are evident from the tropics to the poles.

Climate change also affects the oceans. They both are linked to each other. Ocean reduces the impact of climate change to an extent by acting as a heat sink (Yan *et al.*, 2016). Nevertheless, the massive effects of climate change and its related consequences are being reflected in the global oceans. The average rate of increase in temperature per decade of both the land and ocean is more than twice (0.18°C) in 1981 when compared to that of the 1880s (0.07°C) (NOAA, 2019). The consequences of climate change also include climate extremes (Seneviratne *et al.*, 2012). Global Ocean warming has created drastic climatic variability over the tropical Indo- pacific regions resulting in the most prominent modes of climate variability, the El Niño-Southern Oscillation (ENSO) Indian Ocean Dipole (IOD) (Luo *et al.*, 2009). It also results in decreased dissolved oxygen content, oxygen minimum zones, and ocean acidification even in the offshore regions (FAO, 2018).

The effect of climate change on marine ecosystems can be established by the shift in their distributional range (Nye *et al.*, 2009). These shifts can be detected accompanying the gradual warming or due to extreme climatic events (Mills *et al.*, 2013). The IPCC fifth assessment report suggests that natural climate change at a level lesser than the current anthropogenic climate change can even cause ecosystem disruption, species extinction and ecosystem shifts, thereby posing a great risk to the future. As the temperature warms, the species are forced to shift from tropics to higher latitudes, thereby shrinking their extent (Chen *et al.*,

2009; Chen *et al.*, 2011). The novel regime that the species go into may not fit properly than the current one or it may not be a protected area (Thuiller *et al.*, 2006). One of the most sensitive fish species to the climate extreme, essentially to El Niño southern oscillation is the anchovy (Ñiquen & Bouchon, 2004). In Indian Ocean, as the sea surface temperature rises beyond the threshold of Indian oil sardine, the southern latitudes will witness a decrease in catch especially in the south-west and south-east coast in the near future itself (Vivekanandan *et al.*, 2009).

Various approaches have been used till date to estimate the impact of climate change on species community constitution, their diversity and abundance (Guisan and Zimmermann, 2000). In recent years, predicting the distribution of species is one of the important components in planning conservation strategies and delineating protected areas (Anderson *et al.*, 2003; Elith *et al.*, 2006). Species distribution models (SDM) are one of the common strategies used to find the appropriate niche of species. SDMs deal with the statistical relationship between the suitable climate of the species and their current distribution and thereby predicting its potential distribution in other new environments under the supposition that the species reaction to specific environmental conditions remains the same (Velásquez-Tibatá *et al.*, 2013). Three kinds of approaches define the SDM. They are correlative, mechanistic and hybrid models. The correlation between species presence or abundance with its habitat is utilised in correlative models. Mechanistic models deal with the relationship between the environment of the species and its fitness. The third model is the incorporation of both correlative and mechanistic models (Robinson *et al.*, 2017). Various Species distribution models include Generalised linear Model (GLM), Random Forest (RF), Boosted Regression Tree (BRT), Maximum entropy model (Maxent) etc. Maxent allows species distribution modelling using presence-only data. This study aims to understand the pattern of trends of the remotely sensed climatic variables in the Northern Indian Ocean (NIO). The study also aims to evaluate the probable shifts in the distribution of selected marine fish species in this region.

CHAPTER 2

REVIEW OF LITERATURE

2.1. ENSO

El Niño southern oscillation (ENSO) is a coupled ocean-atmospheric phenomenon involving a periodic departure from expected SST in the central and eastern equatorial Pacific Ocean which has potential to impact weather patterns around the world by generating low- and high-pressure systems and thereby causing irregular wind and precipitation patterns and cycles around two to seven years. ENSO consists mainly of three phases- El Niño, La Nina and a normal/ neutral phase. El Niño and la Nina are the oceanic phenomena whereas the southern oscillation is its atmospheric counterpart. These together comprise the El Niño southern oscillation. Philander (1983) found that southern oscillations have become far more than a see-saw pattern of oscillation of surface pressure between south-east pacific and north Australian zone during the past century. It has become interannual variability of the climate system which can impact the global climate.

There are two forms or types of ENSO events identified in the tropical Pacific Ocean (Wang and Weisberg, 2000; Ashok et al., 2007). They are the Eastern-Pacific (EP) type and the Central-Pacific (CP) type. EP is characterised by SST anomalies over the Eastern pacific cold tongue whereas Central pacific has SST anomaly over the International dateline (Yu and Kao, 2007; Kao and Yu, 2009). The central pacific type is also known as El Niño Modoki (Ashok et al, 2007). Although meteorologists knew of the Southern Oscillation from the 1900s, its association with the oceanic rather than the El Niño phenomenon was not known till the 1960s, and theoretical understanding of these relationships has only begun after that (Eugene et al., 1983).

ENSO is considered as the primary source of interannual variability across the globe. During 1980 to 2010, it increased the average temperature of the Indian Ocean from 25.16 to 26.24°C. After that, in the middle of the 20th century, Indian Ocean showed a brisk warming pattern (Kumar et al., 2014). El Niño are associated with physical and biological changes in the ocean, changes in the distribution of fish species can be imputed to the ENSO climate variability (Brander, 2007). Pacific salmons are also affected by ENSO events. Reduced growth and increased mortality rates are found in salmons immediately after El Niño (NOAA fisheries).

Sockeye salmon shows a northward moving approach during the ENSO period (NOAA fisheries).

The anchovy and sardine catch in the South American coast are affected by ENSO (Bertrand et al., 2004). La Nina event aggregates the skipjack tuna to the western pacific but El Niño distributes it to the east of the dateline (Salinger, 2013). The inspection of the seasonal cycles in the coral fossils and interannual variation (Tudhope et al., 2001) showed a pattern similar to the ENSO cycles in modern coral. So, it is clear that the fossil record of coral indeed is a reflection of the paleo-ENSO system. As there are massive changes in pacific fisheries due to ENSO, its impact can also be seen in Indian as well as Atlantic Ocean fisheries. Fishes like anchovy are affected in the eastern coast due to the ENSO, while in other cases pelagic fishes like tuna, dolphin fishes etc. are available to fishers close to the coast (FAO, 2020).

2.2. Indian Ocean Dipole (IOD)

An internal mode of interannual variability which is unique for both the Pacific and the Atlantic Ocean have been recognised. Such a kind of phenomenon in the Indian Ocean was unidentified until Saji *et al.* (1999) reported the bipolar SST pattern prevailing over the west and East Indian Ocean which was independent of the El Niño southern oscillation. IOD refers to the pattern of SST variation that occurs in the equatorial Indian Ocean interannually, where the positive (negative) IOD represents a positive SST anomaly over western (eastern) Indian Ocean and negative anomaly over eastern (western) Indian Ocean (Saji *et al.*, 1999, Webster *et al.*, 1999). In the eastern equatorial Indian Ocean, the rising trend of anomalies of easterlies and southerlies will cause west and the northward shift of eastern Indian Ocean warm pool respectively that trigger the Indian Ocean dipole (Zhang *et al.*, 2019). The countries which border Indian Ocean such as India, Australia, and Africa are affected by IOD rather than ENSO (Ashok *et al.*, 2001; Ashok *et al.*, 2003)

Indian Ocean warming is the major reason for the increasing Indian Ocean dipole events in the last decade (Ajayamohan and Rao, 2008). The sea surface temperature and wind anomalies are highly coupled in the Indian ocean dipole events (Saji *et al.*, 1999; Saji and Yamagata, 2003). On a decadal time scale the IOD and ENSO activities show an inverse relationship, the stronger decadal ENSO years coincided with years of low IOD events (Saji and

Yamagata, 2003). The Indian Ocean (IO) encountered a remarkable realization of three consecutive positive IO Dipoles (pIODs) between 2006-2008 and Cia (2009) found that climate change is causing the incidence of these events. The unusual co-existence of la nina and positive phase of IOD in the year 2007 depicts that the predictability of pIOD lies in the Indian ocean itself (Luo, *et al.*, 2007). The intensity of Indian Ocean dipole is measured using Dipole Mode Index (DMI), which is the difference between Sea Surface Temperature anomalies of eastern and western Indian Ocean (Vinayachandran *et al.*, 2002). A multi model average indicates that the Eastern Indian ocean warming of the 21st century is slower than the west and models with stronger IOD amplitude generate a slower eastern IO warming rate (Cai, 2011). The ocean conditions are necessary for some Indian Ocean Dipole/Zonal Mode (IODZM) events to occur and the rest are due to the weather noises and it has low predictability (Song and Qian, 2008). Many of the strong Indian Ocean Dipole (IOD) events over the last 50 years have been followed by increased summer monsoon circulation and above average precipitation over central north India (Krishnan, 2009). In general, positive Indian Ocean Dipole (IOD) events appear to be followed by increased summer monsoon flows over the subcontinent and above average precipitation; while heavy monsoons have not always coupled with positive IOD events (Panickal, 2008)

The predictability of IOD can be utilised not only for climate prediction but for the sustainability of various other sectors such as fisheries, agriculture, human health, marine ecosystem, natural disasters *etc* (Yuan and Yamagata 2015). Indian Ocean dipole and ENSO have influence on oceanographic parameters and it affects the distribution of marine fish species of the Indian Ocean (Amri, 2015). IOD curbs the spatial distribution and catch of fish, especially tuna and the catch of yellowfin tuna shows an inverse relationship with IOD which is concentrated in the western Indian ocean- the Arabian Sea and the Madagascar (Lana et al., 2013)

2.3. Indian Ocean Warming

Climate change and rising greenhouse gas concentration in the atmosphere can directly affect marine bodies (Hoegh & Bruno, 2010). Global oceans act as a sink for the rising carbon

dioxide in the atmosphere (Raven & Falkowski, 1999). This is manifested as increasing SST, sea level rise and even as ecosystem disruption.

Analyzing the temperature changes in the ocean not only helps in providing a consistent indication of anthropogenic effects on the climate system but also caters to dependable predictions for future warming (Gabriele *et al.*, 2005). The increased heat content of the Pacific Ocean is balanced by augmented heat transfer from Pacific to Indian Ocean through Indonesia. During the past decade, it results in the enhanced heat content of the Indian Ocean, which accounts for more than 70% increase in heat content in the upper 700m in the global oceans (Sang-Ki *et al.*, 2015). Luo & Jia (2012) proposed that warming in the Indian Ocean relative to the Pacific Ocean may play an important role in modulating 20th and 21st century Pacific climate change. Indian Ocean Sea surface temperature (SST) can potentially affect the global climate. Indian ocean SST is an important variable in ocean atmospheric coupling and its increasing trend will impact the natural modes of variability such as IOD. Between the mid-1950s and mid-1990s, world ocean heat content increased by $\sim 2 \times 10^{23}$ joules, reflecting a mean volume warming of 0.06°C , where the Pacific and Atlantic shows warming from 1950 and Indian Ocean since 1960s and the delayed warming compared to other oceans may be due to the data scarcity in the Indian Ocean region till the 1960s (Levitus, 2000). The tropical Indian Ocean warming trend is greater than other tropical oceans since the last decade (Du and Xie, 2008). There is more downward net heat flux (NHF) over the Tropical Indian Ocean (TIO), which favours TIO warming, and the increase in latent heat flux (LHF) contributes significantly to the NHF (Tao and Weichen, 2015). The Indian ocean SST revealed the strongest basin scale warming by the middle of the 20th century and is identified as the robust warming signal over all oceans according to the measure of signal to noise ratio (Lau and Weng, 1999).

The western tropical Indian Ocean has been warming for more than a century, at a rate faster than other regions of the tropical oceans, and it experienced an unusual 1.2°C warming in SST during 1901 to 2012, while the Indian Ocean Warm Pool increased by 0.7°C (Roxy, 2014). Studies also show that Indian Ocean is warming consistently and its warm pool is expanding abruptly. Warm Pools are regions in the tropical ocean where SST is greater than 28°C . The Indo-Pacific warm pool which is the largest in the world where rigorous air-sea interactions come off and it is a place of active convection (Saraswat *et al.*, 2007). The area of tropical warm pool is expanding since the past 150 years and the rate of expansion is rising from the last

decades (Webster *et al.*, 2006). Hence, the temperature, area and location of the warm pool is changing gradually over the Indian Ocean, which imparts a huge impact on the climate system (Cane and Clement, 1999).

The tropical Pacific confers substantial decadal climate variability to the western Indian Ocean and may imply decadal variability in other regions with strong teleconnections to El Niño Southern Oscillation (Cole and Julia, 2000). It also affects the internal mode of variability in the Indian ocean such as IOD (Saji *et al.*, 1999). The weakened upward or reinforced downward LHF is possibly due to the reduced difference in anomalous sea air temperature due to the reinforced Tropospheric Temperature system (Tao and Weichen, 2015). Anthropogenic impacts and global climate are affecting biodiversity all around the globe. Increased heat content of oceans has negative impacts on the global marine ecosystems. Marine ecosystems play a huge role in sustaining the biology of the earth, still the effects of oceanic changes due to anthropogenic activities are poorly studied (Hoegh-Guldberg, 2010). Western Indian Ocean holds considerable concentration of phytoplankton among all the tropical oceans but remarkably it is one of the largest warming areas among the tropical oceans (Roxy *et al.*, 2016). The upper layer warming and stratification is likely to deteriorate the dissolved oxygen which critically affects the ocean productivity and marine habitat (Keeling *et al.*, 2009). Ocean model prediction suggests that the world's ocean oxygen inventories are declining by one to seven percent within the next century and will continue to decline in the future for a thousand years and more. (Keeling. *et al.*, 2009). Ocean warming will also drive the species to higher latitudes (Laevastu and Rosa, 1963) found that the ocean temperature variation has a role in distribution of tuna fish.

2.4. Climate Change and its influence on the distribution of different species

Globally, spatial distributions of fish stocks are shifting and this has been attributed not only to intensive fishing pressure but also to the recent climate change, with many stocks having been reduced to historically low levels over the past half century. Various species respond to the climatic changes by expanding in the range of the distribution towards poles and contracting their ranges in the equatorward side (Chen *et al.*, 2011; Sunday *et al.*, 2012). However, the

places of rapid temperature change indicated different magnitudes of observed biological responses between species (Angert *et al.*, 2011; Pinsky *et al.*, 2013). Eventhough, variation in the spatial distribution can be attributed to the responsiveness to different climatic variables, the actual response to climate change comprises the interactions of the biotic and abiotic factors together with the changes in all levels of biological organisation (Cahill *et al.*, 2012; Grigaltchik *et al.*, 2012).

Responses to climate change have been observed in different parts of the world and across the ecological hierarchy. Long-term changes in the range sizes of nine out of thirteen tuna species studied have been previously reported globally (Worm and Tittensor, 2011), and range extension or contraction of several fish populations in South East Australia (Last *et al.*, 2011). In addition, studies have suggested that the response of the species towards climate change is size-dependent, where higher distributional shifts are recorded in the smaller sized species as compared to that of the larger sized ones (Genner *et al.*, 2010).

The availability of a standard and consistent outline to evaluate range shifts can facilitate worldwide comparisons of species at each stage of such shifts and should progress predictive capacity (Bates *et al.*, 2014). Especially, various processes that permit species to adapt and endure in a changing climate should be evaluated at each different stage of shifts, and the importance of such processes may differ among stages (Maggini *et al.*, 2011). Utilisation of assorted information sources and careful elucidation of data to quantify which species are at equilibrium with climate in regions undergoing rapid change can help in developing the potential to detect and predict range shifts precisely. However, one of the major limitation in the field of range shift ecology is our inadequate capacity to observe range shifts in order to collect information that is required to parameterize models.

2.5. Distribution of Marine fish species

2.5.1. Global Distribution

Fishes were evolved more than 500 million years ago, and are the first group of vertebrates to ever live on earth and they continue their domination in the water realm. Out of all vertebrate species, more than one-half are contributed by fishes (Nelson, 2006). Eschmeyer and Fong (2014) estimated around 33,059 valid species of fish known from around the world.

Fishes have a wide variety of amazing adaptations that enable them to live in almost all available aquatic environments. Considering the whole marine realm, tropical oceans have an extraordinary diversity of fishes along with other living organisms. (Worm *et al.*, 2006).

Studying the distribution of marine fish species across the world both in time and space is essential for their proper management. Historically, most of the research was focused on the causes and consequences of the difference in marine fish abundance overtime (Hjort, 1914; Cushing, 1990). Climate change has a significant role in the distribution of marine fish species across the world. An increase in sea surface temperature triggered a northward movement of fishes which resulted in the occurrence of increased frequency of sub-tropical species and if it is hindered by any geographical barriers they tend to migrate to deeper and cooler waters (Dulvy *et al.*, 2008).

2.5.2. Indian Context

India is a country rich in biodiversity and this biodiversity richness is truly reflected in the diversity of marine and freshwater fishes. Marine fishes are those who spend at least one of their life cycles in the ocean. The Indian subcontinent along with the island groups of Lakshadweep and Andaman and Nicobar Islands is an integral part of the Indian Ocean. Fish diversity of the Indian subcontinent constitutes 9.7 percent of the total number of known fish species (Eschmeyer and Fong, 2014), and of these, 7.4 percent is contributed by marine fish species alone.

The Indo-Pacific faunal region has the greatest diversity of marine fish species that occur in tropical areas of the Indian and western Pacific oceans. Some of the pioneering studies performed on this region by Randall (1998) showed light into the endemism, disjunctive distributions, and species versus subspecies comparison. Halas and Winterbottom (2009) studied the beginning of the East Indies coral reef biota, coined and defined the “East Indies Triangle”.

The highest number of species diversity in the Indian region is the Andaman and Nicobar archipelago reported with 1431 species (Rajan *et al.*, 2013), and the possible reason for this high species diversity is due to its proximity to and similarity with the Indonesian group of islands. Atoll islands of Lakshadweep archipelago along with its diverse coral reefs exhibit a moderate diversity with 753 species (Rao, 1991). According to the current status of the diversity of Indian

marine fish lists, there is the presence of 1071 species of fish along the west coast of India. Shore fishes of India are mostly derived from the "East Indies Triangle" (Menon, 1961; Krishnan and Mishra, 1993). As all oceans are somehow connected, endemism is not so common among marine fishes. But there are several studies regarding the endemic Indian marine fishes. A study by Mishra *et al.* (2013) has documented the endemic fishes of India. Further studies added 5 more endemic species described from Indian waters (Randall *et al.*, 2013, Bineesh *et al.*, 2013, Mohapatra *et al.*, 2013, Allen *et al.*, 2012)

2.6. Ecological Forecasting Methods

The rapid change in the climate coupled with anthropogenic stresses are posing severe threats to the ecosystems such as shifting of natural habitats, invasion of new species and the emergence of new diseases. So, the modeling of the environmental dynamics with parameters as species distribution and abundance, ecosystem variability and the community composition contributes to the better prediction of the ecosystem movements and thereby facilitates better management decisions, conservation, and sustainability. During earlier days' ecologists developed management decisions utilizing the model from mean and variances of the observed environmental parameters. But faster reformations which occur in the ecosystem as a consequence of climatic variations cannot be quantified precisely by mere historic observations (Smith *et al.*, 2009; Milly, 2008; Craig, 2010). Ecological forecasting makes an attempt to derive a clue about how the environment will behave in the future, based on the current trends and the past data. This includes forecasts of agricultural yield, species distributions (Guisan & Thuiller, 2005), species invasions (Levine & Antonio, 2003), pollinator performance (Corbet *et al.*, 1995), extinction risk (Gotelli & Ellison, 2006), fishery dynamics (Hare *et al.*, 2010); disease dynamics (Ollerenshaw & Smith, 1969) and population size (Ward *et al.*, 2014).

There are mainly two methods for measuring the structural and physical changes occurring in the ecosystem and for better forecasting, namely population models and species distribution models.

2.6.1. Population Models

Models of population dynamics or the ecological population models provide a proper perception about the dynamics and persistence of a population. This model maps the size of

population and age distribution within a population to its decline or extensive growth and produces a better prediction regarding the status of a population. The environmental, as well as interactions with other and similar species, may also be a deciding factor (Uyenoyama *et al.*, 2004). Crowder *et al.*, 1994; Crouse *et al.*, 1987; Caswell, 2001 developed a population model which helps to reverse the population diminishing of the loggerhead sea turtle. The model discloses that the mortality of adults and subadults are the major cause of population decline of these species. So an alternate management action had been taken by installing the TED (Turtle Exclusion Devices) in shrimp trolls and was favorable to the growth of population size of the turtle. Population dynamics models also link the interaction of the environmental variation and the population growth such as the influence of the sea level rise on the extinction of polar bears (Hunter *et al.*, 2010). The overabundant species population is also managed by the help of the population dynamics. Govindarajulu *et al.* (2005) propose the measures for controlling the population of harmful bullfrog of Vancouver Island.

Even though this model is used extensively for predicting the behavior of a population, the amount of uncertainty in the data leads to error in prediction. The complicated biological interactions are not flawlessly implemented by this model unless a sufficient amount of data is supplied.

2.6.2. Species Distribution Models (SDMs)

Species distribution models (SDMs), otherwise called environmental (or ecological) niche modeling (ENM), habitat modeling, predictive habitat distribution modeling, and range mapping (Elith and Leathwick, 2009) are widely used in ecological and biodiversity conservation research for modeling how the species are distributed globally over the geographical area. This model accommodates the tools that incorporate known species occurrences with environmental data (Phillips *et al.*, 2006).

2.6.2.1. Correlative SDMs

Correlative SDMs forecast the influence of climatic variations on the geographical distribution of data. (Thomas *et al.* 2004). In European diadromous fishes the linear combination of predictor attributes best suited for the propagation of the species are developed by Mennesson-Boisneau *et al.* (2006). The statistical records of association of environment to the

species abundance and occurrence are analyzed in these SDMs for identifying the hindering processes to the spread of the species. As per Moilanen & Wintle (2007) the ease of implementation of the Correlative SDMs because of simplicity and the capability to model complex interactions of the environment with less data requirement provides supremacy over other SDMs.

2.6.2.2. Mechanistic SDMs

This model is otherwise called biophysical models or process-based models because it aims at mapping the relationship between the physiology of the species and the surroundings which has an influence on their abundance and distribution. (Kearney *et al.*, 2009). Other than the current radius of the species, the model utilizes the processes or physiological changes within the body of organisms with respect to climate variations and vegetation which helps in the prediction of the future extension possibilities of species range towards a great extent of the ecosystem levels (Porter *et al.*, 2002; Kearney & Porter, 2004; Buckley, 2008; Kearney *et al.*, 2008; Kearney & Porter, 2009). For the complex analysis of interactions between the environment and climatic influences in large scales, the mechanistic SDMs will not be suitable because it requires a large quantity of variables to be considered which makes the model computationally and time constrained to carry out both train and validation phases.

2.6.3. Methods used in the Species Distribution Modelling

Forecasting the geographic ranges of different species with the use of occurrence records (presence or absence) and data of environmental variables from the same locality is the focus of Species distribution modeling (Phillips *et al.*, 2006; Elith and Leathwick, 2009). The species-specific interaction had to be studied in conservation planning measures and the best tool available for this is species bioclimatic envelope models. They shared the same principle of biome envelope models, in which the current distribution of species is used to ‘train’ a model for the future incorporation of predicted climatic conditions (Hannah *et al.*, 2002). Envelopes were constructed using the Geographic Information System (GIS) software or by genetic algorithms or general additive modeling (Peterson *et al.*, 2001; Berry *et al.*, 2002; Midgley *et al.*, 2002). But these models could not model dynamic transitions, interspecific competition, herbivory, dispersal or other factors. By coupling with land-use projection models, application

of the results of bioclimatic envelope models could be used in real-world conservation (Hannah *et al.*, 2002).

2.6.4. Generalized Dissimilarity Models (GDM)

For the modeling of spatial turnover in community composition among pairs of sites as functions of environmental differences between these sites, Generalized Dissimilarity Models (GDM) were used (Ferrier *et al.*, 2007). For the estimation of the probability of occurrence of distribution of a given species, a kernel regression algorithm was used within the transformed environmental space produced by GDM (Lowe, 1995). Elements of matrix regression and generalized linear modeling were combined which allowed the user to model non-linear responses of the environment which captured the ecologically realistic relationships between dissimilarity and ecological distance (Ferrier, 2002).

2.6.5. GLM and GAM models

Non-parametric and non-linear functions were used by Generalised Linear Models (GLM) whereas Generalised Additive Models (GAM) use parametric and combinations of linear, quadratic or cubic terms. GAMS can model complex ecological response shapes than GLM because of greater flexibility (Yee and Mitchell, 1991). GLM and GAM were widely used in species distribution modeling because ecological relationships were modelled realistically and they have strong statistical foundations (Jowett *et al.*, 2008; Alexander, 2016; Rezaei and Sengül, 2018).

2.6.6. Multivariate Adaptive Regression Splines (MARS)

For fitting non-linear responses, an alternative regression-based method called Multivariate Adaptive Regression Splines (MARS) was used. It used piecewise linear fits rather than smooth functions. It was very easy to use in GIS applications for making prediction maps, faster to implement compared to GAMs and had the ability to analyze community data (MARS-COMM) which helped in relating the variation in occurrence of species to the environmental predictors in an analysis, and later evaluating the individual model coefficients for separate species concurrently (Leathwick *et al.*, 2005).

2.6.7. Genetic Algorithm for Rule-set Prediction (GARP)

For the approximation of bioclim species' fundamental ecological niches, several approaches had been used such as BIOCLIM (Nix, 1986), logistic multiple regression (Peeters and Gardeniers, 1998) and Genetic Algorithm for Rule-set Prediction (GARP). GARP was defined by heterogeneous rules that defined the polyhedrons in the ecological niche spaces that were assumed to be livable by a particular species. GARP is a machine-learning approach and also links the occurrence records to the environment variables using envelope, atomic and logistic regression rules. GARP included the properties of both BIOCLIM and logistic multiple regression (Stockwell and Noble, 1992; Stockwell and Peters, 1999). The extensive testing done on the GARP model showed that it has high predictive ability for species geographic distributions (Peterson and Cohoon, 1999; Peterson *et al.*, 2001).

2.6.8. Boosted Regression Trees (BRT)

Boosting Regression Trees were developed in a forward stage-wise manner, where small modifications were done in the model at each step for better fitness of data (Friedman *et al.*, 2000). The use of regression-trees helped in the good selection of relevant variables and it could model interactions. It was upon the weighted versions of the data set where the observation that was poorly fitted in the preceding model and they were accounted for by adjusting the weights (Elith *et al.*, 2006). The correlation between the distributions of adult stages of copepod *Oithona similis* was established using the Boosted Regression tree method (Pinkerton *et al.*, 2010).

2.6.9. Maximum Entropy Modelling (MaxEnt)

According to Phillips *et al.*, 2006, MaxEnt uses the distribution of maximum entropy. Using the background locations and data derived constraints, it approximated the most uniform distribution (Philips *et al.*, 2004; Philips *et al.*, 2006). In this model the complexity of the fitted functions could be chosen, if presence-only species data were used. It was observed that Maximum entropy modeling (MaxEnt) had done better or as well than other modeling techniques (Elith *et al.*, 2006; Hernandez *et al.*, 2006; Philips *et al.*, 2006). Compared to other algorithms, MaxEnt achieved higher success rate and it marked the differences even at low

sample sizes (Pearson *et al.*, 2007). It is observed that species-specific model parameter tuning can enhance models efficiency (Radosavljevic and Anderson, 2014.).

Several studies have recorded the variability in predictions that may arise from distinct MaxEnt background samples, with a specific focus on the extent of the location from which they are chosen (Baasch *et al.*, 2010; Giovanelli *et al.*, 2010; Barve *et al.*, 2011). The outputs obtained from MaxEnt models fall into three categories namely, the raw output, Cumulative output and the logistic output. The difference in the scaling of these three types of outputs plays a crucial role in providing differently appearing prediction maps (Merow *et al.*, 2013).

MaxEnt had used to investigate the distributional patterns of Geckos (*Uroplatus* spp.) for predicting the species distribution (Pearson *et al.*, 2007), American black bear (*Ursus americanus*) for the assessment of denning habitat (Baldwin and Bender, 2008), predicting and mapping of Sage grouse's (*Centrocercus urophasianus*) nesting habitat, Asian slow lorises (*Nycticebus* spp.) was assessed to threats and species distribution analyzed to find conservation urgencies (Thorn *et al.*, 2009).

2.6.10. SDM in marine organisms

A plethora of research outputs and outcomes are obtained in the marine environment using the species distribution modelling. Most of these works are addressing the complex interrelations between the environmental variables and the organisms in the sea, the ongoing negative effects of climate change, the concern about the spread of alien species and the conservation remedies for supporting marine biodiversity (Báez *et al.*, 2010; Gormley *et al.*, 2015; Cheung *et al.*, 2016). SDM's have been restyled to web based cellular automated versions derived from the model, Invasionsoft to forecast the spread of invasive groups (Johnston and Purkis., 2012) and are joined with other common procedures like connectivity analysis for proposing reserve networks for conservation planning (Esselman and Allan, 2011).

In the Baltaic Sea, occurrence and biomass distribution was predicted for twenty-three benthic species using methods like random forests (RF), generalized additive models (GAM), multivariate adaptive regression splines (MARS) and maximum entropy (Max Ent) in which the predictive performance was shown to be high by the Random forest for both occurrence and biomass distribution models (Šiaulyš and Bucas., 2012). An attempt to predict the global biomass of the seafloor and construction of individual and composite maps of the patterns

predicted for this seafloor biomass and abundance of fish and invertebrates were carried out employing Random forest (Wei *et al.*, 2010). Distribution modelling systems such as the Aquamaps that relied on the presence-only data of species to provide global scale prediction of the distribution of marine organisms was also evaluated (Ready *et al.*, 2010). Habitat suitability models were constructed for the macrobenthic species that inhabited the soft sediments of the Belgian Part of the North Sea and total coverage spatial distribution of these macrobenthos were predicted and mapped (Degraer *et al.*, 2008).

The distribution of *Patella rustica* was modelled using the Classification and Regression tree that used the historical distribution data for model training with an aim to use the past and present distribution as a tool for examining its response to climate change (Lima *et al.*, 2007). Patterns of invasion, extinction and species richness of invertebrates were modelled using simulations of environment variables (Jones and Cheung, 2014). The current and future potential distribution of two ecologically and economically important mussels, *Mytilus edulis* and *M. galloprovincialis* were analysed (Fly *et al.*, 2015). Relatively fewer modelling works have been performed in other invertebrates like corals, jellyfishes and anemones.

Species distribution modelling is widely used in research related to marine mammals. Habitat degradation together with the mortality of these mammals as fisheries bycatch result in their population reduction which demands an increased knowledge of the spatial distribution of these marine organisms (Redfern *et al.*, 2006). The social organization, behaviour and the high mobility of these organisms make the data collection and estimation challenging (Barlow, 1999; Ersts and Rosenbaum, 2003). The distribution pattern of fin whales and striped dolphins with respect to the physiographic satellite-based variables were modelled using the Generalised additive model and the prediction and habitat characterisation were done using the CART (Panigada *et al.*, 2008). Habitat preference models were developed for different mammals including bottlenose dolphins *Tursiops truncatus*, harbour porpoises *Phocoena phocoena*, harbour seals *Phoca vitulina* and grey seals *Halichoerus grypus* in the Marine Protected Areas of NE Scotland (Bailey and Thompson, 2009). Genetical studies and spatial analysis through Classification and Regression Tree (CART) was used to delineate the spatial distribution of offshore and coastal ecotypes of bottlenose dolphins in the Northwest Atlantic (Torres *et al.*,

2003). Global distribution of marine mammals were mapped using a Relative Environmental Suitability (RES) model (Kaschner *et al.*, 2006).

The prominent issues related to distribution modelling in the marine scenario can be summed up as insufficiency of data, bias in spatial and temporal data and the scale of spatial and temporal data (Reiss *et al.*, 2014). The difficulty in data collection in marine environments renders a data of low spatial resolution and higher bias (Phillips *et al.*, 2009; Robinson *et al.*, 2011). Responses such as abundance or biomass provide more details than predictions of occurrence only, but require higher quality data (Vierod *et al.*, 2014).

2.6.11. Species Distribution Modelling of marine fishes

The one-fourth of the literature on the marine SDMs cover the distribution of marine fishes and among the marine organisms (Robinson *et al.*, 2011; Monk *et al.*, 2012). Most of the SDMs on them are based on the presence (occurrence) only data for abating the errors (Robinson *et al.*, 2017). The published global occurrence data can be collected from various databases like FishBase (Froese and Pauly, 2007). The most commonly used three approaches to model the distribution of marine fishes are Maxent, AquaMaps and the Sea Around Us Project models (Jones *et al.*, 2012, Ready *et al.*, 2010; Close *et al.*, 2006; Bigg *et al.*, 2008; Cheung *et al.*, 2009). The main objective of the study conducted by Ready *et al.*, 2010 was to compare the prediction using AquaMap of twelve marine species in which nine species were fishes (*Carangoides equula*, *Psettodes erumei*, *Clupea harengus*, *Sardinops sagax*, *Solea solea*, *Trachurus trachurus*, *Squalus megalops*, *Zeus faber*, *Squalus acanthias*) with other modelling approaches such as GARP, GLM, GAM and MaxEnt. DeVaney, 2016 modelled the distribution of deep pelagic eels, the gulper eel *Eurypharynx pelecyanoides* and the bobtail eel *Cyema atrum*, using MaxEnt. The glacial persistence of Atlantic cod was modelled using two approaches among which one was Maxent (Bigg *et al.*, 2008). The spatial and temporal distribution of Atlantic herring (*Clupea harengus*), Atlantic mackerel (*Scomber scombrus*), and butterfish (*Peprilus triacanthus*) were modelled in the Northwest Atlantic shelf area using MaxEnt (Wang *et al.*, 2018). In the studies of Cheung *et al.*, 2009 they projected the distributional range of 1066 species of marine fishes and invertebrates in the year 2050 under the impact of climate change and thereby they predicted the global patterns of local extinction, invasion etc. for the year 2050.

Other approaches are also used for modelling marine fishes. Moore *et al.*, 2009 used SDM for the identification of significant environmental variables that influence the spatial

distribution of demersal fishes and for the assessment of the relationship between them. They modelled the distribution of four demersal fish species using classification trees (CTs) and generalized additive models (GAMs). Swain *et al.*, 2015 in his study titled ‘Spatial distribution of fishes in a Northwest Atlantic ecosystem in relation to risk of predation by a marine mammal’ studied the predation risk on fishes (Atlantic cod, *Gadus morhua* L.; white hake, *Urophycis tenuis* Mitchell; and thorny skate, *Amblyraja radiata* Donovan) by grey seals by comparing the changes in their spatial distribution over the period 1971 – 2012 with that of non – prey species. GAMs were used for modelling the distribution by integrating the effects of predation risk, water temperature and population abundance. Using GAMs, the influence of zooplankton biomass and oceanographic features on the spatial distribution of pre spawning herring *Clupea harengus*, L was studied (Maravelias & Reid, 1997). Schmiing *et al.*, 2013 performed a predictive modelling of selected coastal reef fishes using GAMs in which the relationship between the species and the environment was analysed. Young and Carr, 2015, studied and predicted the distribution, richness and assemblage structure of selected fish species (tubesnout , black surfperch, striped surfperch, kelp greenling, olive rockfish, kelp rockfish, gopher rockfish, black rockfish, black and yellow rockfish and blue rockfish) along the central coast of California, USA using GAMs.

Maxwell *et al.*, 2009 used GLMs for their study focuses on the spatial distribution of the fishes which are mentioned in the title in the parts of the Irish Sea, Celtic Sea and the English Channel. The distribution of eighteen littoral and benthic fishes were predicted by Wiley *et al.*, 2003 using Genetic Algorithm for Rule Set Prediction (GARP).

CHAPTER 3

MATERIAL AND METHODS

3.1. Study area

The area chosen for the present study is the Northern Indian Ocean. This study area comprises of Arabian Sea, Bay of Bengal, Red Sea, the Persian Gulf, Andaman Sea, Gulf of Thailand, Gulf of Aden, and Malacca strait etc. The Indian Ocean includes nearly 20% of the water in the world (Fatima and Jamshed, 2015). The unique feature of the Indian ocean is that it is a closed ocean as unlike the Atlantic and Pacific ocean, it is land-locked in the north and does not extend to the northern hemisphere's cold climate areas. (Bouchard and Crumplin, 2013) The area of the Indian Ocean selected for this study comes under the jurisdiction of various nations.

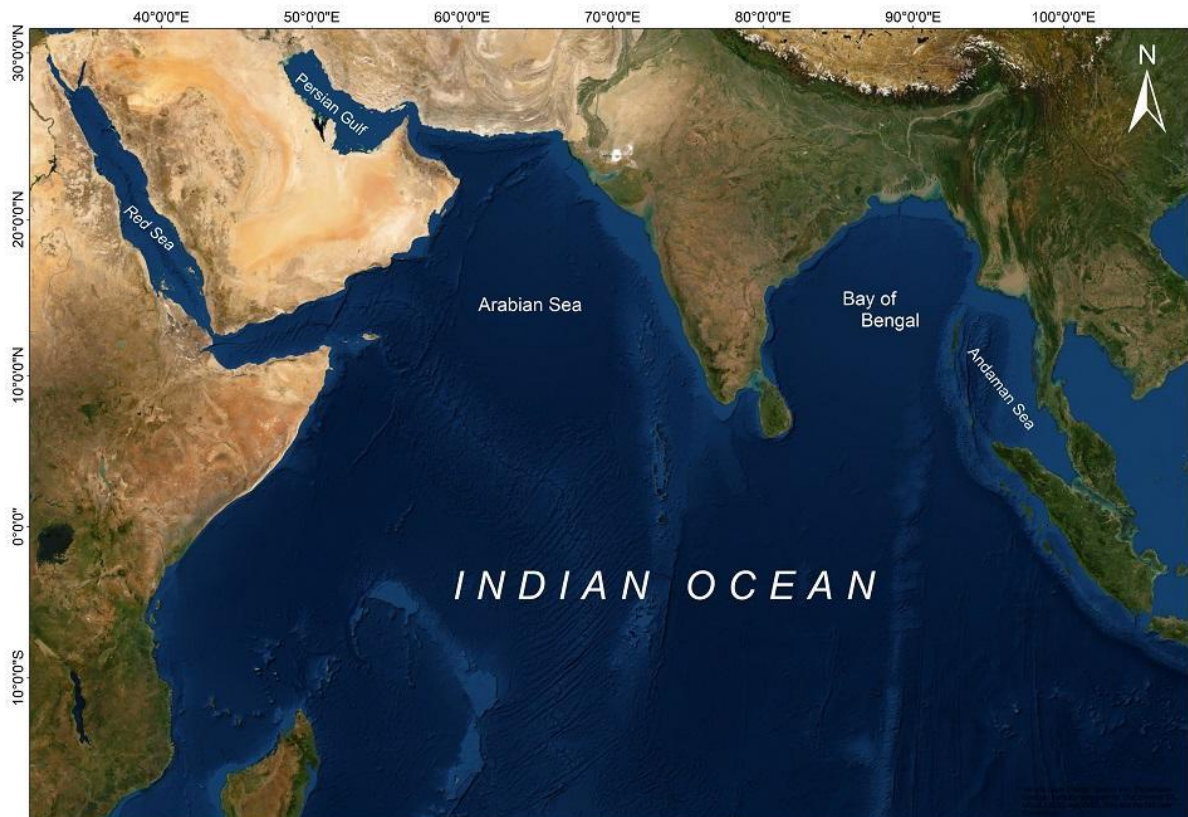


Fig. 1 Satellite Map of Study Area

3.2. Data Sources

3.2.1. EOF Data Source

Sea Surface Temperature (SST) monthly data of 1/12° horizontal resolution for grid points from 20°E to 100°E longitude and 30°N to 20° latitude for the years 1993 to 2018 are utilised. The global reanalysis dataset is an open-source database of Copernicus Marine Environment Monitoring Services (CMEMS) and is maintained by of European Union.

3.2.2. Species Occurrence Data

The species occurrence data of 34 species has been collected from Global Biodiversity Information Facility (GBIF), Fish base, OBIS and CMFRI databases. The distribution points of the species were plotted using ArcGIS software. The fishes selected for the study are -

Alepisaurus ferox Lowe, 1833: They are bathypelagic, oceanodromous (Orlov and Chenko, 2002) mainly inhabit in the tropical and subtropical waters. They belong to IUCN ‘least concern’ category (CITES, 2017).

Spratelloides delicatulus (Bennett, 1832): They are reef- associated fish seen at a depth of 0-50m (Whitehead, 1985). This pelagic (Carpenter *et al.*, 1997), inshore, schooling fish belong to the IUCN ‘least concern’ category (IUCN, 2019).

Sardinella longiceps Valenciennes, 1847: they can be found in the north and western parts on Indian Ocean, Gulf of Aden and Gulf of Oman. This coastal pelagic (Carpenter *et al.*, 1997) breeds only once in a year off the western coast of India.

Stolephorus indicus (van Hasselt, 1823): Indian anchovy is distributed in the Red sea, South Africa, Persian Gulf, Madagascar and Mauritius (Russell and Houston, 1989). Coastal pelagic (Carpenter *et al.*, 1997) schooling species feeds mainly on the zooplanktons.

Uraspis secunda (Poey, 1860): The cottonmouth jack widely distributed in warm water. Distributed in western Indian Ocean (Vaniz, 1984). Adults are mostly oceanic and pelagic.

Seriola rivoliana Valenciennes, 1833: Longfin yellowtail is a reef-associated fish seen at a depth of 5 to 245m (Allen and Erdmann, 2012). Distributed in the Indo-pacific region (Vaniz, 1984).

Megalaspis cordyla (Linnaeus, 1758): Torpedo scad is a reef-associated fish seen at a depth of 20 to 100m (Sakaff and Esseen, 1999). Distributed in the Indo west pacific region.

Elagatis bipinnulata (Quoy & Gaimard, 1825): Rainbow runner is a subtropical reef-associated fish seen at a depth of 0 to 150m (Lieske and Myers, 1994)

Decapterus macarellus (Cuvier, 1833): Mackerel scad is a subtropical circumglobal fish seen at a depth of 0 to 400m (Mundy, 2005). Mainly distributed in Red sea, Gulf of Aden, Seychelles, Mascarenes, South Africa and Sri Lanka

Caranx sexfasciatus Quoy and Gaimond, 1825: Bigeye trevally is a tropical, amphidromous distributed in the Indo-Pacific region (Vaniz, 1984)

Coryphaena hippurus Linnaeus, 1758: Common dolphinfish is a subtropical (Palko *et al.*, 1982), pelagic- neritic, oceanodromous (Riede, 2004). This highly migratory fish (FAO, 1994) occupies the tropical and subtropical waters of Indian Ocean.

Gempylus serpens Cuvier, 1829: Snake mackerel are distributed in the tropical and subtropical seas. They are solitary (Nakamura and Parin, 1993)

Istiophorus platypterus (Shaw, 1792): The Indo-Pacific sailfish is mainly distributed in the tropical and temperate waters. They are epipelagic found above the thermocline.

Makaira nigricans Lacepede, 1802: Blue marlin belongs to the 'vulnerable' category of IUCN (IUCN, 2019). Distributed in the subtropical waters with temperature ranging from 22°C to 31°C (Nakamura, 1985)

Thunnus obesus (Lowe, 1839): Bigeye tuna belong to the ‘vulnerable’ category of IUCN (IUCN, 2019). Changes in the surface temperature and thermocline affect the distribution of this species. (Maigret and Ly, 1986)

Thunnus albacare (Bonnaterre, 1788): Yellowfin tuna occurs above or below the thermocline. This migratory species occupies all the tropical and subtropical seas except Mediterranean Sea. (FAO, 1994). It is a ‘Near threatened’ species (IUCN, 2019).

Thunnus alalunga (Bonnaterre, 1788): Albacore is distributed in all the tropical and temperate seas. It is a ‘Near threatened’ species (IUCN, 2019).

Rastrelliger kanagurta (Cuvier, 1816): Indian mackerel occupies mainly in the Indo- west pacific region. This pelagic neritic schooling species forms feeds on phytoplanktons and small zooplankton (Collette, 2001)

Katsuwonus pelamis (Linnaeus, 1758): Skipjack tuna is a migratory fish which occupies the tropical and warm temperate of all oceans. It is a tropical fish which occupies at a depth of 0 to 260m (Collette, 1995) and temperature 15°C to 30°C. (Collette and Nauen, 1983)

Scomberomorus commerson (Lacepède, 1800): Narrow barred Spanish mackerel occupies a depth range of 10 to 70m (Pauly *et al.*, 1996) in the Indo west pacific regions (Kailola *et al.*, 1993). It belongs to the ‘Near threatened’ category (IUCN, 2019)

Sphyrna barracuda Edwards, 1771: Great barracuda is a subtropical species (Florida Museum of Natural History, 2005) occupying at a depth of 1 to 100m (Sylva, 1990). It is distributed in the Red sea, east coast of Africa (Cervigón, 1993)

Xiphias gladius Linnaeus, 1758: Swordfish occupies tropical and temperate waters of Indian ocean, Pacific and Atlantic Ocean (FAO, 1994). It is a ‘Endangered’ species. (IUCN, 2019).

Canthidermis maculata Bloch, 1786: Rough triggerfish is a sub-tropical reef associated fish occupies at a depth of 1 to 110m (Lieske and Myers, 1994). It is distributed in the western Indian Ocean (Smith and Heemstra, 1986)

Carcharhinus falciformis (Müller and Henle, 1839): Silky shark is mainly distributed in the Indo-pacific region (Compagno *et al.*, 1989). This reef-associated (Riede, 2004) fish prefers 0 to 4000m depth (Florida Museum of Natural History, 2005). This belongs to the ‘Vulnerable’ category (IUCN, 2019).

Carcharhinus plumbeus (Nardo, 1827): Sandbar shark is scattered over the Persian Gulf, Red Sea, and East Africa. It belongs to ‘vulnerable’ category (IUCN, 2019)

Carcharhinus limbatus (Müller and Henle, 1839): Blacktip shark is a ‘Near threatened’ species (IUCN, 2019). It is an anadromous reef-associated fish (Riede, 2004) distributed in the Persian Gulf, Red sea, south Africa (Carpenter *et al.*, 1997)

Carcharhinus brevipinna (Müller and Henle, 1839): Spinner sharks are considered as ‘Vulnerable’ species (IUCN, 2019). They are seen in the tropical and temperate waters of Indo-pacific.

Carcharhinus longimanus (Poey, 1861): Oceanic white tip sharks are highly migratory and distributed in tropical and temperate waters all over the globe. They are considered as ‘Vulnerable’ species (IUCN, 2019)

Sphyrna mokarran (Rüppell, 1837): Great hammerhead are considered as ‘Endangered’ species (IUCN, 2019). They are distributed in the warm temperate and tropical seas (Compagno, 1998)

Sphyrna zygaena (Linnaeus, 1758): Smooth hammerhead is distributed in the Indo pacific region mainly from South Africa to Sri Lanka (Compagna, 1998). They are considered as ‘Vulnerable’ species (IUCN, 2019)

Alopias vulpinus (Bonnaterre, 1788): Thresher are cosmopolitans in tropical and temperate waters (Compagno, 2005). They are considered as ‘Vulnerable’ species (IUCN, 2019)

Rhincodon typus Smith, 1828: Whale sharks are ‘Endangered’ species (IUCN, 2019). Distributed in the tropical and warm temperate waters all over the globe.

Galeocerdo cuvier (Péron & Lesueur, 1822): Tiger sharks are ‘Near threatened’ species (IUCN, 2019). Distributed in the tropical and warm temperate waters all over the globe.

3.2.3. Selection of environmental layers

The environmental parameters which affect the distribution of marine fish are bathymetry, SST mean, SST maximum, SSS mean, chlorophyll a, current. The gridded bathymetry data were collected from GEBCO with 30 arc second resolution. All other variables were obtained from an open-source database- Bio oracle with 5arc minute (approximately 9.2km) resolution. The projection of each layer is made up of GCS_WGS_1984 coordinate system using ArcGIS software and clipped to the extent identical to the study area. This is then interpolated with Inverse Distance Weighting (IDW) using a mask polygon. The rasters were resampled to uniform resolution (9 x 9km). All the files were converted to ASCII in ArcMap.

The datasets for RCP 4.5, 6.0, and 8.5 for the periods 2040-2050 and 2090-2100 were taken from Bio-oracle and GEBCO. It is then reprojected and resampled to the same extend

3.3. Data Analysis

Data analysis is done on anaconda platform using python programming verion 3.7.6

3.3.1. Climatology maps

The monthly climatology is calculated from the monthly mean SST data using climate data operator (CDO). The difference between the monthly mean SST and monthly climatology provides the monthly anomaly

3.3.2. Trend maps

The linear and second order trend has been plotted using the time series data and the first order warming trend per year and for the 25years has also been calculated.

3.3.3. EOF

Empirical Orthogonal Function (EOF) analysis describe time series by using a collection of orthogonal functions (EOFs) in the following way

$$Z(x,y,t) = N \sum_{k=1} PC(t).EOF(x,y)$$

$Z(x,y,t)$ is the original time series as a function of time (t) and space (x,y); $PC(t)$ is the principal component that describes the increasing EOF's amplitude changes over time; $EOF(x, y)$ shows the spatial structure (x, y) of the major factors which may account for the temporal variation of Z .

The SST monthly anomaly data is subjected to empirical orthogonal function (EOF) analysis to find the principal components as well as the dominant modes of variability in spatial and temporal scales. Four EOFs and their subsequent principal components are plotted and analysed. The spatial EOFs are derived by calculating the eigenvalues and eigenvectors of the covariance matrix and principal component time series for each mode is plotted by projecting the resulting eigenvalue to the anomalies (Ehsan *et al.*, 2020)

3.3.4. Correlation

The EOF1 and 2 are taken and correlation analysis has been done using Karl Pearson's rank correlation with Southern Oscillation Index (SOI), Dipole Mode Index (DMI), Multivariate ENSO Index (MEI.v2) and Bivariate El-Niño Southern Oscillation Index (BEST)

3.3.5. Predicting Marine fish Distribution

The maximum entropy model (MaxEnt) is a software package for species distribution modeling. Maxent takes the presence-only data and environmental predictors which affects the species as input and displays the current and future distribution (Merow, 2013). The species data should be given in '.csv' format and environmental layers should be in '.asc' format. The area under the receiver operating characteristic (ROC) curve (AUC) provides a single measure of model performance. The maximum achievable AUC is 1 and the higher value of AUC indicates that the model can accurately differentiate between presence and potentially modeled location (Merow, 2013).

3.3.6. Prediction of Future Distribution

The environmental layer is projected to another layer which contains future environmental data, to predict the future distribution of all the predicted marine fish species. The name of the layer, resolution, and projection should be the same as that of the former layer. Species distribution modeling for RCP 4.5, 6.0 and 8.5 have been done for the year 2040-2050 and 2090-2100 scenarios.

CHAPTER 4 RESULTS

4.1. Climate Variability

4.1.1. Empirical Orthogonal Formula (EOF)

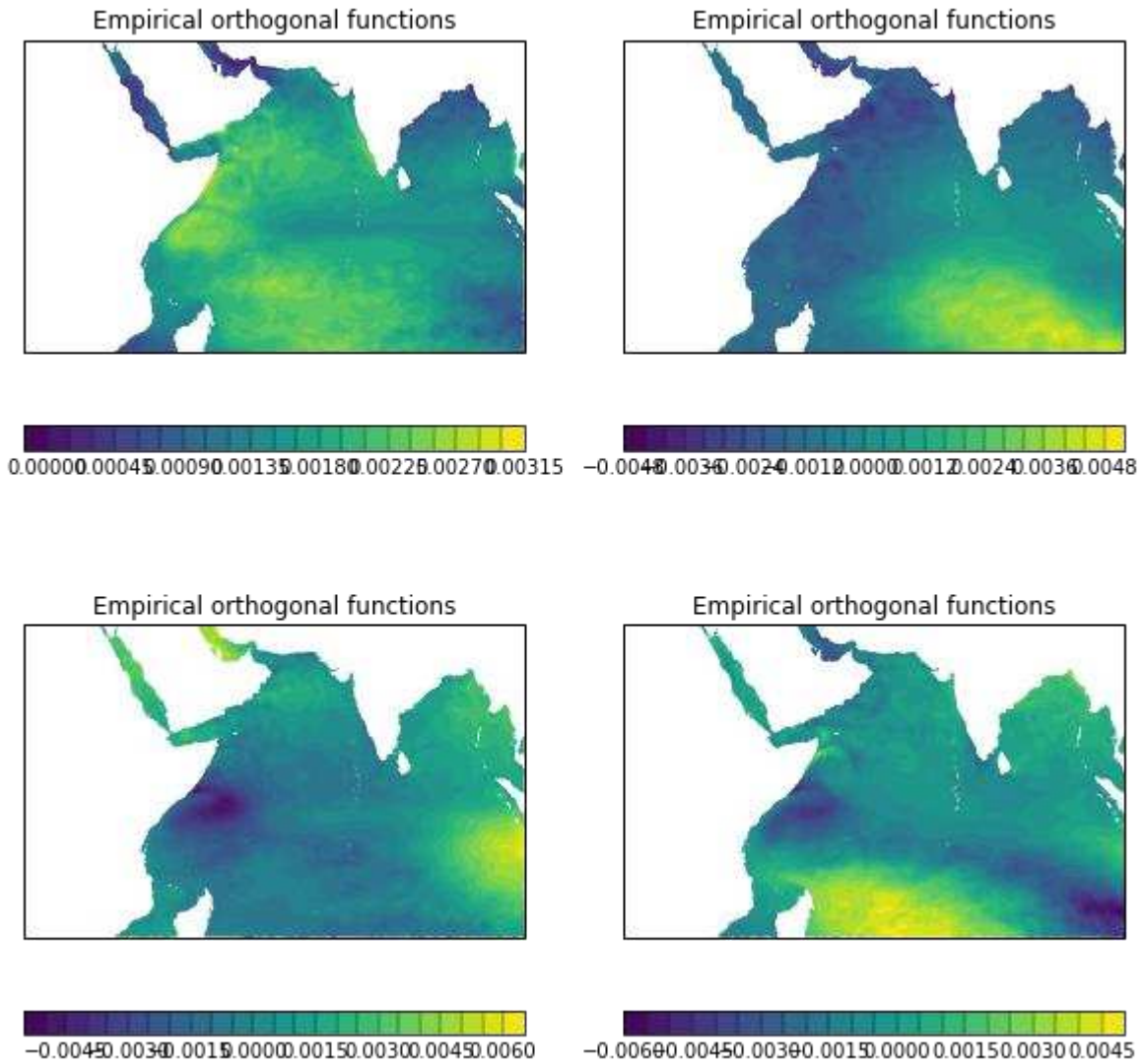


Fig. 2 Empirical Orthogonal Maps (EOF1, EOF2, EOF3, EOF4) maps of SST data in the NIO region

4.1.2. Time Series

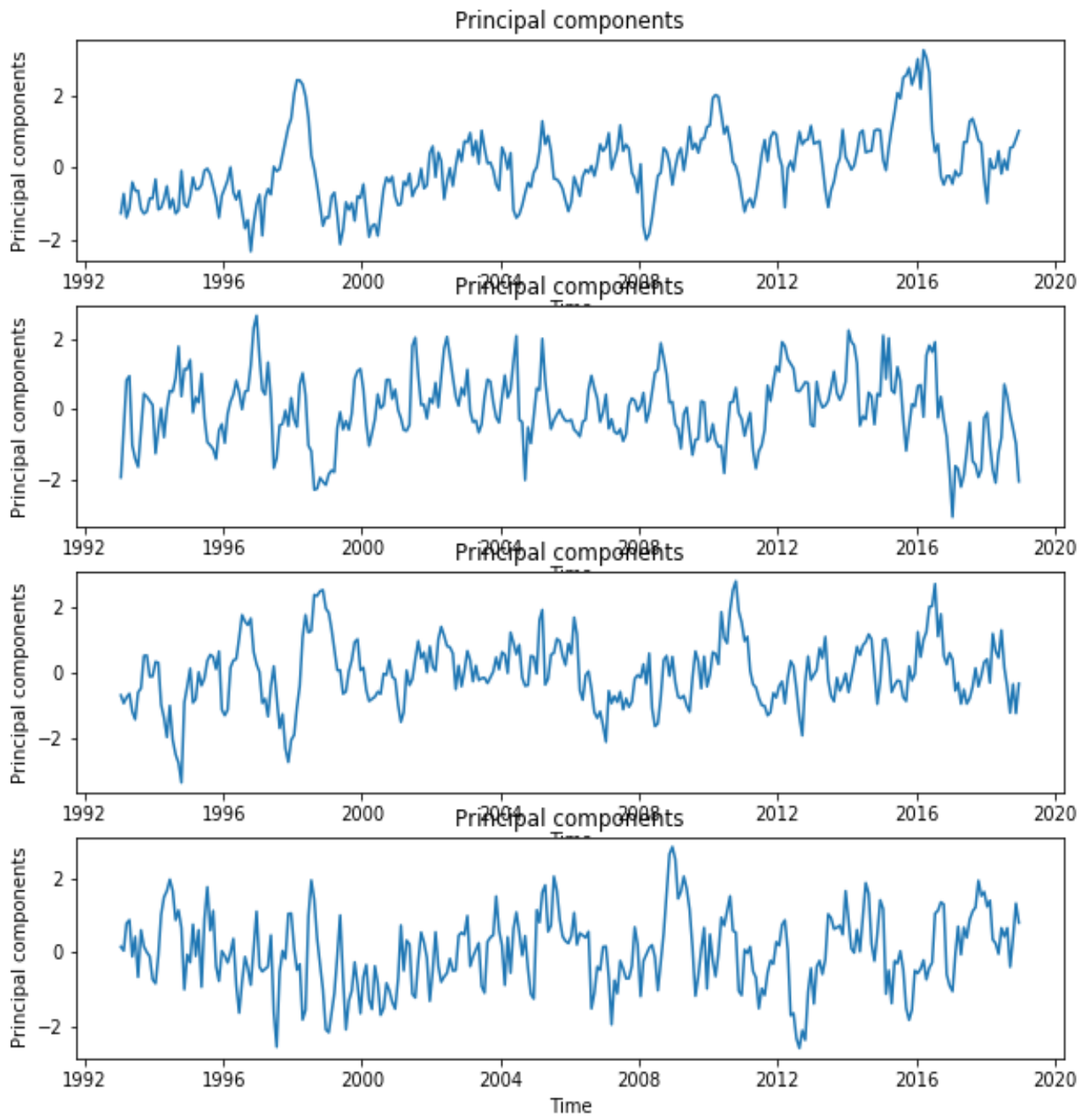


Fig. 3 Trend lines PC1, PC2, PC3 and PC4 of SST data from the NIO region

4.2. Species distributions models

The current distribution and future distribution for the years 2040-2050 and 2090-2100 with RCP 4.5, 6.0 and 8.5 are predicted. The families selected are Clupeidae, Carangidae, Scombridae, Carcharhinidae, Alepisauridae, Corphaenidae, Istiophoridae, Sphyaenidae and Balistidae. The predicted species distribution showing the habitat suitability of each species is shown in the map. The AUC value showing the model predictability is also given in the figure.

4.2.1. *Alepisaurus ferox* Lowe, 1833

Kingdom	Phylum	Class	Order	Family	Genus	Species
Animalia	Chordata	Actinopterygii	Aulopiformes	Alepisauridae	<i>Alepisaurus</i>	<i>ferox</i>

4.2.1.1. Model Evaluation

The area under the curve value for the model is 0.824 with 0.012 standard deviation (Fig. 38). The model prediction for the current distribution shows salinity mean as the greatest percentage contributor with value of 51.9 and permutation importance of 53.6. Distance from the shore, mean temperature, minimum temperature, maximum temperature, current velocity mean and current velocity minimum contribute 11.8%, 10.3%, 8.4%, 7.5%, 6.6% and 3.6% respectively (Table 1). Jackknife test reveals that salinity-mean has the highest gain among all parameters when used in isolation (Fig. 4).

Variable	Percent contribution	Permutation importance
Salinity-Mean	51.9	53.6
Distance from the shore	11.8	12.7
Temperature-Mean	10.3	11.8
Temperature-Min	8.4	7.5
Temperature-Max	7.5	7.3
Current Velocity-Mean	6.6	3.9
Current Velocity-Min	3.6	3.2

Table 1 Table showing the percentage contribution and permutation importance of each environmental variable for the predicted current distribution of *Alepisaurus ferox*

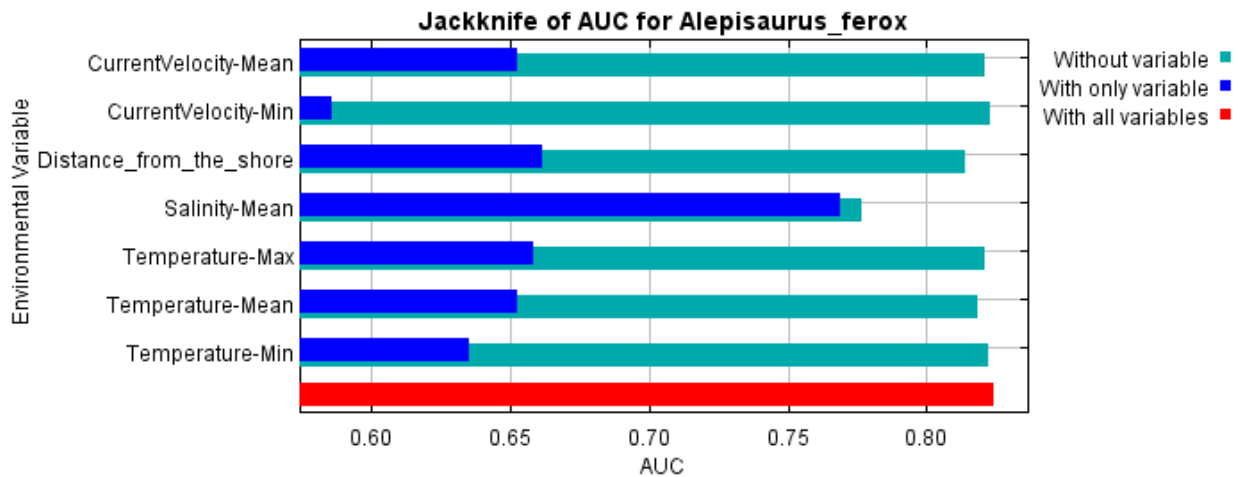


Fig. 4 Jackknife test showing the AUC values when a variable is used in isolation or the variable is excluded from the model

4.2.1.2. Predicted distribution

The predicted current distribution is mainly concentrated in the Western Indian Ocean close to Madagascar and western coast of Madagascar, East coast of Africa, Southern part of Arabian Sea and Bay of Bengal *etc.* with > 75% probability. The predicted distribution for 2040-2050 is concentrated in the same areas as that of the current distribution but the probability of distribution increases for RCP 4.5 with probability > 85% and further rises from RCP 6.0 to 8.5 with probability 50% to 70% (Fig. 39). The extent also shows a gradual increase. The AUC values for RCP 4.5, 6.0 and 8.5 are 0.825 (SD 0.009), 0.831 (SD 0.014) and 0.816 (SD 0.007) respectively (Fig. 4). Salinity mean shows the highest test gain when used in isolation among all the other environmental variables. It is also the one environmental variable which has the maximum percent contribution in both RCPs. The predicted distribution for 2090-2100 shows an abrupt rise in the extent as well as in the probability of distribution (50-70%). The AUC values for RCP 4.5, 6.0 and 8.5 are 0.823 (SD 0.011), 0.824 (SD 0.011) and 0.819 (SD 0.012) respectively (Fig. 4)

4.2.2. *Spratelloides delicatulus* (Bennett, 1832)

Kingdom	Phylum	Class	Order	Family	Genus	Species
Animalia	Chordata	Actinopterygii	Clupeiformes	Clupeidae	<i>Spratelloides</i>	<i>delicatulus</i>

4.2.2.1. Model Evaluation

The area under the curve value for the model is 0.843, with standard deviation is 0.100. The model prediction for the current distribution shows distance from the shore as the greatest percentage contributor with value 45.9 and permutation importance 42.3. (Table 2). Current

velocity mean, temperature minimum, salinity mean, maximum temperature, mean temperature and current velocity minimum contribute 36.4 %, 0.1%, 0.9%, 16.7%, 0%, and 0% respectively Jackknife test reveals that distance from the shore has the highest gain among all parameters when used in isolation (Fig. 5).

Variable	Percent contribution	Permutation importance
Distance from the shore	45.9	42.3
Current Velocity Mean	36.4	28.1
Temperature Min	0.1	0.2
Salinity Mean	0.9	1.8
Temperature Mean	0	0
Current Velocity Min	0	0
Temperature Max	16.7	27.7

Table 2 Table showing the percentage contribution and permutation importance of each environmental variable for the predicted current distribution of *Spratelloides delicatulus*

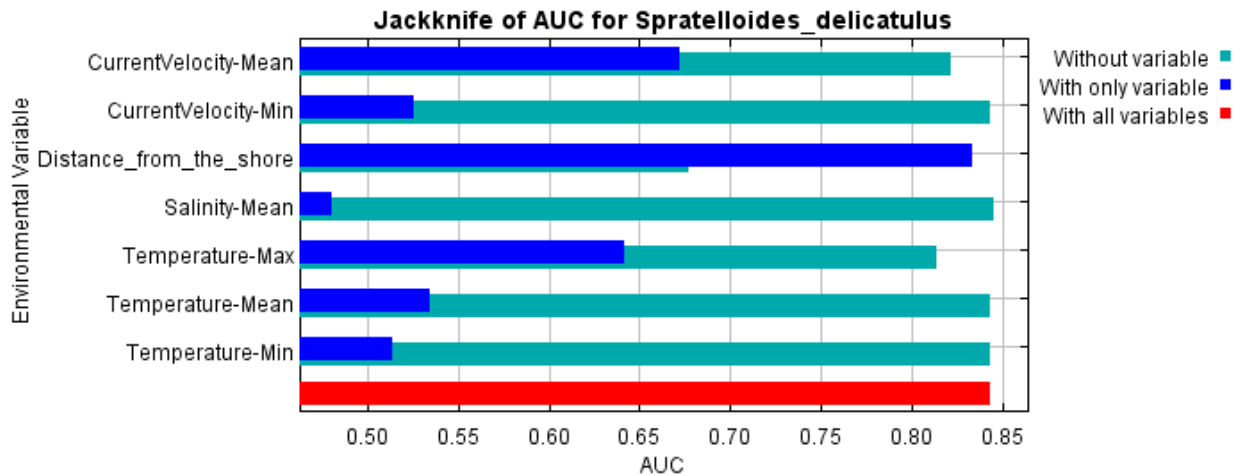


Fig. 5 Jackknife test showing the AUC values when a variable is used in isolation or the variable is excluded from the model

4.2.2.2. Predicted distribution

The predicted current distribution is mainly concentrated in the Western coast of India, north western coast of Srilanka, western coast of Sumatra, north western and north eastern coast of Madagascar and along the Oman coast with probability of distribution 85 to 92 %. The predicted distribution for 2040-2050 is concentrated in the same areas as that of the current distribution but the probability of distribution decreased in RCP 4.5 whereas in RCP 6 of the same decade it regained the distribution similar to current prediction. The prediction of RCP 8.5 showed a very extensive distribution with the species also occupying the coast of Bay of Bengal along the Myanmar and Bangladesh coast, the entire Oman coast, the Persian Gulf and Gulf of Oman and Red sea. (Fig. 41). The extent also shows a considerable increase in year 2040-50 RCP 8.5. The AUC values for RCP 4.5, 6.0 and 8.5 are 0.807 (SD 0.079), 0.774 (SD 0.121) and 0.784 (SD 0.088) respectively (Fig. 40). Distance from the shore shows the highest test gain when used in isolation among all the other environmental variables. It is also the one environmental variable which has the maximum percent contribution in both RCPs. The predicted distribution for 2090-2100 shows a further decline in the extent as well as in the probability of distribution from RCP 4.5 to RCP 8.5 compared to the present prediction as well the RCP scenarios of 2040-50 decade (50-70%). The species considerably reduced its probability of distribution in western coast of India, western Sumatra coast and coast of Madagascar. The AUC values for RCP 4.5, 6.0 and 8.5 are 0.843 (SD 0.052), 0.801 (SD 0.101) and 0.781 (SD 0.094) respectively (Fig. 40).

4.2.3. *Sardinella longiceps* Valenciennes, 1847

Kingdom	Phylum	Class	Order	Family	Genus	Species
Animalia	Chordata	Actinopterygii	Clupeiformes	Clupeidae	<i>Sardinella</i>	<i>longiceps</i>

4.2.3.1. Model Evaluation

The area under the curve value for the model is 0.990 with 0.009 standard deviation (Fig. 42). The model prediction for the current distribution shows distance from the shore as the greatest percentage contributor with value 62.7 and permutation importance 92.1. Current velocity mean, temperature minimum, salinity mean, maximum temperature, mean temperature and current velocity minimum contribute 2.4%, 6.3%, 6.3%, 5%, 15.9% and 1.3% respectively (Table 3). Jackknife test reveals that distance from the shore has the highest gain among all parameters when used in isolation (Fig. 6).

Variable	Percent contribution	Permutation importance
Distance from the shore	62.7	92.1
Current Velocity Mean	2.4	0.2
Temperature Min	6.3	0.3
Salinity Mean	6.3	2
Temperature Mean	15.9	2.1
Current Velocity Min	1.3	1.9
Temperature Max	5	1.4

Table 3 Table showing the percentage contribution and permutation importance of each environmental variable for the predicted current distribution of *Sardinella longiceps*

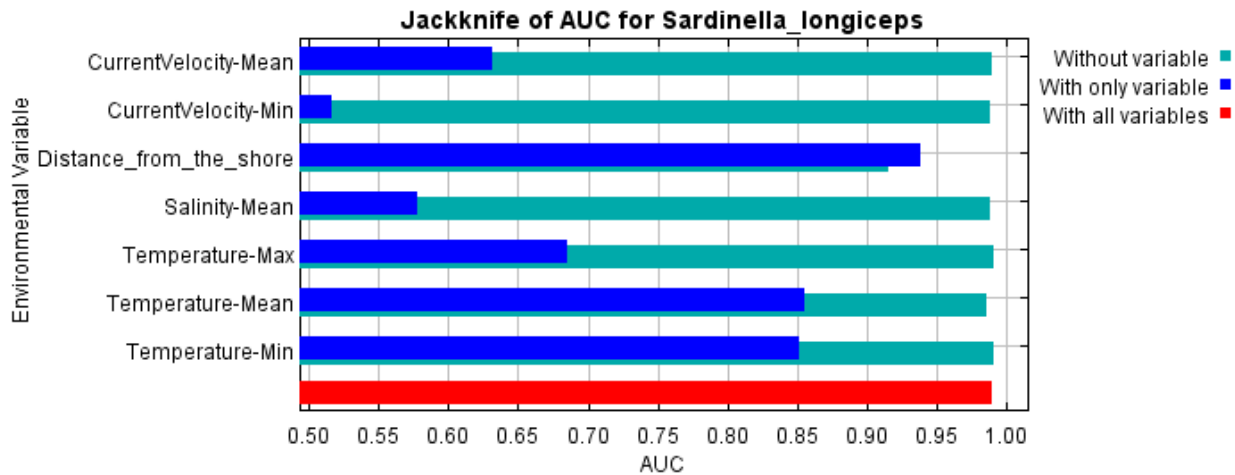


Fig. 6 Jackknife test showing the AUC values for *S. longiceps* when a variable is used in isolation or the variable is excluded from the model

4.2.3.2. Predicted distribution

The predicted current distribution is mainly concentrated in the Western and central coast of India with a probability for the distribution of the species probability of 95- 100%. The eastern coast of Africa, Gulf of Oman and Srilankan coast has a distribution of 60-85% (Fig. 43). The predicted distribution for 2040-2050 shows that in RCP 4.5, the species distribution is concentrated in eastern coast of Africa and Northwestern coast of Madagascar with the same pattern observed in western Indian coast. During RCP 6 of this decade, the eastern Africa and western Madagascar coast shows an increase in the species whereas the concentration in Indian coast is considerably diminished. Under RCP 8.5 of this decade, the species distribution diminishes throughout the northern Indian Ocean. The AUC values for RCP 4.5, 6.0 and 8.5 are 0.988 (SD 0.006), 0.990 (SD 0.005) and 0.984 (SD 0.008) respectively (Fig. 42). Distance from the shore shows the highest test gain when used in isolation among all the other environmental variables. It is also the one environmental variable which has the maximum percent contribution in both RCPs. The predicted distribution of the RCP 4.5 of decade 2090-100 shows the species might regain its distribution in eastern African coast similar to that of RCP 6 of decade 2040-50

decade with an added distribution in the Gujarat coast of India. The pattern is retained in RCP 6 of the decade 2090-2100 but under RCP 8.5 of 2090-2100, it is seen that the distribution of *Sardinella longiceps* above 90% probability is highly restricted only to the western Gujarat coast of India. The AUC values for RCP 4.5, 6.0 and 8.5 are 0.990 (SD 0.007), 0.984 (SD 0.009) and 0.985 (SD 0.011) respectively (Fig. 42)

4.2.4. *Stolephorus indicus* (van Hasselt, 1823)

Kingdom	Phylum	Class	Order	Family	Genus	Species
Animalia	Chordata	Actinopterygii	Clupeiformes	Engraulidae	<i>Stolephorus</i>	<i>indicus</i>

4.2.4.1. Model Evaluation

The area under the curve value for the model is 0.958 with 0.023 standard deviation (Fig. 44). The model prediction for the current distribution shows Distance from shore has the greatest percentage contributor with value 73 and permutation importance 85.3. Temperature minimum temperature mean and salinity mean contribute 9.2%, 1.8% and 9.1% respectively (Table 4). Jackknife test reveals that Distance from shore has the highest gain among all parameters when used in isolation (Fig. 7).

Variable	Percent contribution	Permutation importance
Distance from the shore	73	85.3
Current Velocity Mean	4.7	1.8
Temperature Min	9.2	3.7
Salinity Mean	9.1	6.6
Temperature Mean	1.8	0.5
Current Velocity Min	1.7	1.3
Temperature Max	0.5	0.7

Table 4 Table showing the percentage contribution and permutation importance of each environmental variable for the predicted current distribution of *Stolephorus indicus*

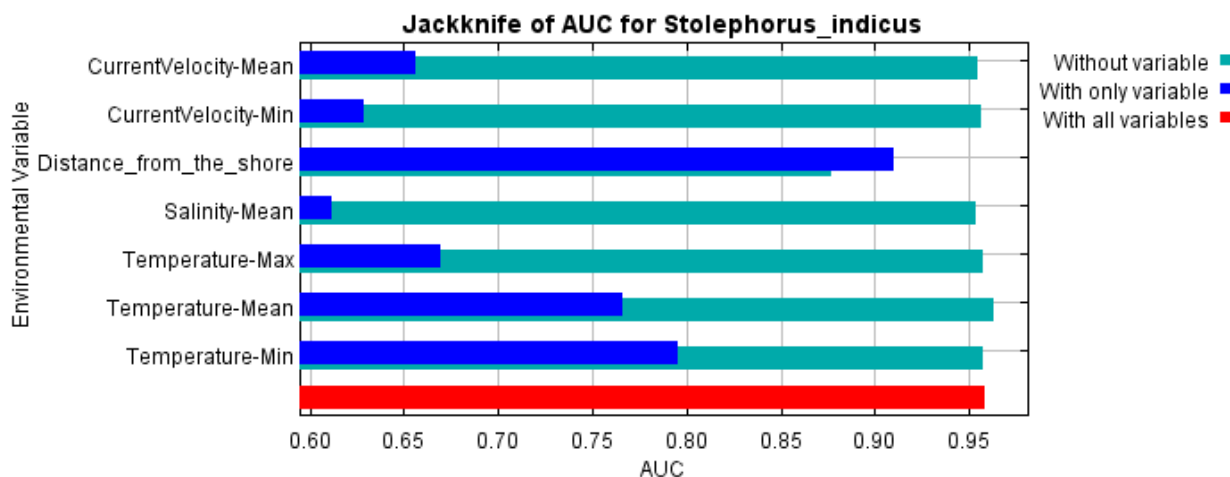


Fig. 7 Jackknife test showing the AUC values of *S. indicus* when a variable is used in isolation or the variable is excluded from the model

4.2.4.2. Predicted distribution

The predicted current distribution is mainly concentrated in the eastern and Western coast of India, eastern coast of Africa, western Madagascar, Andaman Sea, Red sea, Sumatra coast *etc.* with > 71% probability (Fig. 45). The predicted distribution for 2040-2050 is concentrated in the same areas as that of the current distribution but the probability of distribution decreases from RCP 4.5, 6.0 to RCP 8.5 with probability 50% to 70%. The extent also shows a gradual

decrease. The AUC values for RCP 4.5, 6.0 and 8.5 are 0.967(0.017), 0.964 (SD 0.021) and 0.957 (SD 0.030) respectively (Fig. 44). Distance from shore shows the highest test gain when used in isolation among all the other environmental variables. It is also the one environmental variable which has the maximum percent contribution in both RCPs. The predicted distribution for 2090-2100 shows a further decline in the extent as well as in the probability of distribution (50-70%). The AUC values for RCP 4.5, 6.0 and 8.5 are 0.865(0.289), 0.958 (SD 0.044) and 0.961 (SD 0.022) respectively (Fig. 44)

4.2.5. *Uraspis secunda* (Poey, 1860)

Kingdom	Phylum	Class	Order	Family	Genus	Species
Animalia	Chordata	Actinopterygii	Perciformes	Carangidae	<i>Uraspis</i>	<i>secunda</i>

4.2.5.1. Model Evaluation

The area under the curve value for the model is 0.914 with 0.018 standard deviation (Fig. 46). The model prediction for the current distribution shows salinity mean as the greatest percentage contributor with value 47.1 and permutation importance 52.8. Temperature mean, current velocity mean, temperature-min contribute 21.3%, 11.4% and 9.6% respectively (Table 5). Jackknife test reveals that Salinity mean has the highest gain among all parameters when used in isolation (Fig. 8).

Variable	Percent contribution	Permutation importance
Salinity-Mean	47.1	52.8
Temperature-Mean	21.3	23.3
CurrentVelocity-Mean	11.4	6.2
Temperature-Min	9.6	5.9
Temperature-Max	4	5
Distance from the shore	3.3	5.2
Current Velocity Min	3.2	1.6

Table 5 Table showing the percentage contribution and permutation importance of each environmental variable for the predicted current distribution of *Uraspis secunda*

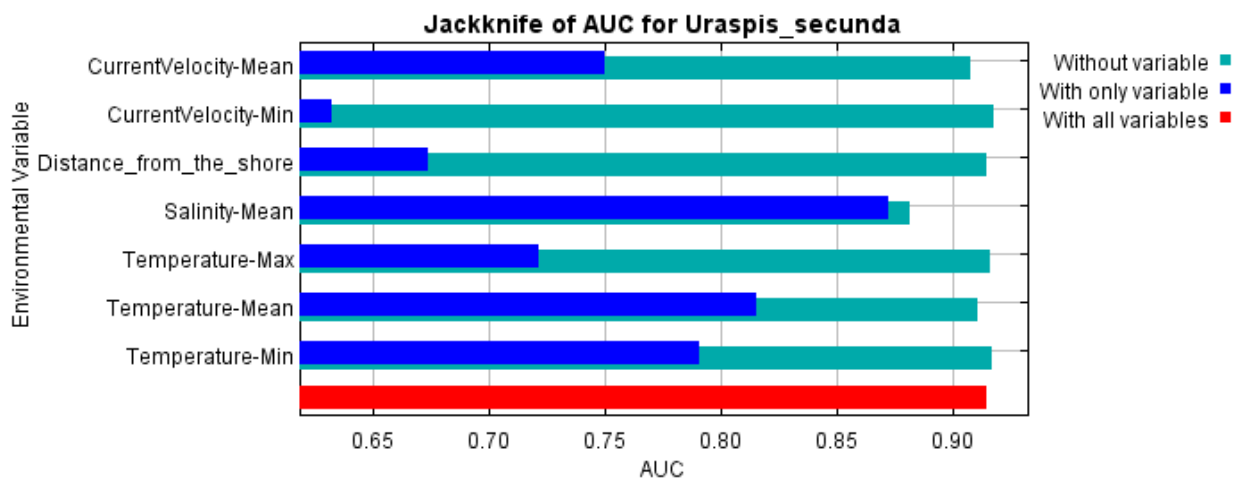


Fig. 8 Jackknife test showing the AUC values of *U. secunda* when a variable is used in isolation or the variable is excluded from the model

4.2.5.2. Predicted distribution

The predicted current distribution is mainly concentrated in a small region in the Western coast of Madagascar with >85% and also along western Indian Ocean close to Madagascar with 75% probability (Fig. 45). The predicted distribution for 2040-2050 is concentrated in the same areas as that of the current distribution but the probability of distribution decreases from RCP 6.0 to RCP 8.5 with probability 50% to 75%. The extent also shows a gradual decrease. The

AUC values for RCP 4.5, RCP 6.0 and 8.5 are 0.909 (SD 0.025), 0.918 (SD 0.012) and 0.927 (SD 0.013) respectively (Fig. 46). Salinity mean shows the highest test gain when used in isolation among all the other environmental variables. It is also the one environmental variable which has the maximum percent contribution in both RCPs. The predicted distribution for 2090-2100 shows a further decline in the extent as well as in the probability of distribution (50-70%). The AUC values for RCP 4.5, RCP 6.0 and 8.5 are 0.920 (SD 0.017), 0.902 (SD 0.017) and 0.916 (SD 0.013) respectively (Fig. 46)

4.2.6. *Seriola rivoliana* Valenciennes, 1833

Kingdom	Phylum	Class	Order	Family	Genus	Species
Animalia	Chordata	Actinopterygii	Perciformes	Carangidae	<i>Seriola</i>	<i>rivoliana</i>

4.2.6.1. Model Evaluation

The area under the curve value for the model is 0.901 with 0.022 standard deviation (Fig. 48). The model prediction for the current distribution shows Salinity-Mean as the greatest percentage contributor with value 46.5 and permutation importance 46.1. Current Velocity-Mean, Temperature-Min and Mean temperature contribute 18.6%, 9.8% and 9.4% respectively (Table 6). Jackknife test reveals that Salinity-Mean has the highest gain among all parameters when used in isolation (Fig. 9).

Variable	Percent contribution	Permutation importance
Salinity-Mean	46.5	46.1
Current Velocity-Mean	18.6	15.6
Temperature-Min	9.8	11
Temperature-Mean	9.4	13.4
Temperature-Max	7.8	6.2
Distance from the shore	4.7	5.2
Current Velocity-Min	3.2	2.5

Table 6 Table showing the percentage contribution and permutation importance of each environmental variable for the predicted current distribution of *Seriola rivoliana*

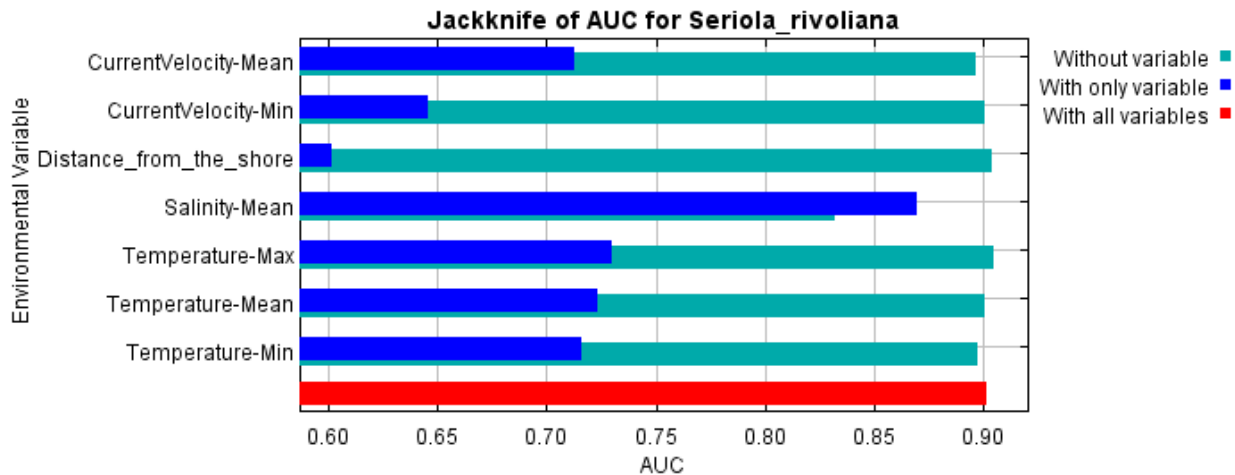


Fig. 9 Jackknife test showing the AUC values of *Seriola rivoliana* when a variable is used in isolation or the variable is excluded from the model

4.2.6.2. Predicted distribution

The predicted current distribution is mainly concentrated in the Western Indian Ocean close to Madagascar and western coast of Madagascar with > 75% probability (Fig. 49). The predicted distribution for 2040-2050 is concentrated in the same areas as that of the current distribution but the probability of distribution decreases from RCP 6.0 to RCP 8.5 with probability 50% to 75%. The extent also shows a gradual decrease. The AUC values for RCP 4.5, RCP 6.0 and 8.5

are 0.893 (SD 0.019), 0.895 (SD 0.007) and 0.890 (SD 0.026) respectively (Fig. 48). Salinity mean shows the highest test gain when used in isolation among all the other environmental variables. It is also the one environmental variable which has the maximum percent contribution in both RCPs. The predicted distribution for 2090-2100 shows a further decline in the extent as well as in the probability of distribution (50-70%). The AUC values for RCP 4.5, RCP 6.0 and 8.5 are 0.904 (SD 0.020), 0.896 (SD 0.018) and 0.889 (SD 0.027) respectively (Fig. 48).

4.2.7. *Megalaspis cordyla* (Linnaeus, 1758)

Kingdom	Phylum	Class	Order	Family	Genus	Species
Animalia	Chordata	Actinopterygii	Perciformes	Carangidae	<i>Megalaspis</i>	<i>cordyla</i>

4.2.7.1. Model Evaluation

The area under the curve value for the model is 0.959 with 0.014 standard deviation (Fig. 50). The model prediction for the current distribution shows distance from the shore as the greatest percentage contributor with value 93.3 and permutation importance 92. Current Velocity-Mean, current velocity-min and temperature-max contribute 5.2%, 1.2% and 0.3% respectively (Table 7). Jackknife test reveals that Distance from the shore has the highest gain among all parameters when used in isolation (Fig. 10).

Variable	Percent contribution	Permutation importance
----------	----------------------	------------------------

Distance from the shore	93.3	92
Current Velocity-Mean	5.2	6.2
Current Velocity-Min	1.2	0.2
Temperature-Max	0.3	1.5
Temperature-Min	0	0.1
Temperature-Mean	0	0
Salinity-Mean	0	0

Table 7 Table showing the percentage contribution and permutation importance of each environmental variable for the predicted current distribution of *Megalaspis cordyla*

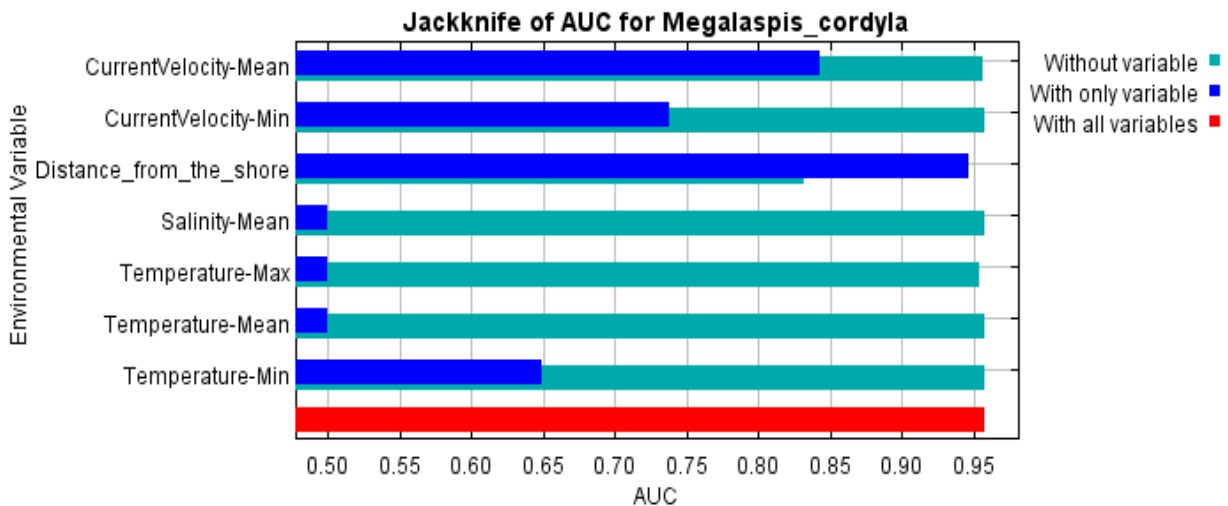


Fig. 10 Jackknife test showing the AUC values of *Megalaspis cordyla* when a variable is used in isolation or the variable is excluded from the model

4.2.7.2. Predicted distribution

The predicted current distribution is mainly concentrated in the Western and Eastern coast of India, coast of Burma, Thailand, Malaysia Madagascar, Red sea *etc.* with > 85% probability (Fig. 51). The predicted distribution for 2040-2050 is concentrated in the same areas as that of the current distribution but the probability of distribution decreases from RCP 6.0 to

RCP 8.5 with probability 50% to 75%. The extent also shows a gradual decrease. The AUC values for RCP 4.5, RCP 6.0 and 8.5 are 0.950 (SD 0.013), 0.957 (SD 0.014) and 0.948 (SD 0.021) respectively (Fig. 50). Distance from the shore shows the highest test gain when used in isolation among all the other environmental variables. It is also the one environmental variable which has the maximum percent contribution in both RCPs. The predicted distribution for 2090-2100 shows a further decline in the extent as well as in the probability of distribution (50-70%). The AUC values for RCP 4.5, RCP 6.0 and 8.5 are 0.957 (SD 0.016), 0.957 (SD 0.016) and 0.963 (SD 0.019) respectively (Fig. 50)

4.2.8. *Elagatis bipinnulata* (Quoy & Gaimard, 1825)

Kingdom	Phylum	Class	Order	Family	Genus	Species
Animalia	Chordata	Actinopterygii	Perciformes	Carangidae	<i>Elagatis</i>	<i>bipinnulata</i>

4.2.8.1. Model Evaluation

The area under the curve value for the model is 0.913 with 0.008 standard deviation (Fig. 52). The model prediction for the current distribution shows the salinity mean as the greatest percentage contributor with value 56.1 and permutation importance 56.1. Mean temperature, maximum temperature and salinity contribute 13.3%, 8.2% and 3% respectively (Table 8). Jackknife test reveals that salinity mean has the highest gain among all parameters when used in isolation (Fig. 11).

Variable	Percent contribution	Permutation importance
Distance from the shore	4.2	4.8
Current Velocity Mean	9.4	4.6
Temperature Min	11.9	11.3
Salinity Mean	56.1	56.1
Temperature Mean	15.4	18.9
Current Velocity Min	0.5	0.5
Temperature Max	2.5	3.7

Table 8 Table showing the percentage contribution and permutation importance of each environmental variable for the predicted current distribution of *Elagatis bipinnulata*

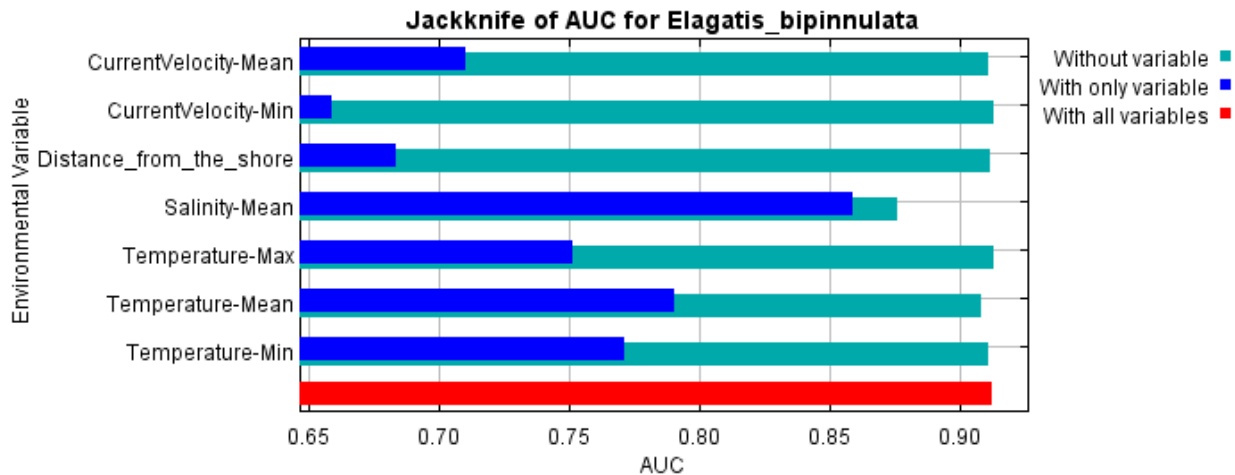


Fig. 11 Jackknife test showing the AUC values of *Elagatis bipinnulata* when a variable is used in isolation or the variable is excluded from the model

4.2.8.2. Predicted distribution

The predicted current distribution is mainly concentrated in the south west coast of India and east coast of Africa to Madagascar with > 75% probability (Fig. 53). The predicted distribution for 2040-2050 is concentrated in the same areas as that of the current distribution but the probability of distribution decreases from RCP4.5 to 6.0 and shows a slight increase in RCP 8.5 with probability 50% to 75%. The extent also shows a gradual decrease. The AUC

values for RCP4.5, 6.0 and 8.5 are 0.912 (SD 0.007), 0.911(SD 0.006) and 0.912 (SD 0.008) respectively (Fig. 52). Salinity mean shows the highest test gain when used in isolation among all the other environmental variables. It is also the one environmental variable which has the maximum percent contribution in both RCPs. The predicted distribution for 2090-2100 shows a further decline in the extent as well as in the probability of distribution (50-70%). The AUC values for RCP4.5, 6.0 and 8.5 are 0.911 (SD 0.005), 0.0912(SD 0.006) and 0.913 (SD 0.011) respectively (Fig. 52)

4.2.9. *Decapterus macarellus* (Cuvier, 1833)

Kingdom	Phylum	Class	Order	Family	Genus	Species
Animalia	Chordata	Actinopterygii	Perciformes	Carangidae	<i>Decapterus</i>	<i>macarellus</i>

4.2.9.1. Model Evaluation

The area under the curve value for the model is 0.945 with 0.011 standard deviation (Fig. 54). The model prediction for the current distribution shows salinity mean as the greatest percentage contributor with value 42.8 and permutation importance 43.3. Mean temperature, maximum temperature and current velocity contribute 23.5%, 5.4% and 7.4% respectively (Table 9). Jackknife test reveals that Salinity mean has the highest gain among all parameters when used in isolation (Fig. 2).

Variable	Percent contribution	Permutation importance
Distance from the shore	8.9	9.4
Current Velocity Mean	7.4	5.6
Temperature Min	11.2	9
Salinity Mean	42.8	43.3
Temperature Mean	23.5	28.1
Current Velocity Min	0.8	1.3
Temperature Max	5.4	3.3

Table 9 Table showing the percentage contribution and permutation importance of each environmental variable for the predicted current distribution of *Decapterus macarellus*

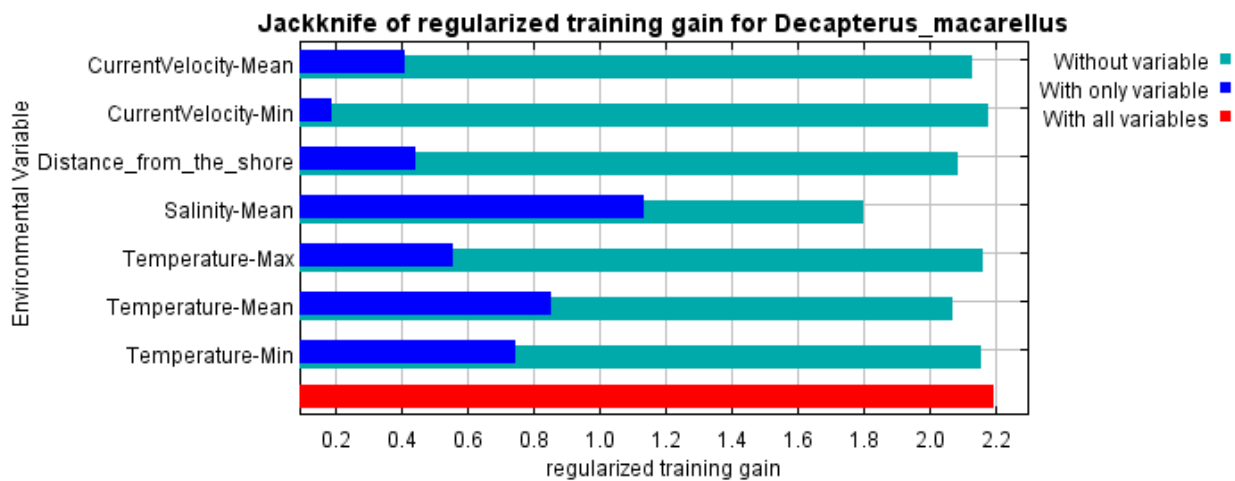


Fig. 12 Jackknife test showing the AUC values of *Decapterus macarellus* when a variable is used in isolation or the variable is excluded from the model

4.2.9.2. Predicted distribution

The predicted current distribution is mainly concentrated in the Western coast of Africa near Madagascar with > 71% probability (Fig. 55). The predicted distribution for 2040-2050 is concentrated in the same areas as that of the current distribution but the probability of distribution decreases from RCP 4.5 to RCP 8.5. The AUC values for RCP 4.5, 6.0 and 8.5 are

0.941(SD 0.009) 0.938 (SD 0.008) and 0.943 (SD 0.015) respectively (Fig. 54). Salinity mean shows the highest test gain when used in isolation among all the other environmental variables. It is also the one environmental variable which has the maximum percent contribution in both RCPs. The predicted distribution for 2090-2100 shows a further decline in the extent as well as in the probability of distribution (50-70%). The AUC values for RCP 4.5, 6.0 and 8.5 are 0.936 (SD 0.011) 0.932 (SD 0.013) and 0.937 (SD 0.066) respectively (Fig. 54)

4.2.10. *Caranx sexfasciatus* Quoy & Gaimard, 1825

Kingdom	Phylum	Class	Order	Family	Genus	Species
Animalia	Chordata	Actinopterygii	Perciformes	Carangidae	<i>Caranx</i>	<i>sexfasciatus</i>

4.2.10.1. Model Evaluation

The area under the curve value for the model is 0.839 with 0.032 standard deviation (Fig. 56). The model prediction for the current distribution shows distance from the shore as the greatest percentage contributor with value 28.3 and permutation importance 32.8. Salinity mean, mean temperature, maximum temperature, minimum temperature, current velocity mean and current velocity minimum contribute 23.8 %, 17.9%, 14.7%, 6.5%, 6.3% and 2.6% respectively (Table 10). Jackknife test reveals that Salinity- mean has the highest gain among all parameters when used in isolation (Fig. 12).

Variable	Percent contribution	Permutation importance
Distance from the shore	28.3	32.8
Salinity-Mean	23.8	24.4
Temperature-Mean	17.9	11
Temperature-Max	14.7	5.1
Temperature-Min	6.5	13
Current Velocity-Mean	6.3	6.5
Current Velocity-Min	2.6	7.4

Table 9 Table showing the percentage contribution and permutation importance of each environmental variable for the predicted current distribution of *Caranx sexfasciatus*

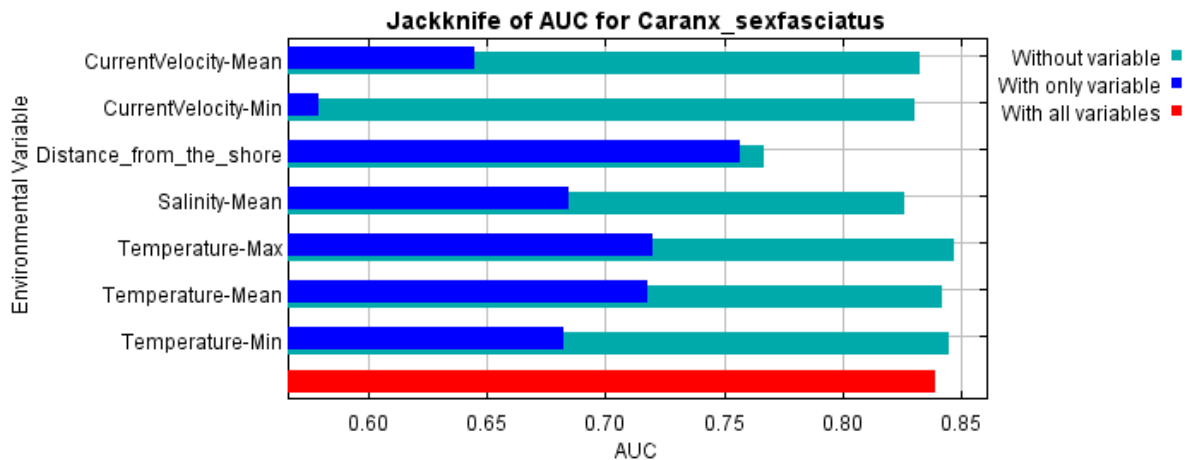


Fig. 13 Jackknife test showing the AUC values of *Caranx sexfasciatus* when a variable is used in isolation or the variable is excluded from the model

4.2.10.2. Predicted distribution

The predicted current distribution is mainly concentrated in the western coast of India, Western coast of Madagascar, the part of Indian Ocean which is west to the Madagascar, Southern part of Arabian Sea, *etc.* with > 75% probability (Fig. 57). The predicted distribution for 2040-2050 is concentrated in the same areas as that of the current distribution but the probability of distribution decreases from RCP 6.0 to RCP 8.5 with probability 50% to 65. The extent also shows a gradual decrease. The AUC values for RCP 4.5, 6.0 and 8.5 are 0.838 (SD

0.052), 0.855 (SD 0.038) and 0.810 (SD 0.087) respectively (Fig. 56). Distance from the shore shows the highest test gain when used in isolation among all the other environmental variables. It is also the one environmental variable which has the maximum percent contribution in both RCPs. The predicted distribution for 2090-2100 shows a further decline in the extent as well as in the probability of distribution (50-70%). The AUC values for RCP 4.5, 6.0 and 8.5 are 0.846 (SD 0.033), 0.854 (SD 0.035) and 0.849 (SD 0.047) respectively (Fig. 56)

4.2.11. *Coryphaena hippurus* Linnaeus, 1758

Kingdom	Phylum	Class	Order	Family	Genus	Species
Animalia	Chordata	Actinopterygii	Perciformes	Coryphaenidae	<i>Coryphaena</i>	<i>hippurus</i>

4.2.11.1. Model Evaluation

The area under the curve value for the model is 0.873 with 0.019 standard deviation (Fig. 58). The model prediction for the current distribution shows salinity mean as the greatest percentage contributor with value 35.2 and permutation importance 41.4. Minimum temperature, maximum temperature, current velocity mean, temperature mean, distance from the shore and current velocity minimum contribute 20.8%, 11.6%, 11.5%, 10.7%, 9.3% and 0.9% respectively (Table 11). Jackknife test reveals that salinity mean has the highest gain among all parameters when used in isolation (Fig. 13).

Variable	Percent contribution	Permutation importance
Salinity Mean	35.2	41.4
Temperature Min	20.8	28.1
Temperature Max	11.6	0.9
Current Velocity Mean	11.5	2.9
Temperature Mean	10.7	23.8
Distance from the shore	9.3	2.8
Current Velocity Min	0.9	0.1

Table 10 Table showing the percentage contribution and permutation importance of each environmental variable for the predicted current distribution of *Coryphaena hippurus*

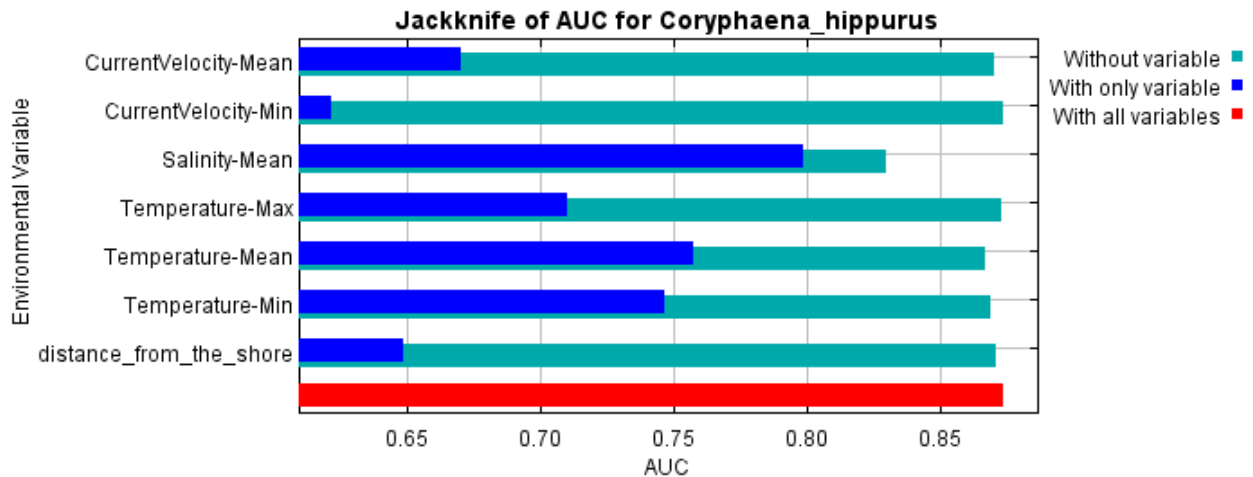


Fig. 14 Jackknife test showing the AUC values of *Coryphaena hippurus* when a variable is used in isolation or the variable is excluded from the model

Predicted distribution

The predicted current distribution is mainly concentrated in the south western coast of India, western coast of Africa near Madagascar with > 77% probability (Fig. 59). The predicted distribution for 2040-2050 is concentrated in the same areas as that of the current distribution but the probability of distribution decreases from RCP 6.0 to RCP 8.5 with probability 50% to 75%. The extent also shows a gradual decrease. The AUC values for RCP4.5, 6.0 and 8.5 are 0.878 (SD 0.006), 0.879 (SD 0.009) and 0.874 (SD 0.007) respectively (Fig. 58). Salinity mean

shows the highest test gain when used in isolation among all the other environmental variables. It is also the one environmental variable which has the maximum percent contribution in both RCPs. The predicted distribution for 2090-2100 shows an increase in distribution in RCP 4.5 and decline in the extent further. The AUC values for RCP4.5, 6.0 and 8.5 are 0.874 (SD 0.009), 0.878 (SD 0.008) and 0.876 (SD 0.008) respectively (Fig. 58)

4.2.12. *Gempylus serpens* Cuvier, 1829

Kingdom	Phylum	Class	Order	Family	Genus	Species
Animalia	Chordata	Actinopterygii	Perciformes	Gempylidae	<i>Gempylus</i>	<i>serpens</i>

4.2.12.1. Model Evaluation

The area under the curve value for the model is 0.814 with 0.053 standard deviation (Fig. 60). The model prediction for the current distribution shows current velocity minimum as the greatest percentage contributor with value 31 and permutation importance 15.7. salinity Mean, distance from the shore, temperature maximum, temperature mean , temperature minimum, and current velocity mean contribute 22.7%,19.7%, 9.7%, 9.4%, 6.2% and 1.3% respectively (Table 12). Jackknife test reveals that salinity mean has the highest gain among all parameters when used in isolation (Fig. 15).

Variable	Percent contribution	Permutation importance
Current Velocity Min	31	15.7
Salinity Mean	22.7	30.1
Distance from the shore	19.7	25
Temperature Max	9.7	0.5
Temperature Mean	9.4	21.4
Temperature Min	6.2	3.6
Current Velocity Mean	1.3	3.7

Table 11 Table showing the percentage contribution and permutation importance of each environmental variable for the predicted current distribution of *Gempylus serpens*

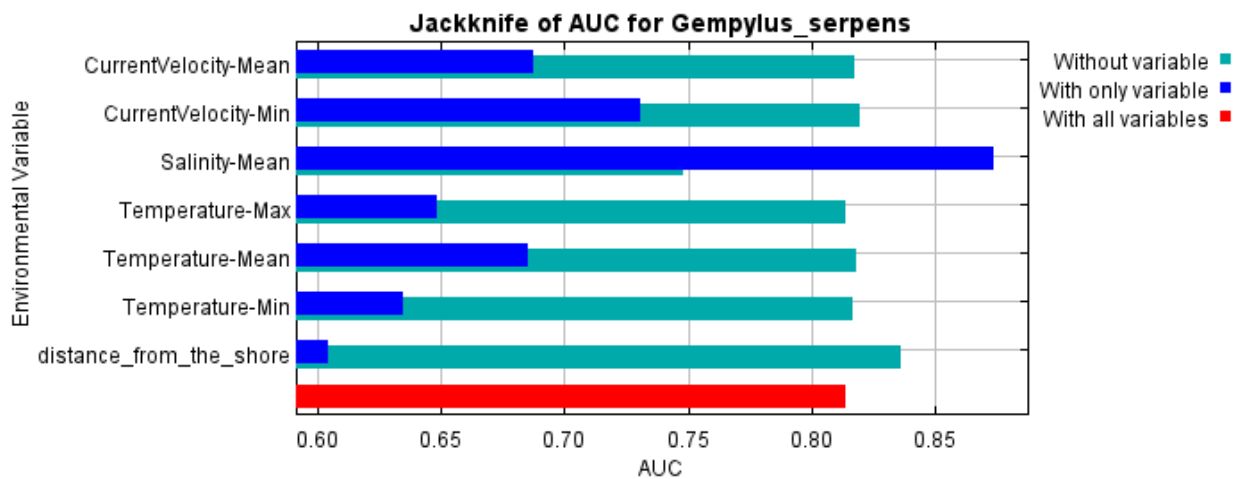


Fig. 15 Jackknife test showing the AUC values of *Gempylus serpens* when a variable is used in isolation or the variable is excluded from the model

4.2.12.2. Predicted distribution

The predicted current distribution is mainly concentrated in the Western coast of Africa, with >75% probability (Fig. 61). The predicted distribution for 2040-2050 is concentrated in the same areas as that of the current distribution but the extent of distribution decreases from RCP 4.5 to RCP 8.5. The AUC values for RCP 4.5, 6.0 and 8.5 are 0.806 (SD 0.070), 0.800 (SD 0.063) and

0.810 (SD 0.087) respectively (Fig. 60). Salinity mean shows the highest test gain when used in isolation among all the other environmental variables. Current velocity is the environmental variable which has the maximum percent contribution in all RCPs. The predicted distribution for 2090-2100 shows a slight increase in the extent. The AUC values for RCP 4.5, 6.0 and 8.5 are 0.788 (SD 0.057), 0.800 (SD 0.63) and 0.751 (SD 0.093) respectively (Fig. 60)

4.2.13. *Istiophorus platypterus* (Shaw, 1792)

Kingdom	Phylum	Class	Order	Family	Genus	Species
Animalia	Chordata	Actinopterygii	Perciformes	Istiophoridae	<i>Istiophorus</i>	<i>platypterus</i>

4.2.13.1. Model Evaluation

The area under the curve value for the model is 0.837 with 0.021 standard deviation (Fig. 62). The model prediction for the current distribution shows salinity mean as the greatest percentage contributor with value 44.8 and permutation importance 40. Current velocity mean, Temperature minimum, Distance from the shore, maximum temperature, mean temperature and current velocity minimum contribute 4.3%, 12.8%, 12%, 18.1%, 7.9% and 0% respectively (Table 13). Jackknife test reveals that salinity mean has the highest gain among all parameters when used in isolation (Fig. 16)

Variable	Percent contribution	Permutation importance
Distance from the shore	12	12.6
Current Velocity Mean	4.3	3.2
Temperature Min	12.8	16.6
Salinity Mean	44.8	40
Temperature Mean	7.9	20.2
Current Velocity Min	0	0.4
Temperature Max	18.1	7

Table 12 Table showing the percentage contribution and permutation importance of each environmental variable for the predicted current distribution of *Istiophorus platypterus*

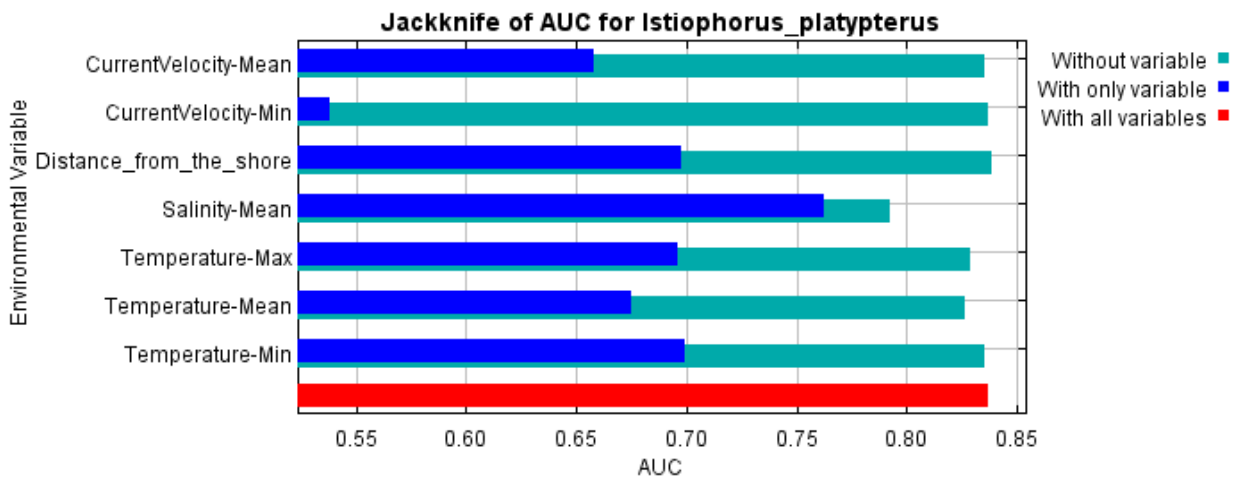


Fig. 16 Jackknife test showing the AUC values of *Istiophorus platypterus* when a variable is used in isolation or the variable is excluded from the model

4.2.13.2. Predicted distribution

The predicted current distribution is mainly concentrated in the Persian Gulf, the eastern coast of Africa, western coast of Madagascar, Gulf of Aden, Red sea, Arabian Sea and towards the north western Indian Ocean with > 50% probability (Fig. 63). The predicted distribution for 2040-2050 is concentrated in the same areas as that of the current distribution but the probability of distribution in Gulf of Aden decreases from RCP 4.5 to RCP 8.5 with probability less than

80 %. The extend of the species is also reduced throughout the eastern African coast with the probability decreasing to almost below 40% in many portions during the RCP 8.5 of this decade. The AUC values for RCP 4.5, 6.0 and 8.5 are 0.846(SD 0.010), 0.837(SD 0.022) and 0.844 (SD 0.012) respectively (Fig. 62). Salinity mean shows the highest test gain when used in isolation among all the other environmental variables. It is also the one environmental variable which has the maximum percent contribution in all RCPs. The predicted distribution for 2090-2100 shows a further decline in the extent of this species throughout the North western Indian Ocean with probability of distribution diminished to less than 40 % in many of the regions. The AUC values for RCP 4.5, 6.0 and 8.5 are 0.851 (SD 0.014), 0.844 (SD 0.011) and 0.842(SD 0.012) respectively (Fig. 62)

4.2.14. *Makaira nigricans* Lacepède, 1802

Kingdom	Phylum	Class	Order	Family	Genus	Species
Animalia	Chordata	Actinopterygii	Perciformes	Istiophoridae	<i>Makaira</i>	<i>nigricans</i>

4.2.14.1. Model Evaluation

The area under the curve value for the model is 0.832 with 0.071 standard deviation (Fig. 64). The model prediction for the current distribution shows Salinity mean as the greatest percentage contributor with value 50.8 and permutation importance 50.4. Temperature minimum, current velocity mean, temperature mean, distance from the shore, maximum temperature and current velocity minimum contribute 31.9%, 11.5%, 3.2%, 1.4%, 0.6% and 0.6% respectively (Table 14). Jackknife test reveals that Salinity mean has the highest gain among all parameters when used in isolation (Fig. 17).

Variable	Percent contribution	Permutation importance
Distance from the shore	1.4	1.5
Current Velocity Mean	11.5	9
Temperature Min	31.9	34.5
Salinity Mean	50.8	50.4
Temperature Mean	3.2	3.2
Current Velocity Min	11.5	9
Temperature Max	0.6	0.4

Table 13 Table showing the percentage contribution and permutation importance of each environmental variable for the predicted current distribution of *Makaira nigricans*

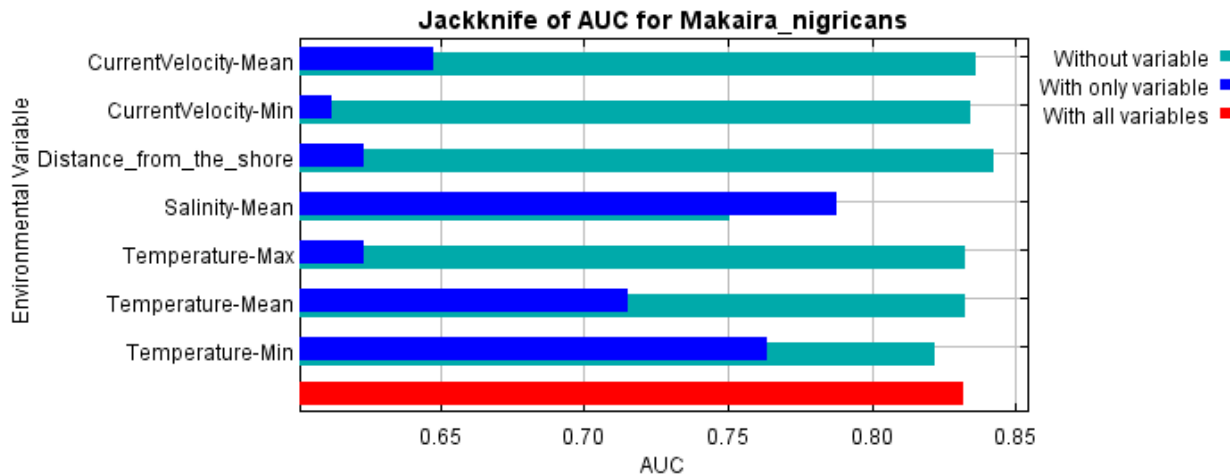


Fig. 17 Jackknife test showing the AUC values of *Makaira nigricans* when a variable is used in isolation or the variable is excluded from the model

4.2.14.2. Predicted distribution

The predicted current distribution is mainly concentrated in the Southwestern parts of Indian Ocean with > 83% probability (Fig. 65). The predicted distribution for 2040-2050 is concentrated in the same areas as that of the current distribution but the probability of distribution decreases from RCP 4.5, RCP 6.0 to RCP 8.5 with probability 67% to 50%. The extent also shows a gradual decrease. The AUC values for RCP 4.5, 6.0 and 8.5 are 0.814 (SD 0.063), 0.868 (SD

0.066) and 0.868 (SD 0.047) respectively (Fig. 64). Salinity mean shows the highest test gain when used in isolation among all the other environmental variables. It is also the one environmental variable which has the maximum percent contribution in both RCPs. The predicted distribution for 2090-2100 shows a further decline in the extent as well as in the probability of distribution (67-33%). The AUC values for RCP 4.5, 6.0 and 8.5 are 0.839 (SD 0.064), 0.821(SD 0.069) and 0.823 (SD 0.077) respectively (Fig. 64).

4.2.15. *Kajikia albida* (Poey, 1860)

Kingdom	Phylum	Class	Order	Family	Genus	Species
Animalia	Chordata	Actinopterygii	Perciformes	Istiophoridae	<i>Kajikia</i>	<i>albida</i>

4.2.15.1. Model Evaluation

The area under the curve value for the model is 0.762 with 0.130 standard deviation (Fig. 66). The model prediction for the current distribution shows current velocity minimum as the greatest percentage contributor with value 65.1 and permutation importance 66.6. Salinity-mean, distance from the shore and minimum temperature contribute 21.4%, 8.9% and 4.6% respectively (Table 15). Jackknife test reveals that Current velocity minimum has the highest gain among all parameters when used in isolation (Fig. 18).

Variable	Percent contribution	Permutation importance
CurrentVelocity Min	65.1	66.6
Salinity Mean	21.4	25.3
Temperature Min	4.64	4.3
Distance from the shore	8.9	3.8
CurrentVelocity Mean	0	0
Temperature Mean	0	0
Temperature Max	0	0

Table 14 Table showing the percentage contribution and permutation importance of each environmental variable for the predicted current distribution of *Kajikia albida*

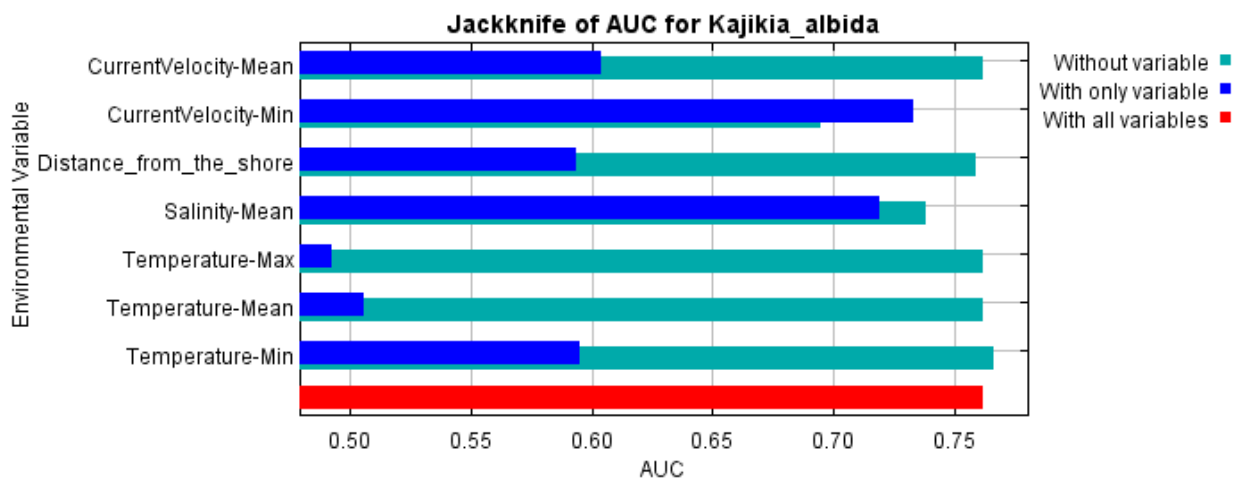


Fig. 18 Jackknife test showing the AUC values of *Kajikia albida* when a variable is used in isolation or the variable is excluded from the model

4.2.15.2. Predicted distribution

The predicted current distribution is mainly concentrated in the Eastern coast of Africa, western and southern part of Arabian Sea, Indian Ocean, Western coast of Madagascar, Eastern coast of India, Red sea *etc.* with > 85% probability (Fig. 67). The predicted distribution for 2040-2050 is concentrated in the same areas as that of the current distribution but the probability of

distribution decreases from RCP 6.0 to RCP 8.5 with probability 50% to 75%. The extent also shows a gradual decrease. The AUC values for RCP 4.5, 6.0 and 8.5 are 0.854 (SD 0.029), 0.792 (SD 0.075) and 0.809 (SD 0.075) respectively (Fig. 66). Current velocity minimum shows the highest test gain when used in isolation among all the other environmental variables. It is also the one environmental variable which has the maximum percent contribution in both RCPs. The predicted distribution for 2090-2100 shows a further decline in the extent as well as in the probability of distribution (50-70%). The AUC values for RCP 4.5, 6.0 and 8.5 are 0.816 (SD0.088), 0.790 (SD 0.075) and 0.795 (SD 0.072) respectively (Fig. 66)

4.2.16. *Istiompax indica* (Cuvier, 1832)

Kingdom	Phylum	Class	Order	Family	Genus	Species
Animalia	Chordata	Actinopterygii	Perciformes	Istiophoridae	<i>Istiompax</i>	<i>indica</i>

4.2.16.1. Model Evaluation

The area under the curve value for the model is 0.850 with 0.019 standard deviation (Fig. 68). The model prediction for the current distribution shows salinity mean as the greatest percentage contributor with value 38.4 and permutation importance 39.3. Minimum temperature, current velocity mean, temperature mean, distance from the shore, maximum temperature and current velocity minimum contribute 22.7%, 13.3%, 9.6%, 8.4%, 6% and 1.6% respectively (Table 16). Jackknife test reveals that salinity mean has the highest gain among all parameters when used in isolation (Fig. 19).

Variable	Percent contribution	Permutation importance
Salinity Mean	38.4	39.3
Temperature Min	22.7	18.7
Current velocity mean	13.3	9.3
Temperature Mean	9.6	18.7
Distance from the shore	8.4	5.8
Temperature Max	6	6.7
Current Velocity Min	1.6	1.5

Table 15 Table showing the percentage contribution and permutation importance of each environmental variable for the predicted current distribution of *Istiompax indica*

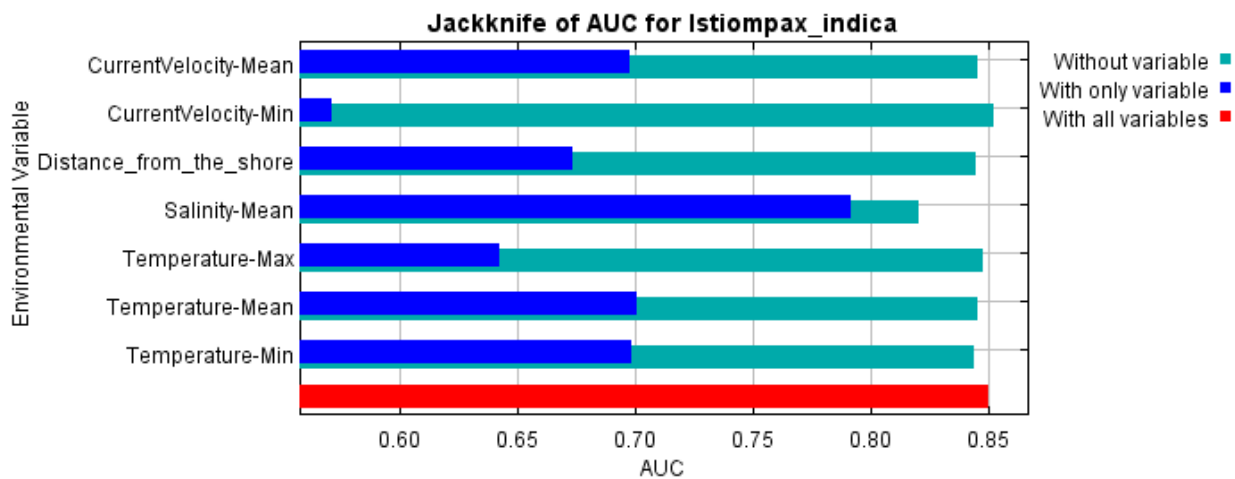


Fig. 19 Jackknife test showing the AUC values of *Istiompax indica* when a variable is used in isolation or the variable is excluded from the model

4.2.16.2. Predicted distribution

The predicted current distribution is mainly concentrated in the south western coast of India, and east Africa near Madagascar with > 85% probability (Fig. 69). The predicted distribution for 2040-2050 is concentrated in the same areas as that of the current distribution but the probability of distribution decreases from RCP 4.5 to RCP 8.5. The extent also shows a

gradual decrease. The AUC values for RCP 4.5, 6.0 and 8.5 are 0.835 (SD 0.014), 0.847 (SD 0.024) and 0.841 (SD 0.013) respectively (Fig. 68). Salinity mean shows the highest test gain when used in isolation among all the other environmental variables. It is also the one environmental variable which has the maximum percent contribution in all RCPs. The predicted distribution for 2090-2100 shows a further decline in the extent as well as in the probability of distribution (50-70%). The AUC values for RCP 4.5, 6.0 and 8.5 are 0.81 (SD 0.018), 0.865 (SD 0.014) and 0.851 (SD 0.024) respectively (Fig. 68).

4.2.17. *Thunnus obesus* (Lowe, 1839)

Kingdom	Phylum	Class	Order	Family	Genus	Species
Animalia	Chordata	Actinopterygii	Perciformes	Scombridae	<i>Thunnus</i>	<i>obesus</i>

4.2.17.1. Model Evaluation

The area under the curve value for the model is 0.814 with 0.005 standard deviation (Fig. 70). The model prediction for the current distribution shows salinity mean as the greatest percentage contributor with value 35.3 and permutation importance 57.8. Current velocity Mean, temperature maximum, distance from the shore, temperature minimum, temperature mean and current velocity minimum contribute 26%, 12.1%, 10.8%, 7.8%, 7.5% and 0.6% respectively (Table 17). Jackknife test reveals that salinity mean has the highest gain among all parameters when used in isolation (Fig. 20).

Variable	Percent contribution	Permutation importance
Distance from the shore	10.8	5.3
Current Velocity Mean	26	2.8
Temperature Min	7.8	4.2
Salinity Mean	35.3	57.8
Temperature Mean	7.5	20
Current Velocity Min	0.6	1
Temperature Max	12.1	8.9

Table 16 Table showing the percentage contribution and permutation importance of each environmental variable for the predicted current distribution of *Thunnus obesus*

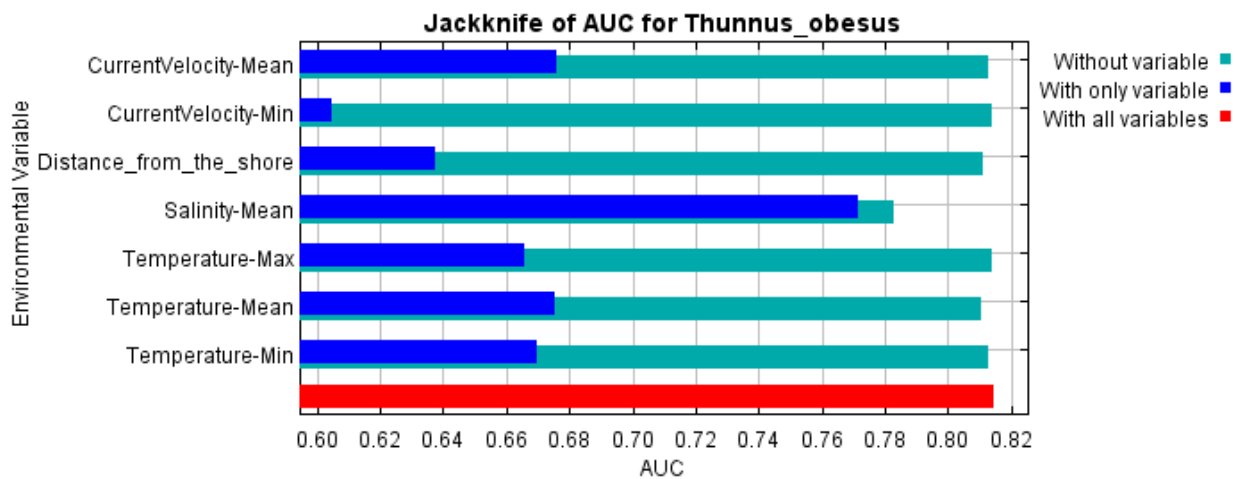


Fig. 20 Jackknife test showing the AUC values of *Thunnus obesus* when a variable is used in isolation or the variable is excluded from the model

4.2.17.2. Predicted distribution

The predicted current distribution is mainly concentrated in the Western coast of Africa and eastern coast of Madagascar with > 85% probability (Fig. 71). The predicted distribution for 2040-2050 is concentrated below the Indian sub-continent but the probability of distribution increased from RCP 4.5 to RCP 8.5 with probability >85% . The AUC values for RCP 4.5, 6.0

and 8.5 are 0.813 (SD 0.007), 0.815 (SD 0.005) and 0.819 (SD 0.006) respectively (Fig. 70). Salinity mean shows the highest test gain when used in isolation among all the other environmental variables. It is also the one environmental variable which has the maximum percent contribution in both RCPs. The predicted distribution for 2090-2100 shows a further increase in the extent as well as in the probability of distribution. The AUC values for RCP4.5, 6.0 and 8.5 are 0.815 (SD 0.006), 0.810 (SD 0.07) and 0.811 (SD 0.004) respectively (Fig. 70)

4.2.18. *Thunnus albacares* (Bonnaterre, 1788)

Kingdom	Phylum	Class	Order	Family	Genus	Species
Animalia	Chordata	Actinopterygii	Perciformes	Scombridae	<i>Thunnus</i>	<i>albacares</i>

4.2.18.1. Model Evaluation

The area under the curve value for the model is 0.787 with 0.007 standard deviation (Fig. 72). The model prediction for the current distribution shows Salinity mean as the greatest percentage contributor with value 57 and permutation importance 51.8. Mean temperature, minimum temperature, current velocity mean, maximum temperature, distance from the shore and current velocity minimum contribute 16.5, 12.1%, 6.8%, 5.2%, 2.1% and 0.3 % respectively (Table 18). Jackknife test reveals that salinity mean has the highest gain among all parameters when used in isolation (Fig. 21).

Variable	Percent contribution	Permutation importance
Distance from the shore	2.1	3.4
Current Velocity Mean	6.8	4.7
Temperature Min	12.1	11.9
Salinity Mean	57	51.8
Temperature Mean	16.5	21.4
Current Velocity Min	0.3	0.5
Temperature Max	5.2	6.3

Table 17 Table showing the percentage contribution and permutation importance of each environmental variable for the predicted current distribution of *Thunnus albacares*

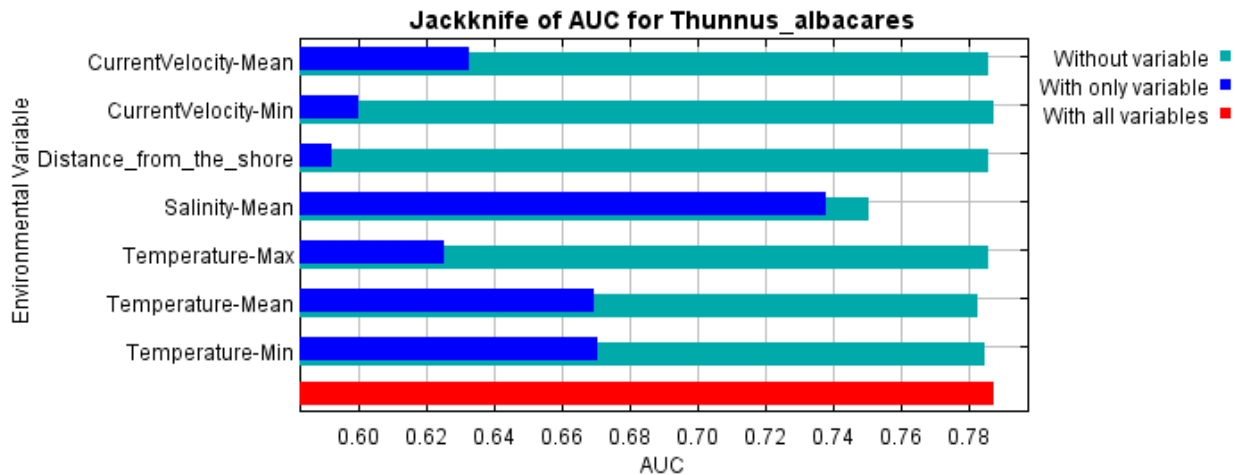


Fig. 21 Jackknife test showing the AUC values of *Thunnus albacares* when a variable is used in isolation or the variable is excluded from the model

Predicted distribution

The predicted current distribution is mainly concentrated in the north western Indian Ocean, Eastern African coast, Gulf of Aden, western coast of Madagascar and in some parts of Western coast of India with a probability greater than 40%. The probability of distribution greater than 85% is seen in the eastern coast of Madagascar, Indian Ocean region above the Madagascar and some portions of Gulf of Aden (Fig. 73). The predicted distribution for 2040-2050 is in the same areas as that of the current distribution but the probability of distribution

increases to a higher level of almost 100% in RCP 4.5 in most regions of the North western Indian Ocean with the first appearance of this species in the Bay of Bengal. The western coast of India also shows a distribution probability of around 85%. During RCP 4.5 and RCP 6, the distribution tends to move towards the region of Indian mainland and in RCP 8.5 of decade 2040-50, the distribution gets restricted to the portion of Indian Ocean located south and south west of Kerala coast. The extent also shows a gradual decrease. The AUC values for RCP 4.5, 6.0 and 8.5 are 0.786 (SD 0.008), 0.788 (SD 0.004) and 0.786 (SD 0.005) respectively (Fig. 72). Salinity mean shows the highest test gain when used in isolation among all the other environmental variables. It is also the one environmental variable which has the maximum percent contribution in both RCPs. The predicted distribution for 2090-2100 shows a further increase in the extent as well as in the probability of distribution as from RCP 4.5 to 8.5, the distribution spread to most of the north western North Indian ocean as well as to the north eastern Indian ocean, more parts of Arabian sea, parts of Gulf of Oman and western Sumatran coast with a distribution probability of 50 to 100%. The AUC values for RCP 4.5, 6.0 and 8.5 are 0.785 (SD 0.004), 0.785 (SD 0.006) and 0.786 (SD 0.005) respectively (Fig. 72)

4.2.19. *Thunnus alalunga* (Bonneterre, 1788)

Kingdom	Phylum	Class	Order	Family	Genus	Species
Animalia	Chordata	Actinopterygii	Perciformes	Scombridae	<i>Thunnus</i>	<i>alalunga</i>

4.2.19.1. Model Evaluation

The area under the curve value for the model is 0.805 with 0.010 standard deviation (Fig. 74). The model prediction for the current distribution shows salinity mean as the greatest percentage contributor with value 52.9 and permutation importance 64.8. Distance from the shore, minimum temperature, maximum temperature, current velocity minimum, current velocity mean and mean temperature contribute 23.1%, 7.2%, 6.7%, 5.9%, 3.4% and 0.8% respectively (Table 19). Jackknife test reveals that salinity mean has the highest gain among all parameters when used in isolation (Fig. 22).

Variable	Percent contribution	Permutation importance
Salinity Mean	52.9	64.8
Distance from the shore	23.1	11.5
Temperature Min	7.2	8.7
Temperature Max	6.7	5.4
Current Velocity Min	5.9	3.6
Current Velocity Mean	3.4	4.2
Temperature Mean	0.8	1.8

Table 18 Table showing the percentage contribution and permutation importance of each environmental variable for the predicted current distribution of Thunnus alalunga

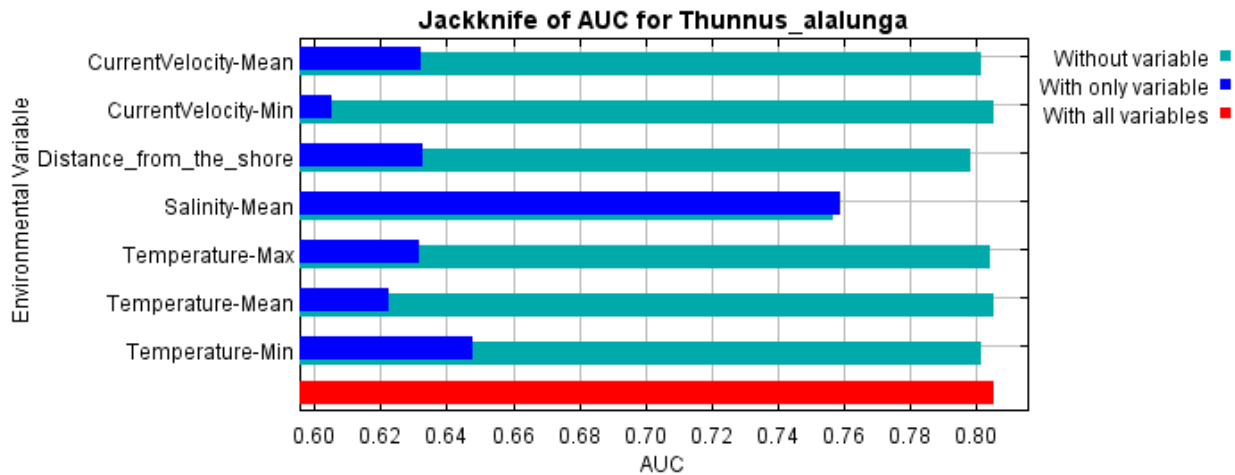


Fig. 22 Jackknife test showing the AUC values of *Thunnus alalunga* when a variable is used in isolation or the variable is excluded from the model

4.2.19.2. Predicted distribution

The predicted current distribution is mainly concentrated in the Southern part of Arabian sea, eastern part of Africa, Indian ocean, Madagascar sea, Southern coast of India *etc.* with > 75% probability (Fig. 75). The predicted distribution for 2040-2050 is concentrated in the same areas as that of the current distribution but the probability of distribution decreases from RCP 6.0 to RCP 8.5 with probability 50 % to 65 % . The extent also shows a gradual decrease. The AUC values for RCP 4.5, 6.0 and 8.5 are 0.815 (SD 0.012), 0.808 (SD 0.012) and 0.812 (SD 0.012) respectively (Fig. 74). Salinity mean shows the highest test gain when used in isolation among all the other environmental variables. It is also the one environmental variable which has the maximum percent contribution in both RCPs. The predicted distribution for 2090-2100 shows a further decline in the extent as well as in the probability of distribution (50-60%) . The AUC values for RCP 4.5, 6.0 and 8.5 are 0.807 (SD 0.013), 0.820 (SD 0.011) and 0.809 (SD 0.011) respectively (Fig. 74).

4.2.20. *Rastrelliger kanagurta* (Cuvier, 1816)

Kingdom	Phylum	Class	Order	Family	Genus	Species
Animalia	Chordata	Actinopterygii	Perciformes	Scombridae	<i>Rastrelliger</i>	<i>kanagurta</i>

4.2.20.1. Model Evaluation

The area under the curve value for the model is 0.906 with 0.024 standard deviation (Fig. 76). The model prediction for the current distribution shows distance from the shore as the greatest percentage contributor with value 84.8 and permutation importance 86.8. The current velocity mean, minimum sea surface temperature, mean salinity, sea surface temperature means, and current velocity minimum contribute 9.9%, 3.1%, 1.1%, 0.5% and 0.4% respectively (Table 20). Jackknife test reveals that distance from the shore has the highest gain among all parameters when used in isolation (Fig. 23).

Variable	Percent contribution	Permutation importance
Distance from the shore	84.8	86.8
Current Velocity Mean	9.9	7.6
Temperature Min	3.1	3.5
Salinity Mean	1.1	1.5
Temperature Mean	0.5	0.7
Current Velocity Min	0.4	0
Temperature Max	0.3	0

*Table 19 Table showing the percentage contribution and permutation importance of each environmental variable for the predicted current distribution of *Rastrelliger kanagurta**

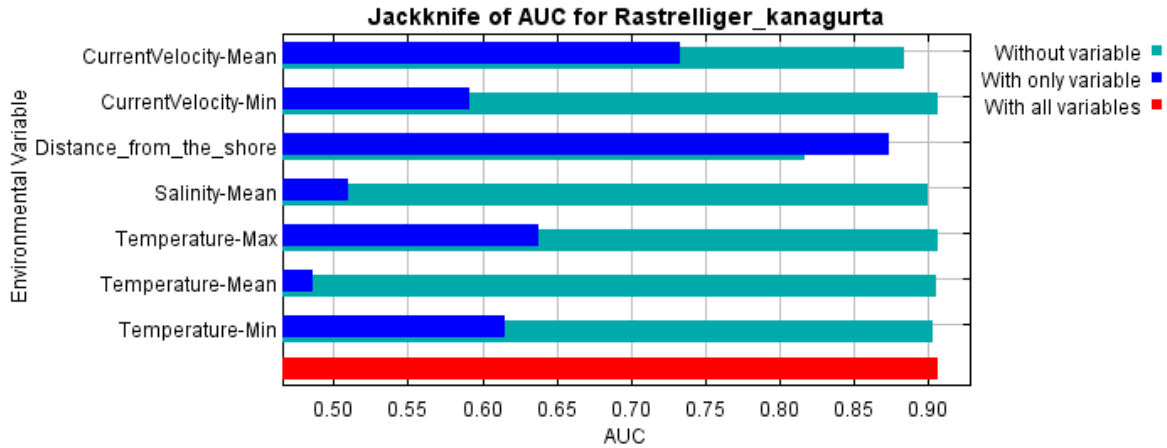


Fig. 23 Jackknife test showing the AUC values of *Rastrelliger kanagurta* when a variable is used in isolation or the variable is excluded from the model

4.2.20.2. Predicted distribution

The predicted current distribution is mainly concentrated in the Western coast of India, Andaman Sea, Persian Gulf, Red sea, Madagascar *etc.* with > 85% probability (Fig. 77). The predicted distribution for 2040-2050 is concentrated in the same areas as that of the current distribution. The AUC values for RCP 4.5, 6.0 and 8.5 are 0.919 (SD 0.025), 0.933(SD 0.016) and 0.910 (SD 0.028) respectively (Fig. 76). Distance from the shore shows the highest test gain when used in isolation among all the other environmental variables. It is also the one environmental variable which has the maximum percent contribution in both RCPs. The predicted distribution for 2090-2100 shows a northward shift in distribution in RCP8.5. The AUC values for RCP 4.5, 6.0 and 8.5 are 0.914 (SD 0.013), 0.911 (SD 0.037) and 0.915 (SD 0.021) respectively (Fig. 76)

4.2.21. *Katsuwonus pelamis* (Linnaeus, 1758)

Kingdom	Phylum	Class	Order	Family	Genus	Species
Animalia	Chordata	Actinopterygii	Perciformes	Scombridae	<i>Katsuwonus</i>	<i>pelamis</i>

4.2.21.1. Model Evaluation

The area under the curve value for the model is 0.849 with 0.007 standard deviation (Fig. 78). The model prediction for the current distribution shows salinity mean as the greatest percentage contributor with value 34.4 and permutation importance 55.4. Current velocity mean, minimum temperature, maximum temperature, distance from the shore, mean temperature and current velocity minimum contribute 20.7%, 15.6%, 11.9%, 8.9%, 0.1% and 3% respectively (Table 21). Jackknife test reveals that Salinity mean has the highest gain among all parameters when used in isolation (Fig. 24).

Variable	Percent contribution	Permutation importance
Salinity-Mean	34.4	55.4
Current Velocity-Mean	20.7	4.7
Temperature-Min	15.6	10.6
Temperature-Max	11.9	7.9
Distance from the shore	8.9	7.4
Temperature-Mean	8.3	13.8
Current Velocity-Min	0.1	0.2

*Table 20 Table showing the percentage contribution and permutation importance of each environmental variable for the predicted current distribution of *Katsuwonus pelamis**

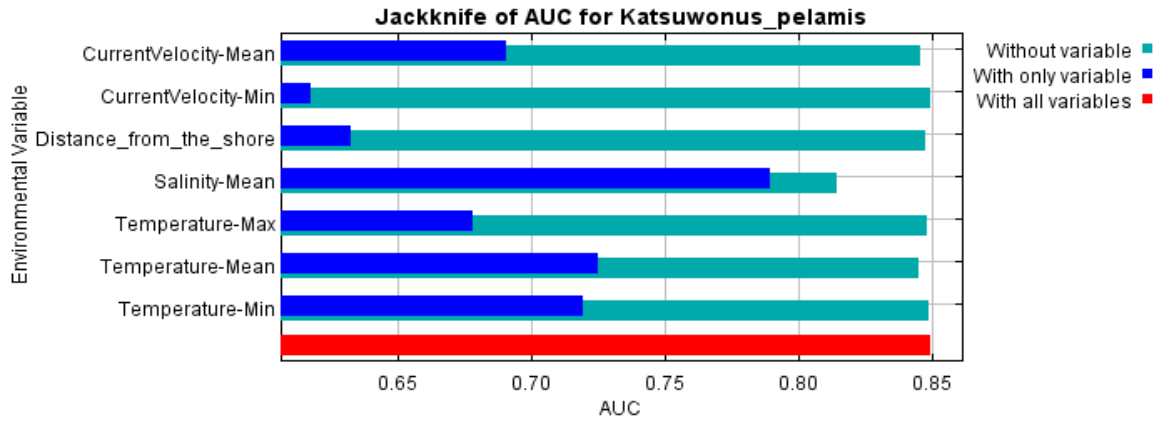


Fig. 24 Jackknife test showing the AUC values of *Katsuwonus pelamis* when a variable is used in isolation or the variable is excluded from the model

Predicted distribution

The predicted current distribution is mainly concentrated in the Eastern coast of Africa, western coast of Madagascar, South west part of Arabian sea, the part of Indian Ocean which is west to the Madagascar *etc.* with > 75% probability (Fig. 79). The predicted distribution for 2040-2050 is concentrated in the same areas as that of the current distribution but the probability of distribution further decreased from RCP 6.0 to RCP 8.5. The extent also shows a gradual decrease. The AUC values for RCP 4.5, 6.0 and 8.5 are 0.849 (SD 0.007), 0.849 (SD 0.006) and 0.844 (SD 0.005) respectively (Fig. 78). Salinity mean shows the highest test gain when used in isolation among all the other environmental variables. It is also the one environmental variable which has the maximum percent contribution in both RCPs. The predicted distribution for 2090-2100 shows a further decline in the extent as well as in the probability of distribution (50-70%). The AUC values for RCP 4.5, 6.0 and 8.5 are 0.850 (SD 0.006), 0.8490 (SD 0.006) and 0.847 (SD 0.004) respectively (Fig. 78).

4.2.22. *Scomberomorus commerson* (Lacepède, 1800)

Kingdom	Phylum	Class	Order	Family	Genus	Species
Animalia	Chordata	Actinopterygii	Perciformes	Scombridae	<i>Scomberomorus</i>	<i>commerson</i>

4.2.22.1. Model Evaluation

The area under the curve value for the model is 0.780 with 0.047 standard deviation (Fig. 80). The model prediction for the current distribution shows distance from the shore as the greatest percentage contributor with value 55.7 and permutation importance 82.1. Current velocity mean , maximum temperature, mean temperature , current velocity minimum , salinity mean and minimum temperature contribute 24.1%, 9.9% , 4.4% , 2.5% , 1.8% and 1.6% respectively (Table 22). Jackknife test reveals that distance from the shore has the highest gain among all parameters when used in isolation (Fig. 25).

Variable	Percent contribution	Permutation importance
Distance from the shore	55.7	82.1
CurrentVelocity-Mean	24.1	1.3
Temperature-Max	9.9	6.7
Temperature-Mean	4.4	3.9
CurrentVelocity-Min	2.5	2.5
Salinity-Mean	1.8	1
Temperature-Min	1.6	2.7

Table 21 Table showing the percentage contribution and permutation importance of each environmental variable for the predicted current distribution of Scomberomorus commerson

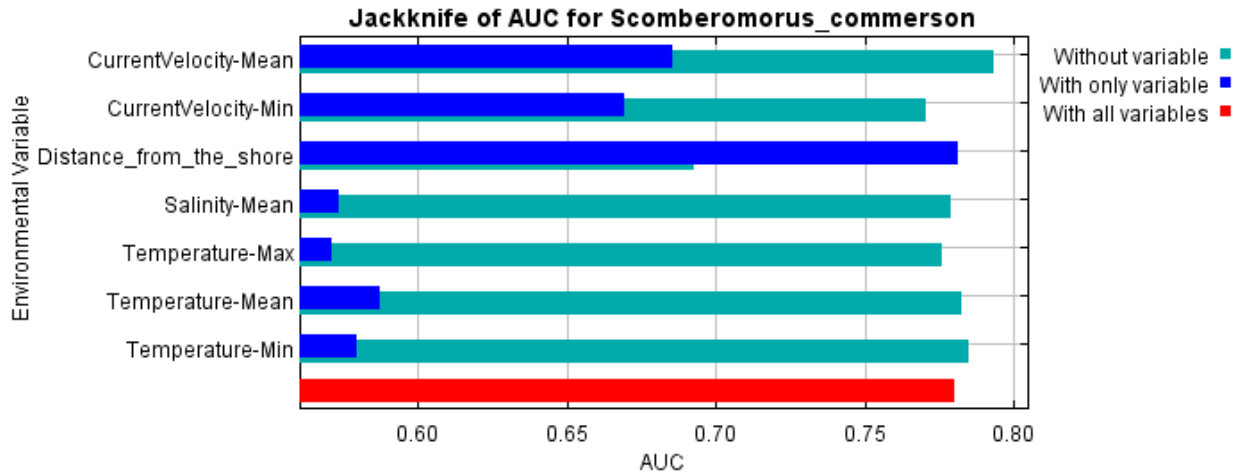


Fig. 25 Jackknife test showing the AUC values of *Scomberomorus commerson* when a variable is used in isolation or the variable is excluded from the model

4.2.22.2. Predicted distribution

The predicted current distribution is mainly concentrated in the Western and Eastern coast of India, coast of Thailand, Malaysia, Madagascar, Red sea *etc.* with > 80% probability (Fig. 81). The predicted distribution for 2040-2050 is concentrated in the same areas as that of the current distribution but the probability of distribution decreases from RCP 8.5 to RCP 6 with probability 50% to 75%. The extent also shows a gradual decrease. The AUC values for RCP 4.5, 6.0 and 8.5 are 0.755 (SD 0.084), 0.777 (SD 0.101) and 0.778 (SD 0.091) respectively (Fig. 80). Distance from the shore shows the highest test gain when used in isolation among all the other environmental variables. It is also the one environmental variable which has the maximum percent contribution in both RCPs. The predicted distribution for 2090-2100 shows a further decline in the extent as well as in the probability of distribution (50-70%). The AUC values for RCP 4.5, 6.0 and 8.5 are 0.756(SD 0.086), 0.763 (SD 0.0118) and 0.771 (SD 0.099) respectively (Fig. 80).

4.2.23. *Sphyraena barracuda* (Edwards, 1771)

Kingdom	Phylum	Class	Order	Family	Genus	Species
Animalia	Chordata	Actinopterygii	Perciformes	Sphyraenidae	<i>Sphyraena</i>	<i>barracuda</i>

4.2.23.1. Model Evaluation

The area under the curve value for the model is 0.849 with 0.018 standard deviation (Fig. 82). The model prediction for the current distribution shows Salinity-Mean as the greatest percentage contributor with value 46.9 and permutation importance 45.7. Temperature-Mean, Temperature-Min and Distance from the shore contribute 17%, 16.9% and 9.3% respectively (Table 23). Jackknife test reveals that Salinity-Mean has the highest gain among all parameters when used in isolation (Fig. 26).

Variable	Percent contribution	Permutation importance
Salinity-Mean	46.9	45.7
Temperature-Mean	17	24.7
Temperature-Min	16.9	8.7
Distance from the shore	9.3	10.9
Temperature-Max	4.2	6
Current Velocity-Mean	4.1	2.3
Current Velocity-Min	1.7	1.6

Table 23 Table 22 Table showing the percentage contribution and permutation importance of each environmental variable for the predicted current distribution of *Sphyraena barracuda*

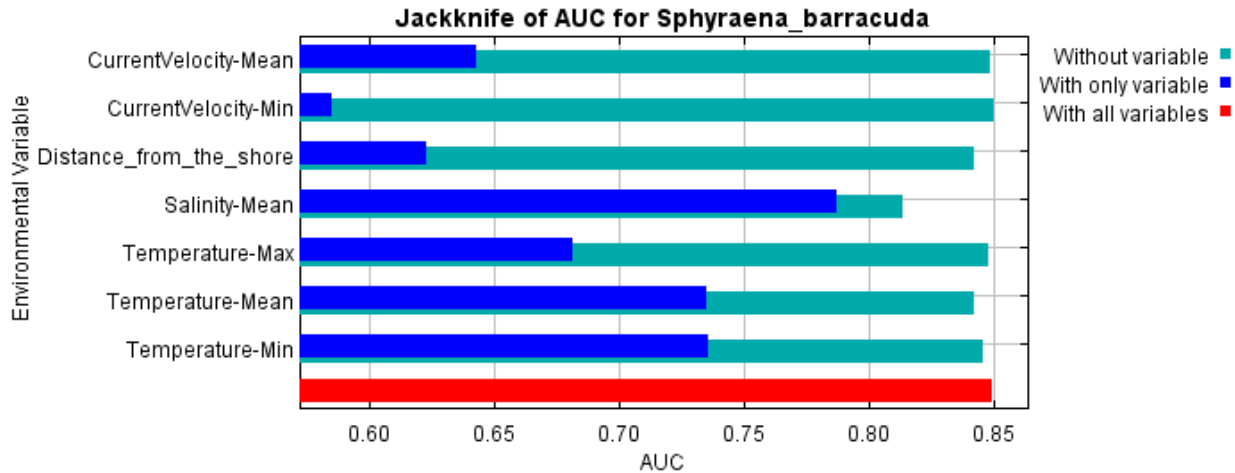


Fig. 26 Jackknife test showing the AUC values of *Sphyraena barracuda* when a variable is used in isolation or the variable is excluded from the model

4.2.23.2. Predicted distribution

The predicted current distribution is mainly concentrated in the Western Indian Ocean close to Madagascar and also along the west coast of Madagascar with > 75% probability (Fig. 83). The predicted distribution for 2040-2050 is concentrated in the same areas as that of the current distribution but the probability of distribution increases for RCP 6.0 with probability >85% decreases for RCP 8.5 with probability 50% to 75% . The extent also shows a gradual decrease. The AUC values for RCP 4.5, RCP 6.0 and 8.5 are 0.854 (0.015), 0.854 (SD 0.013) and 0.853 (SD 0.016) respectively (Fig. 82). Salinity mean shows the highest test gain when used in isolation among all the other environmental variables. It is also the one environmental variable which has the maximum percent contribution in both RCPs. The predicted distribution for 2090-2100 shows a further decline in the extent as well as in the probability of distribution (50-70%) for RCP 6.0 but slight increase is seen for RCP 8.5. The AUC values for RCP 4.5, RCP 6.0 and 8.5 are 0.851 (SD 0.014), 0.850 (SD 0.010) and 0.848 (SD 0.016) respectively (Fig. 82).

4.2.24. *Canthidermis maculata* (Bloch, 1786)

Kingdom	Phylum	Class	Order	Family	Genus	Species
Animalia	Chordata	Actinopterygii	Tetraodontiformes	Balistidae	<i>Canthidermis</i>	<i>maculata</i>

4.2.24.1. Model Evaluation

The area under the curve value for the model is 0.912 with 0.006 standard deviation (Fig. 84). The model prediction for the current distribution shows Salinity mean as the greatest percentage contributor with value 37 and permutation importance 44.7. Current velocity mean, Temperature minimum, Temperature mean, Distance from the shore, Temperature maximum and Current velocity minimum contribute 16.2%, 15.6%, 13.1%, 9%, 8.2%, 1% respectively (Table 24). Jackknife test reveals that Salinity mean has the highest gain among all parameters when used in isolation (Fig. 27).

Variable	Percent contribution	Permutation importance
Distance from the shore	9	9.9
Current Velocity Mean	16.2	4.8
Temperature Min	15.6	17.2
Salinity Mean	37	44.7
Temperature Mean	13.1	21.4
Current Velocity Min	1	0
Temperature Max	8.2	1.9

Table 23 Table showing the percentage contribution and permutation importance of each environmental variable for the predicted current distribution of Canthidermis maculata

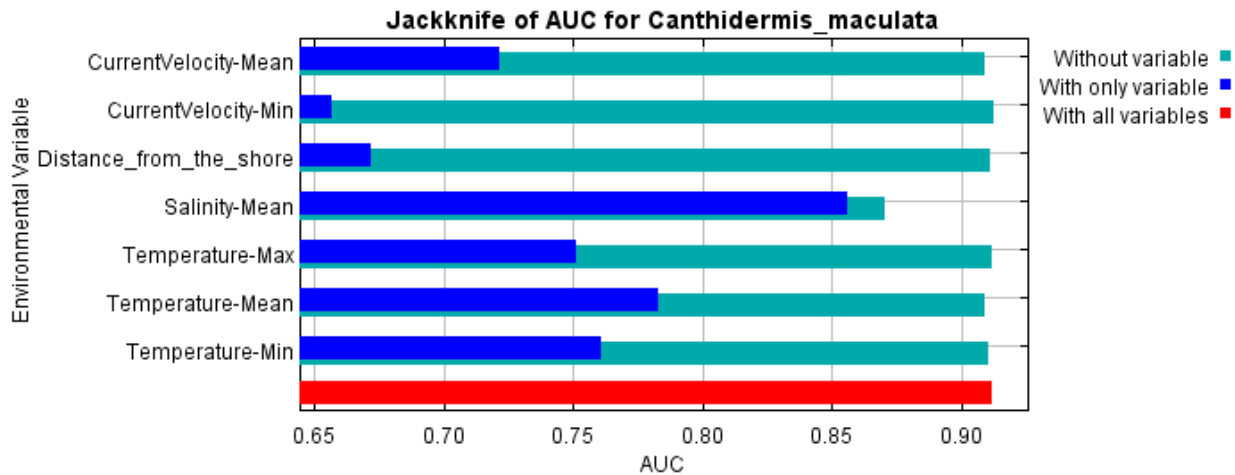


Fig. 27 Jackknife test showing the AUC values of *Canthidermis maculata* when a variable is used in isolation or the variable is excluded from the model

4.2.24.2. Predicted distribution

The predicted current distribution is mainly concentrated in the Southwest Arabian Sea with > 77 % probability (Fig. 3). The predicted distribution for 2040-2050 is concentrated in the same areas as that of the current distribution but the probability of distribution decreases from RCP 4.5, RCP 6.0 and RCP 8.5 with probability 46% to 69% . The extent also shows a gradual decrease. The AUC values for RCP 4.5, 6.0 and 8.5 are 0.908 (SD 0.010), 0.909 (SD 0.007) and 0.903 (SD 0.007) respectively (Fig. 4). Salinity mean shows the highest test gain when used in isolation among all the other environmental variables. It is also the one environmental variable which has the maximum percent contribution in both RCPs. The predicted distribution for 2090-2100 shows a further decline in the extent as well as in the probability of distribution (62 %) . The AUC values for RCP 4.5, 6.0 and 8.5 are 0.909 (SD0.006), 0.910 (SD 0.008) and 0.913 (SD 0.009) respectively (Fig. 4).

4.2.25. *Carcharhinus falciformis* (Müller & Henle, 1839)

Kingdom	Phylum	Class	Order	Family	Genus	Species
Animalia	Chordata	Elasmobranchii	Carcharhiniformes	Carcharhinidae	<i>Carcharhinus</i>	<i>falciformis</i>

4.2.25.1. Model Evaluation

The area under the curve value for the model is 0.876 with 0.008 standard deviation (Fig. 86). The model prediction for the current distribution shows salinity mean as the greatest percentage contributor with value 47 and permutation importance 41.8. Mean temperature, maximum temperature, current velocity mean, SST minimum, distance from the shore and current velocity minimum contribute 27.2 %, 9%, 6.5%, 6.2%, 3.7% and 0.4% respectively (Table 25). Jackknife test reveals that salinity mean has the highest gain among all parameters when used in isolation (Fig. 28).

Variable	Percent contribution	Permutation importance
Salinity Mean	47	41.8
Temperature Mean	27.2	30.1
Temperature Maximum	9	9.5
Current velocity mean	6.5	4
Temperature minimum	6.2	8.8
Distance from the shore	3.2	5.3
Current velocity minimum	0.4	0.5

Table 24 Table showing the percentage contribution and permutation importance of each environmental variable for the predicted current distribution of *Carcharhinus falciformis*

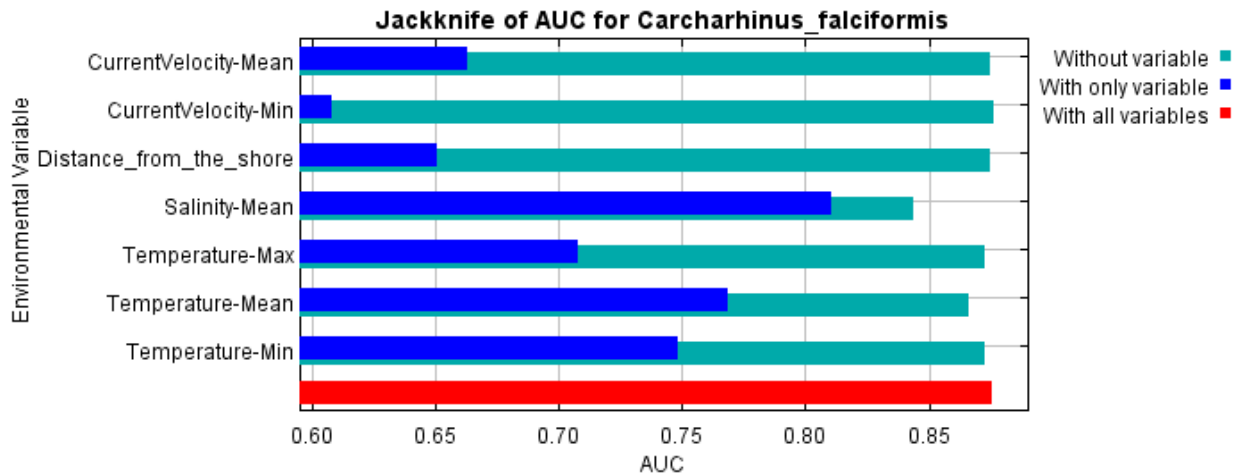


Fig. 28 Jackknife test showing the AUC values of Carcharhinus falciformis when a variable is used in isolation or the variable is excluded from the model

4.2.25.2. Predicted distribution

The predicted current distribution is mainly concentrated in the south west part of Indian Ocean and in the western coast of Africa to Madagascar with > 77% probability (Fig. 87). The predicted distribution for 2040-2050 is concentrated in the same areas as that of the current distribution but the probability of distribution decreases in RCP 4.5 and RCP 6.0, but RCP8.5 shows an increased distribution probability >80% just below the coast of India . The AUC values for RCP4.5, 6.0 and 8.5 are 0.879 (SD 0.009), 0.876 (SD 0.007) and 0.879 (SD 0.004) respectively (Fig. 86). Salinity mean shows the highest test gain when used in isolation among all the other environmental variables. It is also the one environmental variable which has the maximum percent contribution in both RCPs. The predicted distribution for 2090-2100 shows a further decline in the extent as well as in the probability of distribution. The AUC values for RCP 4.5, 6.0 and 8.5 are 0.878 (SD 0.006), 0.881 (SD 0.004) and 0.878 (SD 0.006) respectively (Fig. 86)

4.2.26. *Carcharhinus plumbeus* (Nardo, 1827)

Kingdom	Phylum	Class	Order	Family	Genus	Species
Animalia	Chordata	Elasmobranchii	Carcharhiniformes	Carcharhinidae	<i>Carcharhinus</i>	<i>plumbeus</i>

4.2.26.1. Model Evaluation

The area under the curve value for the model is 0.904 with 0.021 standard deviation (Fig. 88). The model prediction for the current distribution shows distance from the shore as the greatest percentage contributor with value 41.5 and permutation importance 33. The current velocity mean, minimum sea surface temperature, mean salinity, sea surface temperature mean, current velocity minimum and temperature maximum contribute 16.8%, 23.8%, 6%, 23.8%, 0.1% and 9.3% respectively (Table 26). Jackknife test reveals that distance from the shore has the highest gain among all parameters when used in isolation (Fig. 29).

Variable	Percent contribution	Permutation importance
Distance from the shore	41.5	33
CurrentVelocity Mean	16.8	13.5
Temperature Min	23.8	45.4
Salinity Mean	6	4
Temperature Mean	23.8	1.6
CurrentVelocity Min	0.1	0.2
Temperature Max	9.3	2.2

Table 25 Table showing the percentage contribution and permutation importance of each environmental variable for the predicted current distribution Carcharhinus plumbeus

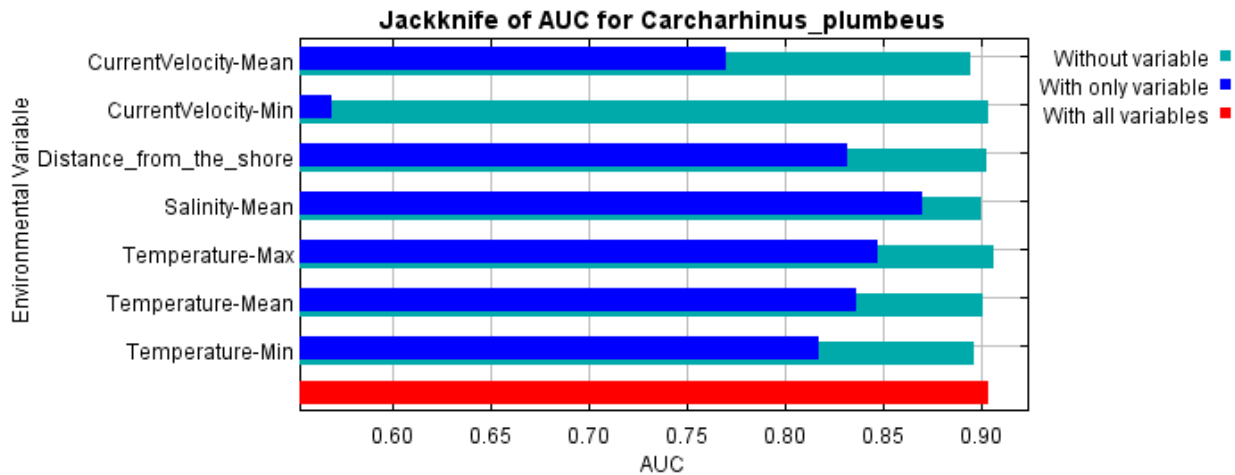


Fig. 29 Jackknife test showing the AUC values of Carcharhinus plumbeus when a variable is used in isolation or the variable is excluded from the model

4.2.26.2. Predicted distribution

The predicted current distribution has the highest concentration in the western part of the northern Indian Ocean, away from the region of Madagascar with a probability of > 85% (Fig. 89). According to the current predicted model, the species distribution can also be found in the western Madagascar coast, in some regions of north eastern African coast, Gujarat coast with a probability of 46% to 69%. The predicted distribution for RCP 4.5 in 2040 - 50 exhibits a reduced probability of the species but it shows a new appearance in the region of northern Indian ocean, slightly far from the Sumatra. The probability distribution in RCP 6 shows a slight reduction compared to that of RCP 4 but it is greatly diminished during RCP 8.5. The AUC values for RCP 4.5, RCP 6.0 and 8.5 are 0.902 (SD 0.016), 0.914 (SD 0.012) and 0.890 (SD 0.023) respectively (Fig. 88). Distance from the shore shows the highest test gain when used in isolation among all the other environmental variables. It is also the one environmental variable which has the maximum percent contribution in all RCPs. The predicted distribution for RCP 4.5 of 2090-2100 shows a similar pattern of distribution to that of in 2040-50 but their extent is minimized. The distribution and extent of the species further decline in the RCP 6 and 8.5 of

2090 - 100. The AUC values for RCP 4.5, RCP 6.0 and 8.5 are 0.912 (SD 0.011), 0.916 (SD 0.018) and 0.902 (SD 0.023) respectively (Fig. 88)

4.2.27. *Carcharhinus limbatus* (Müller & Henle, 1839)

Kingdom	Phylum	Class	Order	Family	Genus	Species
Animalia	Chordata	Elasmobranchii	Carcharhiniformes	Carcharhinidae	<i>Carcharhinus</i>	<i>limbatus</i>

4.2.27.1. Model Evaluation

The area under the curve value for the model is 0.841 with 0.023 standard deviation (Fig. 90). The model prediction for the current distribution shows salinity mean as the greatest percentage contributor with value 29.5 and permutation importance 22.6. Distance from the shore, current velocity mean, sea surface temperature minimum, sea surface temperature mean, current velocity minimum, sea surface temperature maximum contribute 26.4%, 7%, 8.2%, 3.6%, 2.5% and 22.9% respectively (Table 27). Jackknife test reveals that salinity mean has the highest gain among all parameters when used in isolation (Fig. 30).

Variable	Percent contribution	Permutation importance
Distance from the shore	26.4	37
Current Velocity Mean	7	15.3
Temperature Min	8.2	8.7
Salinity Mean	29.5	22.6
Temperature Mean	3.6	5.1
Current Velocity Min	2.5	3
Temperature Max	22.9	8.3

Table 26 Table showing the percentage contribution and permutation importance of each environmental variable for the predicted current distribution of *Carcharhinus limbatus*

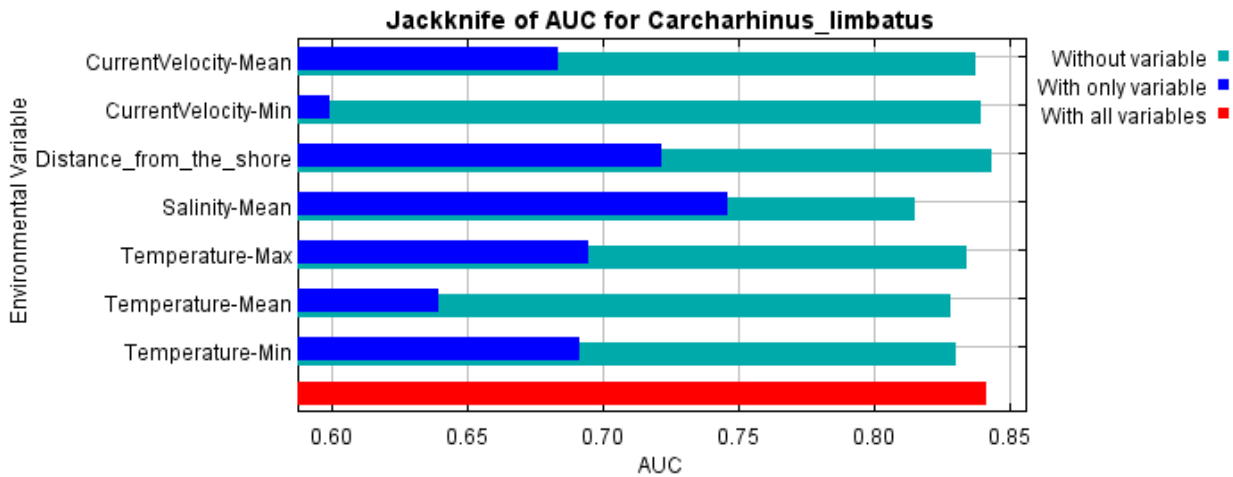


Fig. 30 Jackknife test showing the AUC values of *Carcharhinus limbatus* when a variable is used in isolation or the variable is excluded from the model

4.2.27.2. Predicted distribution

The predicted current distribution is mainly concentrated in the Gulf of Aden, under south west of India and in some regions of north east Africa with > 85% probability (Fig. 91). According to the predicted model, during RCP 4.5, 2040-2050 the probability of distribution increases. The probability distribution of the species in Srilanka coast will increase from 71% to more than 85%. In RCP 6, a migration towards North West of the study area and when it comes to RCP 8.5, a drastic decline in the probability distribution and in extent can be observed. The AUC values for RCP 4.5, 6.0 and 8.5 are 0.835 (SD 0.032), 0.849 (SD 0.018) and 0.849 (SD 0.028) respectively (Fig. 90). Salinity mean shows the highest test gain when used in isolation among all the other environmental variables. It is also the one environmental variable which has the maximum percent contribution in both RCPs. The predicted distribution for 2090-2100 shows an increase in the probability of distribution (50-70%). The AUC values for RCP

4.5, 6.0 and 8.5 are 0.823 (SD 0.028), 0.842 (SD 0.027) and 0.846 (SD 0.027) respectively (Fig. 90)

4.2.28. *Carcharhinus brevipinna* (Müller & Henle, 1839)

Kingdom	Phylum	Class	Order	Family	Genus	Species
Animalia	Chordata	Elasmobranchii	Carcharhiniformes	Carcharhinidae	<i>Carcharhinus</i>	<i>brevipinna</i>

4.2.28.1. Model Evaluation

The area under the curve value for the model is 0.950 with 0.037 standard deviation (Fig. 93). The model prediction for the current distribution shows sea surface temperature minimum as the greatest percentage contributor with value 26 and permutation importance 44.4. Distance from the shore, current velocity mean, salinity mean, temperature mean, current velocity minimum and sea surface temperature maximum contribute 9.9%, 21%, 19.1%, 4.7%, 1.1% and 18.2% respectively (Table 28). Jackknife test reveals that sea surface temperature minimum has the highest gain among all parameters when used in isolation (Fig. 31).

Variable	Percent contribution	Permutation importance
Distance from the shore	9.9	3.5
Current Velocity Mean	21	31.2
Temperature Min	26	44.4
Salinity Mean	19.1	15.9
Temperature Mean	4.7	0.3
Current Velocity Min	1.1	0.4
Temperature Max	18.2	4.3

Table 27 Table showing the percentage contribution and permutation importance of each environmental variable for the predicted current distribution of *Carcharhinus brevipinna*

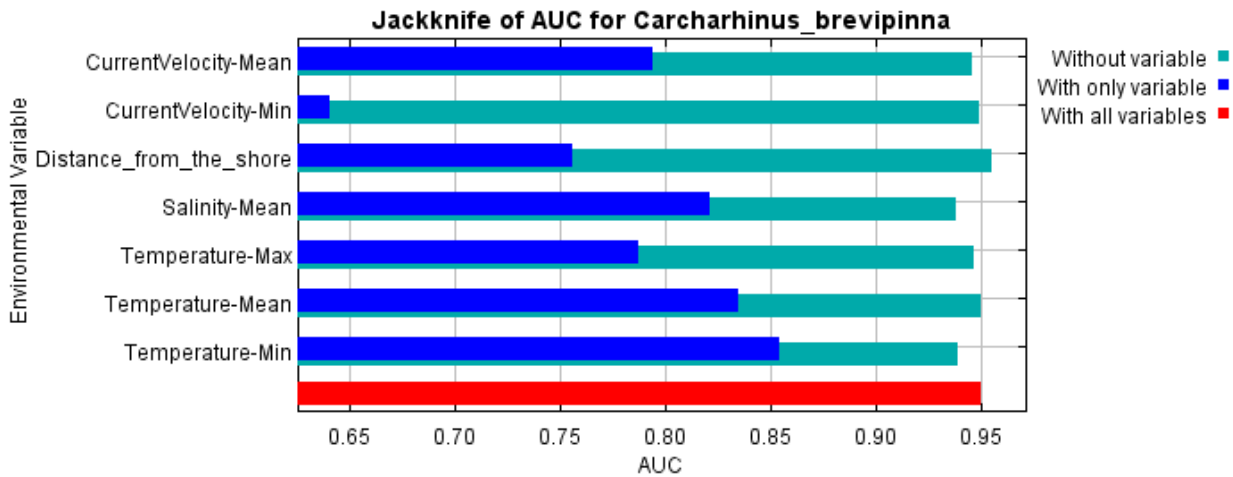


Fig. 31 Jackknife test showing the AUC values of *Carcharhinus brevipinna* when a variable is used in isolation or the variable is excluded from the model

Predicted distribution

The predicted current distribution is mainly concentrated in the western region of the Madagascar coast, in the south west region of the study area located in the north east region of the Madagascar and in the west coast of India with > 85% probability (Fig. 93). The predicted distribution for RCP 4.5 and 6, 2040-2050 is concentrated in the same areas as that of the current distribution but the probability of distribution decreases. But in RCP 8.5, the probability of distribution as well as the extent increases even more than that in the present. The AUC values for RCP 4.5, 6.0 and 8.5 are 0.967 (SD 0.011), 0.937(SD 0.033), 0.949(SD 0.031) respectively (Fig. 92). Sea surface temperature minimum shows the highest test gain when used in isolation among all the other environmental variables. It is also the one environmental variable which has the maximum percent contribution in both RCPs. The predicted distribution for RCP 4.5, 2090-2100 shows a decline in the probability of distribution but RCP 6 exhibits its opposite. An interesting observation of RCP 6 is that species in the west coast of India migrate upwards whereas species in the eastern part of the Madagascar shift downwards. In RCP 8, the probability

distribution of the species increases in the northern part of the study area and it declines in the southern part . The AUC values for RCP 4.5, 6.0 and 8.5 are 0.939 (SD 0.039), 0.946 (SD 0.024) and 0.912 (SD 0.081) respectively (Fig. 92)

4.2.29. *Carcharhinus longimanus* (Poey, 1861)

Kingdom	Phylum	Class	Order	Family	Genus	Species
Animalia	Chordata	Elasmobranchii	Carcharhiniformes	Carcharhinidae	<i>Carcharhinus</i>	<i>longimanus</i>

4.2.29.1. Model Evaluation

The area under the curve value for the model is 0.812 with 0.018 standard deviation (Fig. 95). The model prediction for the current distribution shows salinity mean as the greatest percentage contributor with value 40.3 and permutation importance 37.8. The current velocity mean, Temperature minimum, Distance from the shore, maximum temperature, mean temperature and current velocity minimum contribute 15 %, 6.8%, 14.1%, 12.1%, 10.3% and 1.5% respectively (Table 29). Jackknife test reveals that salinity mean has the highest gain among all parameters when used in isolation (Fig. 32).

Variable	Percent contribution	Permutation importance
Distance from the shore	14.1	10.4
Current Velocity Mean	15	6.7
Temperature Min	6.8	8.6
Salinity Mean	40.3	37.8
Temperature Mean	10.3	19
Current Velocity Min	1.5	2.9
Temperature Max	12.1	14.6

Table 28 Table showing the percentage contribution and permutation importance of each environmental variable for the predicted current distribution of *Carcharhinus longimanus*

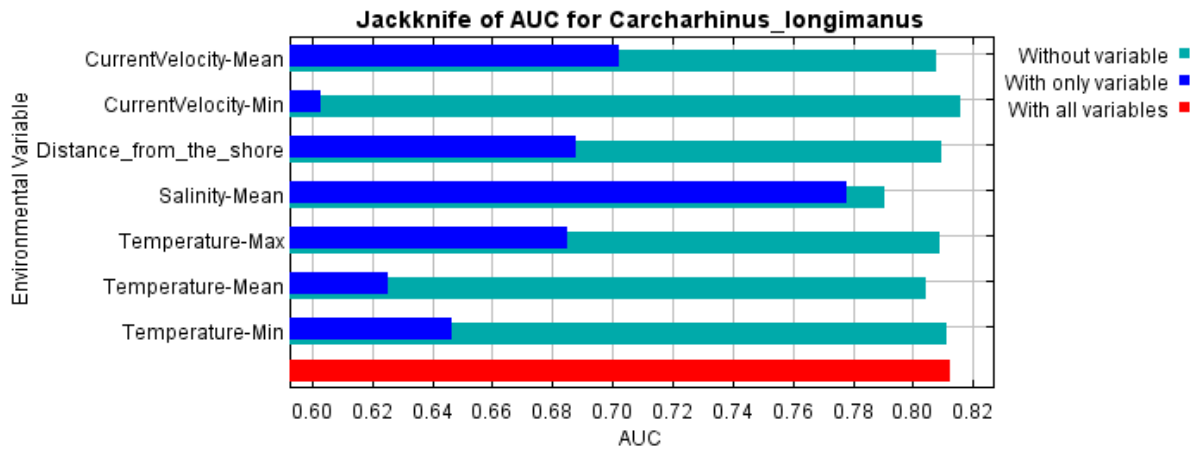


Fig. 32 Jackknife test showing the AUC values of *Carcharhinus longimanus* when a variable is used in isolation or the variable is excluded from the model

4.2.29.2. Predicted distribution

The prediction of current distribution shows the range of species with > 85% probability in the north eastern side of Africa where distribution seems to be continuous and in the portion of Indian Ocean located to the east of Madagascar. The western coast of India and some parts of Bay of Bengal shows 50 to 85% probability of distribution (Fig. 95). Under RCP 4.5 of the decade 2040-2050, the range of species shows a shift away from the Madagascar and eastern African coast, moving towards the Arabian Sea. The probability of distribution increased in the

southern central Bay of Bengal under this RCP scenario with greater than 60% probability distribution. From eastern Africa shows a patchy distribution of species with > 50% probability. In RCP 8.5 the range as well as the probability of distribution reduced considerably and appearance of species is seen only in the Indian Ocean region to the south of India and Srilanka with a probability range of 43 to 86%. The AUC values for RCP 4.5, 6.0 and 8.5 are 0.805 (SD 0.021), 0.813 (SD 0.020) and 0.821 (SD 0.016) respectively (Fig. 94). Salinity mean shows the highest test gain when used in isolation among all the other environmental variables. It is also the one environmental variable which has the maximum percent contribution in all RCPs. The RCP 4.5 and 6 of 2090-2100 shows similar distribution patterns of RCP 6 of previous decade except that the probability is diminished in oceanic area near to India and Srilanka and an increase in distribution of the species in the oceanic region located to the eastern side of Madagascar. The predicted distribution of RCP 8.5 of the decade differs from the present prediction in that the distribution tends to shift more towards the north-eastern region of Indian Ocean and the area having probability greater than 85% distribution shows a notable reduction. The AUC values for RCP 4.5, 6.0 and 8.5 are 0.805 (SD 0.024), 0.809 (SD 0.017) and 0.819 (SD 0.013) respectively (Fig. 94).

4.2.30. *Sphyrna mokarran* (Rüppell, 1837)

Kingdom	Phylum	Class	Order	Family	Genus	Species
Animalia	Chordata	Elasmobranchii	Carcharhiniformes	Sphyrnidae	<i>Sphyrna</i>	<i>mokarran</i>

4.2.30.1. Model Evaluation

The area under the curve value for the model is 0.923 with 0.037 standard deviation (Fig. 97). The model prediction for the current distribution shows salinity as the greatest percentage contributor with value 28.4 and permutation importance 45.9. (Table 30). The current velocity mean, Temperature minimum, Distance from the shore, maximum temperature, mean temperature and current velocity mean contribute 19.7 %, 18.7%, 11.6%, 11.6%, 9.9 and 0.2% respectively. Jackknife test reveals that Salinity-Mean has the highest gain among all parameters when used in isolation (Fig. 33).

Variable	Percent contribution	Permutation importance
Distance from the shore	11.6	3.9
Current Velocity Mean	19.7	6.9
Temperature Min	18.7	31.7
Salinity Mean	28.4	45.9
Temperature Mean	9.9	8.3
Current Velocity Min	0.2	1
Temperature Max	11.6	2.3

Table 29 Table showing the percentage contribution and permutation importance of each environmental variable for the predicted current distribution of *Sphyrna mokarran*

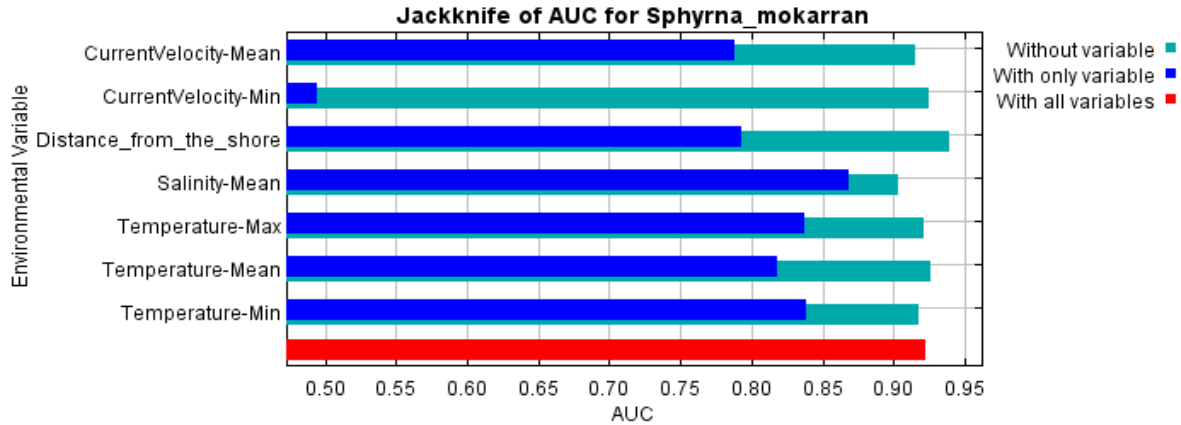


Fig. 33 Jackknife test showing the AUC values of *Sphyrna mokarran* when a variable is used in isolation or the variable is excluded from the model

4.2.30.2. Predicted distribution

The predicted current distribution is mainly concentrated in the southern Arabian sea above the Madagascar with a probability ranging from 46% to 96% and its presence in south western coast of India (Fig. 97). On comparing the predicted distribution with the 2040-2050 decade it is observed that even though the concentration is diminished, the range of the species is extended and is shifted towards the eastern coast of Africa from RCP 4.5 to 8.5. The AUC values for RCP 4.5, 6.0 and 8.5 are 0.945(SD 0.018), 0.929 (SD 0.019) and 0.937 (SD 0.027) respectively (Fig. 96). Salinity mean shows the highest test gain when used in isolation among all the other environmental variables. It is also the one environmental variable which has the maximum percent contribution in all RCPs. The predicted distribution for 2090-2100 implies the range of the species gets diminished to eastern part of Madagascar and it completely shifted towards the north western coast of India. The AUC values for RCP 4.5, 6.0 and 8.5 are 0.940 (SD 0.015), 0.944 (SD 0.021) and 0.942 (SD 0.011) respectively (Fig. 96)

4.2.31. *Sphyrna zygaena* (Linnaeus, 1758)

Kingdom	Phylum	Class	Order	Family	Genus	Species
Animalia	Chordata	Elasmobranchii	Carcharhiniformes	Sphyrnidae	<i>Sphyrna</i>	<i>zygaena</i>

4.2.31.1. Model Evaluation

The area under the curve value for the model is 0.844 with 0.036 standard deviation (Fig. 98). The model prediction for the current distribution shows sea surface temperature minimum as the greatest percentage contributor with value 39.2 and permutation importance 52.3. The distance from the shore, current velocity mean, mean salinity, sea surface temperature mean, current velocity minimum and sea surface temperature maximum contribute 38%, 0.9%, 14.4%, 4.8%, 0.1% and 2.5% respectively (Table 31). Jackknife test reveals that sea surface temperature minimum has the highest gain among all parameters when used in isolation (Fig. 34).

Variable	Percent contribution	Permutation importance
Distance from the shore	38	52.3
Current Velocity Mean	0.9	4.4
Temperature Min	39.2	52.3
Salinity Mean	14.4	23.9
Temperature Mean	4.8	3
Current Velocity Min	0.1	0.1
Temperature Max	2.5	2.9

*Table 30 Table showing the percentage contribution and permutation importance of each environmental variable for the predicted current distribution of *Sphyrna zygaena**

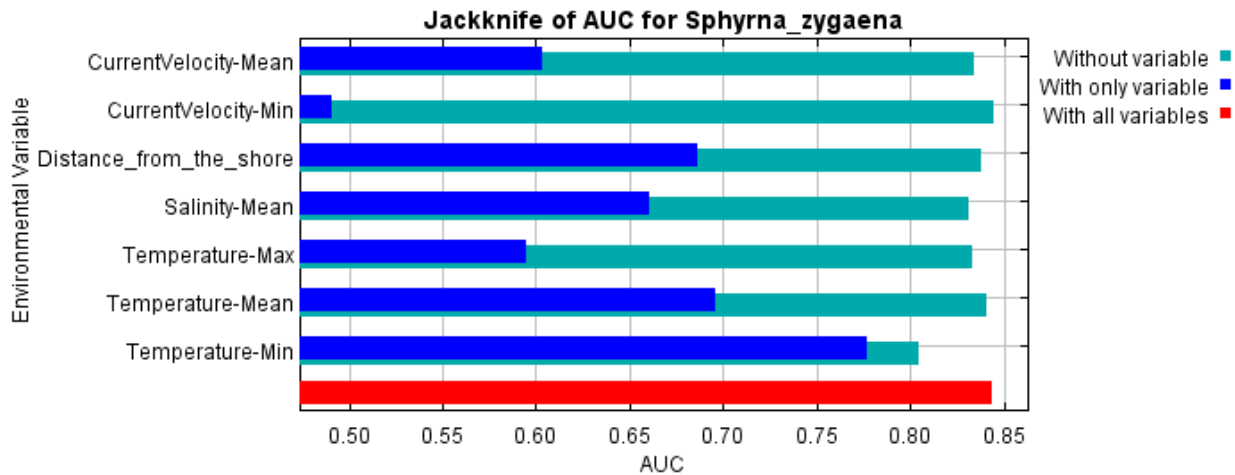


Fig. 34 Jackknife test showing the AUC values of *Sphyrna zygaena* when a variable is used in isolation or the variable is excluded from the model

4.2.31.2. Predicted distribution

The predicted current distribution is mainly concentrated in the Gulf of Aden, in some regions of the coast of Red sea, Maharashtra coast *etc.* with > 85% probability (Fig. 99). The predicted distribution for 2040-2050 exhibits an upward shift in the distribution of the species. The AUC values for RCP 4.5, 6.0 and 8.5 are 0.842(SD 0.054), 0.840(SD 0.054) and 0.829 (SD 0.044) respectively (Fig. 98). Sea surface temperature minimum shows the highest test gain when used in isolation among all the other environmental variables. It is also the one environmental variable which has the maximum percent contribution in all RCPs. The predicted distribution of RCP 4.5 and 6 of 2090 - 100 shows a northward shift but their range is decreased in comparison with that of 2040 - 50. In RCP 8.5, the distribution is concentrated in the north west regions of the study area with a probability of >85% . The AUC values for RCP 4.5, 6.0 and 8.5 are 0.842 (SD 0.028), 0.846 (SD 0.050) and 0.807 (SD 0.038) respectively (Fig. 98)

4.2.32. *Alopias vulpinus* (Bonnaterre, 1788)

Kingdom	Phylum	Class	Order	Family	Genus	Species
Animalia	Chordata	Elasmobranchii	Lamniformes	Alopiidae	<i>Alopias</i>	<i>vulpinus</i>

4.2.32.1. Model Evaluation

The area under the curve value for the model is 0.827 with 0.037 standard deviation (Fig. 100). The model prediction for the current distribution shows salinity mean as the greatest percentage contributor with value 26.3 and permutation importance 22.4. The maximum temperature, The minimum temperature, mean temperature, current velocity mean, current velocity minimum and distance from the shore contribute 21.9%, 15.4%, 16.2%, 7.9%, 2.9% and 9.3% respectively (Table 32). Jackknife test reveals that Salinity-Mean has the highest gain among all parameters when used in isolation (Fig. 35).

Variable	Percent contribution	Permutation importance
Distance from the shore	9.8	6
Current Velocity Mean	8.4	6.1
Temperature Min	14.2	23
Salinity Mean	27.3	21.6
Temperature Mean	13.8	28.1
Current Velocity Min	3.5	4.5
Temperature Max	23	10.8

*Table 31 Table showing the percentage contribution and permutation importance of each environmental variable for the predicted current distribution of *Alopias vulpinus**

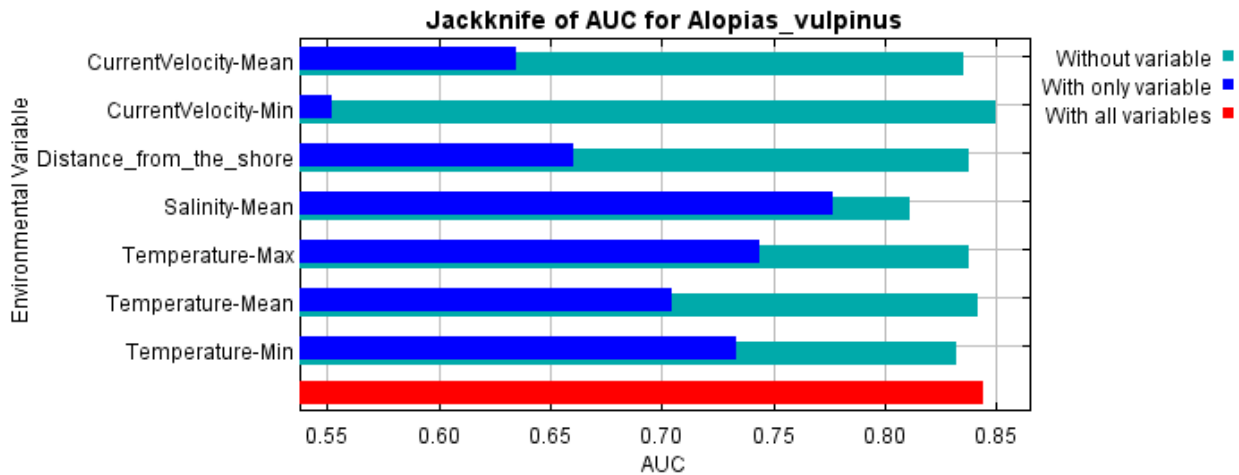


Fig. 35 Jackknife test showing the AUC values of Alopias vulpinus when a variable is used in isolation or the variable is excluded from the model

4.2.32.2. Predicted distribution

The predicted current distribution is mainly concentrated in the eastern coast of Africa, Gulf of Aden and eastern part of Madagascar with > 85% probability (Fig. 101). The predicted distribution for 2040-2050 is concentrated in the same areas as that of the current distribution but the probability of distribution decreases from RCP 6.0 to RCP 8.5 with probability. The AUC values for RCP 4.5, 6.0 and 8.5 are 0.840 (SD 0.028), 0.839 (SD 0.032) and 0.847 (SD 0.020) respectively (Fig. 100). Salinity-Mean shows the highest test gain when used in isolation among all the other environmental variables. It is also the one environmental variable which has the maximum percent contribution in both RCPs. The predicted distribution for 2090-2100 shows an increase in the extent from RCP 4.5 to 8.5. The AUC values for RCP 4.5, 6.0 and 8.5 are 0.858 (SD 0.021), 0.827 (SD 0.030) and 0.823 (SD 0.031) respectively (Fig. 100).

4.2.33. *Rhincodon typus* Smith, 1828

Kingdom	Phylum	Class	Order	Family	Genus	Species
Animalia	Chordata	Elasmobranchii	Orectolobiformes	Rhincodontidae	<i>Rhincodon</i>	<i>typus</i>

4.2.33.1. Model Evaluation

The area under the curve value for the model is 0.901 with 0.021 standard deviation (Fig. 102). The model prediction for the current distribution shows distance from the shore as the greatest percentage contributor with value 51.1 and permutation importance 65.6. current velocity mean, salinity mean, SST maximum, SST minimum, SST mean and current velocity minimum contribute 13.7%, 13%, 8.6%, 8.4%, 4.4% and 0.8% respectively (Table 33). Jackknife test reveals that distance from the shore has the highest gain among all parameters when used in isolation (Fig. 36).

Variable	Percent contribution	Permutation importance
Distance from the shore	51.1	65.6
Current Velocity Mean	13.7	8.7
Temperature Min	13	8.3
Salinity Mean	8.6	5.3
Temperature Mean	8.4	5.7
Current Velocity Min	8.4	5.3
Temperature Max	0.8	1.2

Table 32 Table showing the percentage contribution and permutation importance of each environmental variable for the predicted current distribution of *Rhincodon typus*

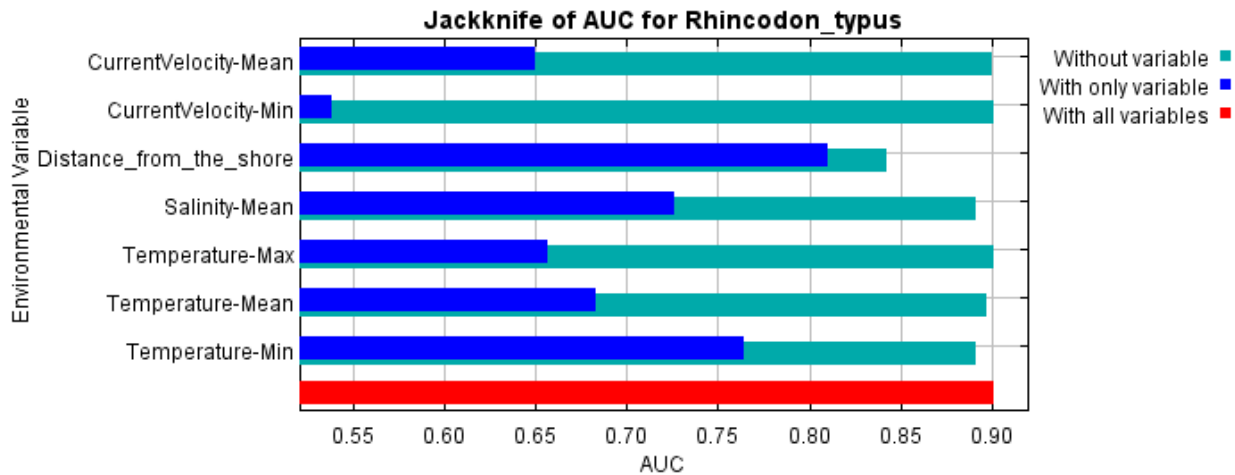


Fig. 36 Jackknife test showing the AUC values of Rhincodon typus when a variable is used in isolation or the variable is excluded from the model

Predicted distribution

The predicted current distribution is mainly concentrated in the Western coast of India, Persian Gulf, Red sea, Madagascar *etc.* with > 77% probability (Fig. 103). The predicted distribution for 2040-2050 of distribution decreases from RCP 4.5 to RCP 8.5. The AUC values for RCP4.5, 6.0 and 8.5 are 0.883 (SD 0.014), 0.885(SD 0.020) and 0.893 (SD 0.026) respectively (Fig. 102). Distance from the shore shows the highest test gain when used in isolation among all the other environmental variables. It is also the one environmental variable which has the maximum percent contribution in both RCPs. The predicted distribution for 2090-2100 shows a further decline in the extent. The AUC values for RCP 4.5, 6.0 and 8.5 are 0.882 (SD 0.025), 0.893(Sd 0.015) and 0.888 (SD 0.031) respectively (Fig. 102)

4.2.34. *Galeocerdo cuvier* Smith, 1828

Kingdom	Phylum	Class	Order	Family	Genus	Species
Animalia	Chordata	Elasmobranchii	Orectolobiformes	Rhincodontidae	<i>Rhincodon</i>	<i>typus</i>

4.2.34.1. Model Evaluation

The area under the curve value for the model is 0.911 with 0.015 standard deviation (Fig. 104). The model prediction for the current distribution shows distance from the shore as the greatest percentage contributor with value 35.5 and permutation importance 30.8. Minimum temperature, current velocity mean, maximum temperature salinity mean, and temperature mean, current velocity minimum contribute 19.2%, 18.6%, 17.2%, 5.3%, 3.4% and 0.9% respectively (Table 34). Jackknife test reveals that temperature maximum has the highest gain among all parameters when used in isolation (Fig. 37).

Variable	Percent contribution	Permutation importance
Distance from the shore	35.5	30.8
Temperature Min	19.2	10.7
Current velocity mean	18.6	16.1
Temperature maximum	17.2	19.3
Salinity Mean	5.3	8.3
Temperature mean	3.4	11.3
Current velocity min	0.9	3.5

Table 33 Table showing the percentage contribution and permutation importance of each environmental variable for the predicted current distribution

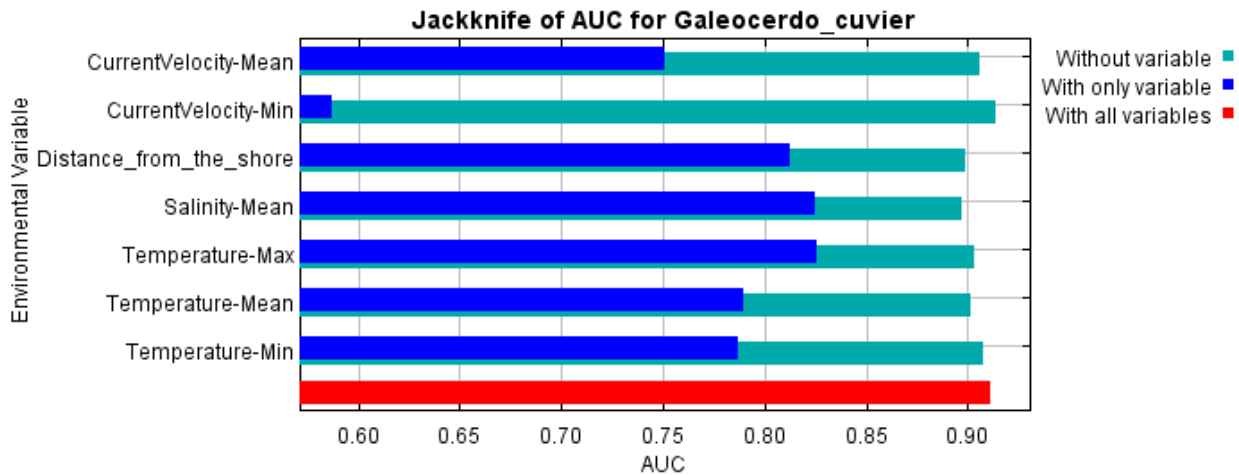


Fig. 37 Jackknife test showing the AUC values of Galeocerdo cuvier when a variable is used in isolation or the variable is excluded from the model

Predicted distribution

The predicted current distribution is mainly concentrated in the eastern part of Madagascar, eastern coast of Africa *etc.* with > 85% probability (Fig. 105). The predicted distribution for 2040-2050 is concentrated in the same areas as that of the current distribution but the probability of distribution decreases from RCP 4.5 to RCP 8.5 with probability 50% to 75%. The extent also shows a gradual decrease. The AUC values for RCP 4.5, 6.0 and 8.5 are 0.911 (SD 0.018), 0.921(SD 0.013) and 0.912 (SD 0.012) respectively (Fig. 104). Temperature maximum shows the highest test gain when used in isolation among all the other environmental variables. Distance from the shore is the environmental variable which has the maximum percent contribution in all RCPs. The predicted distribution for 2090-2100 shows a further decline in the extent as well as in the probability of distribution (50-70%). The AUC values for RCP 4.5, 6.0 and 8.5 are 0.915 (SD 0.011), 0.908 (SD 0.016) and 0.907 (SD 0.022) respectively (Fig. 104).

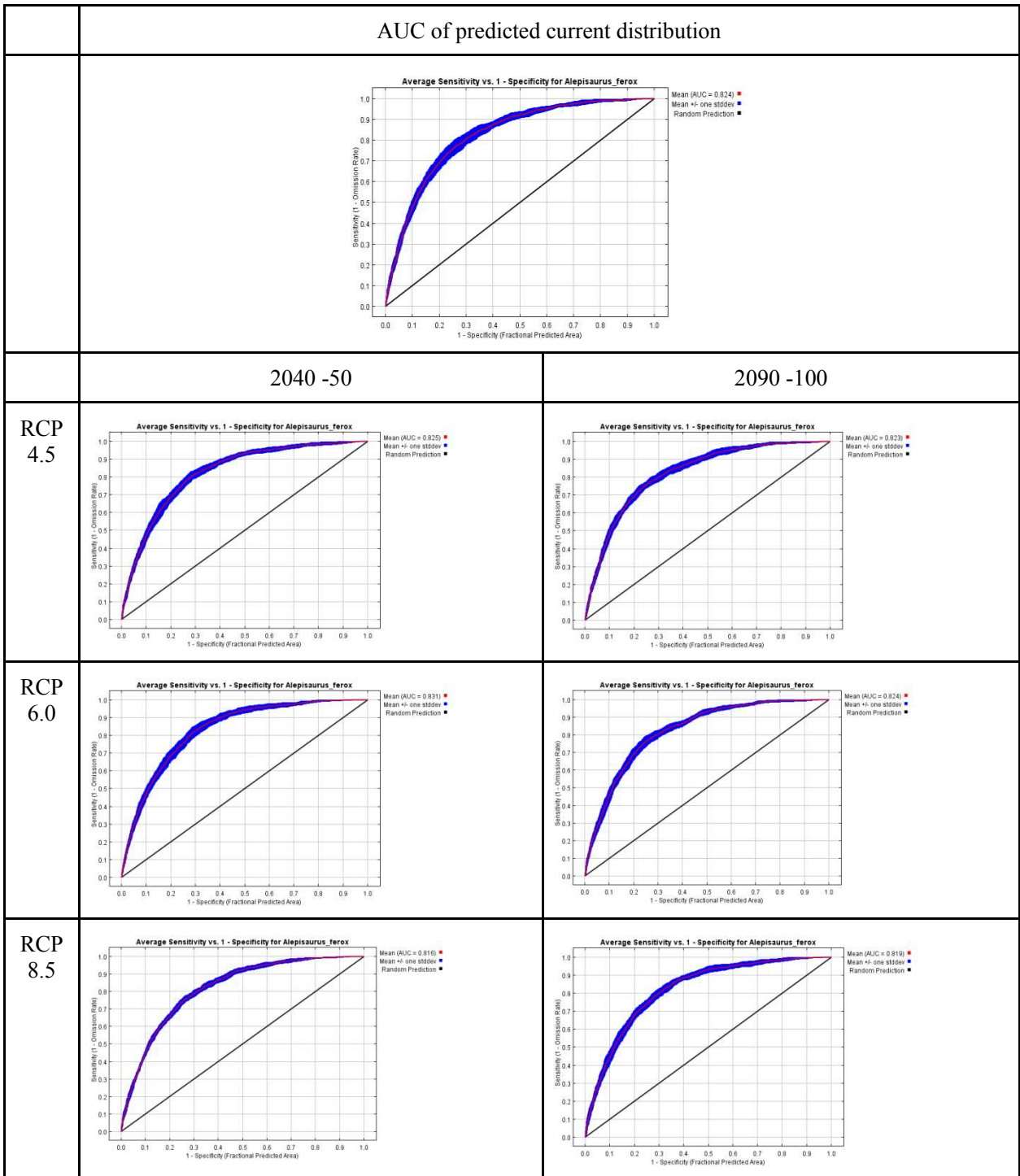


Fig. 38 The average sensitivity vs. 1- specificity graph for *A. ferox* showing the mean Area Under the Curve (AUC) and standard deviation for the predicted current distribution the predicted future distributions

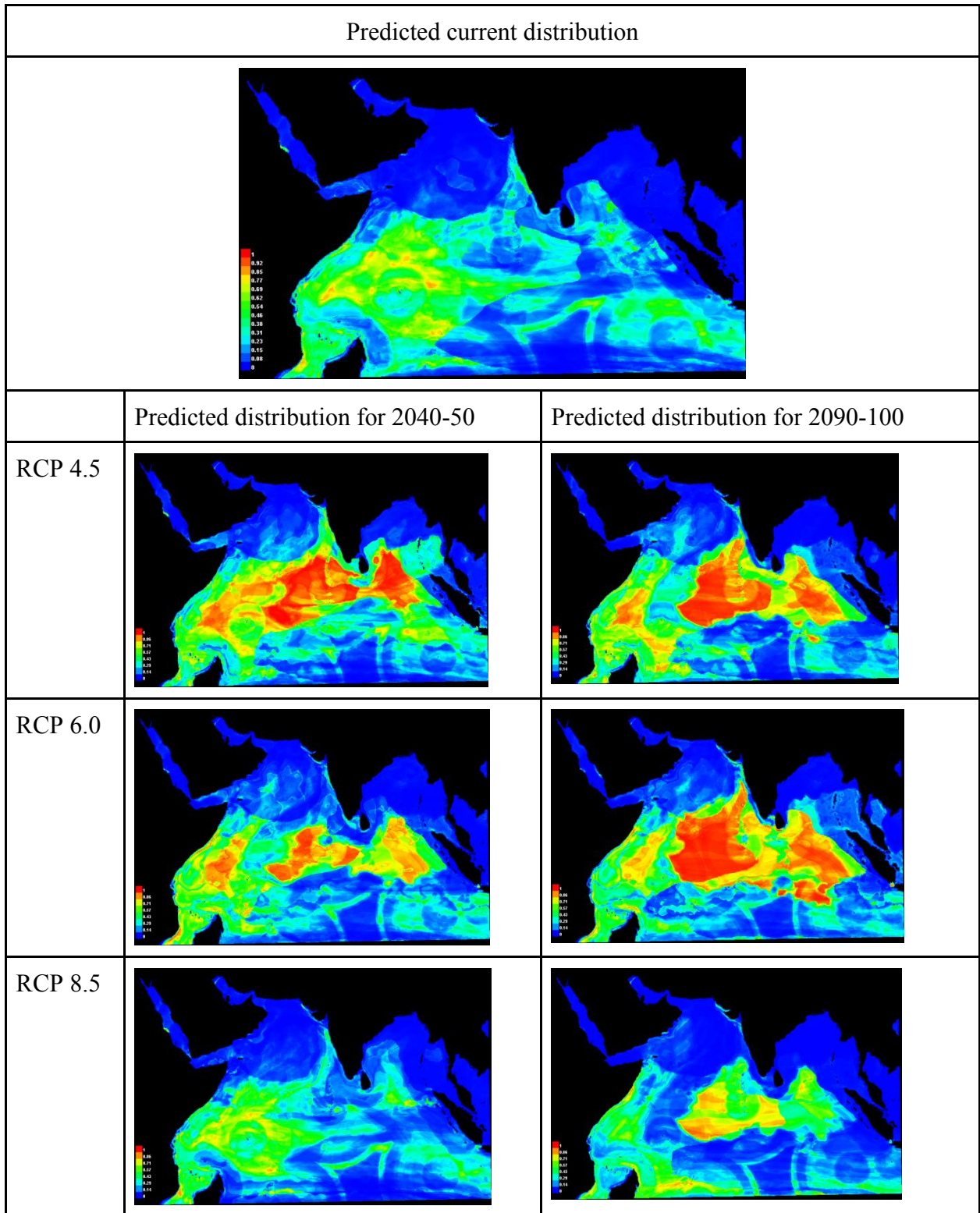


Fig. 39 Map showing the predicted current and future distributions of *A. ferox*

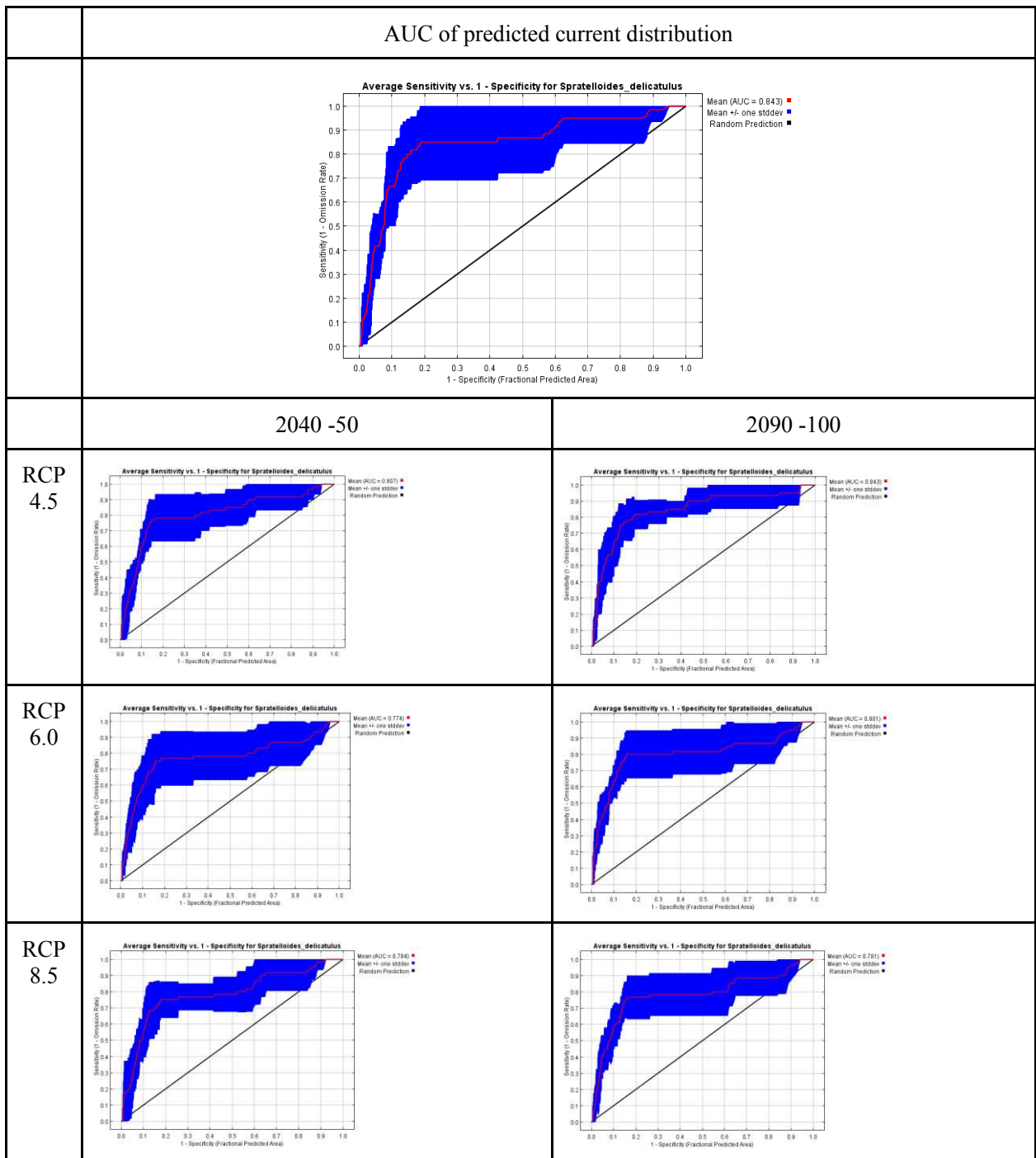


Fig. 40 The average sensitivity vs. 1- specificity graph for *Spratelloides delicatulus* showing the mean Area Under the Curve (AUC) and standard deviation for the predicted current distribution the predicted future distributions

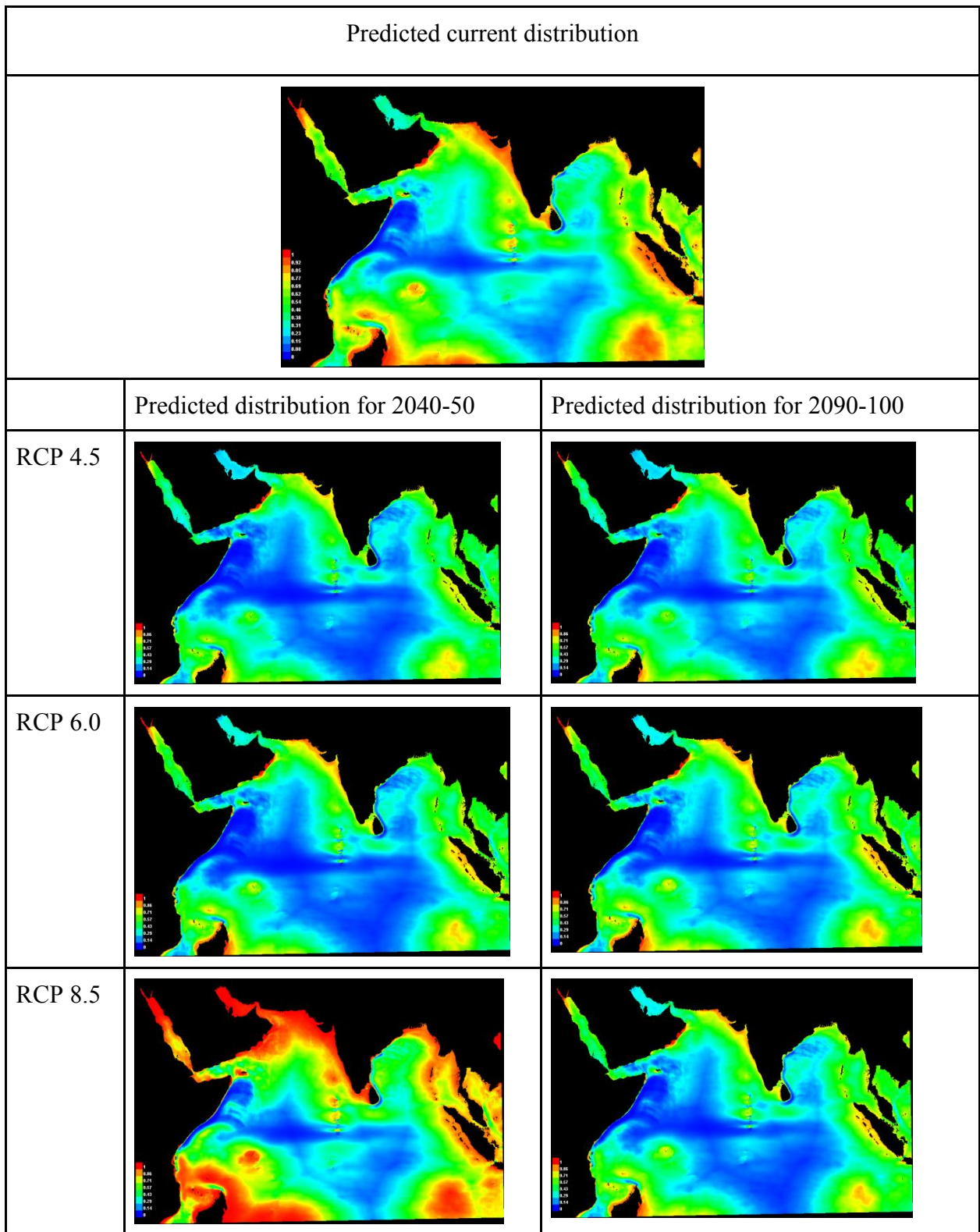


Fig. 41 Map showing the predicted current and future distributions of *Spratelloides delicatulus*

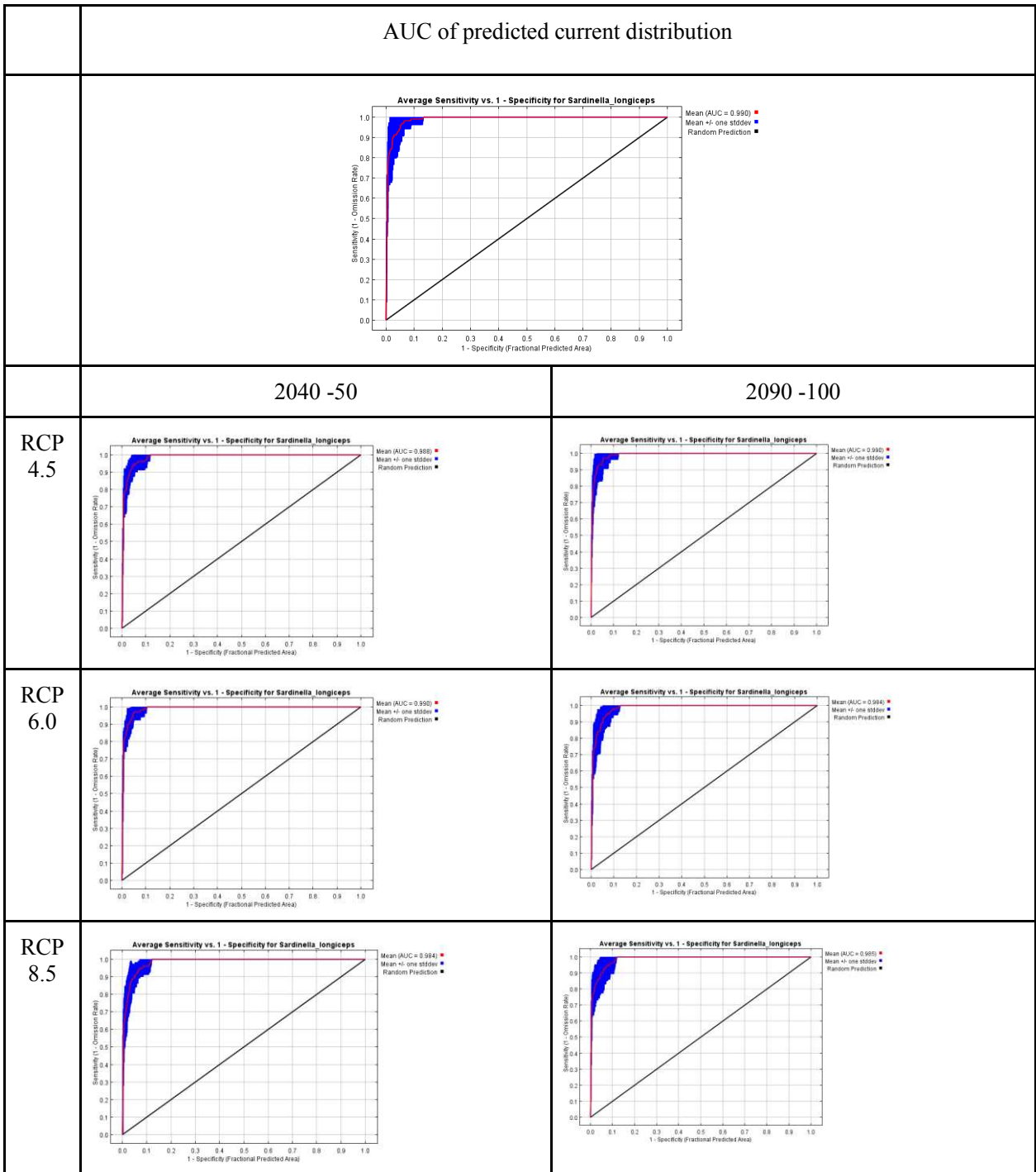


Fig. 42 The average sensitivity vs. 1- specificity graph for *Sardinella longiceps* showing the mean Area Under the Curve (AUC) and standard deviation for the predicted current distribution the predicted future distributions

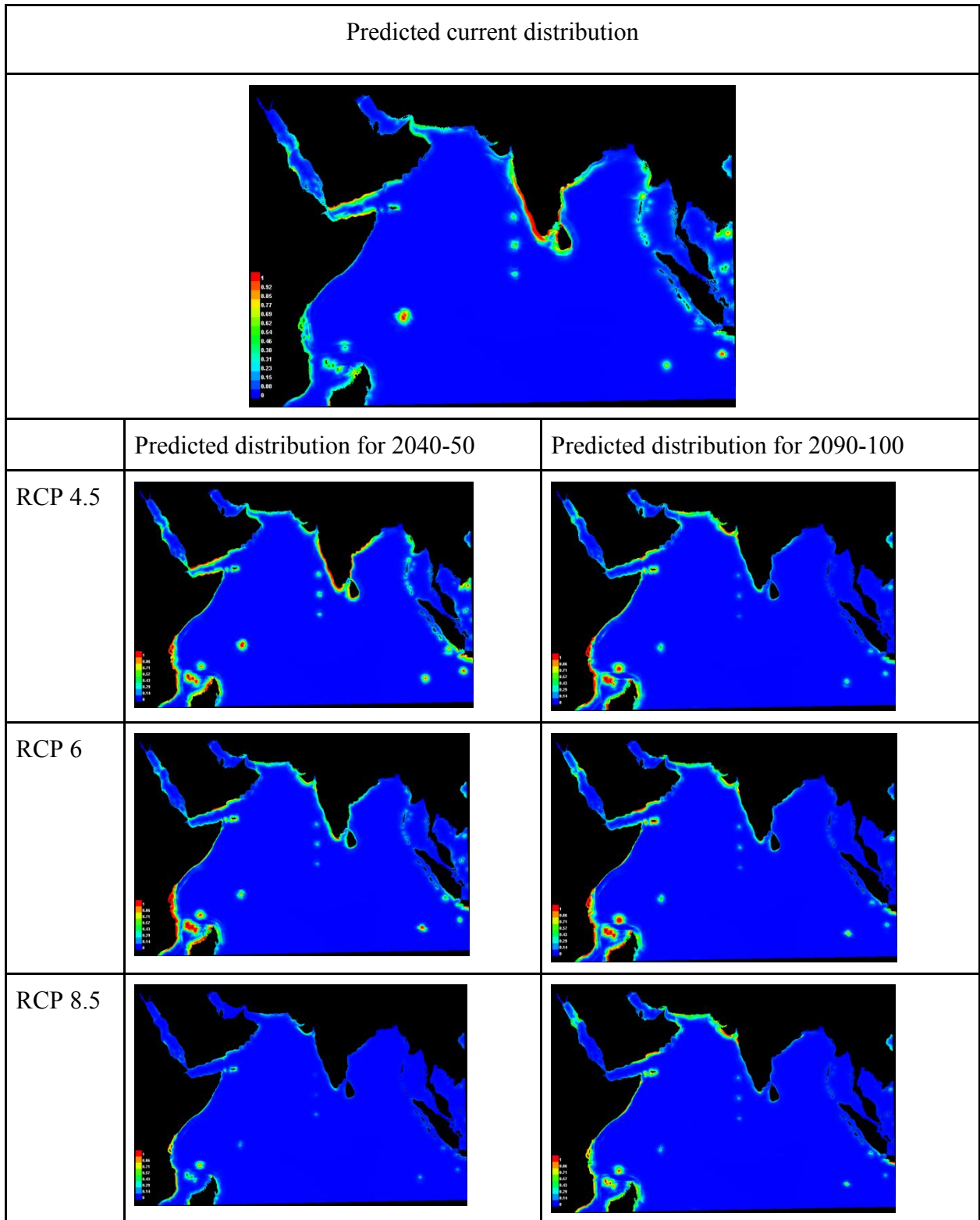


Fig. 43 Map showing the predicted current and future distributions of *Sardinella longiceps*

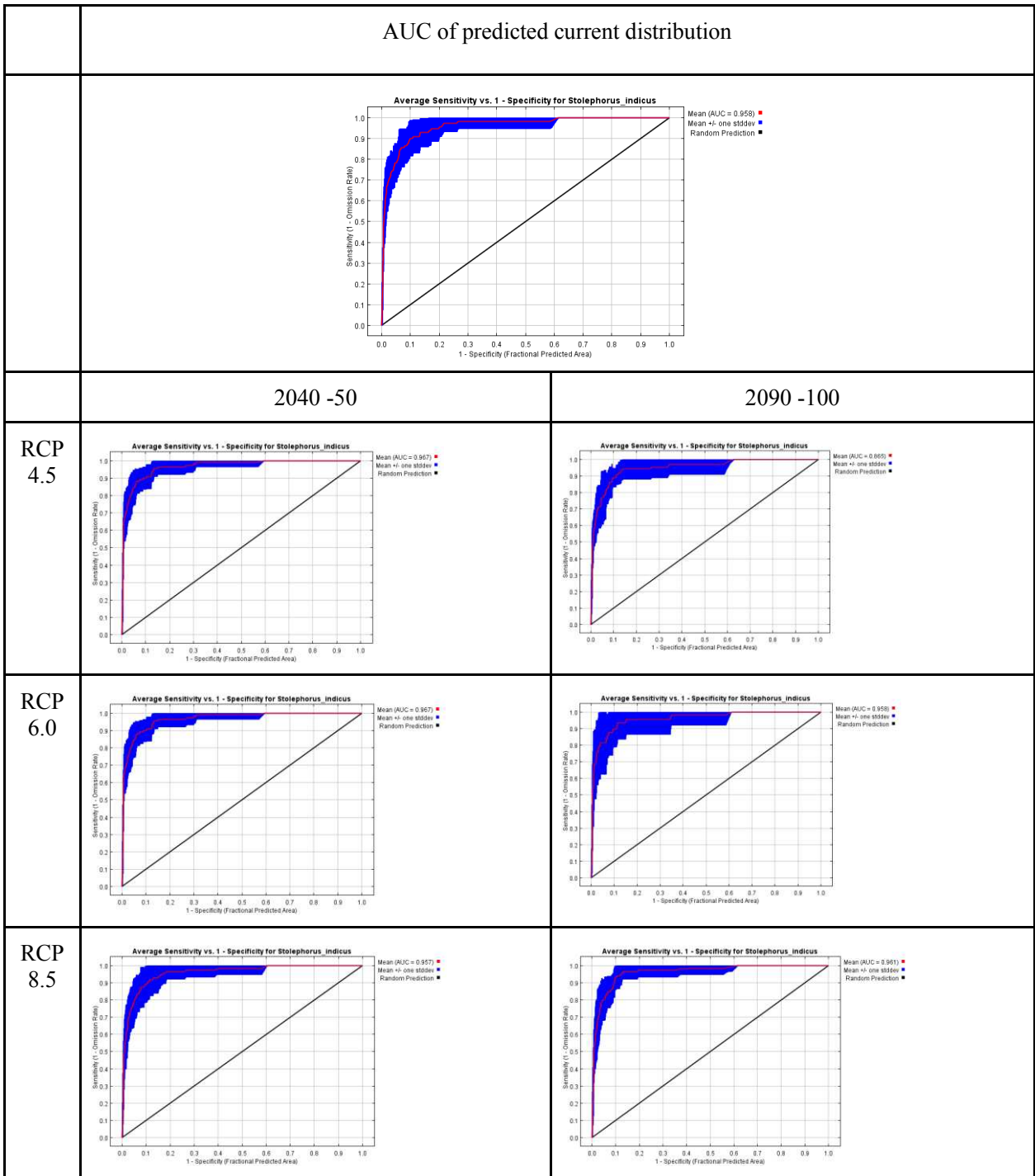


Fig. 44 The average sensitivity vs. 1- specificity graph for *Stolephorus indicus* showing the mean Area Under the Curve (AUC) and standard deviation for the predicted current distribution the predicted future distributions

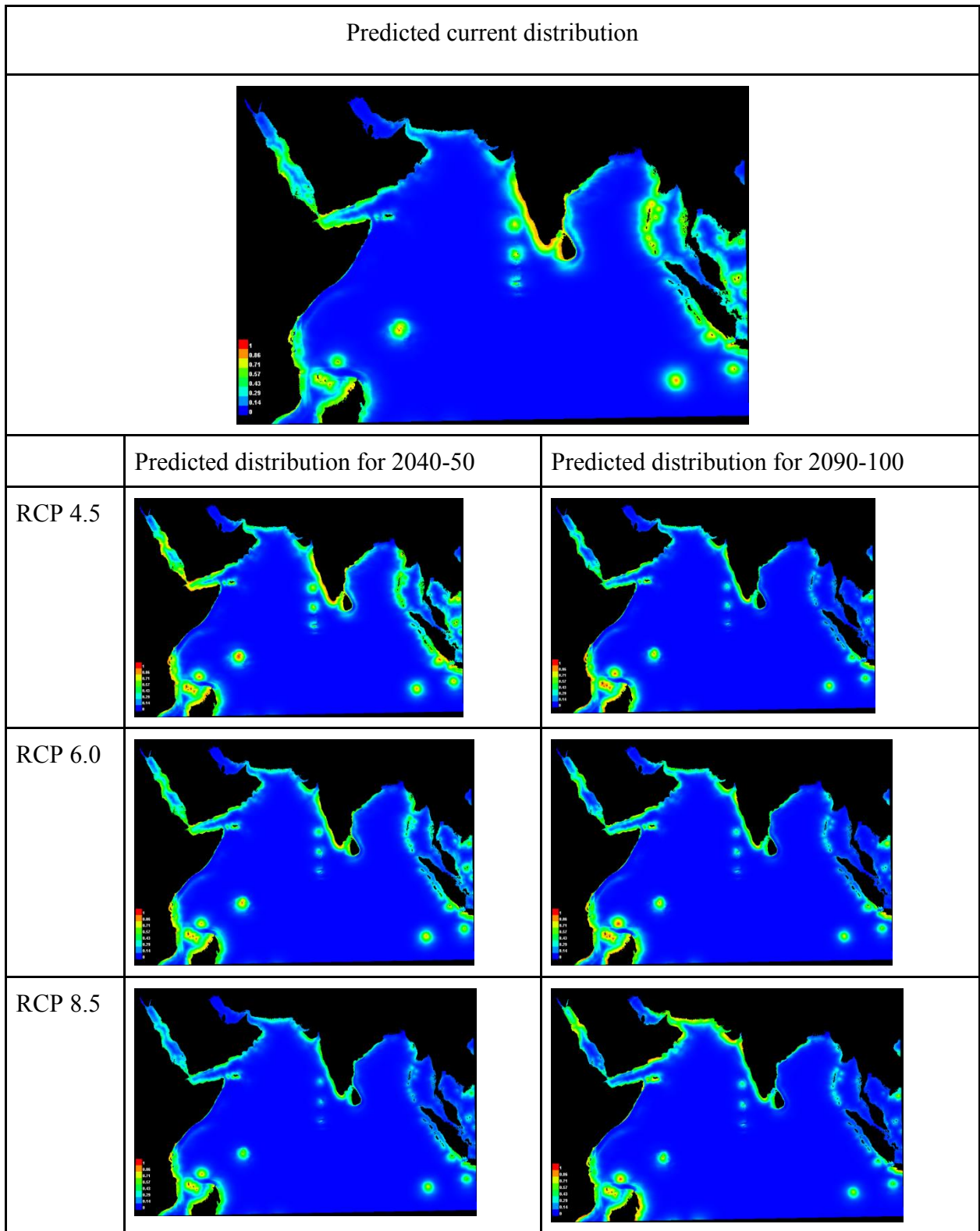


Fig. 45 Map showing the predicted current and future distributions of *Stolephorus indicus*

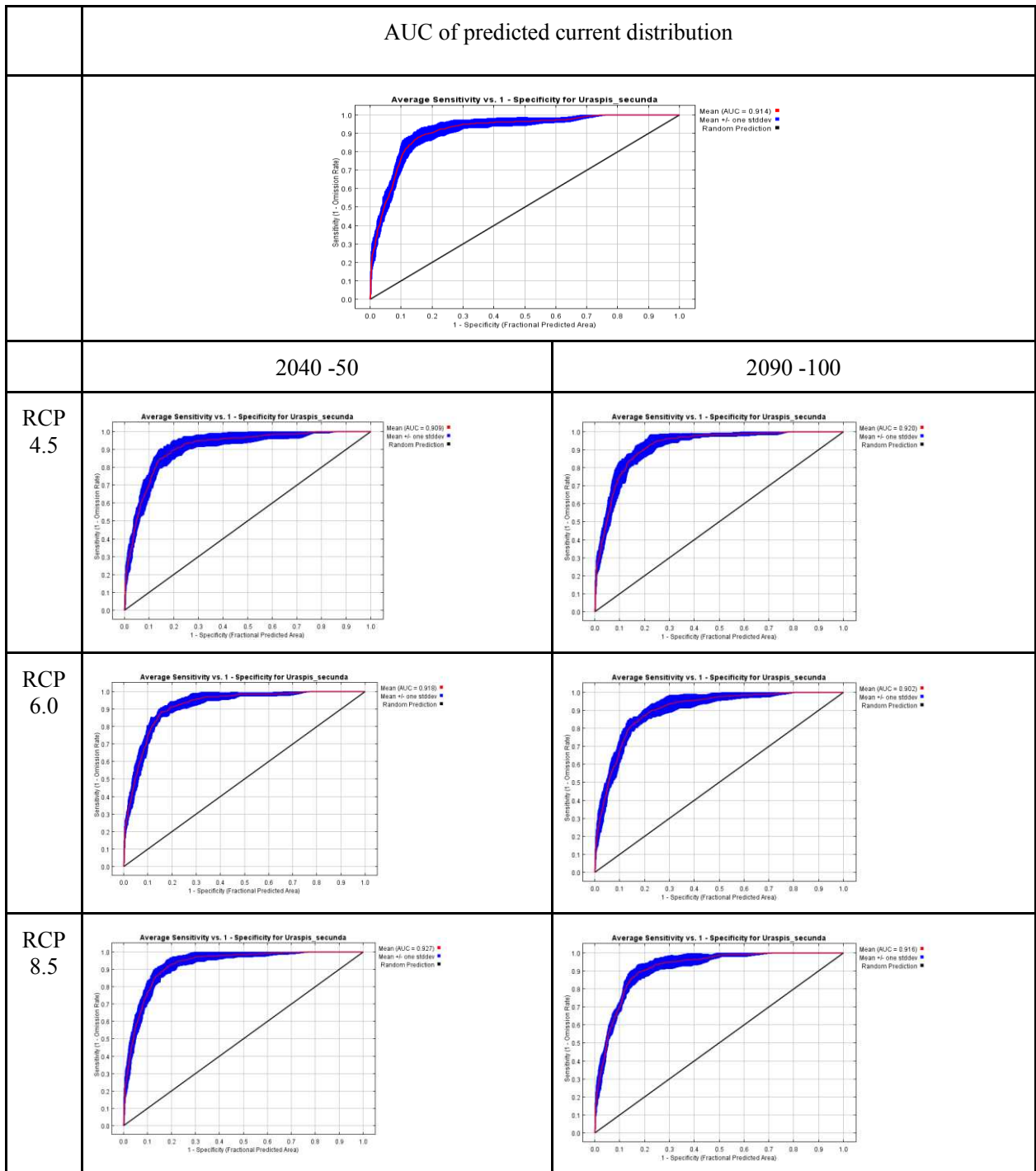


Fig. 46 The average sensitivity vs. 1- specificity graph for *Uraspis secunda* showing the mean Area Under the Curve (AUC) and standard deviation for the predicted current distribution the predicted future distributions

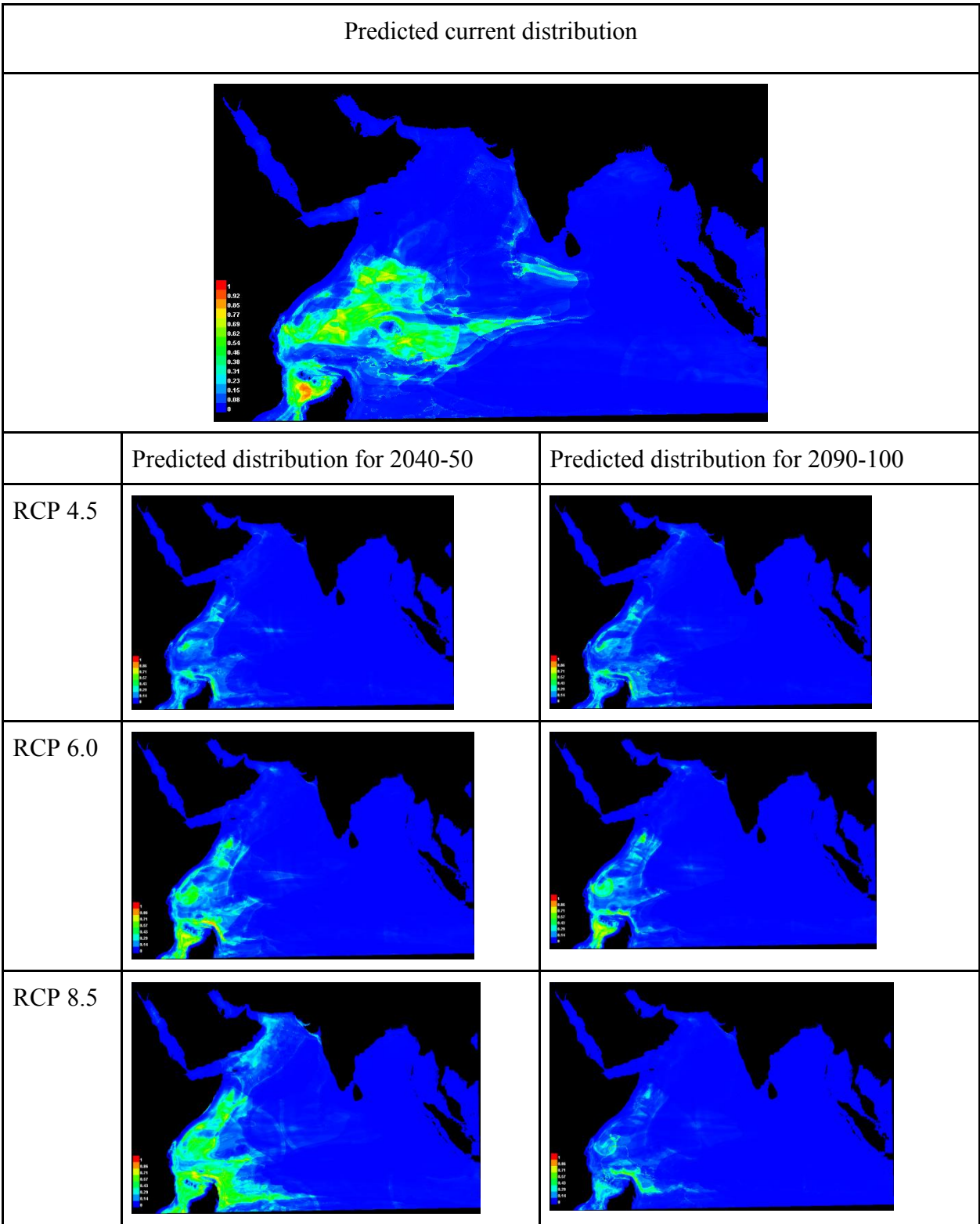


Fig. 47 Map showing the predicted current and future distributions of *Uraspis secunda*

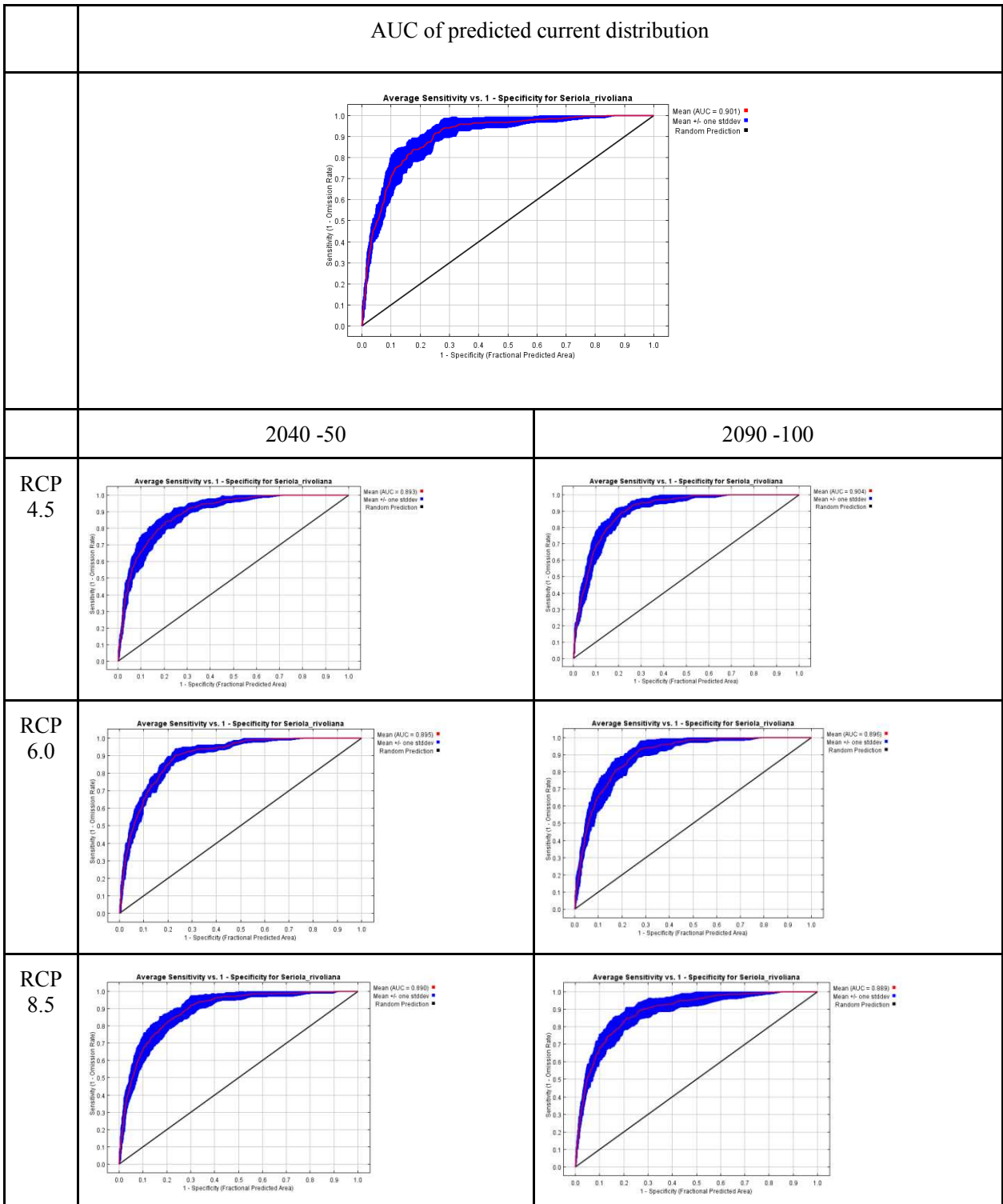


Fig. 48 The average sensitivity vs. 1- specificity graph for Seriola rivoliانا showing the mean Area Under the Curve (AUC) and standard deviation for the predicted current distribution the predicted future distributions

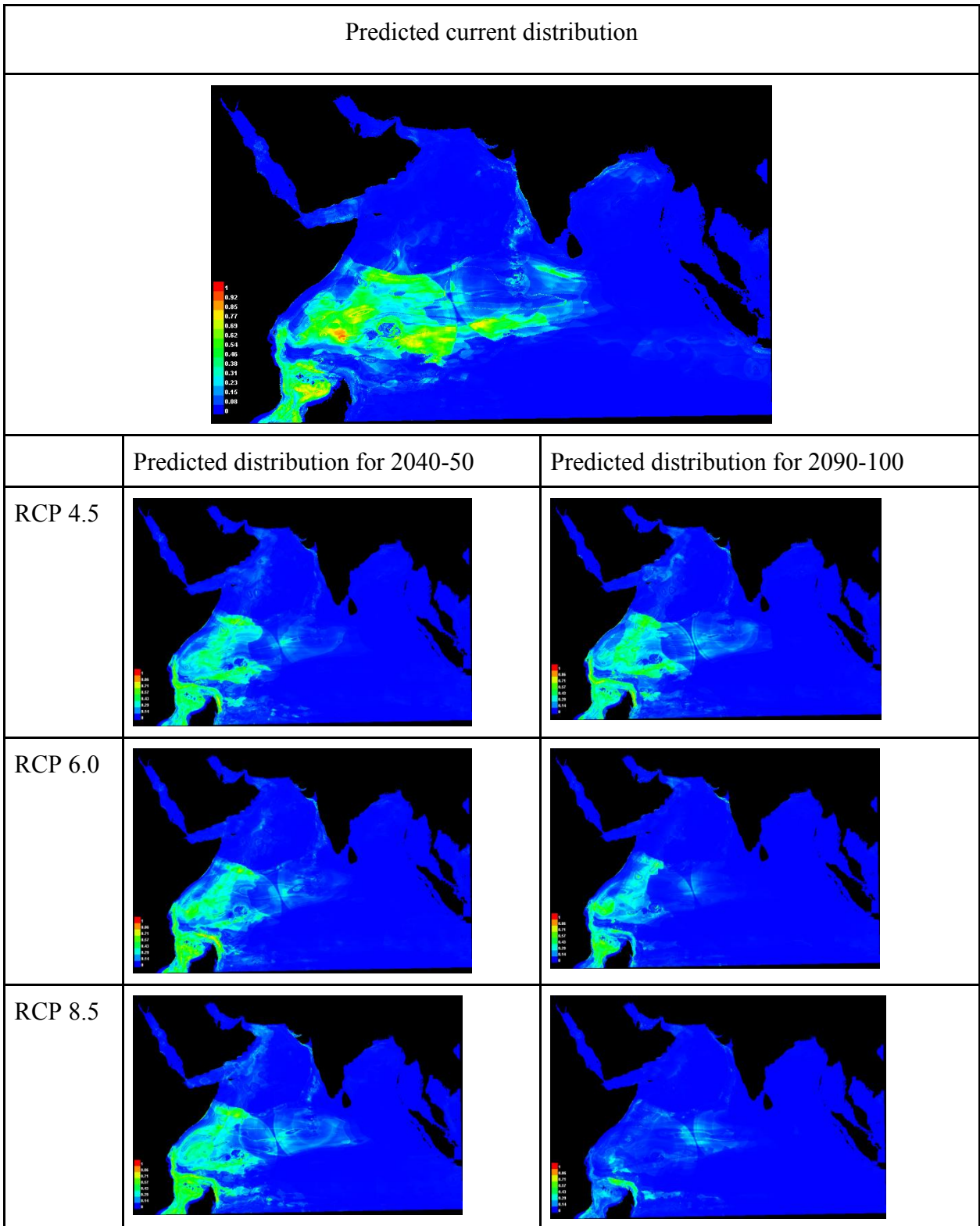


Fig. 49 Map showing the predicted current and future distributions of *Seriola rivoliana*

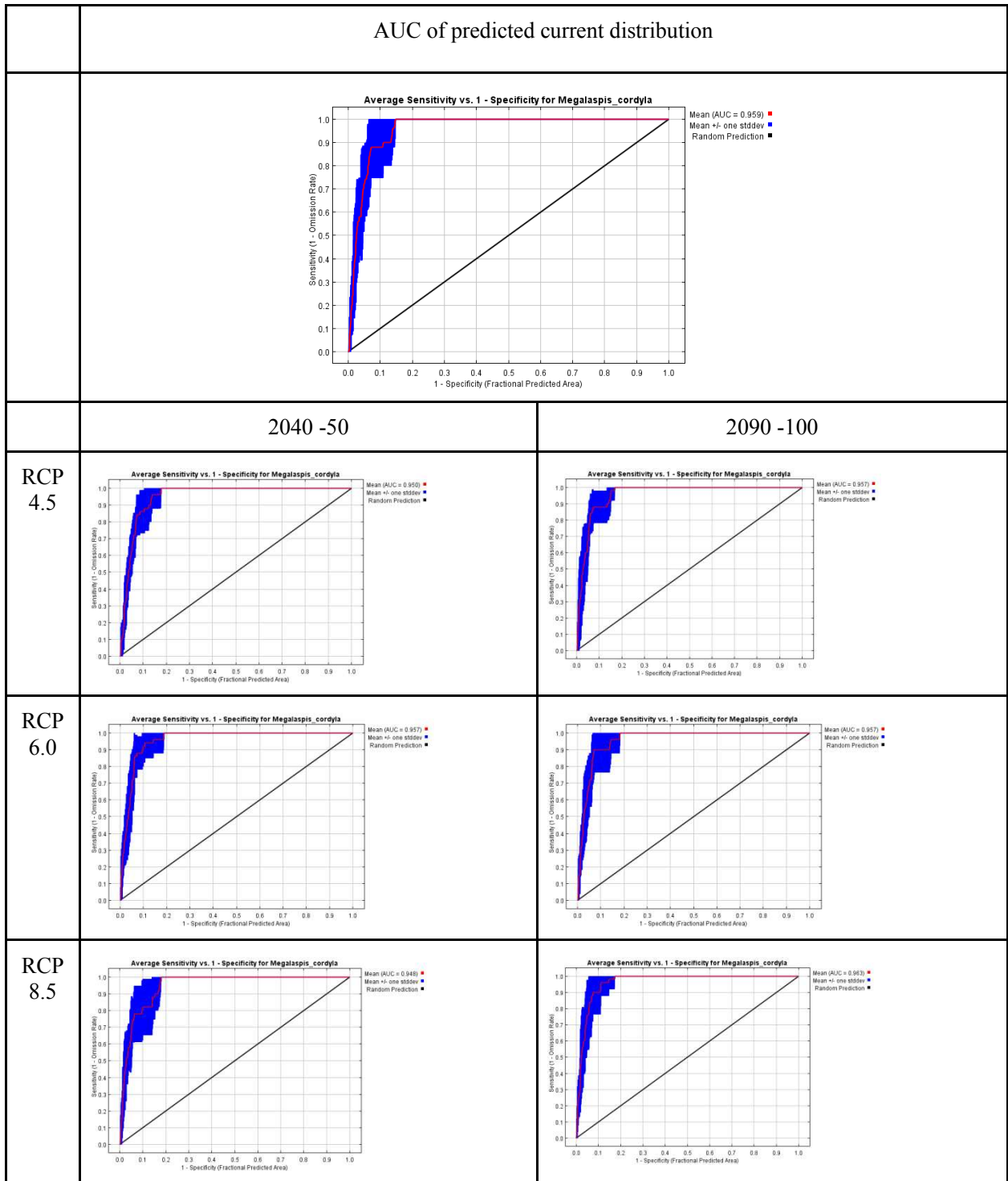


Fig. 50 The average sensitivity vs. 1- specificity graph for *Megalaspis cordyla* showing the mean Area Under the Curve (AUC) and standard deviation for the predicted current distribution the predicted future distributions.

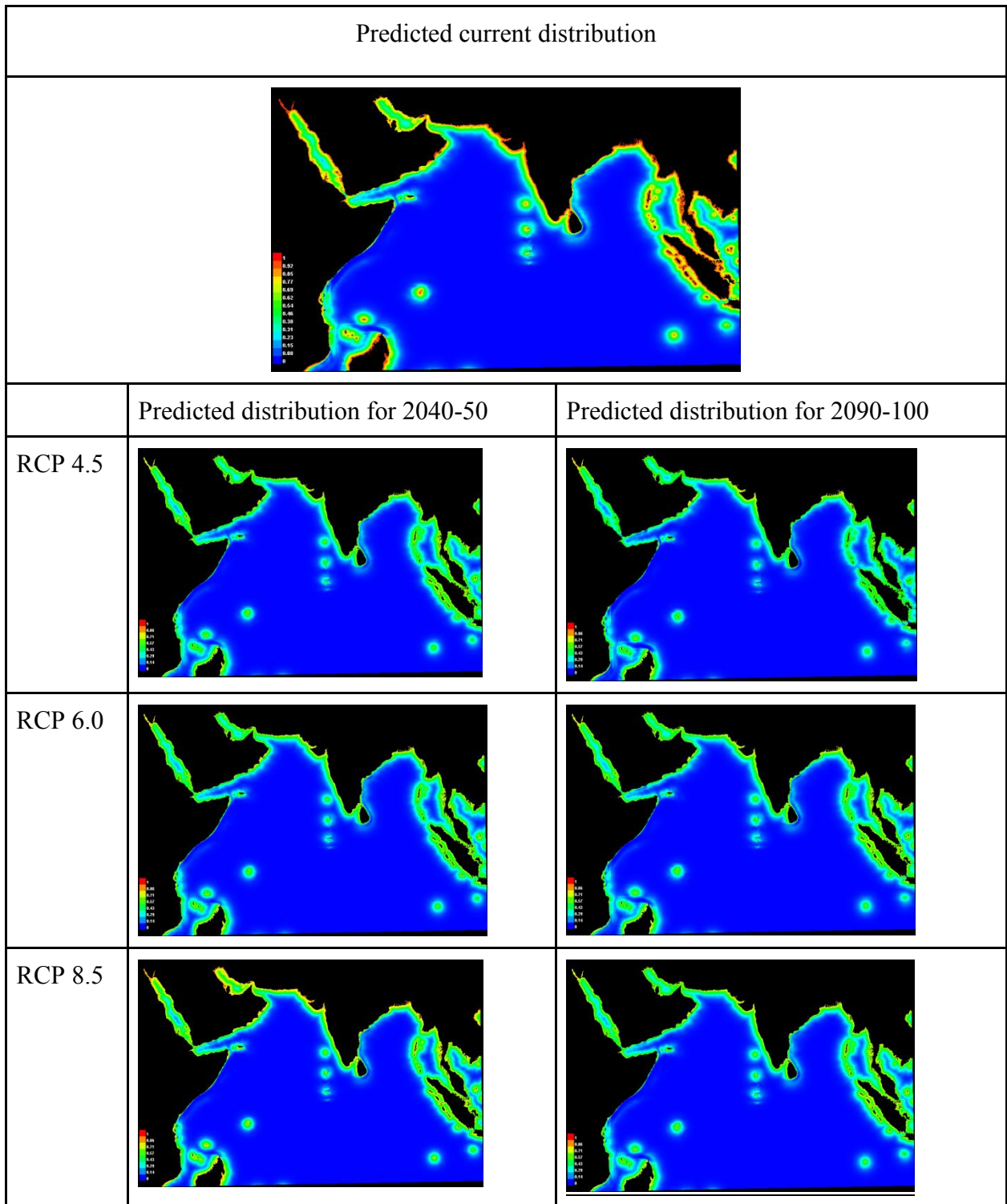


Fig. 51 Map showing the predicted current and future distributions of *Megalaspis cordyla*

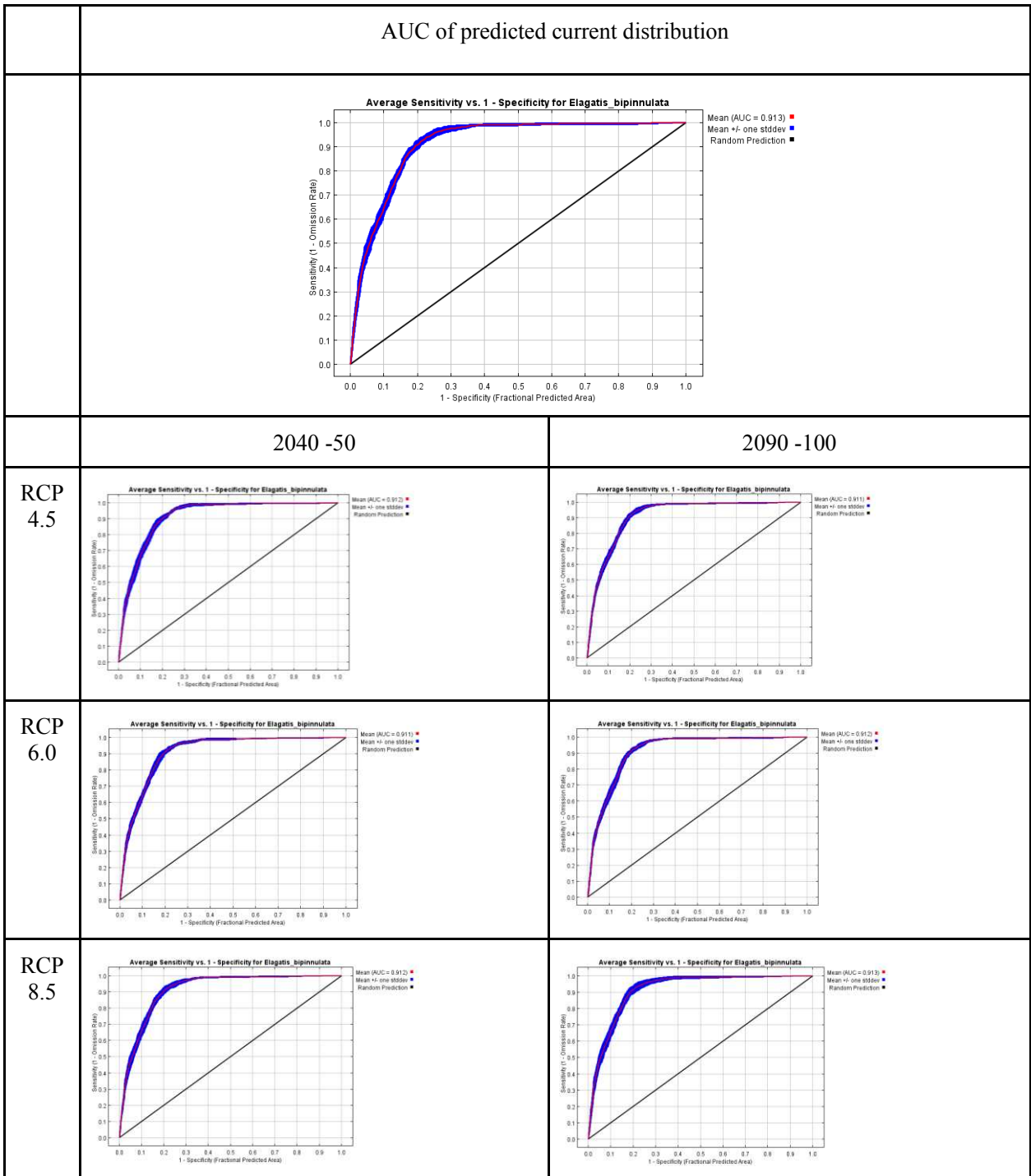


Fig. 52 The average sensitivity vs. 1- specificity graph for *Elagatis bipinnulata* showing the mean Area Under the Curve (AUC) and standard deviation for the predicted current distribution the predicted future distributions

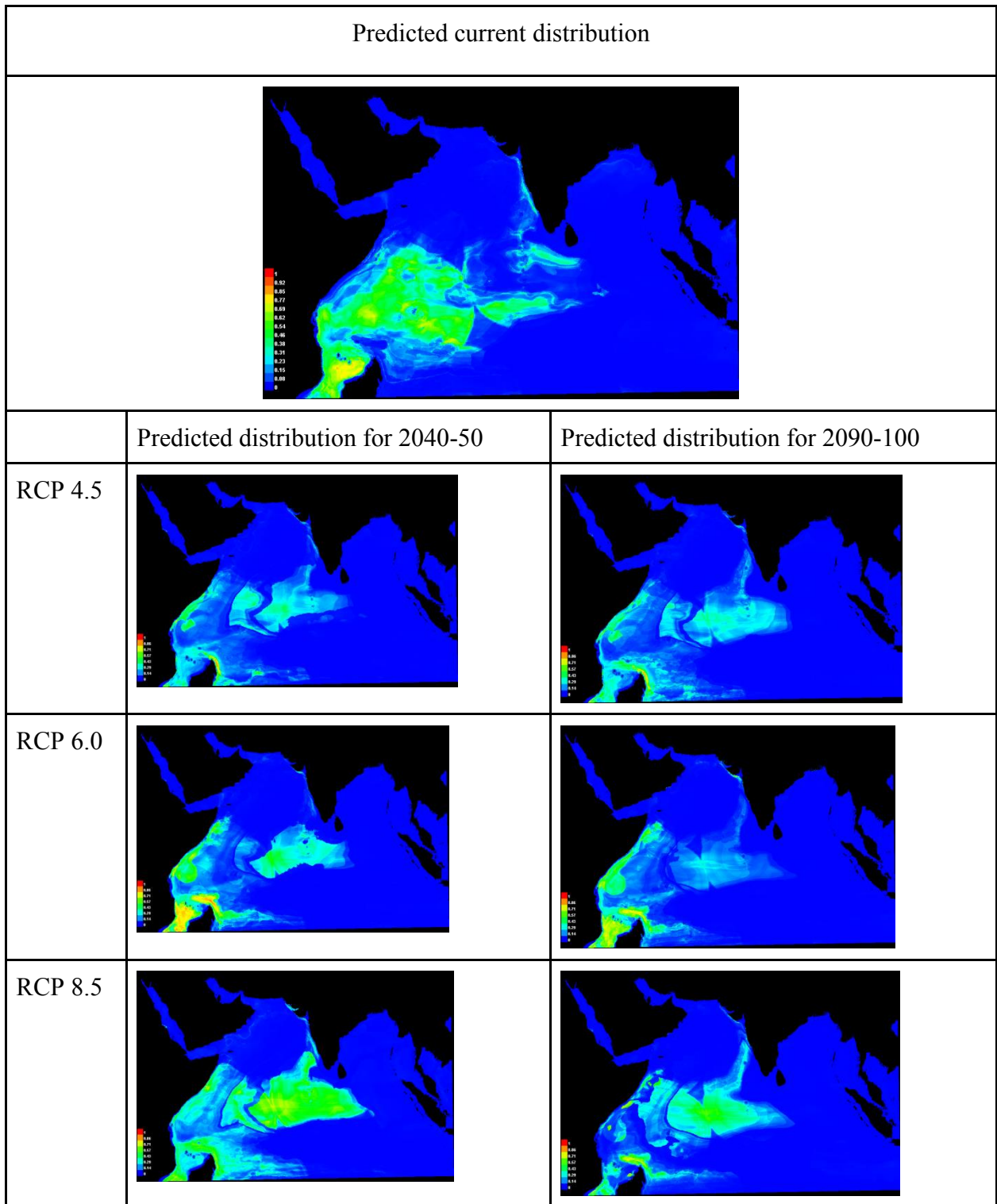


Fig. 53 Map showing the predicted current and future distributions of *Elagatis bipinnulata*

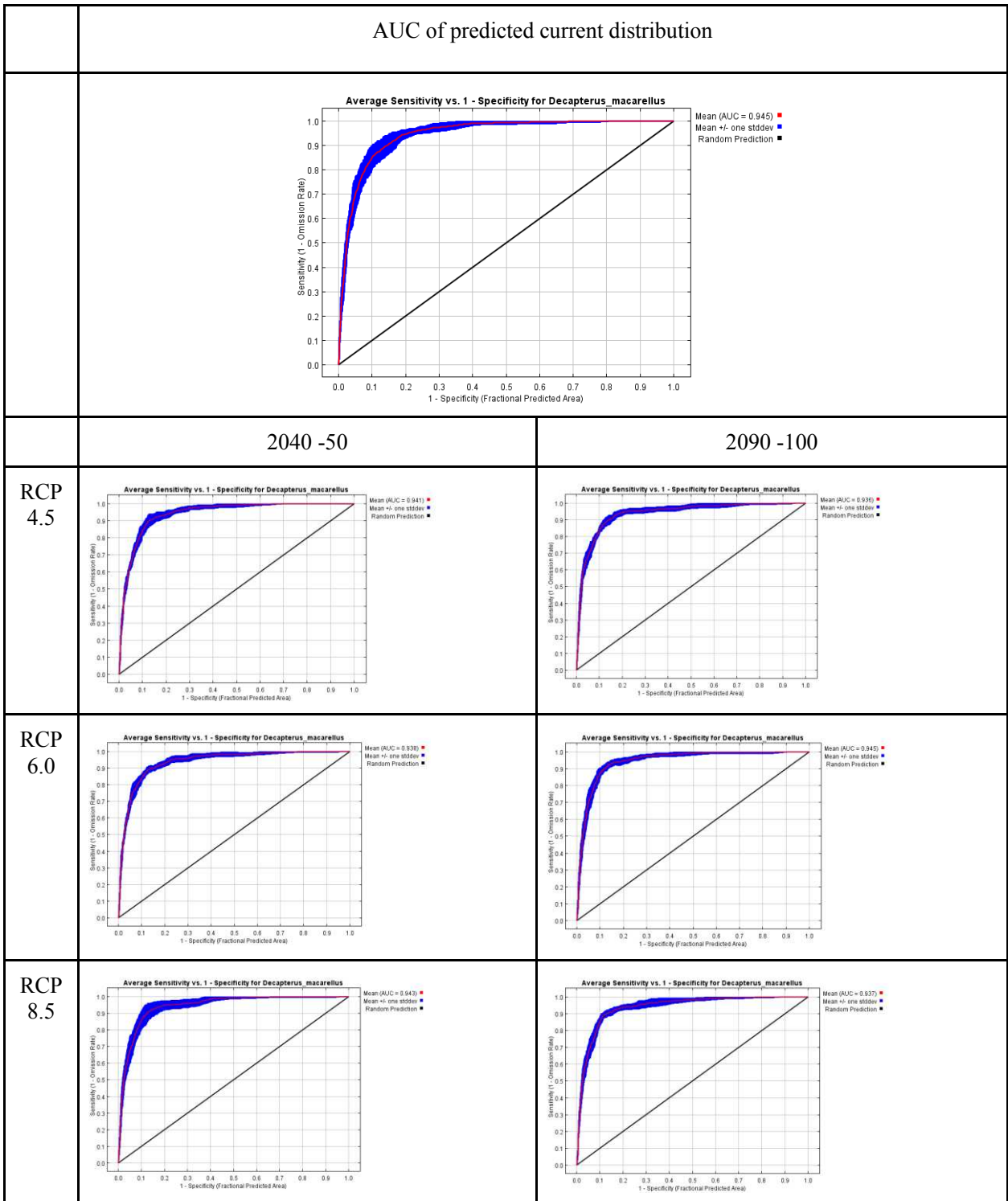


Fig. 54 The average sensitivity vs. 1- specificity graph for *Decapterus macarellus* showing the mean Area Under the Curve (AUC) and standard deviation for the predicted current distribution the predicted future distributions

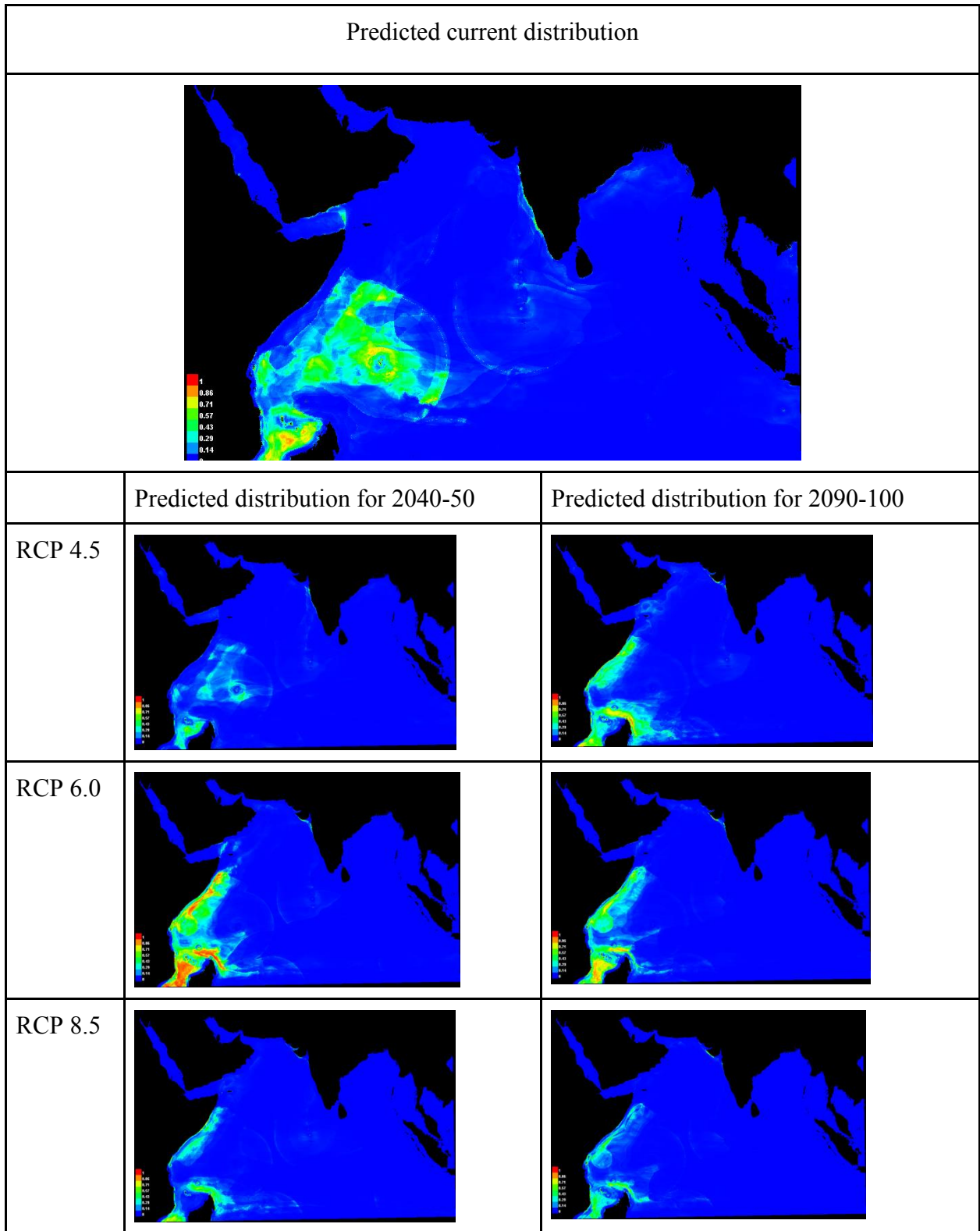


Fig. 55 Map showing the predicted current and future distributions of *Decapterus macarellus*

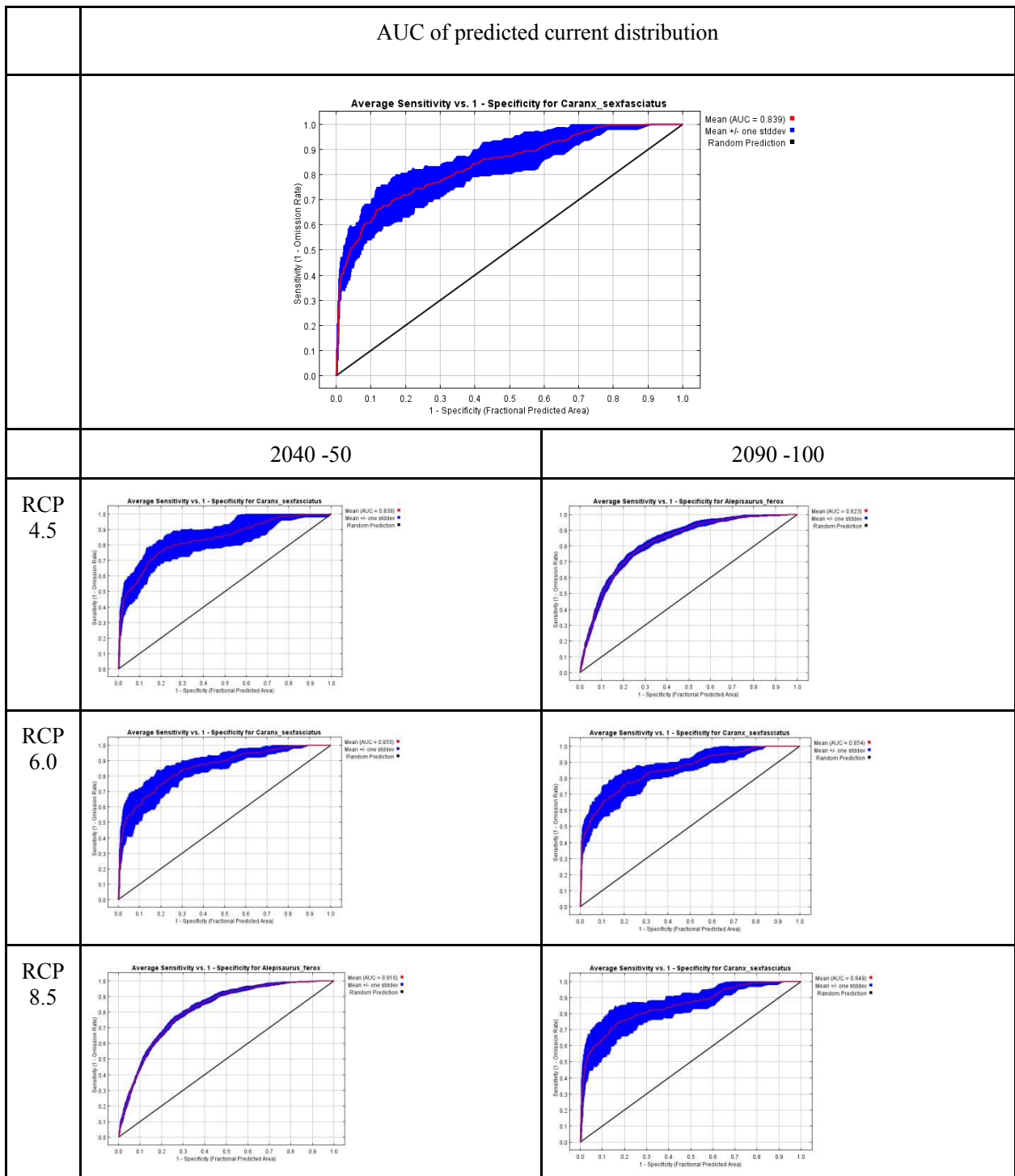


Fig. 56 The average sensitivity vs. 1-specificity graph for *Caranx sexfasciatus* showing the mean Area Under the Curve (AUC) and standard deviation for the predicted current distribution the predicted future distributions

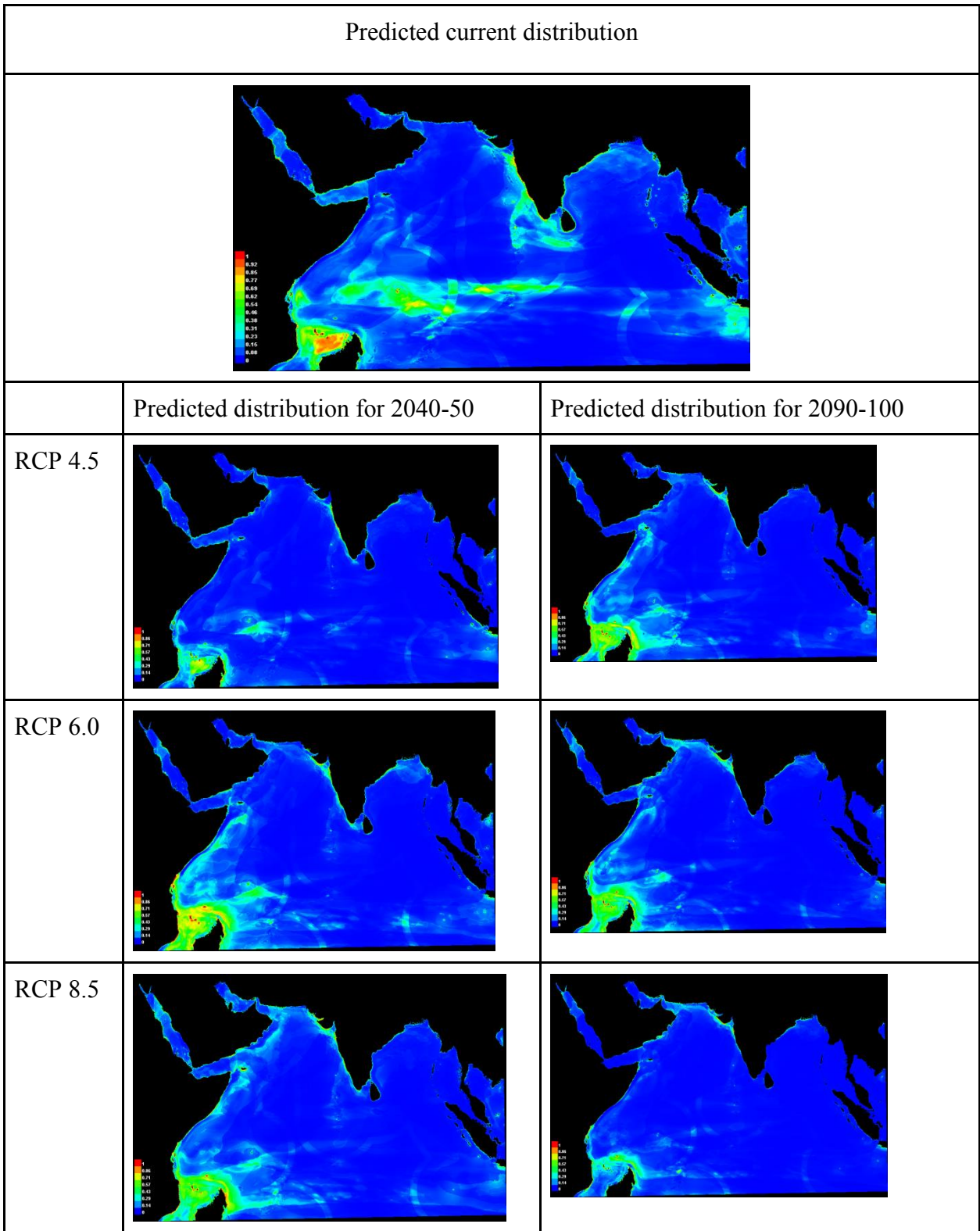


Fig. 57 Map showing the predicted current and future distributions of *C. sexfasciatus*

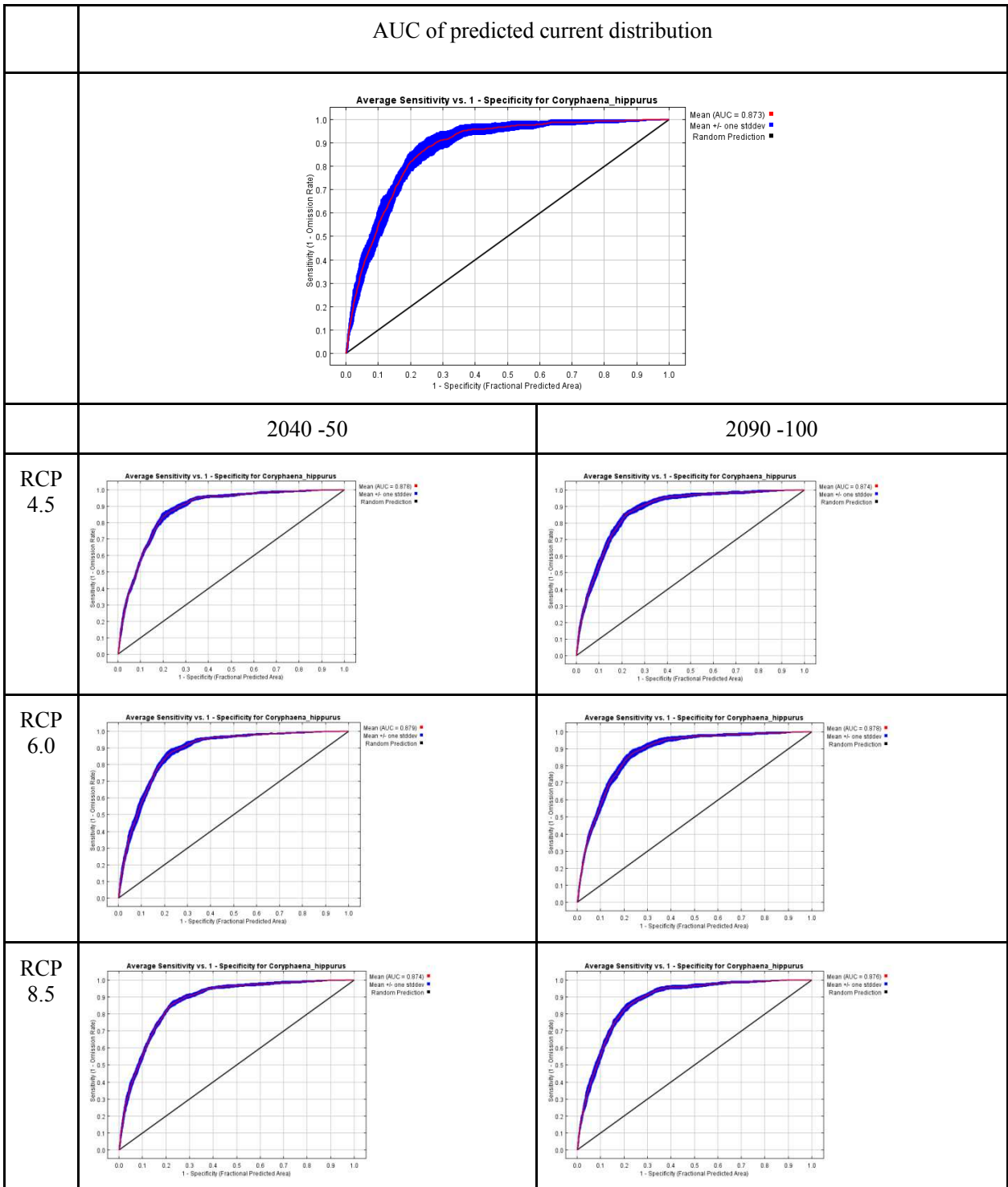


Fig. 58 The average sensitivity vs. 1- specificity graph for *Coryphaena hippurus* showing the mean Area Under the Curve (AUC) and standard deviation for the predicted current distribution the predicted future distributions

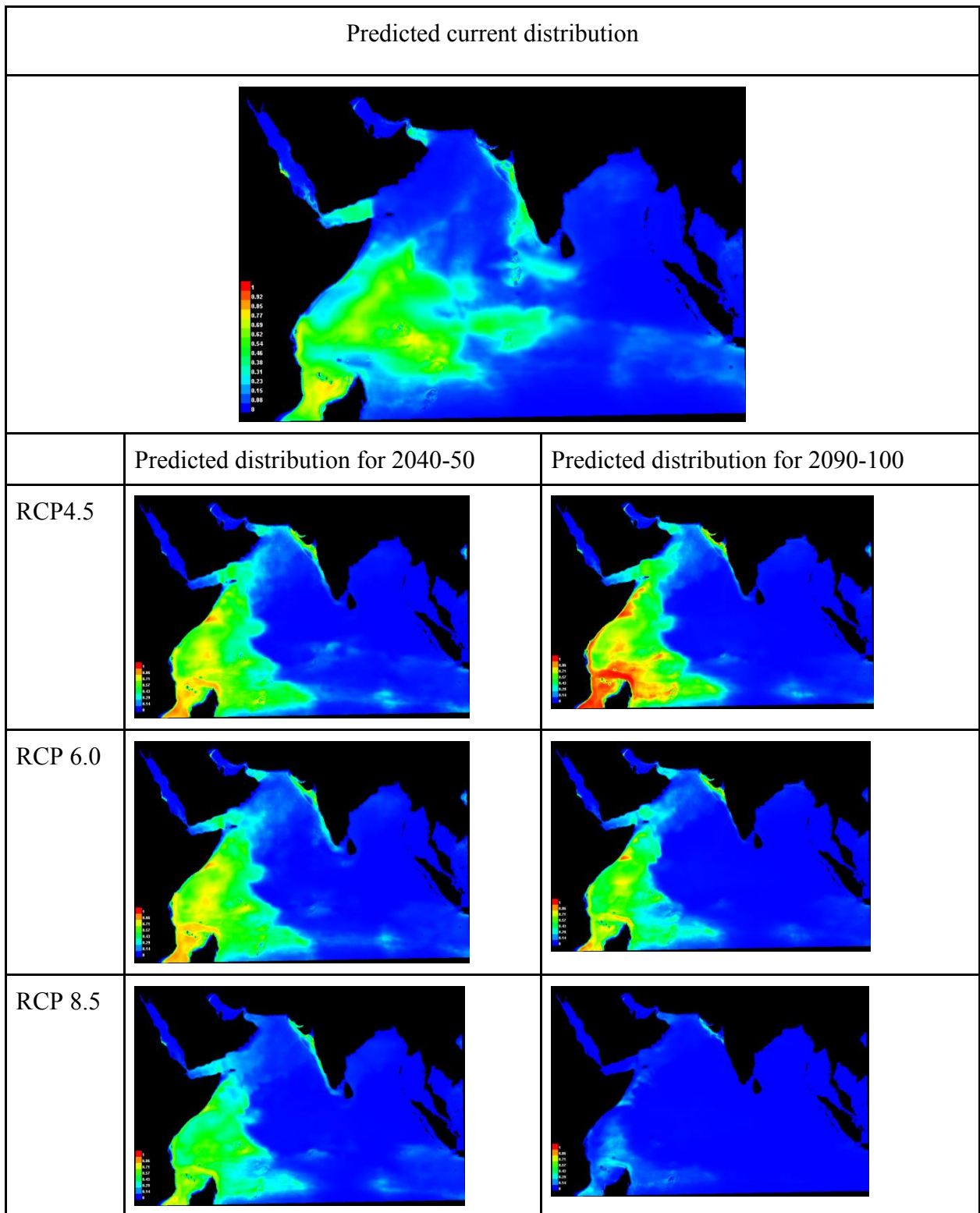


Fig. 59 Map showing the predicted current and future distributions of *Coryphaena hippurus*

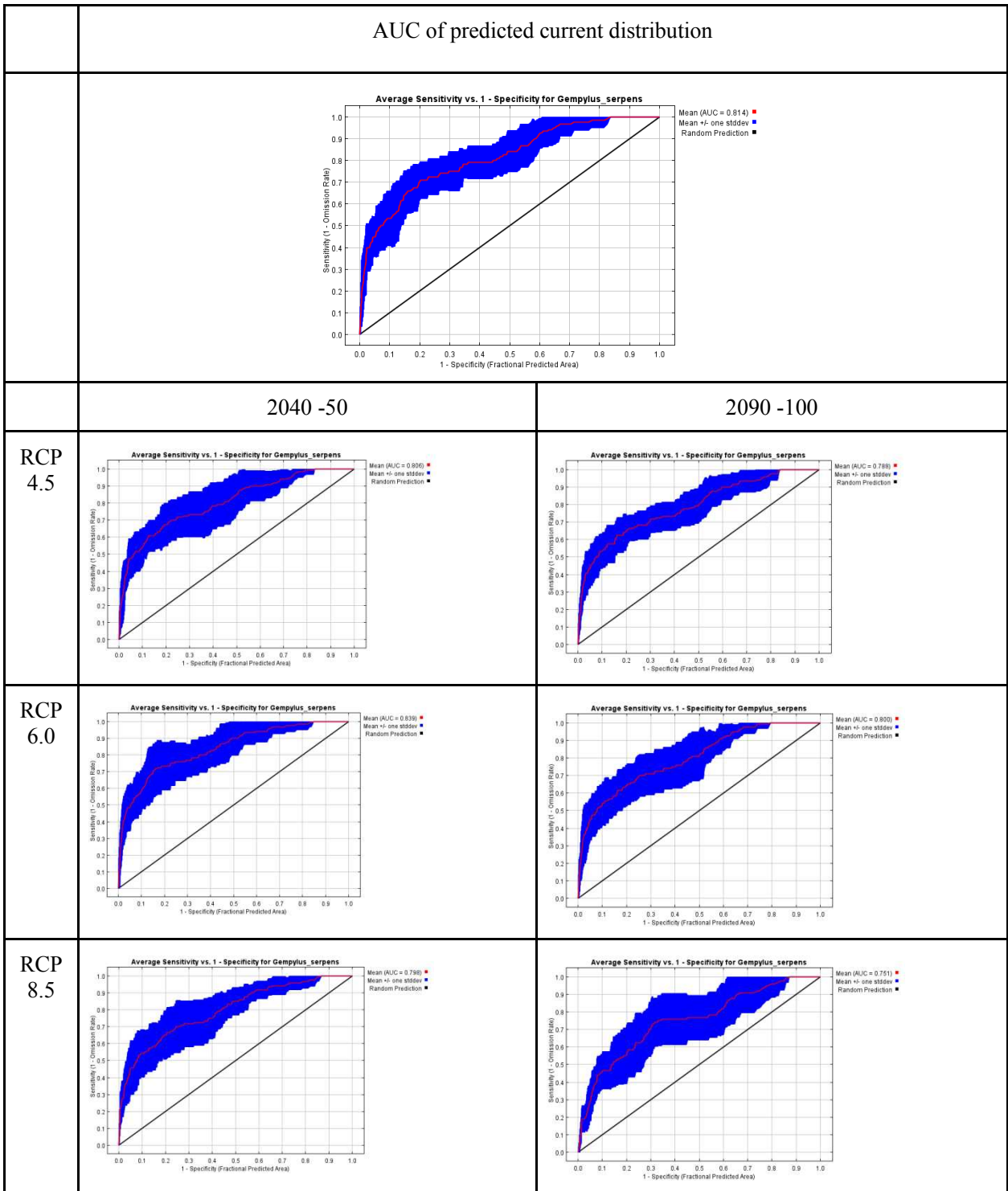


Fig. 60 The average sensitivity vs. 1- specificity graph for *Gempylus serpens* showing the mean Area Under the Curve (AUC) and standard deviation for the predicted current distribution the predicted future distributions

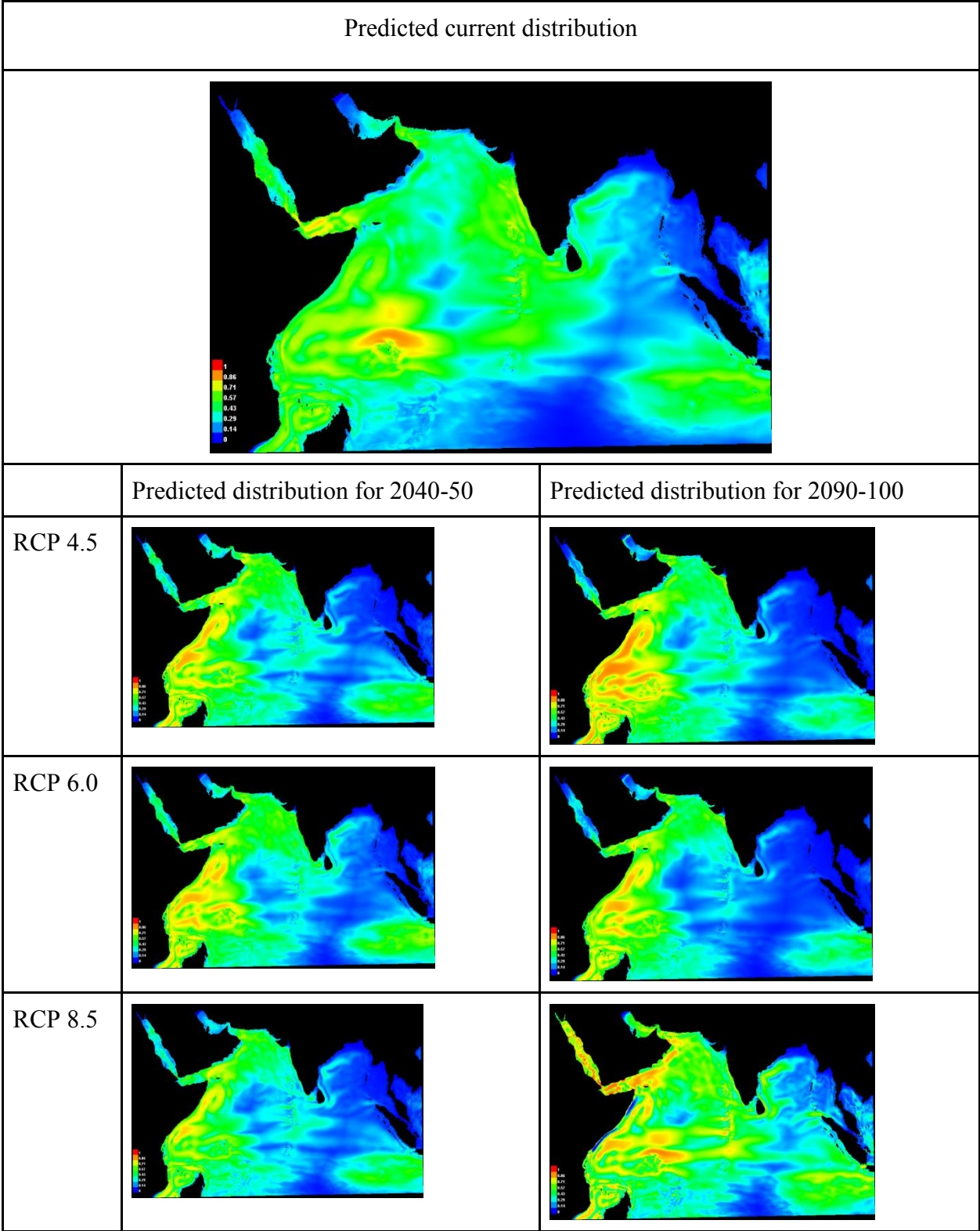


Fig. 61 Map showing the predicted current and future distributions of *Gempylus serpens*

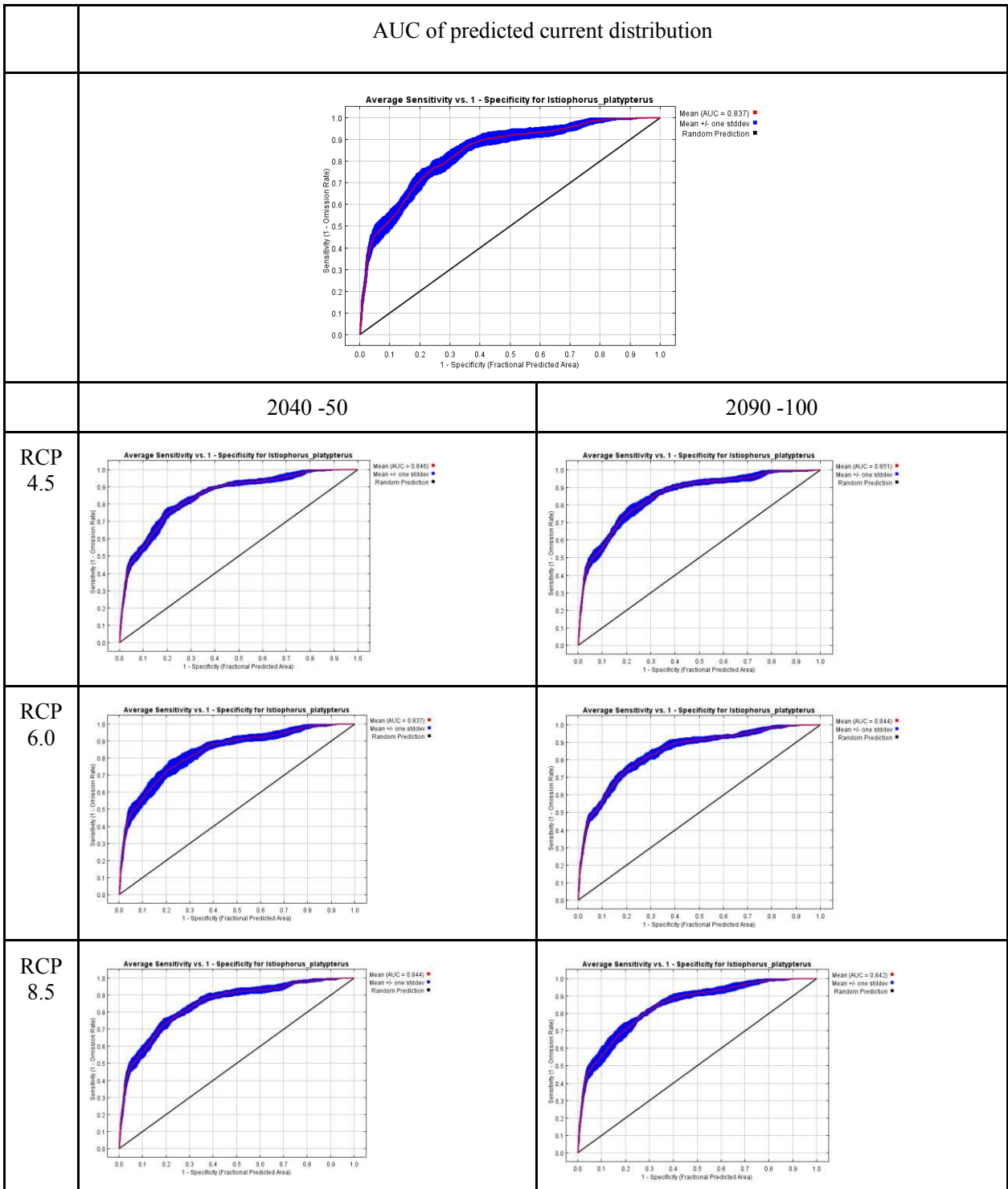


Fig. 62 The average sensitivity vs. 1- specificity graph for *Istiophorus platypterus* showing the mean Area Under the Curve (AUC) and standard deviation for the predicted current distribution the predicted future distributions

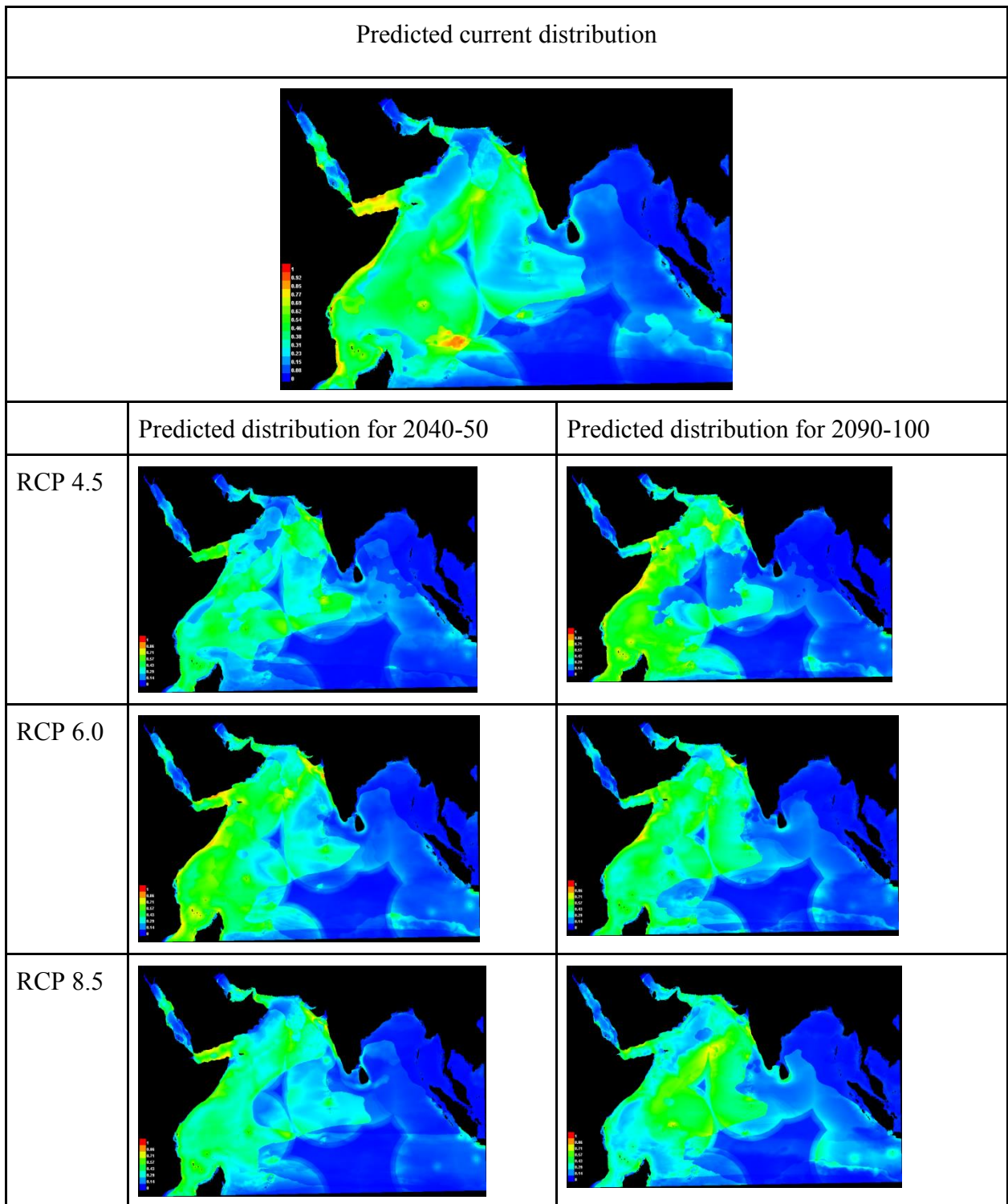


Fig. 63 Map showing the predicted current and future distributions of *Istiophorus platypterus*

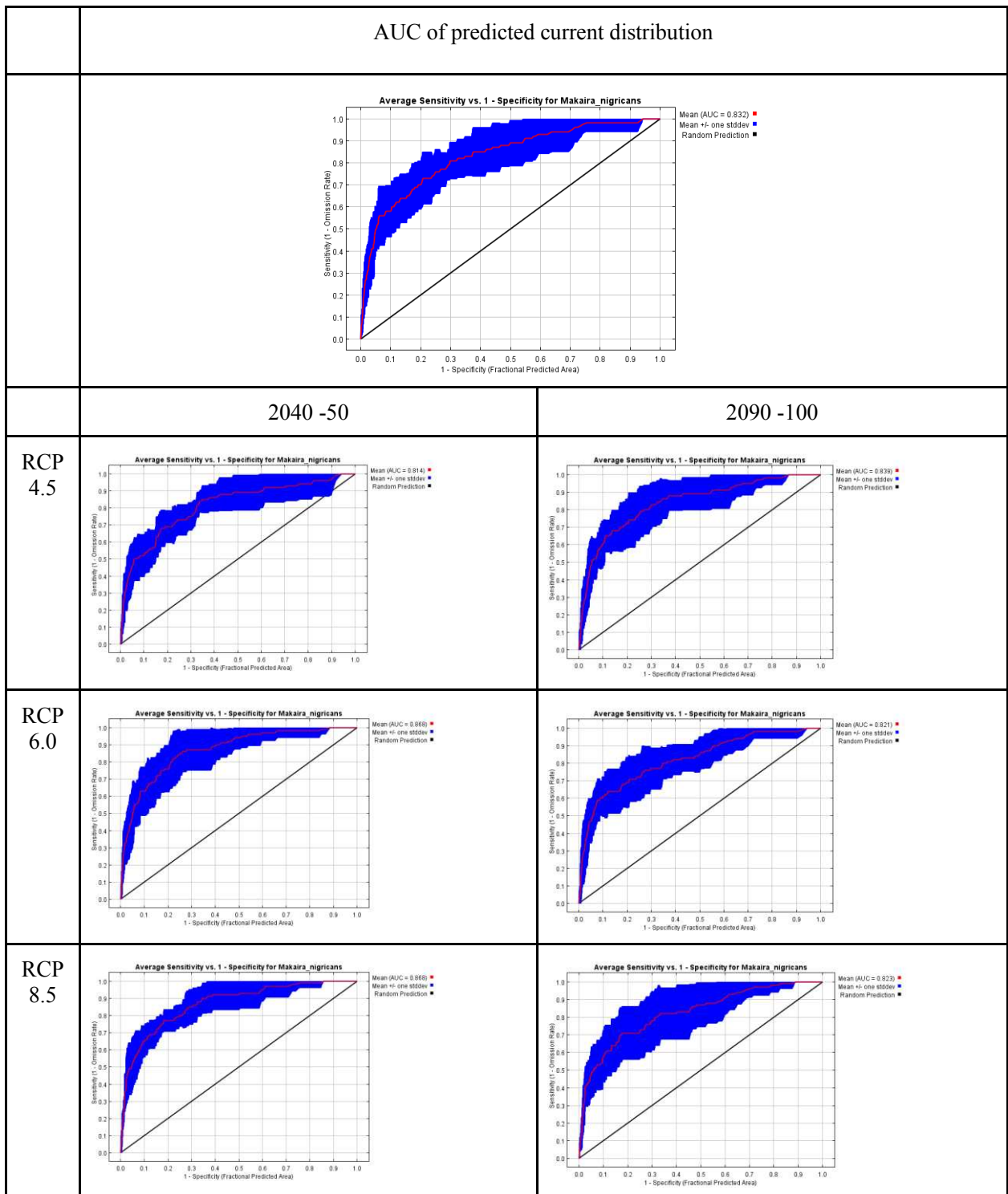


Fig. 64 The average sensitivity vs. 1- specificity graph for *Makaira nigricans* showing the mean Area Under the Curve (AUC) and standard deviation for the predicted current distribution the predicted future distributions

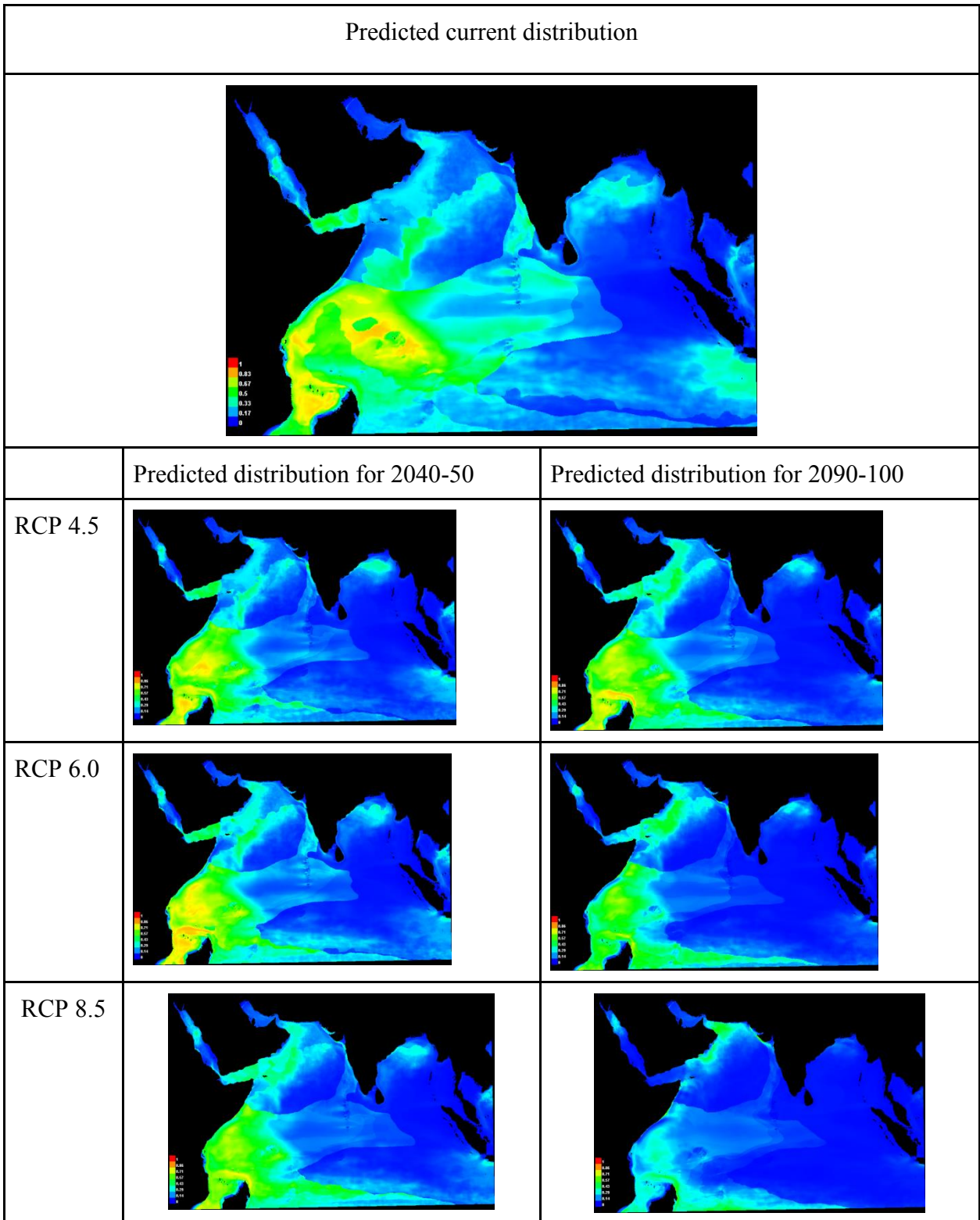


Fig. 65 Map showing the predicted current and future distributions of *Makaira nigricans*

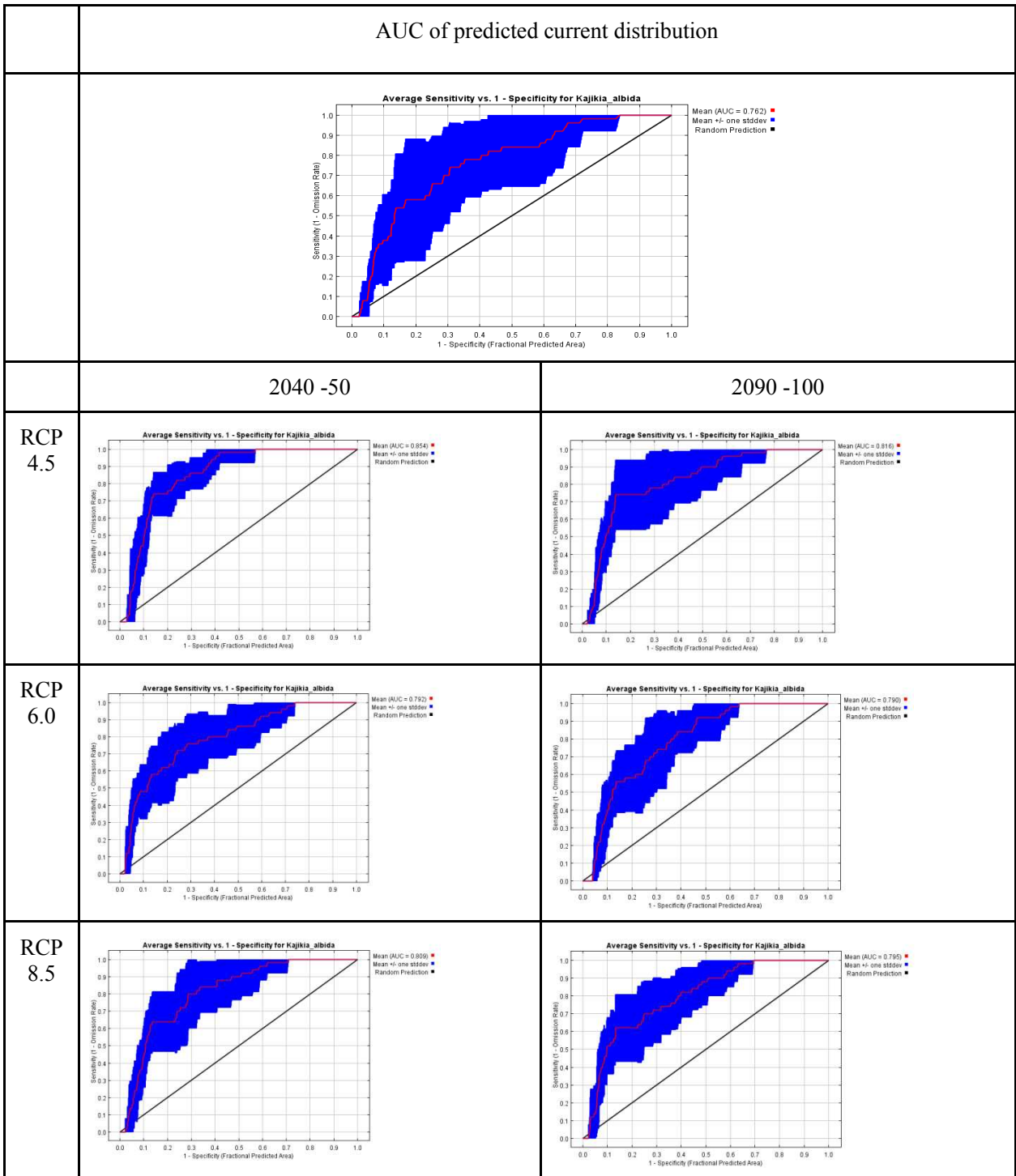


Fig. 66 The average sensitivity vs. 1- specificity graph for Kajikia albida showing the mean Area Under the Curve (AUC) and standard deviation for the predicted current distribution the predicted future distributions

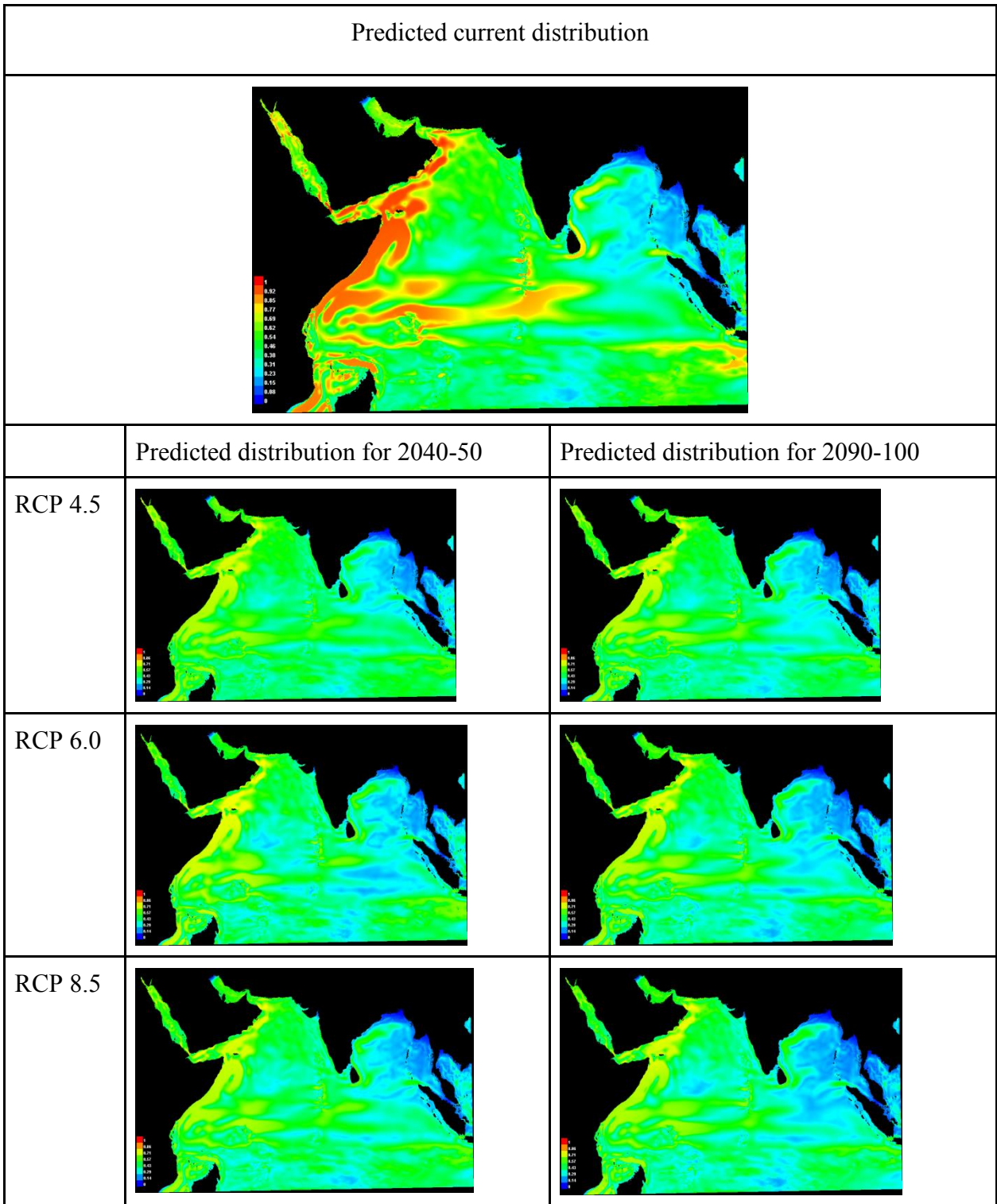


Fig. 67 Map showing the predicted current and future distributions of *Kajikia albida*

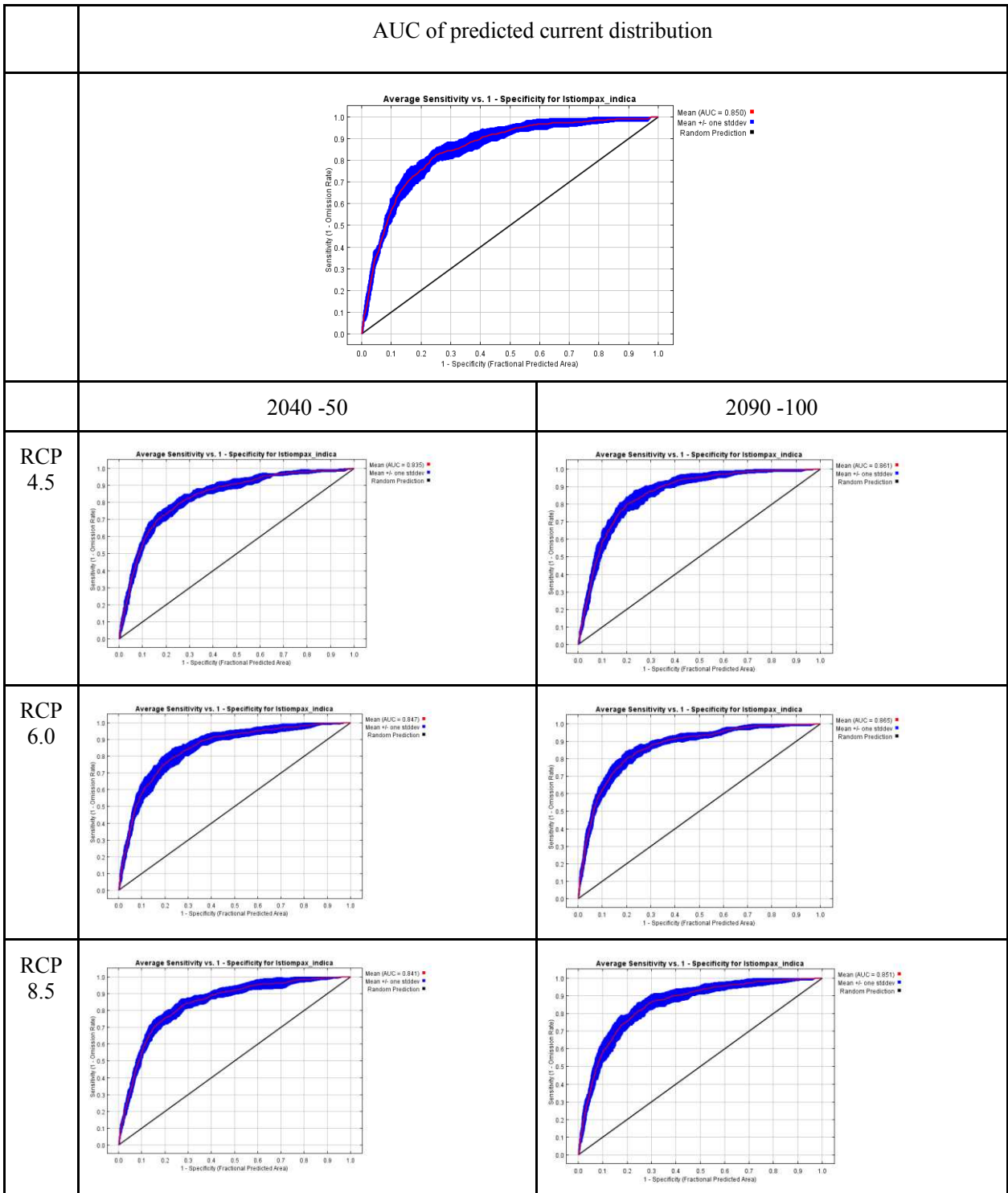


Fig. 68 The average sensitivity vs. 1- specificity graph for *Istiompax indica* showing the mean Area Under the Curve (AUC) and standard deviation for the predicted current distribution the predicted future distributions

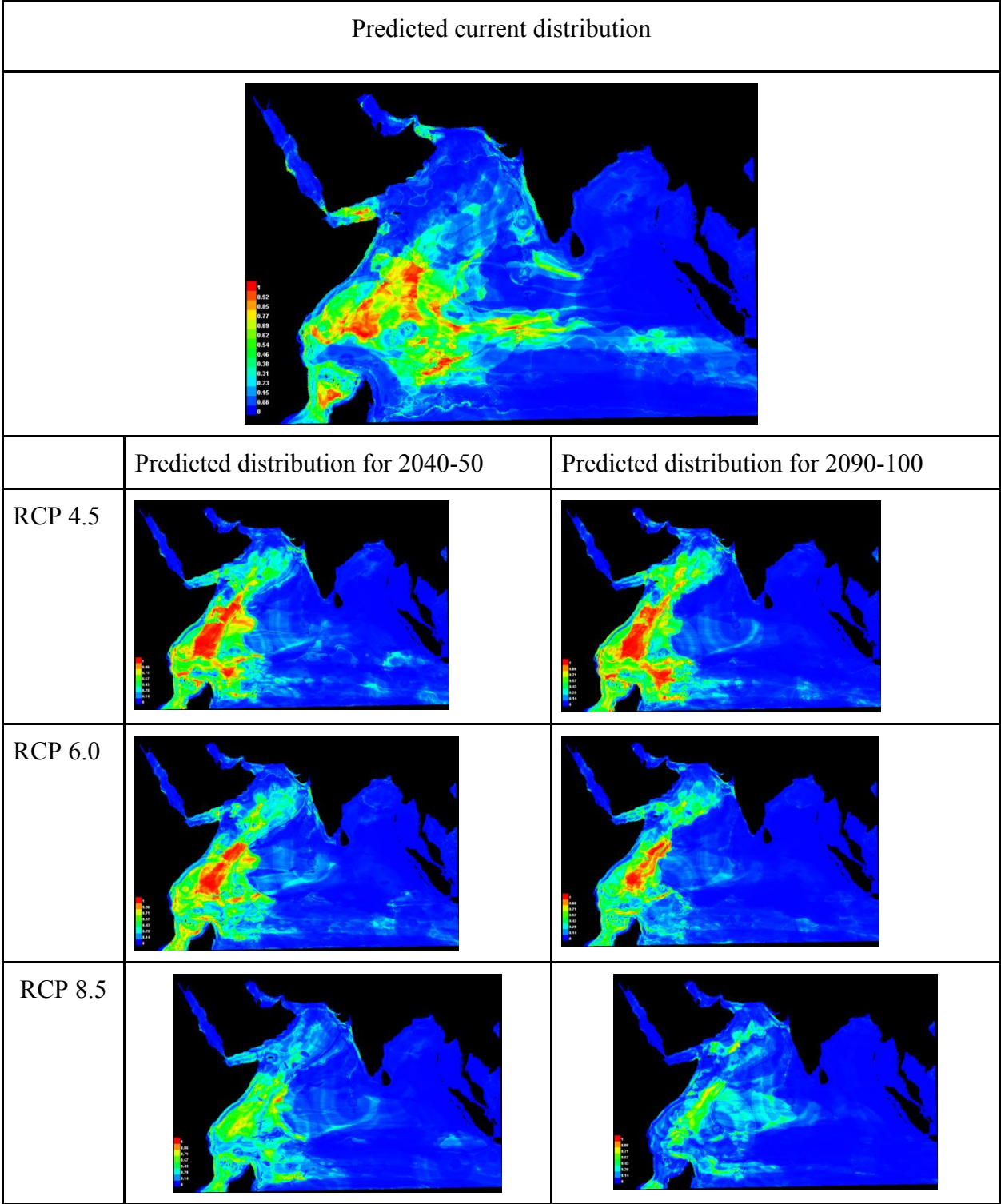


Fig. 69 Map showing the predicted current and future distributions of *Istiompax indica*

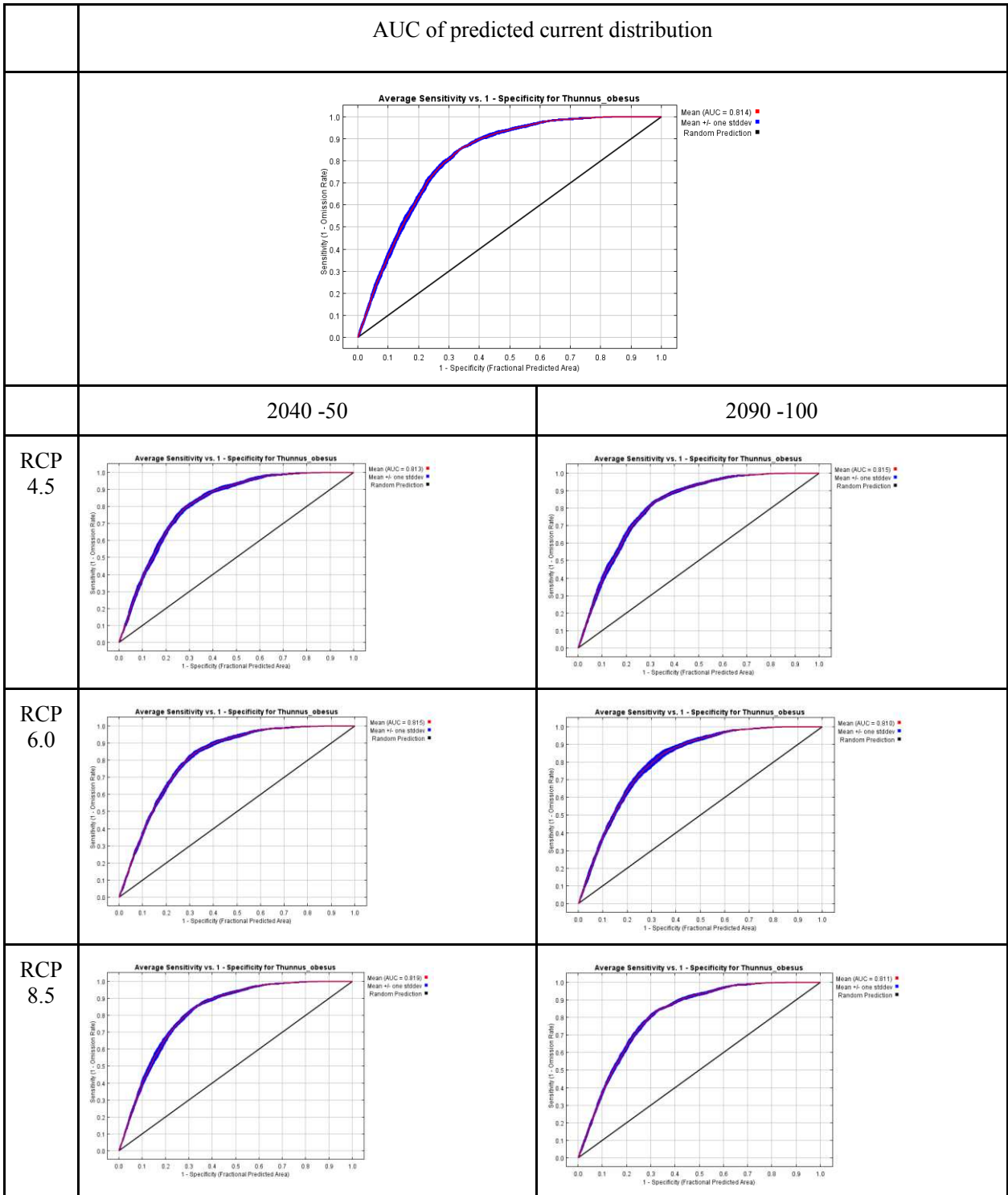


Fig. 70 The average sensitivity vs. 1- specificity graph for *Thunnus obesus* showing the mean Area Under the Curve (AUC) and standard deviation for the predicted current distribution the predicted future distributions

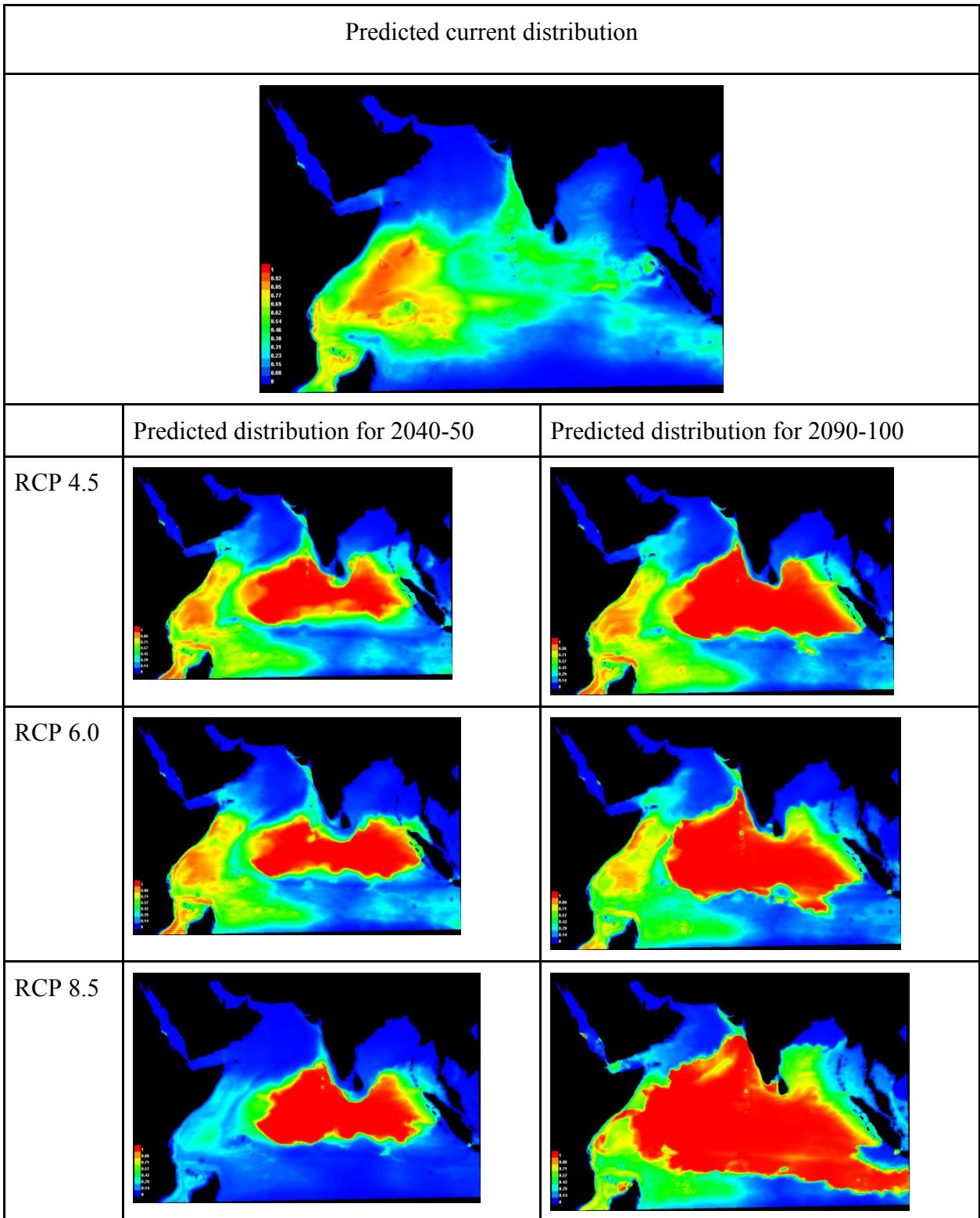


Fig. 71 Map showing the predicted current and future distributions of *Thunnus obesus*

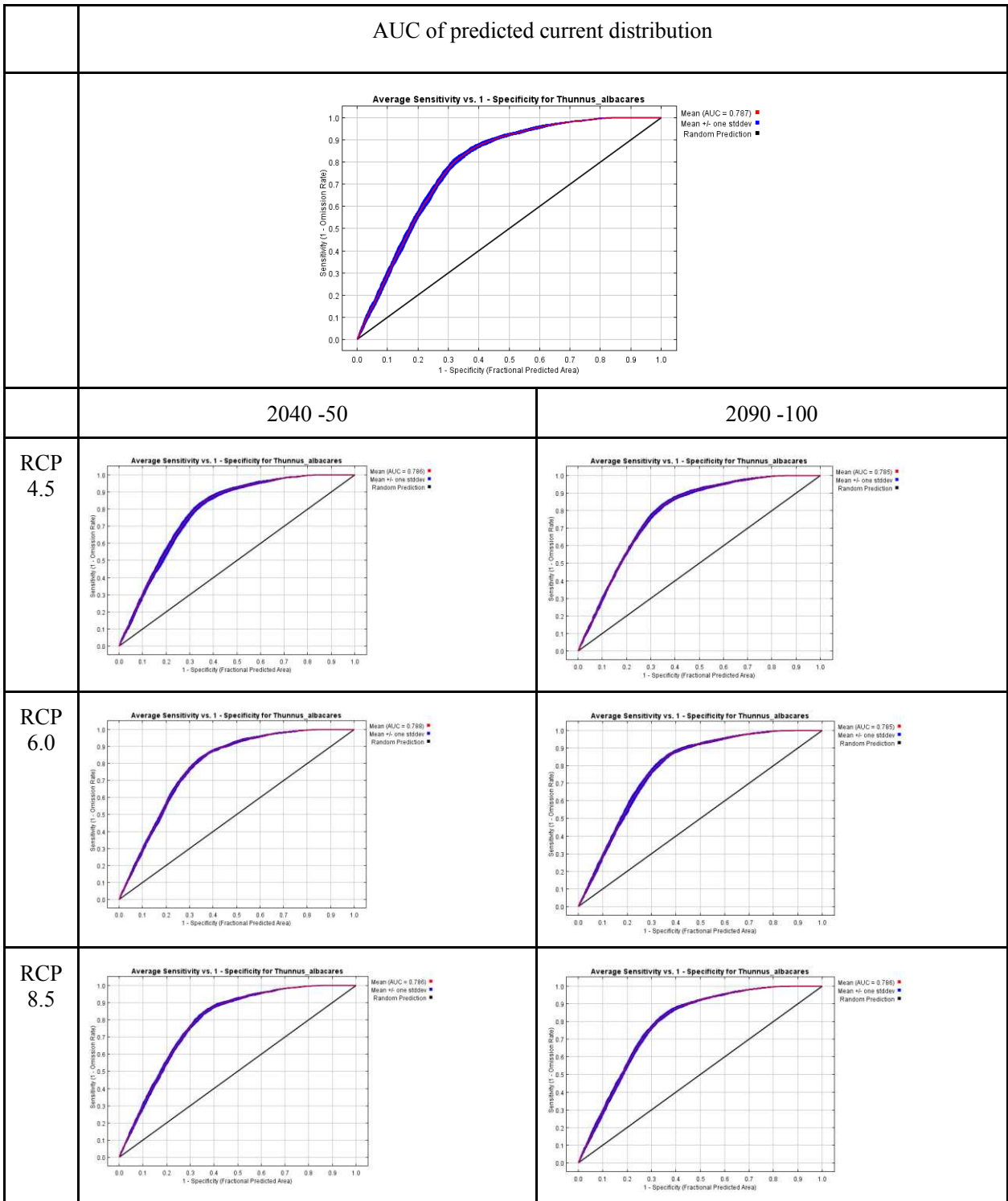


Fig. 72 The average sensitivity vs. 1- specificity graph for *Thunnus albacares* showing the mean Area Under the Curve (AUC) and standard deviation for the predicted current distribution the predicted future distributions

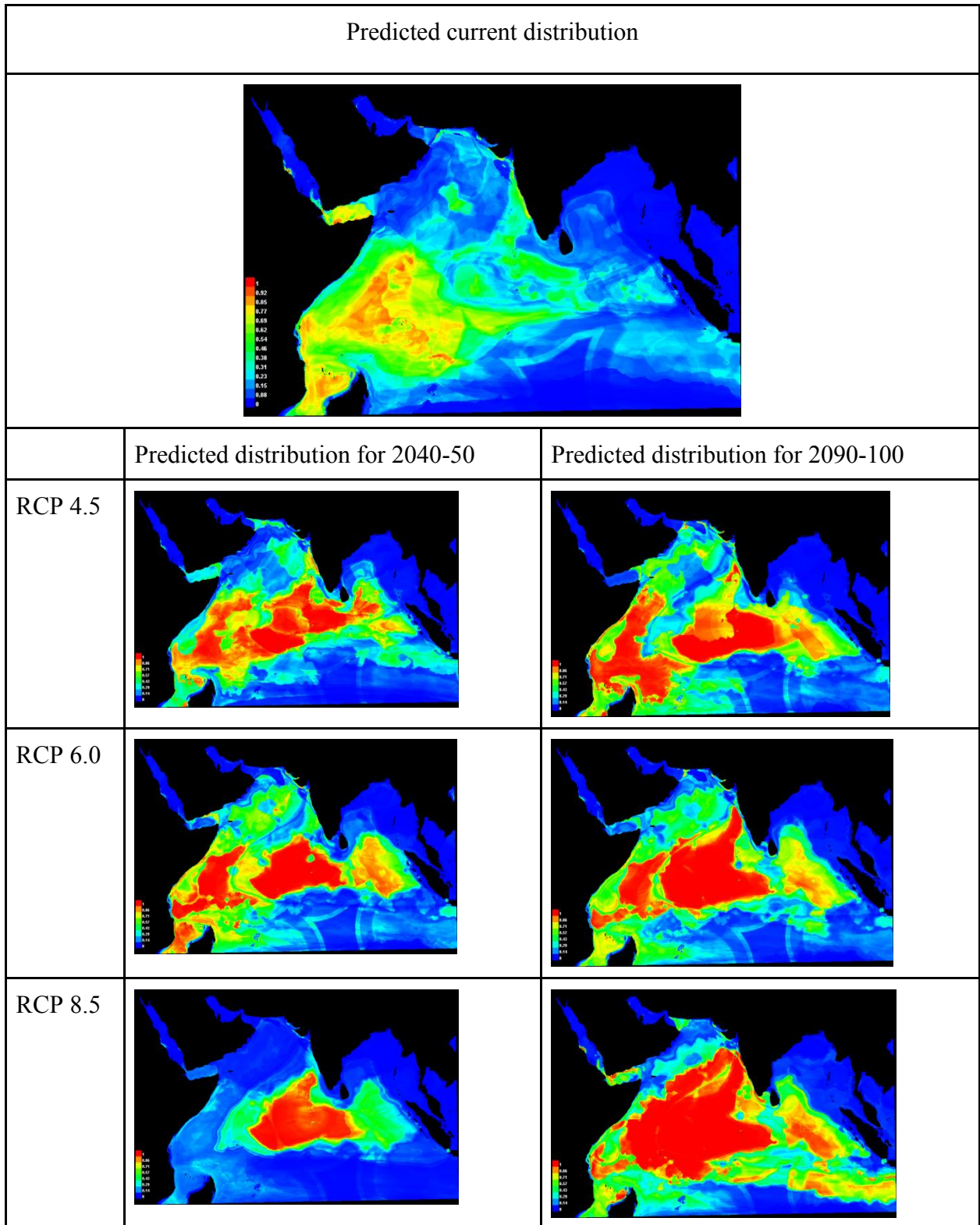


Fig. 73 Map showing the predicted current and future distributions of *Thunnus albacares*

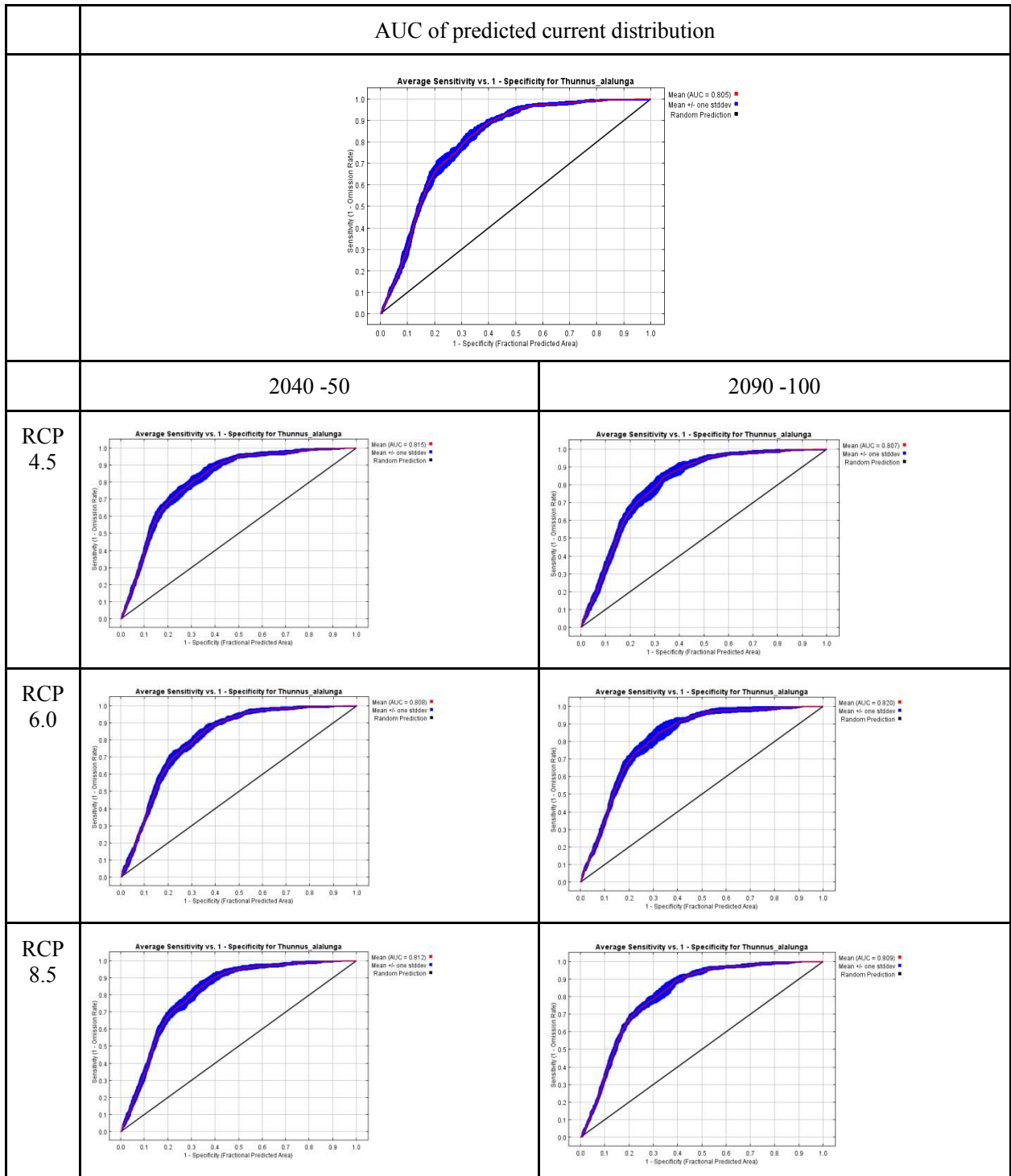


Fig. 74 The average sensitivity vs. 1- specificity graph for *T. alalunga* showing the mean Area Under the Curve (AUC) and standard deviation for the predicted current distribution the predicted future distributions

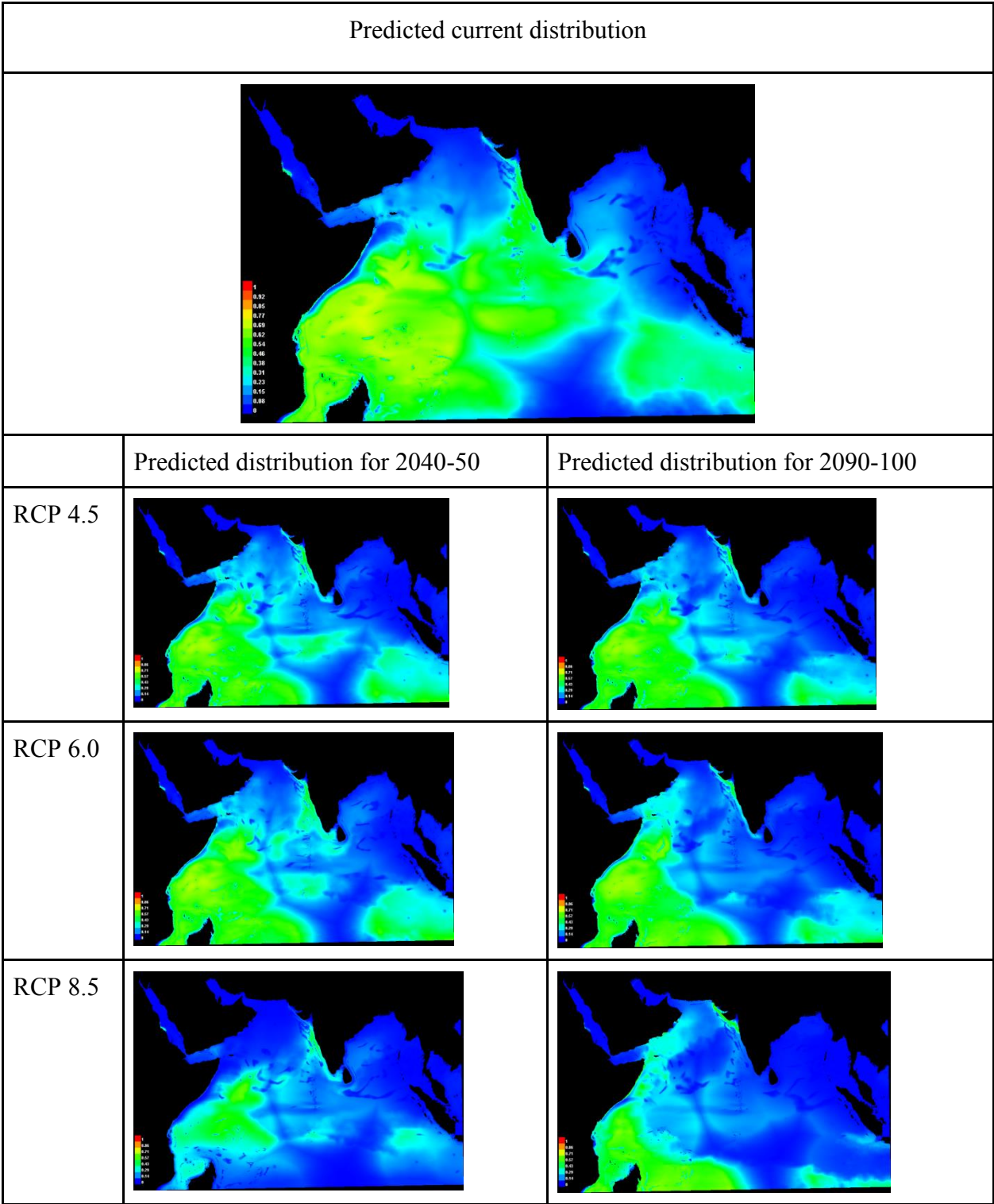


Fig. 74 Map showing the predicted current and future distributions of *T. alalunga*

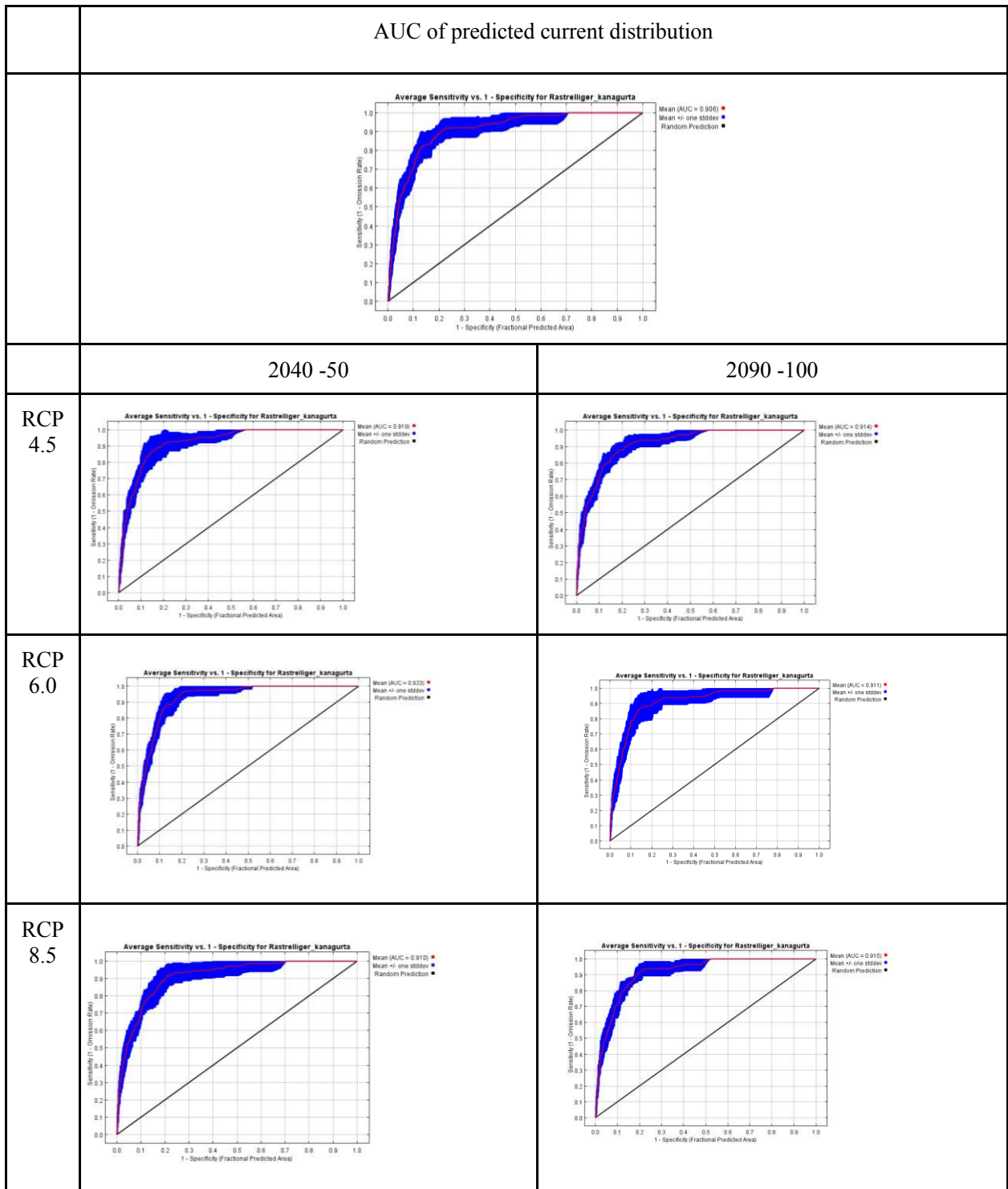


Fig. 75 The average sensitivity vs. 1- specificity graph for *R. kanagurta* showing the mean Area Under the Curve (AUC) and standard deviation for the predicted current distribution the predicted future distributions

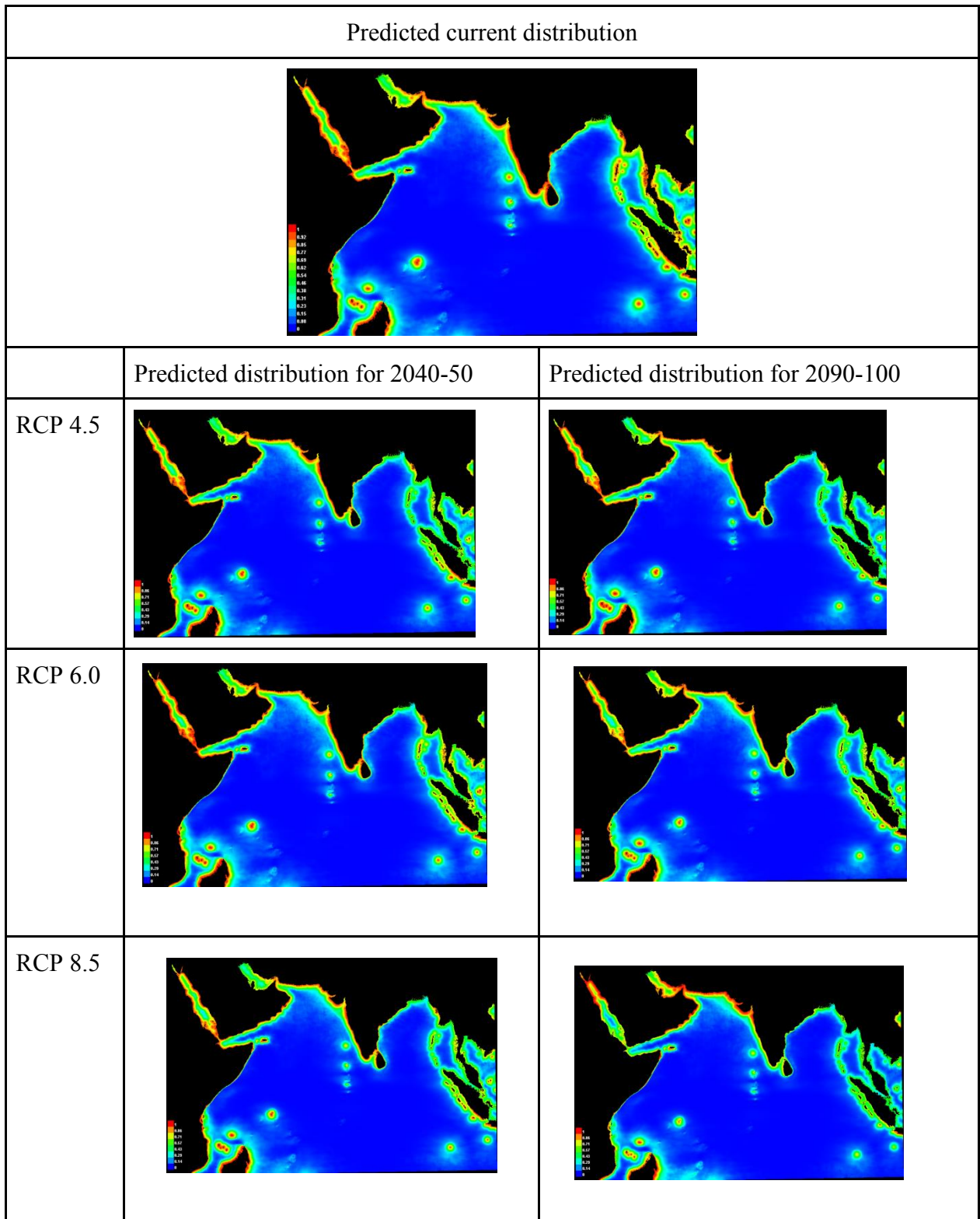


Fig. 76 Map showing the predicted current and future distributions of *R. kanagurta*

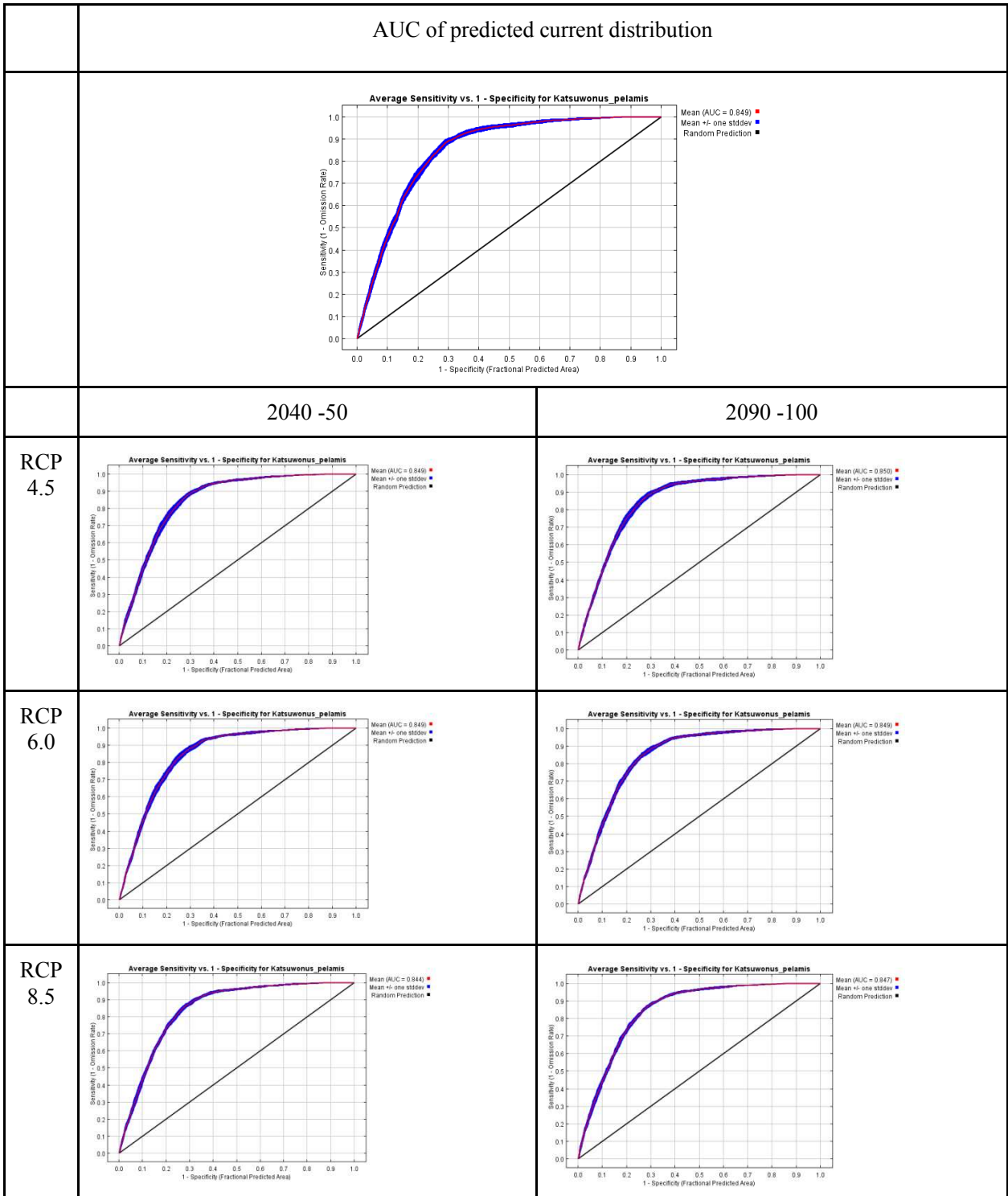


Fig. 77 The average sensitivity vs. 1- specificity graph for *Katsuwonus pelamis* showing the mean Area Under the Curve (AUC) and standard deviation for the predicted current distribution the predicted future distributions

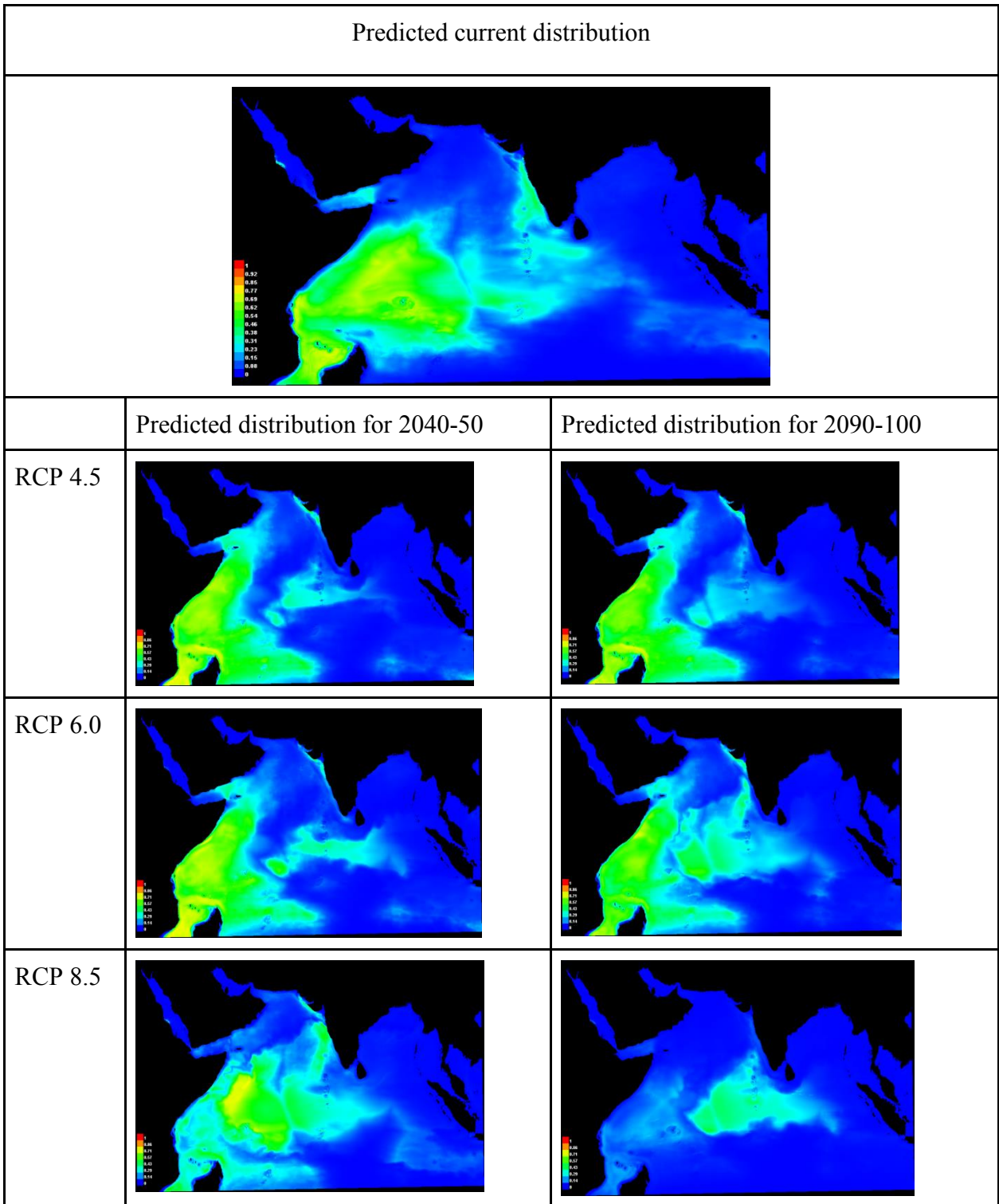


Fig. 78 Map showing the predicted current and future distributions *K. pelamis*

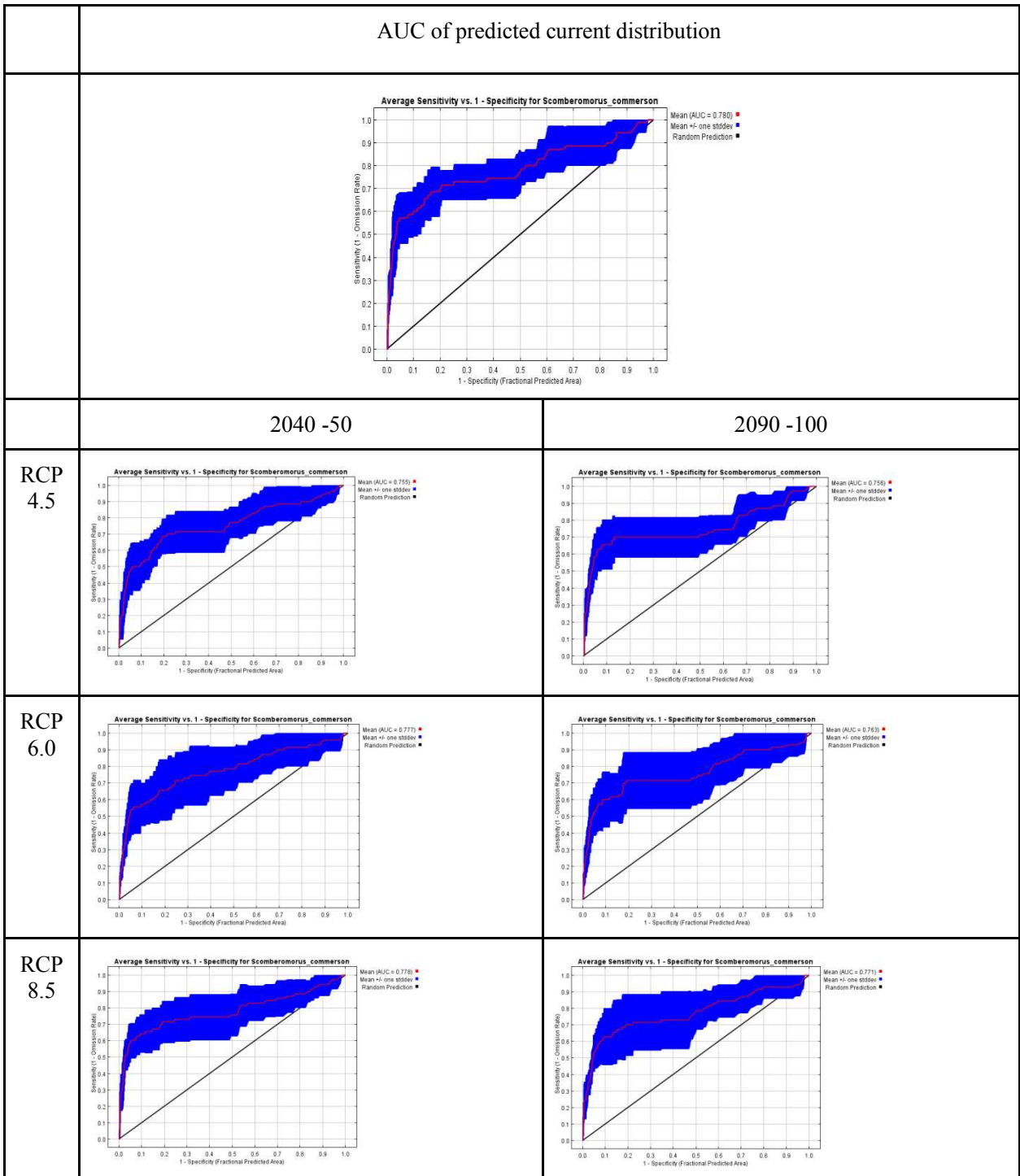


Fig. 79 The average sensitivity vs. 1- specificity graph for *Scomberomorus commerson* showing the mean Area Under the Curve (AUC) and standard deviation for the predicted current distribution the predicted future distributions

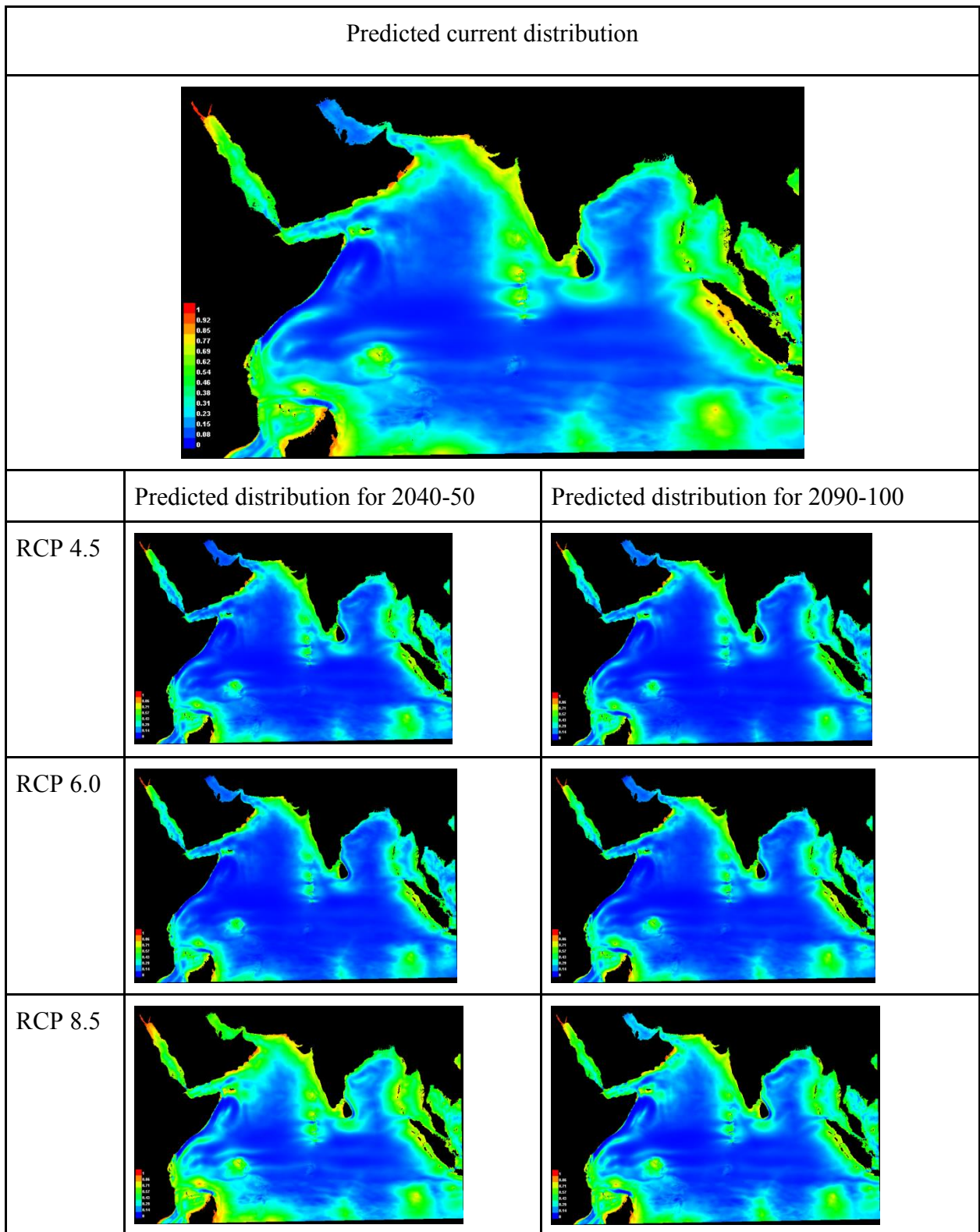


Fig. 80 Map showing the predicted current and future distributions of *S. commerson*

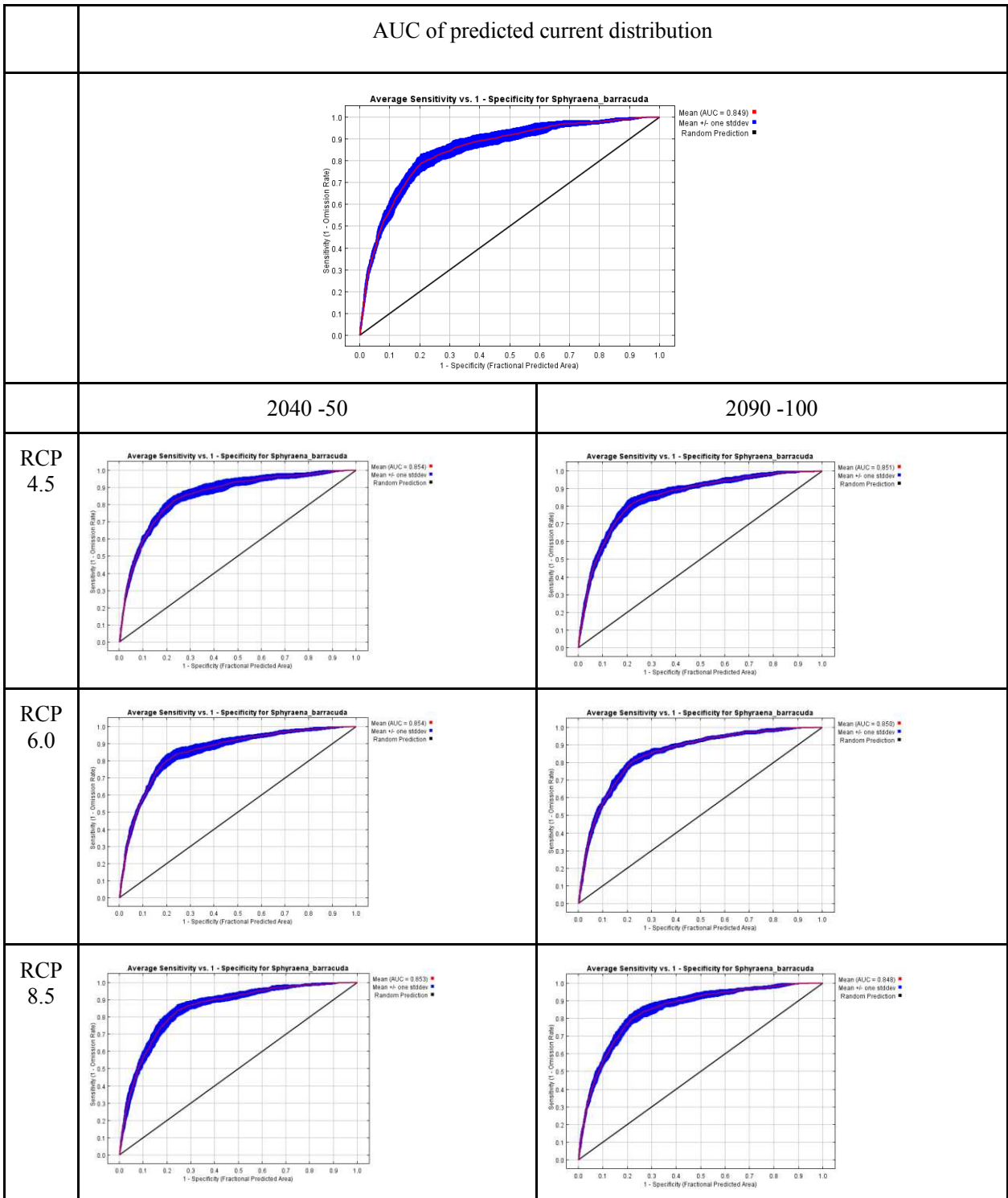


Fig. 81 The average sensitivity vs. 1- specificity graph for *Sphyaena barracuda* showing the mean Area Under the Curve (AUC) and standard deviation for the predicted current distribution the predicted future distributions

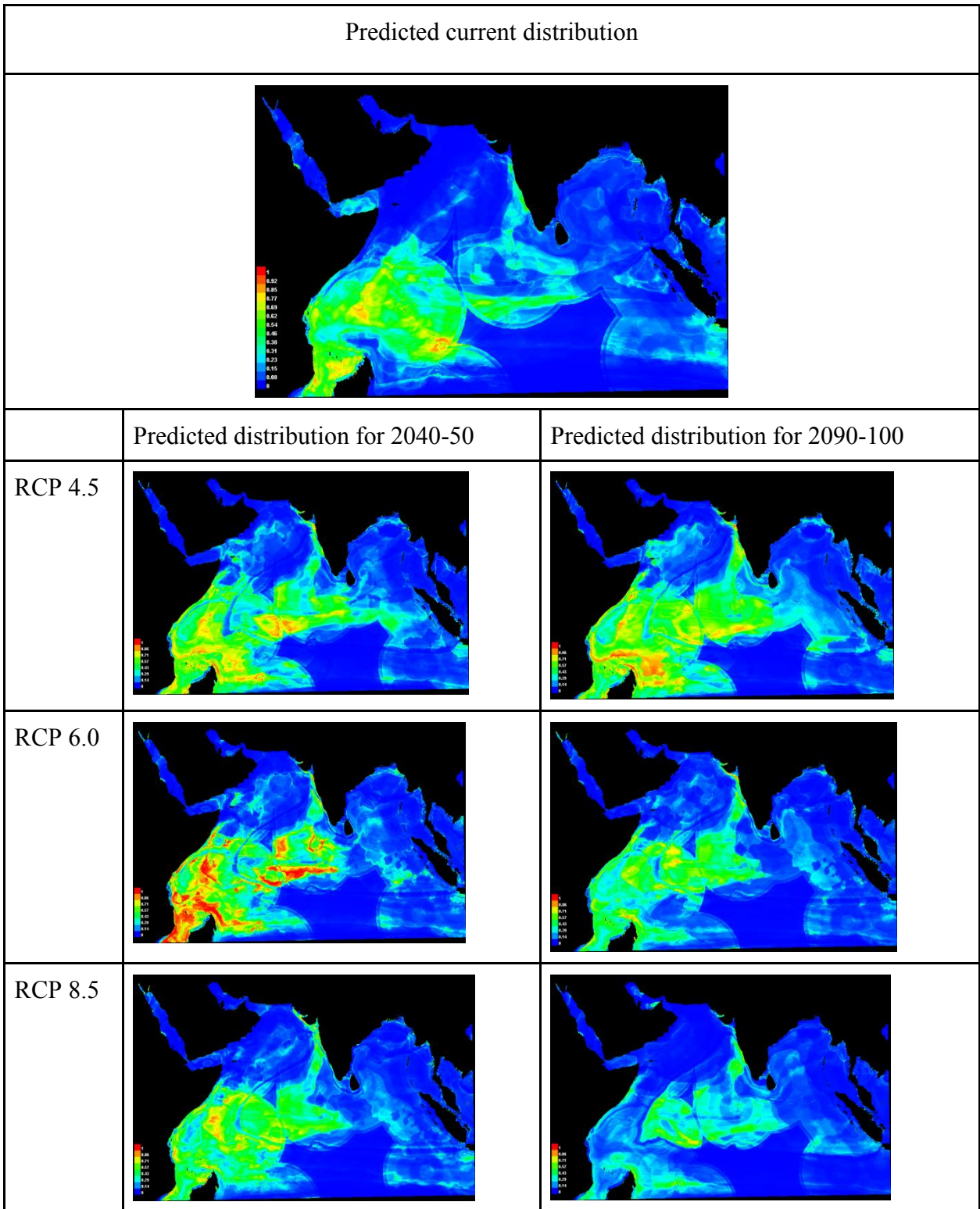


Fig. 82 Map showing the predicted current and future distributions of *Sphyraena barracuda*

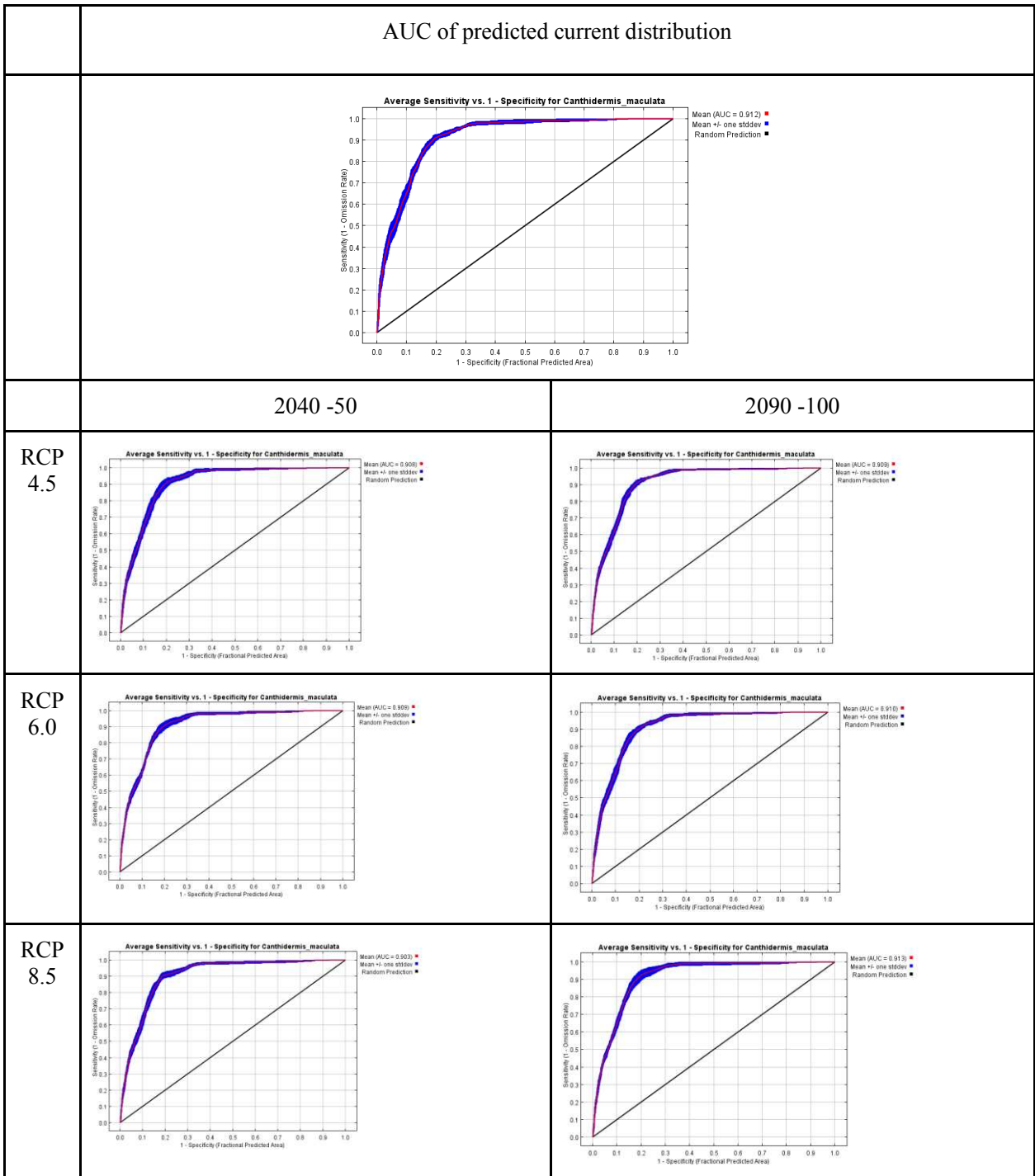


Fig. 83 The average sensitivity vs. 1-specificity graph for *Canthidermis maculata* showing the mean Area Under the Curve (AUC) and standard deviation for the predicted current distribution the predicted future distributions

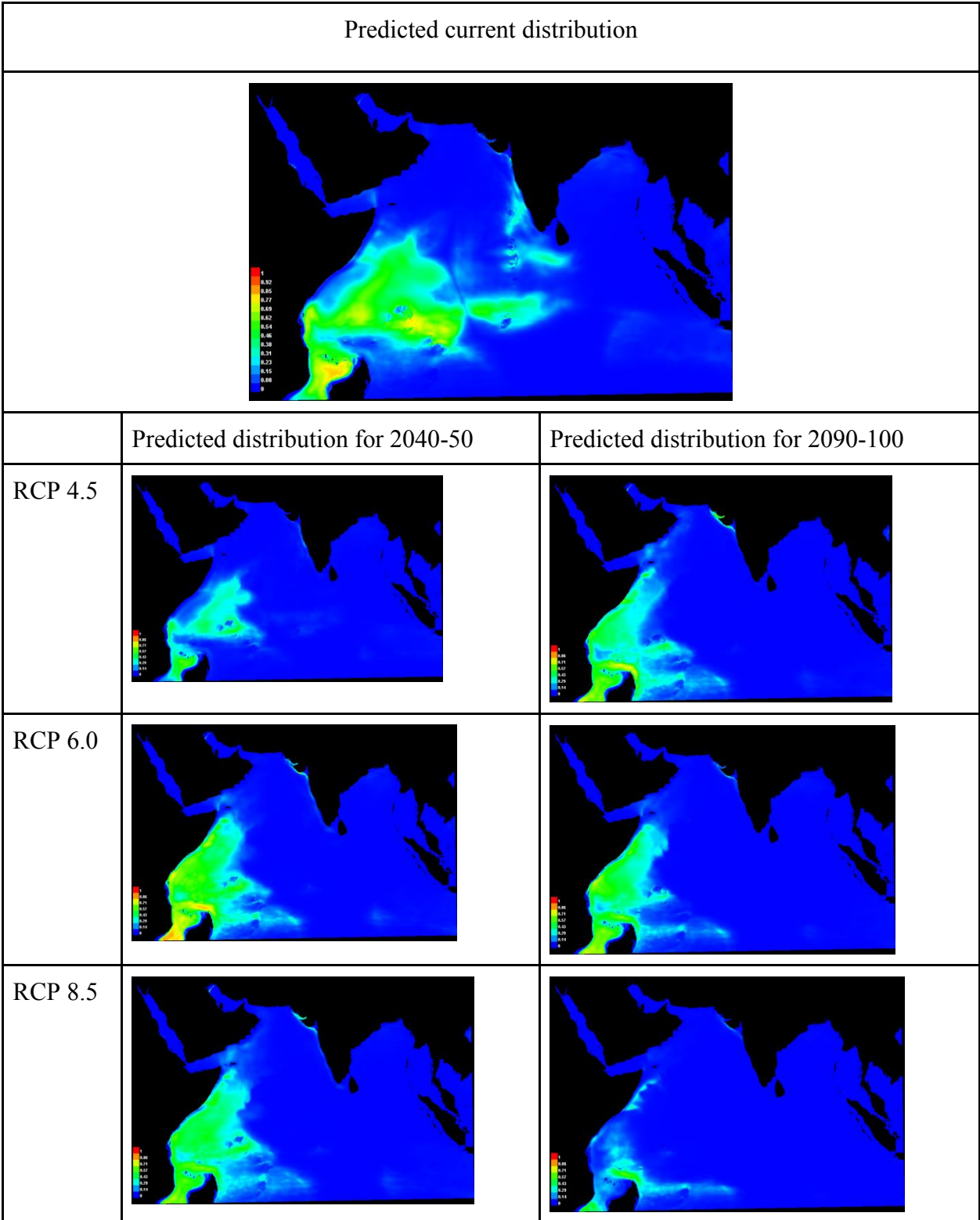


Fig. 84 Map showing the predicted current and future distributions of *Canthidermis maculata*

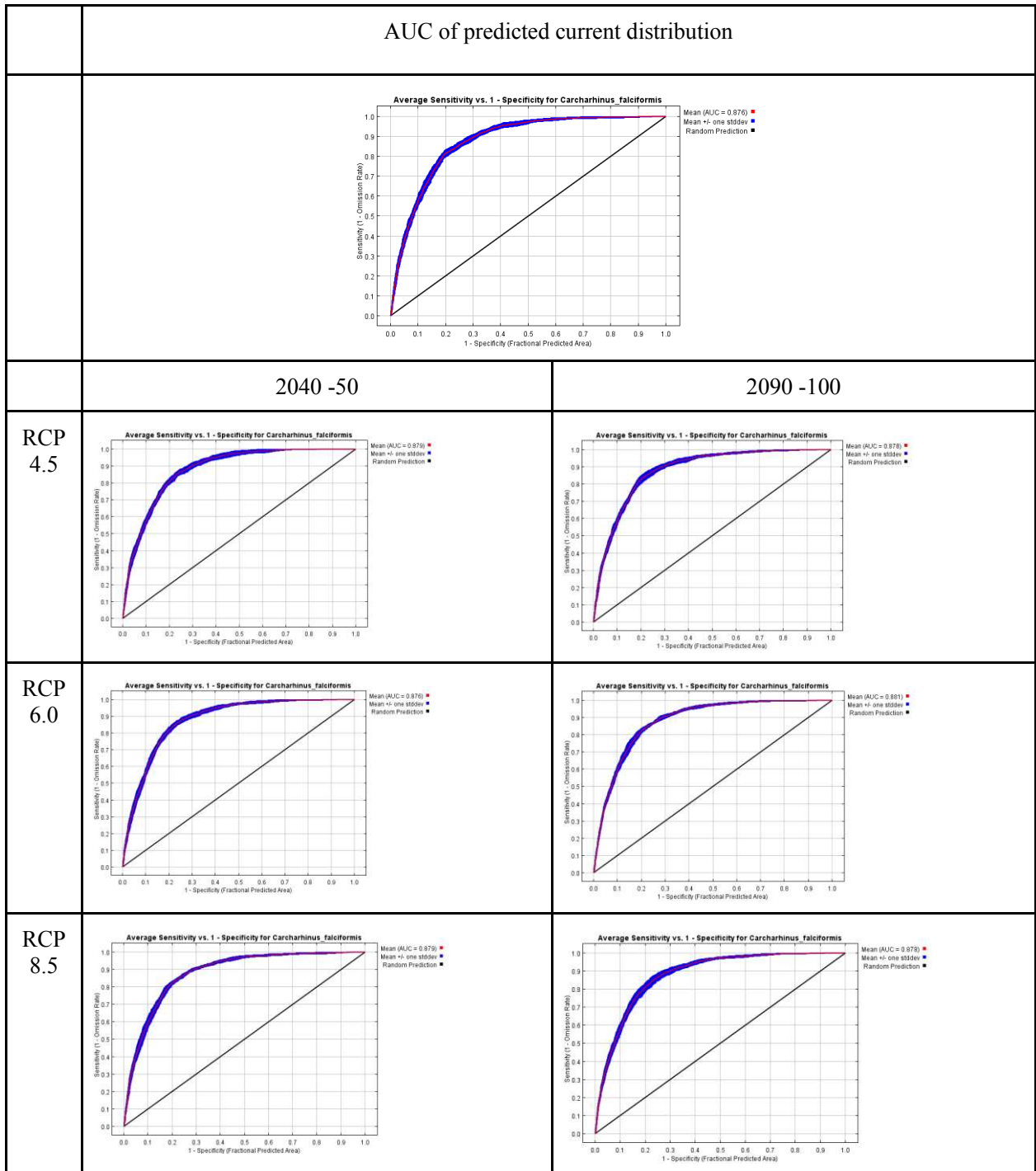


Fig. 85 The average sensitivity vs. 1- specificity graph for *Carcharhinus falciformis* showing the mean Area Under the Curve (AUC) and standard deviation for the predicted current distribution the predicted future distributions

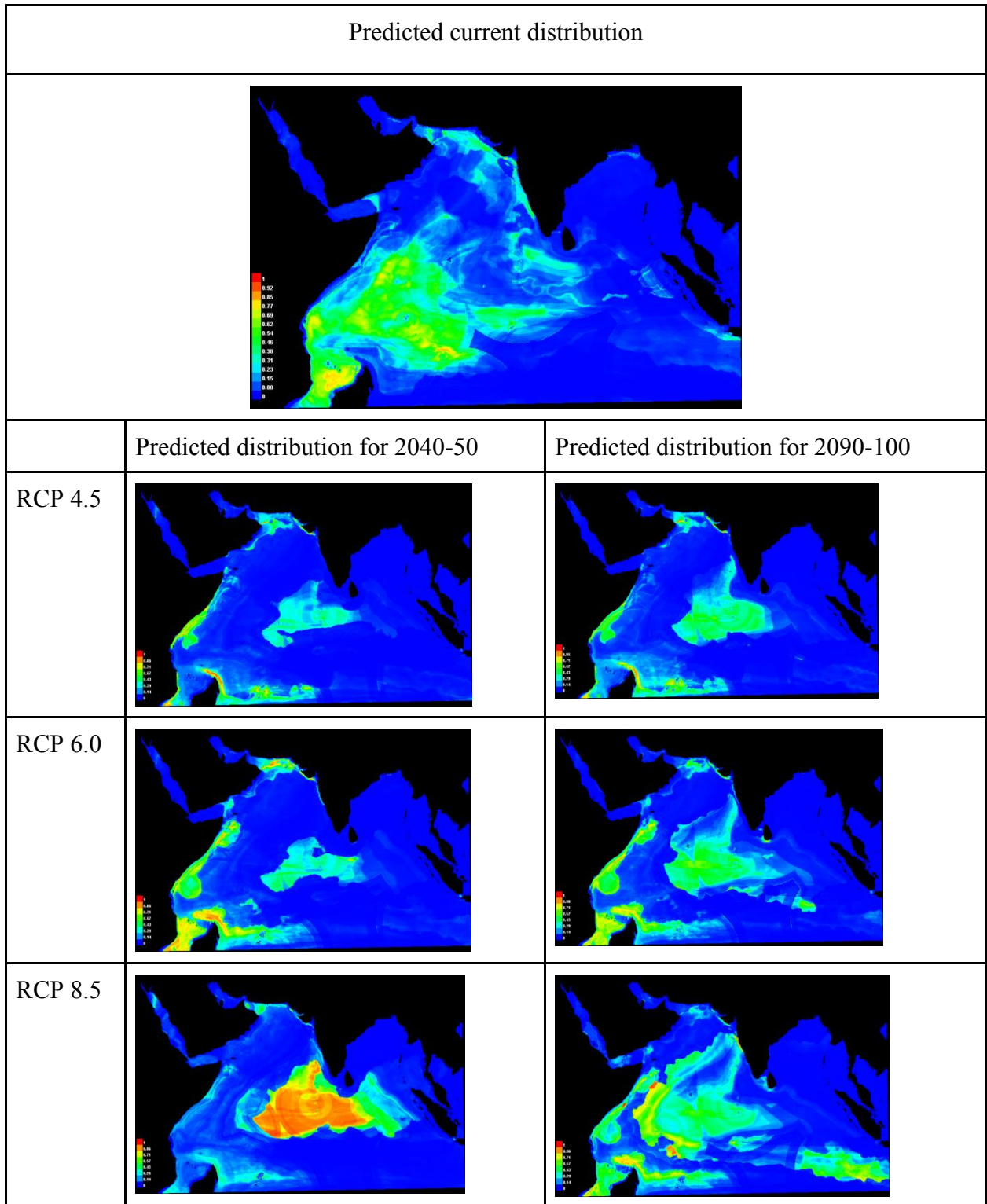


Fig. 86 Map showing the predicted current and future distributions of *Carcharhinus falciformis*

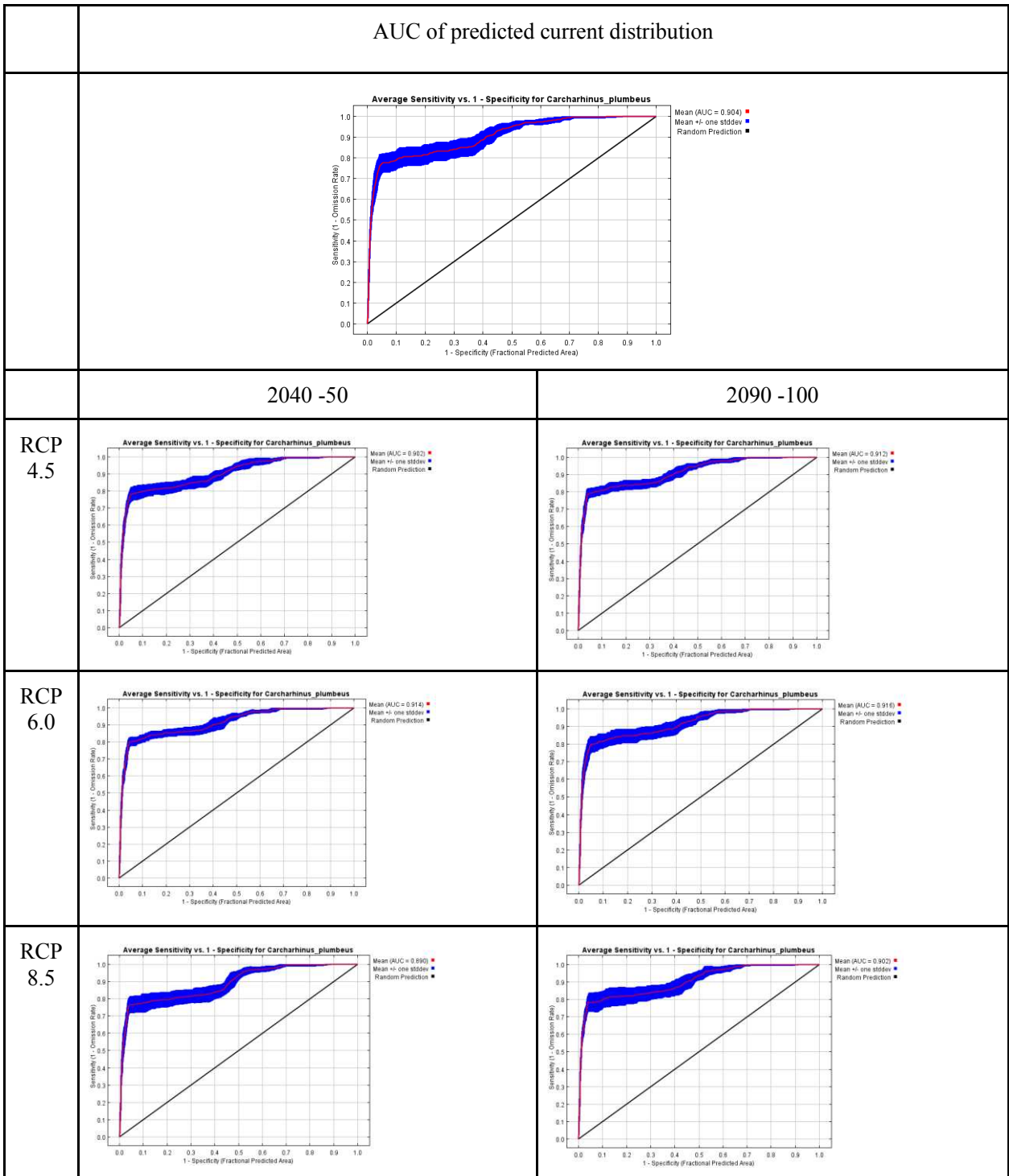


Fig. 87 The average sensitivity vs. 1- specificity graph for *Carcharhinus plumbeus* showing the mean Area Under the Curve (AUC) and standard deviation for the predicted current distribution the predicted future distributions

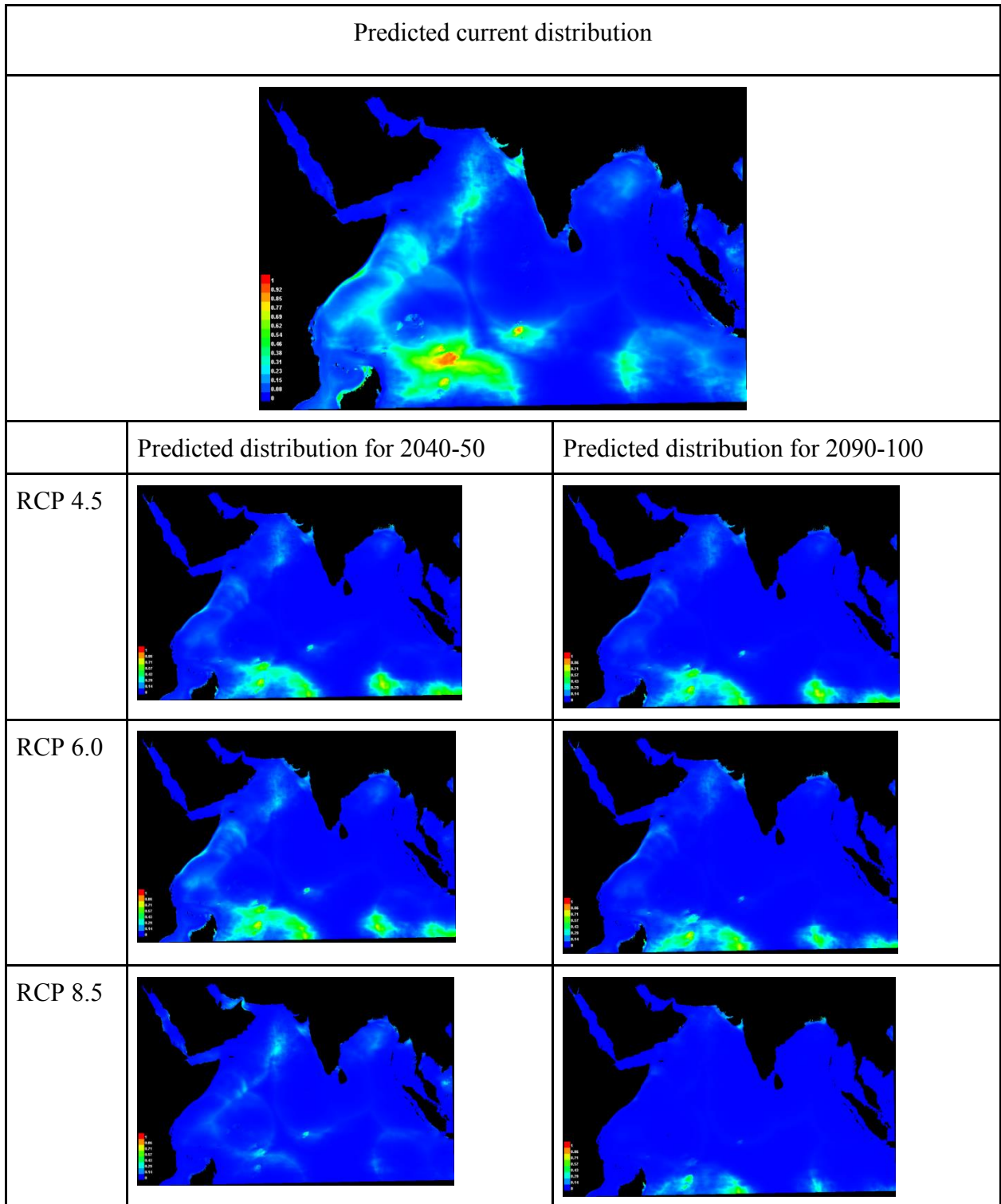


Fig. 88 Map showing the predicted current and future distributions of *Carcharhinus plumbeus*

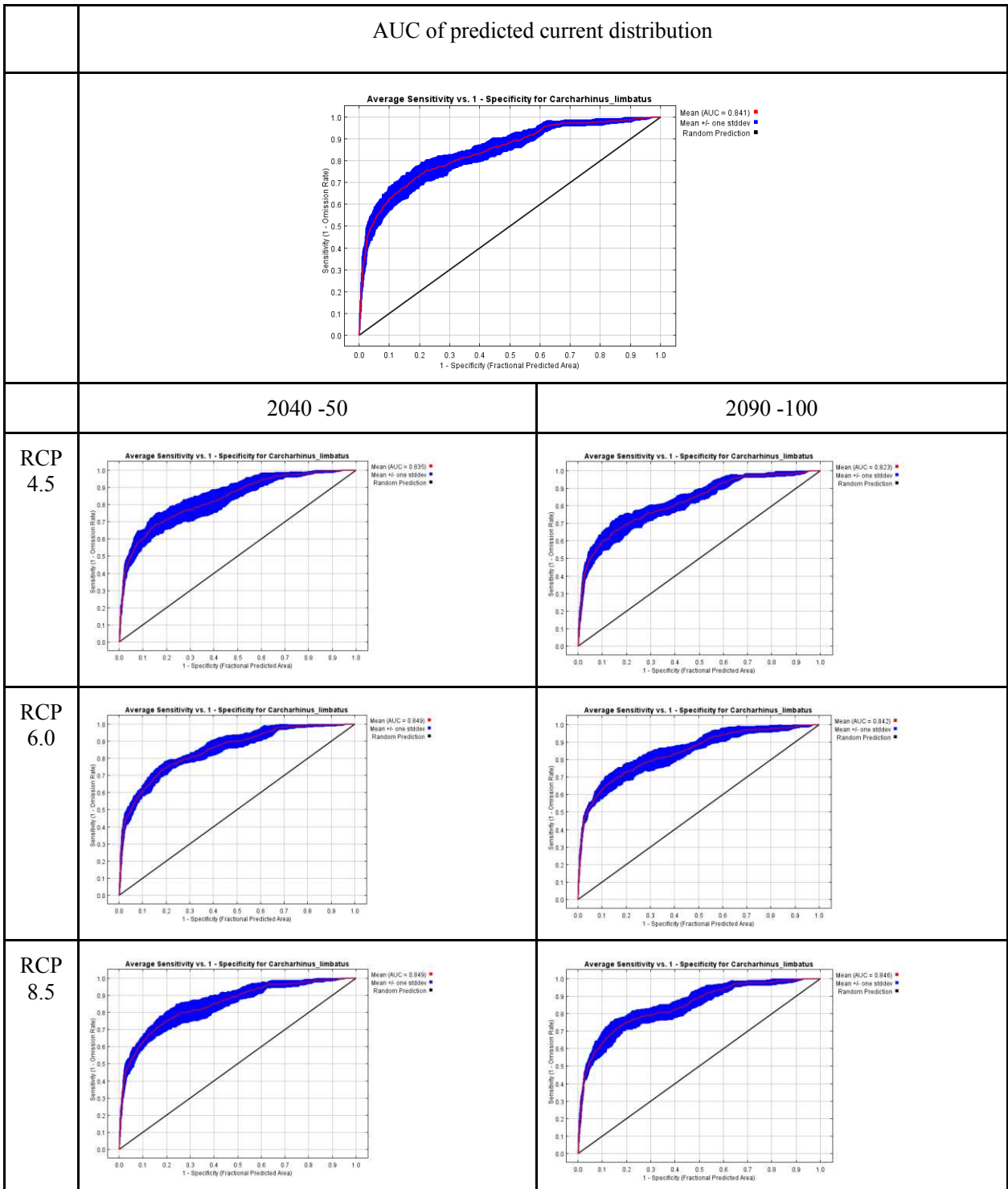


Fig. 89 The average sensitivity vs. 1- specificity graph for *Carcharhinus limbatus* showing the mean Area Under the Curve (AUC) and standard deviation for the predicted current distribution the predicted future distributions

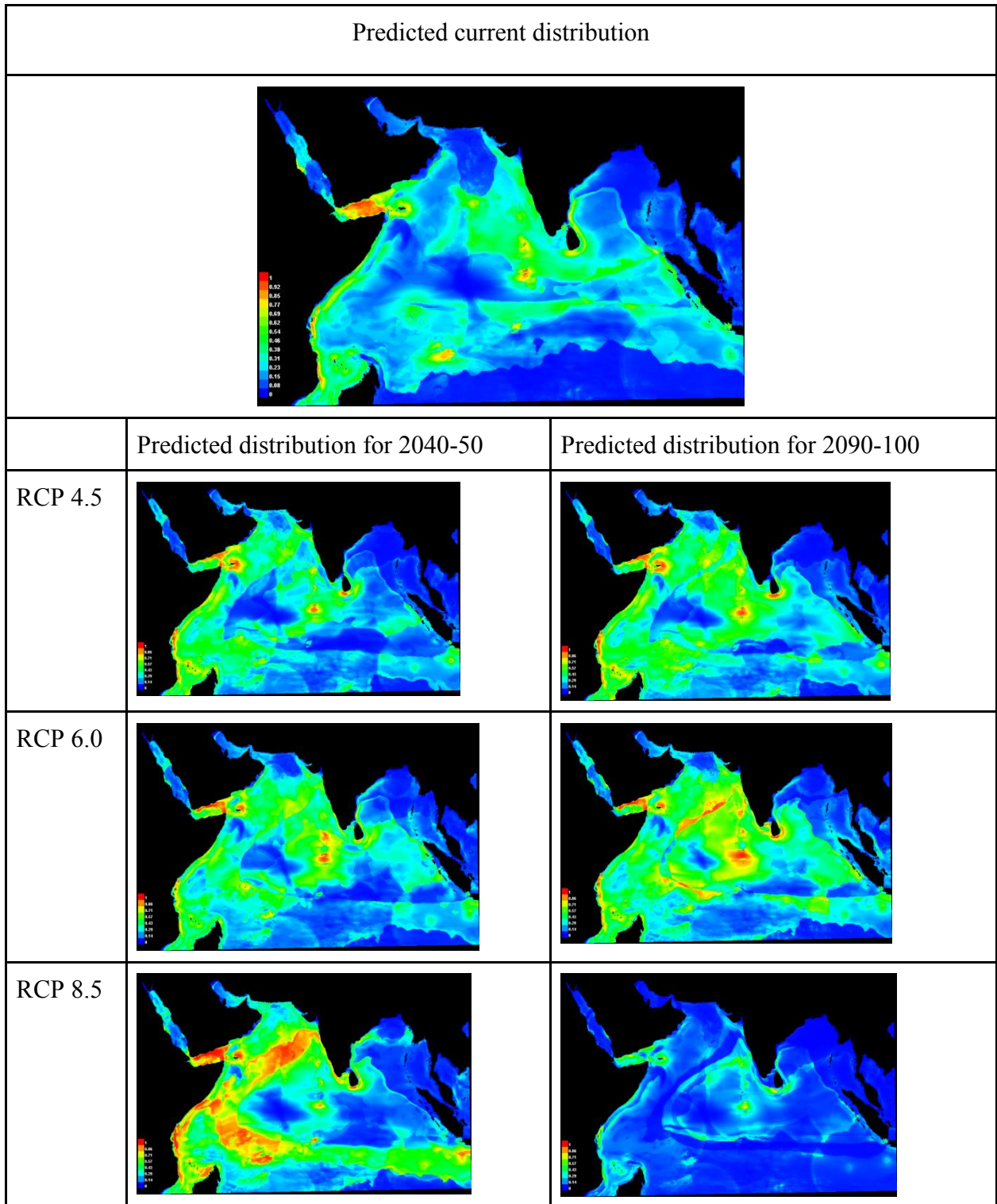


Fig. 90 Map showing the predicted current and future distributions of *Carcharhinus limbatus*

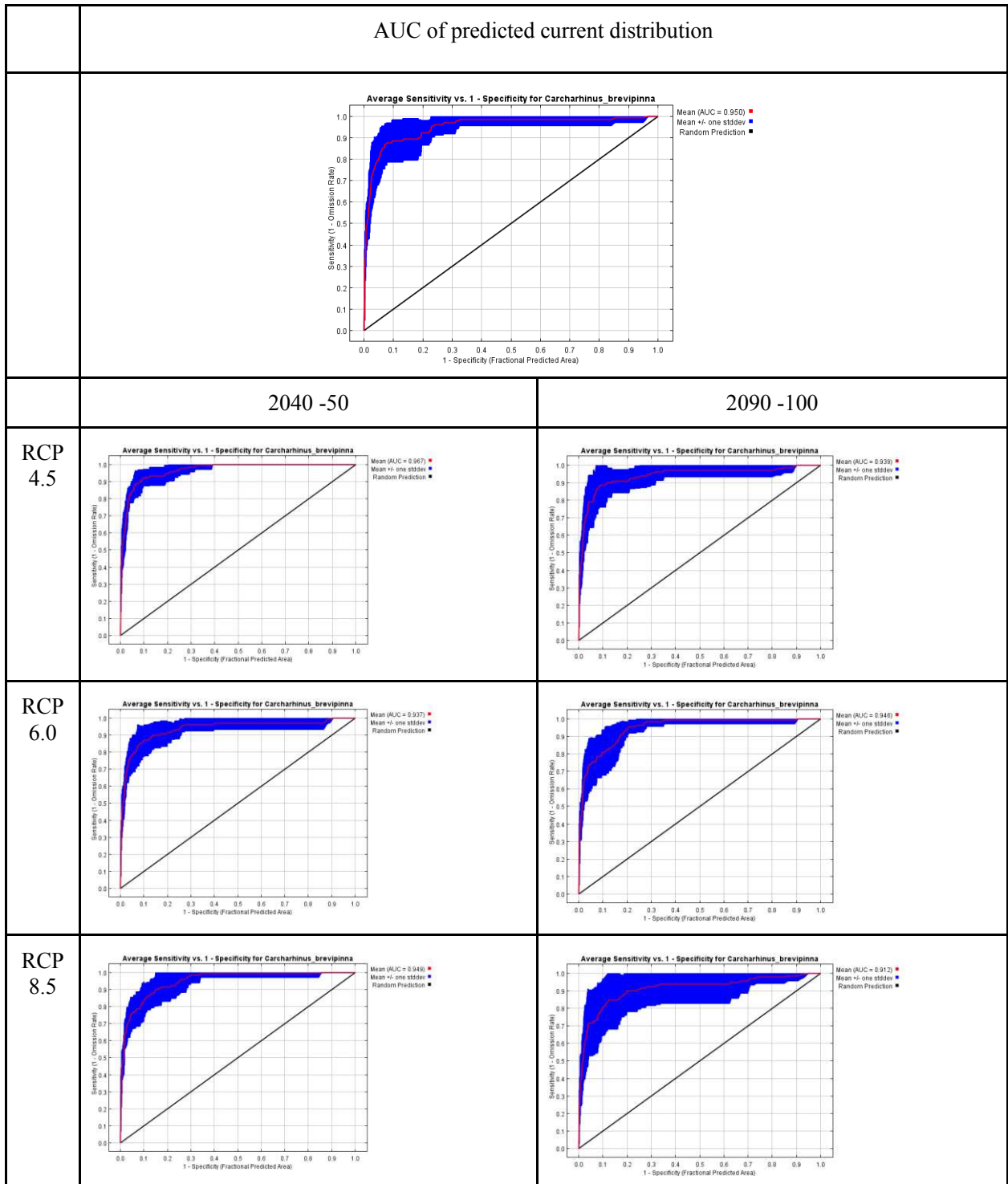


Fig. 91 The average sensitivity vs. 1- specificity graph for *Carcharhinus brevipinna* showing the mean Area Under the Curve (AUC) and standard deviation for the predicted current distribution the predicted future distributions

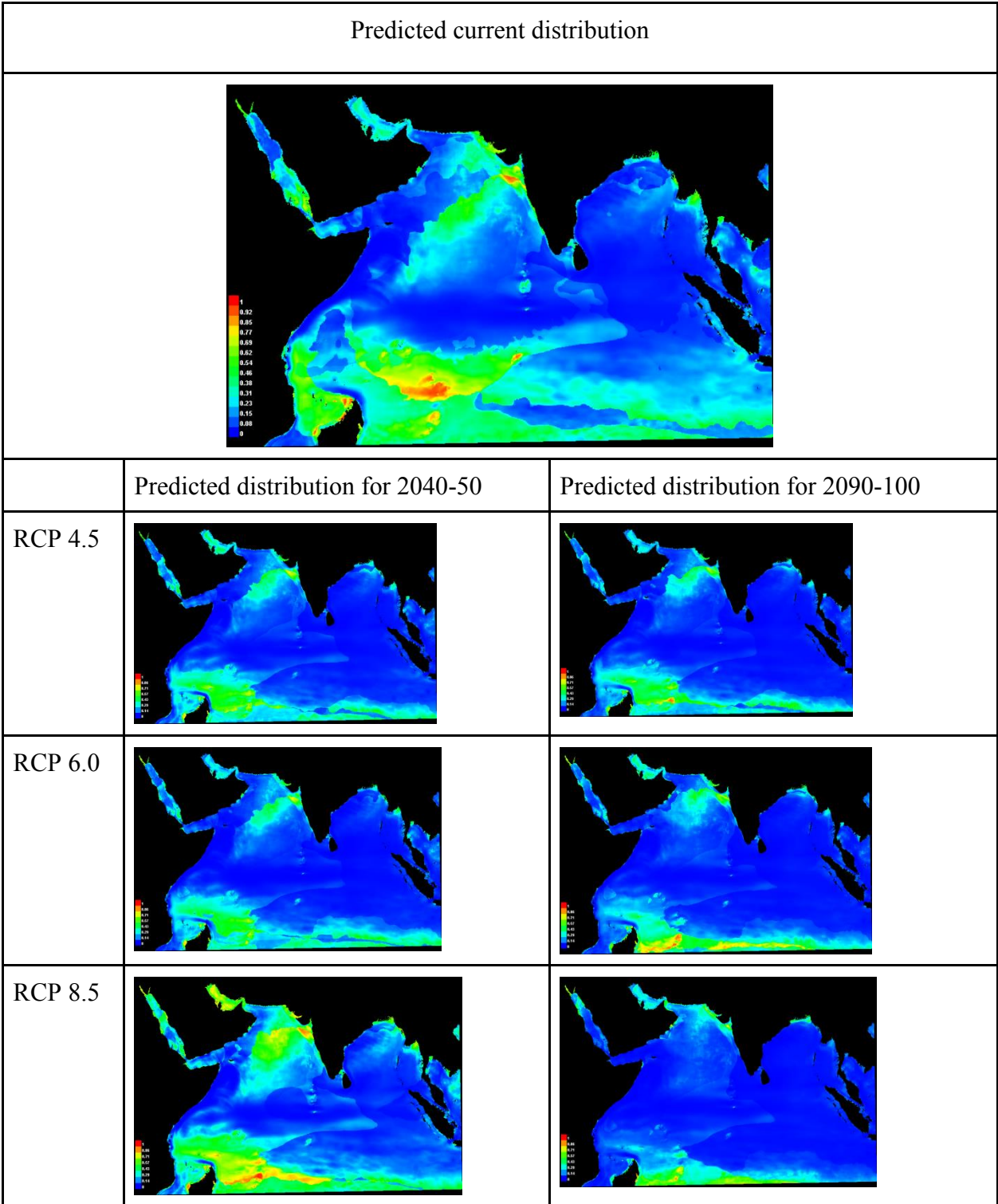


Fig. 92 Map showing the predicted current and future distributions of *Carcharhinus brevipinna*

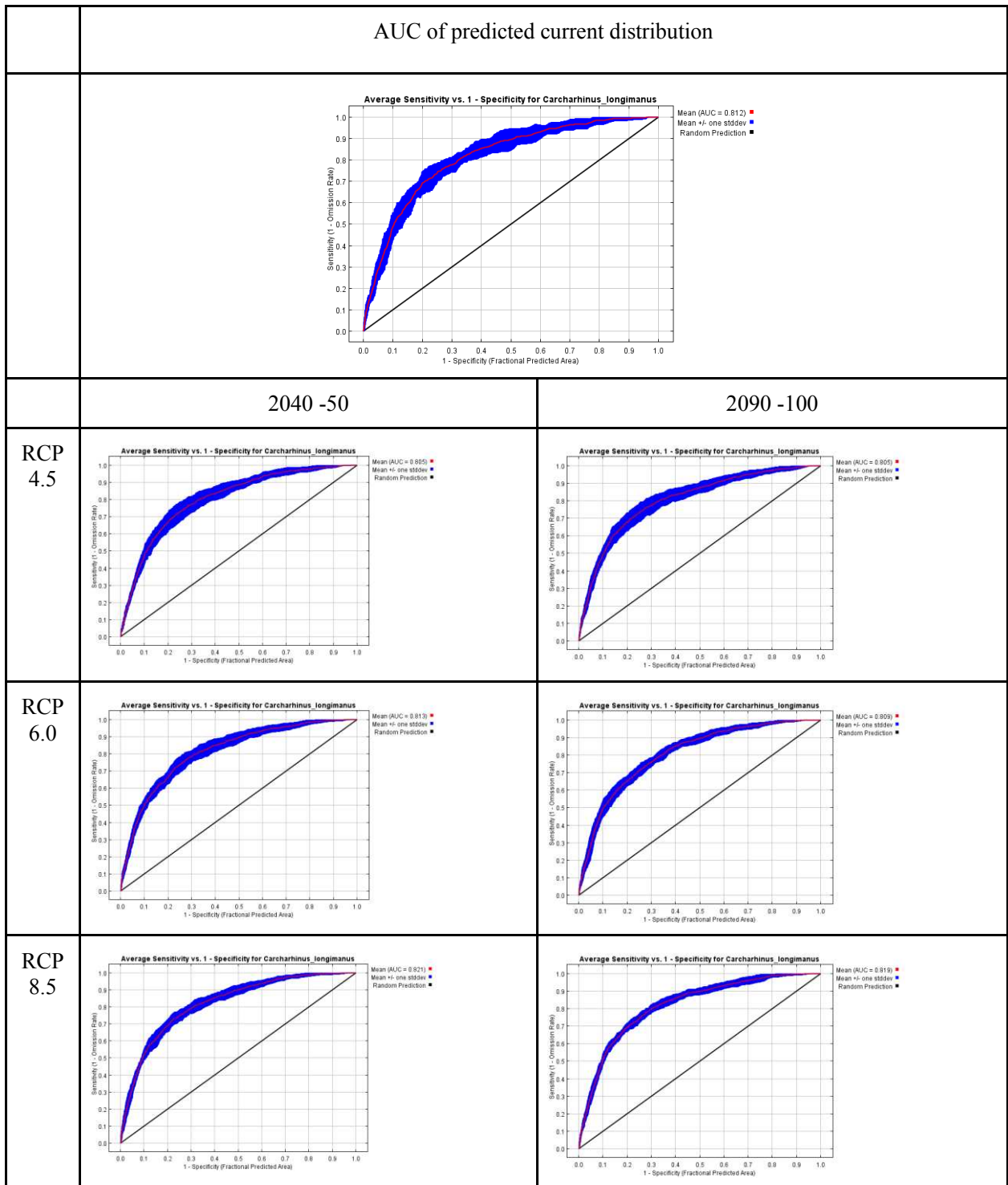


Fig. 93 The average sensitivity vs. 1- specificity graph for *Carcharhinus longimanus* showing the mean Area Under the Curve (AUC) and standard deviation for the predicted current distribution the predicted future distributions

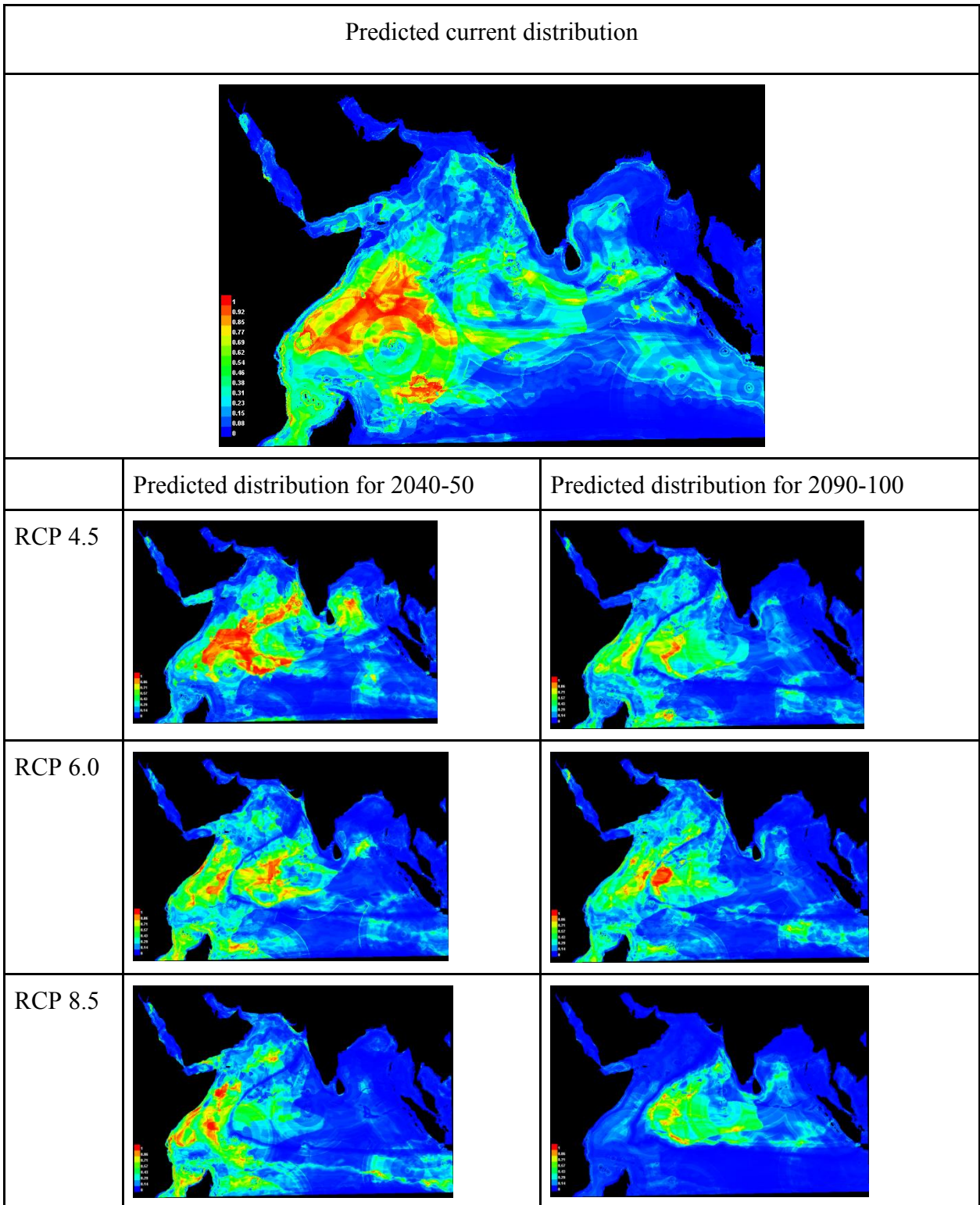


Fig. 94 Map showing the predicted current and future distributions of *Carcharhinus longimanus*

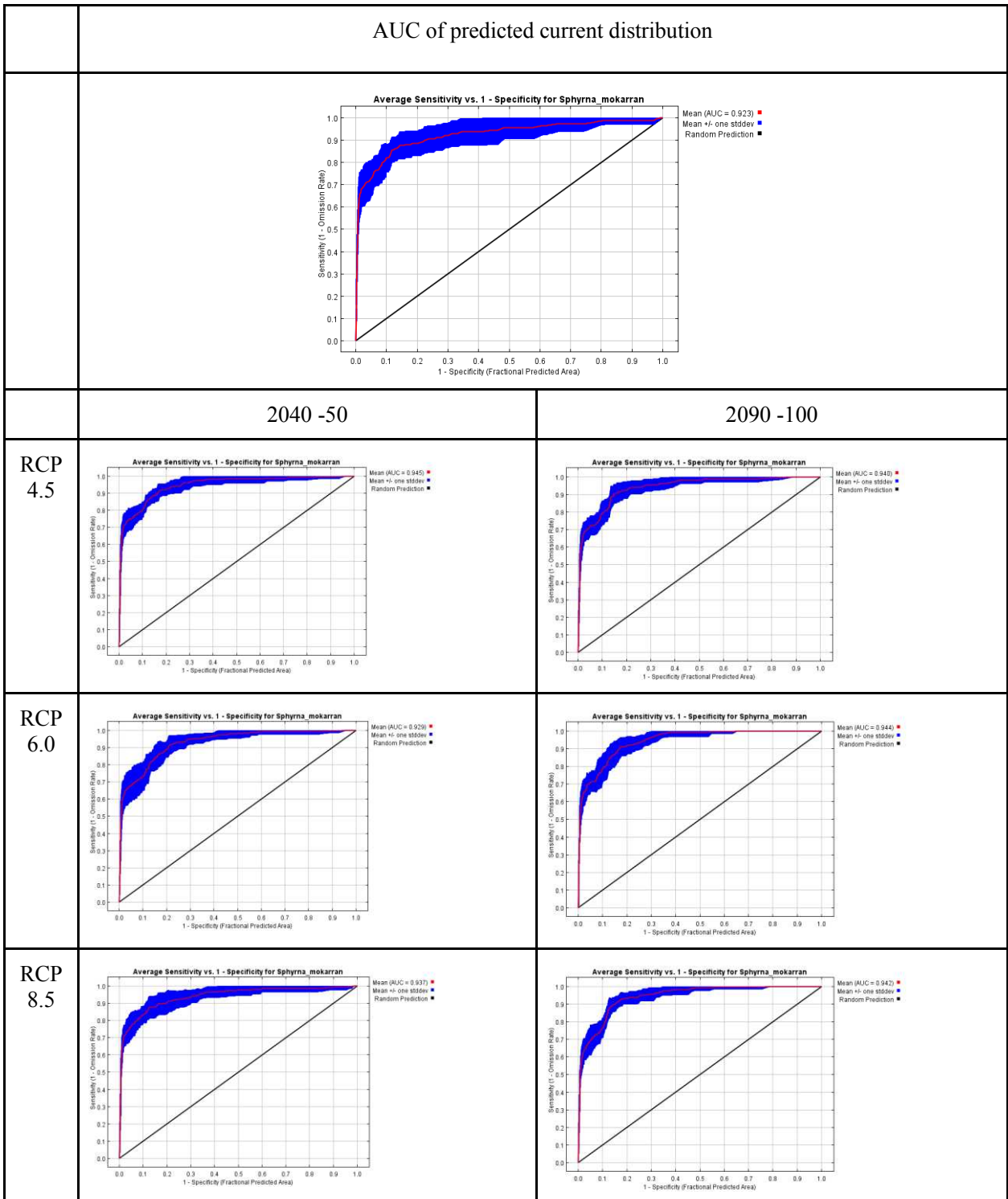


Fig. 95 The average sensitivity vs. 1- specificity graph for *Sphyrna mokarran* showing the mean Area Under the Curve (AUC) and standard deviation for the predicted current distribution the predicted future distributions

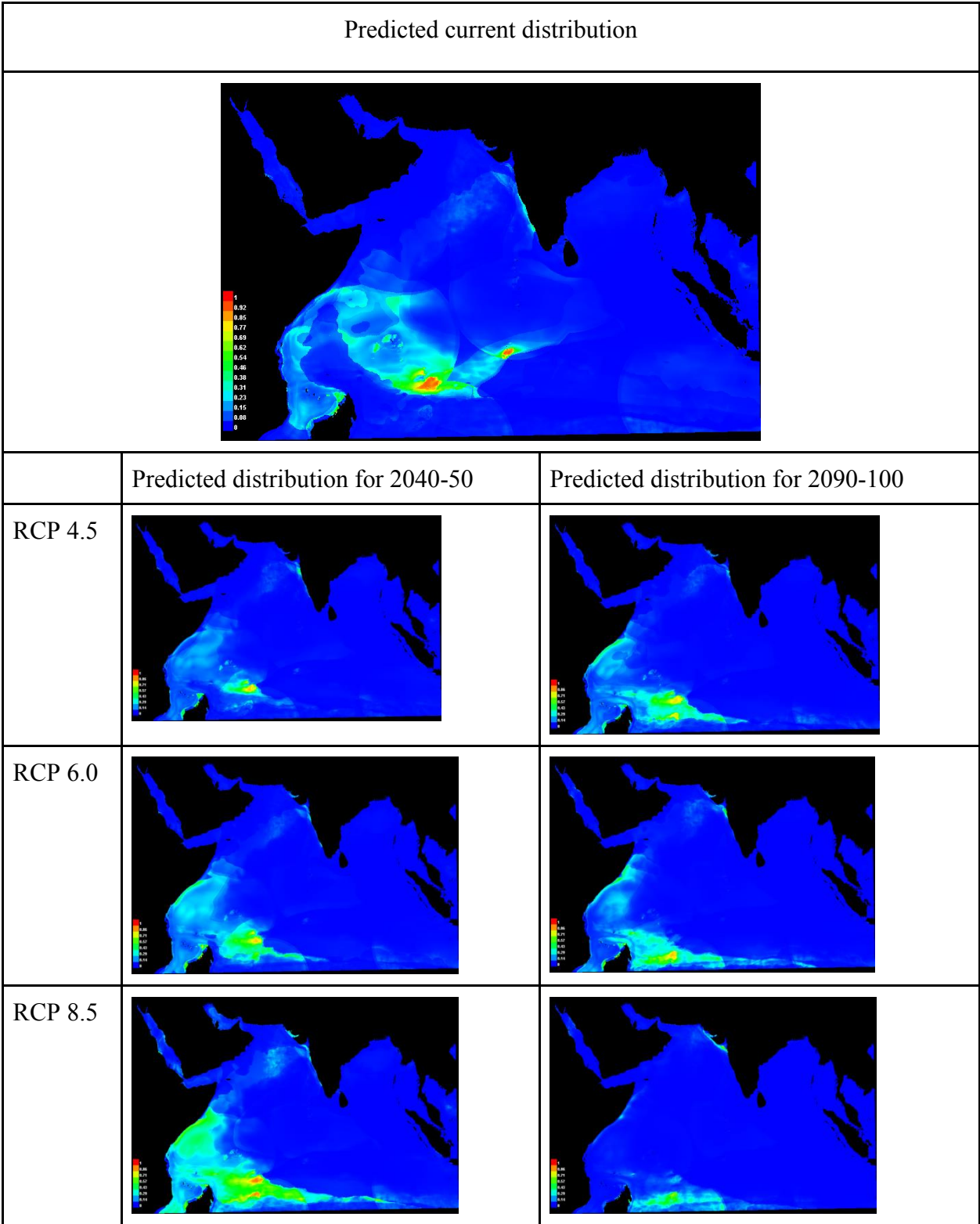


Fig. 96 Map showing the predicted current and future distributions of *Sphyrna mokarran*

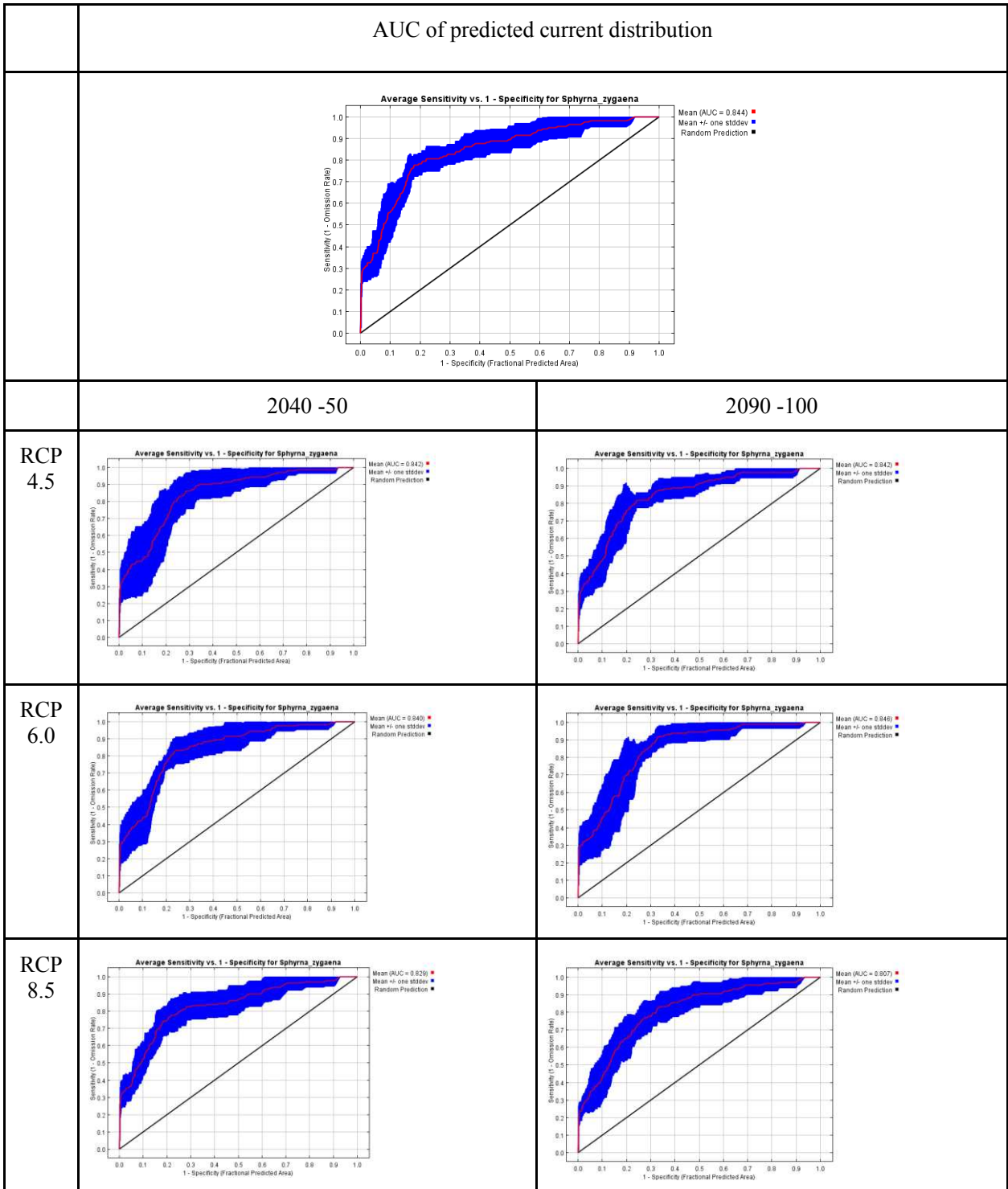


Fig. 97 The average sensitivity vs. 1- specificity graph for *Sphyrna zygaena* showing the mean Area Under the Curve (AUC) and standard deviation for the predicted current distribution the predicted future distributions

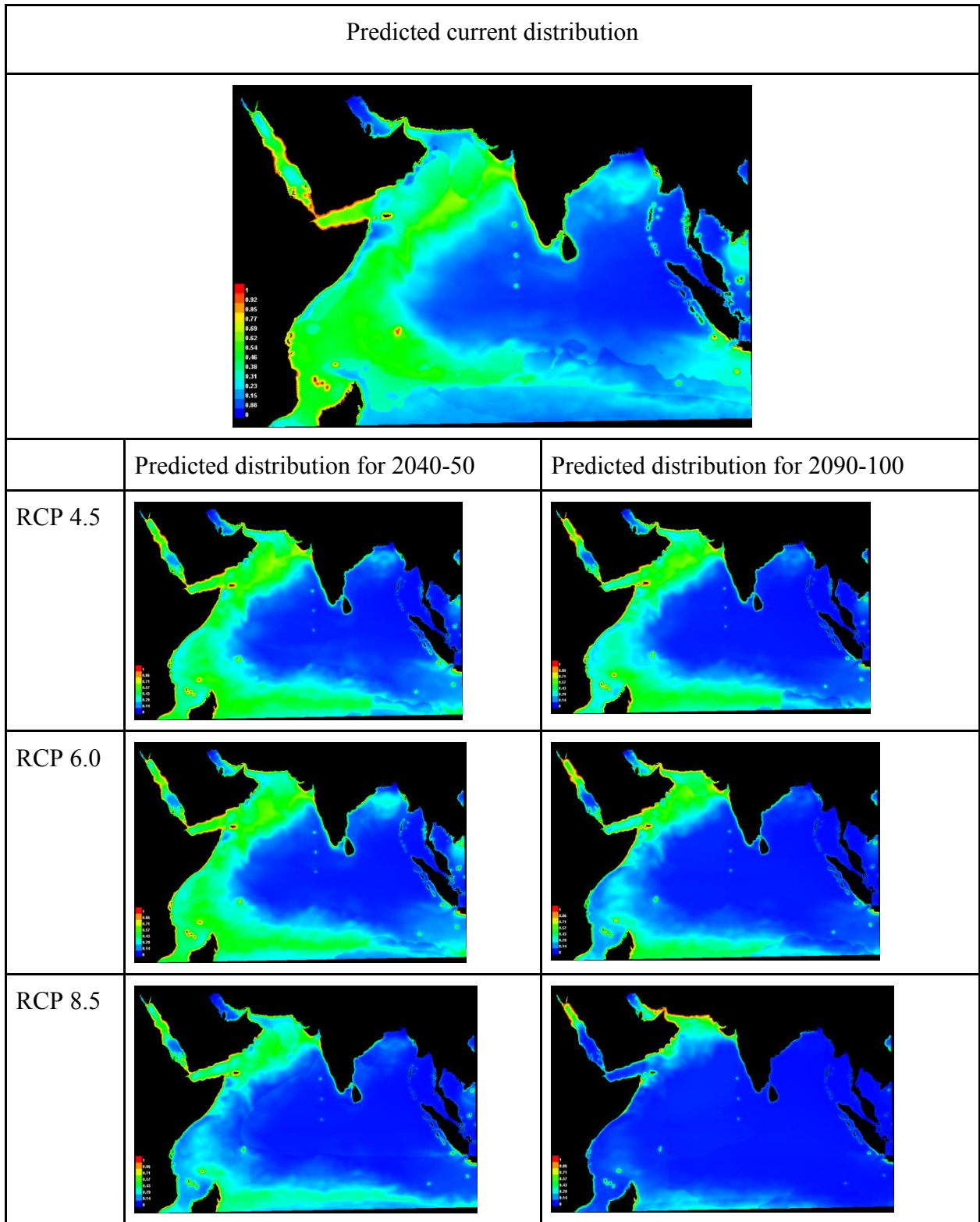


Fig. 98 Map showing the predicted current and future distributions of *Sphyrna zygaena*

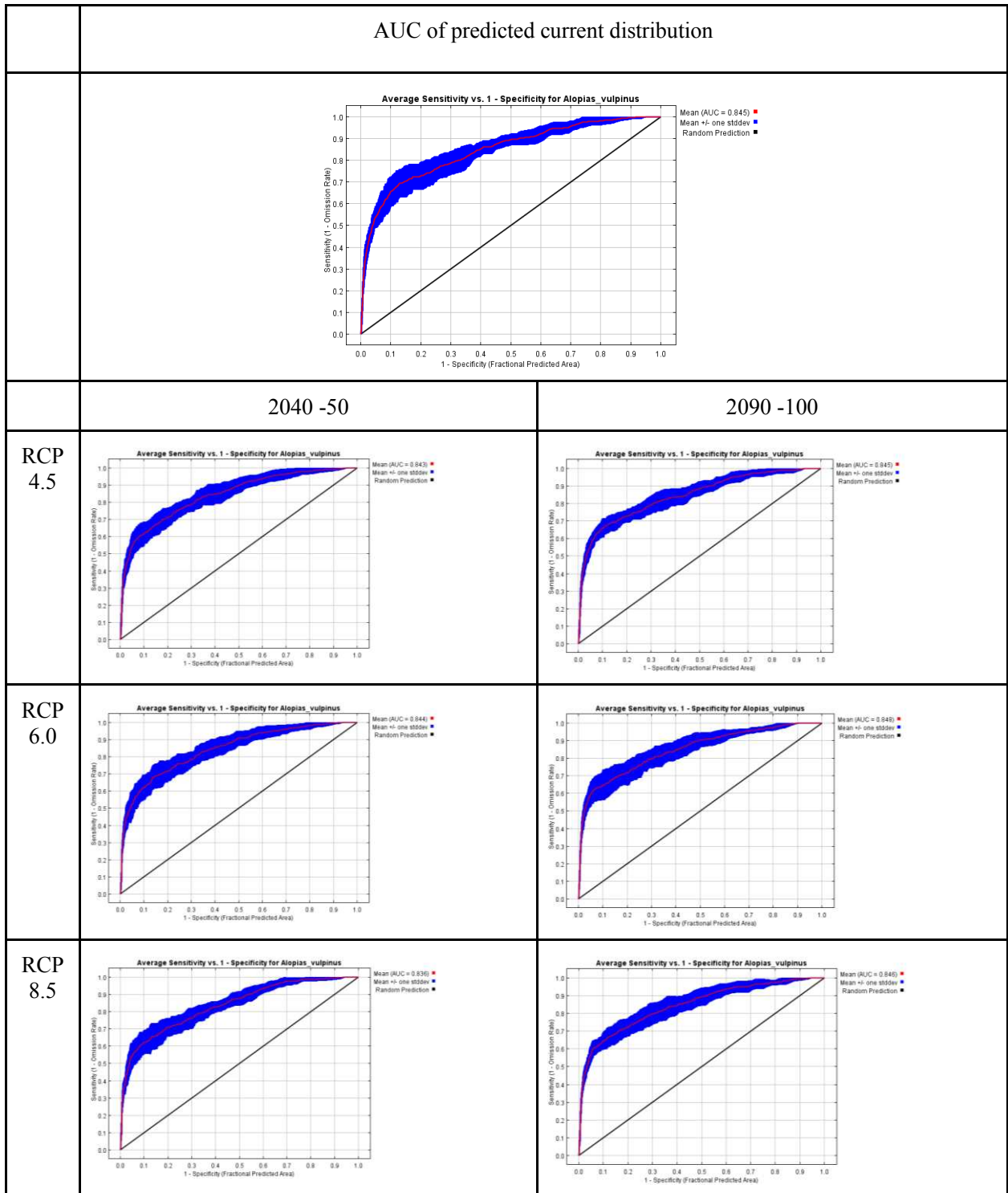


Fig. 99 The average sensitivity vs. 1- specificity graph for *Alopias vulpinus* showing the mean Area Under the Curve (AUC) and standard deviation for the predicted current distribution the predicted future distributions

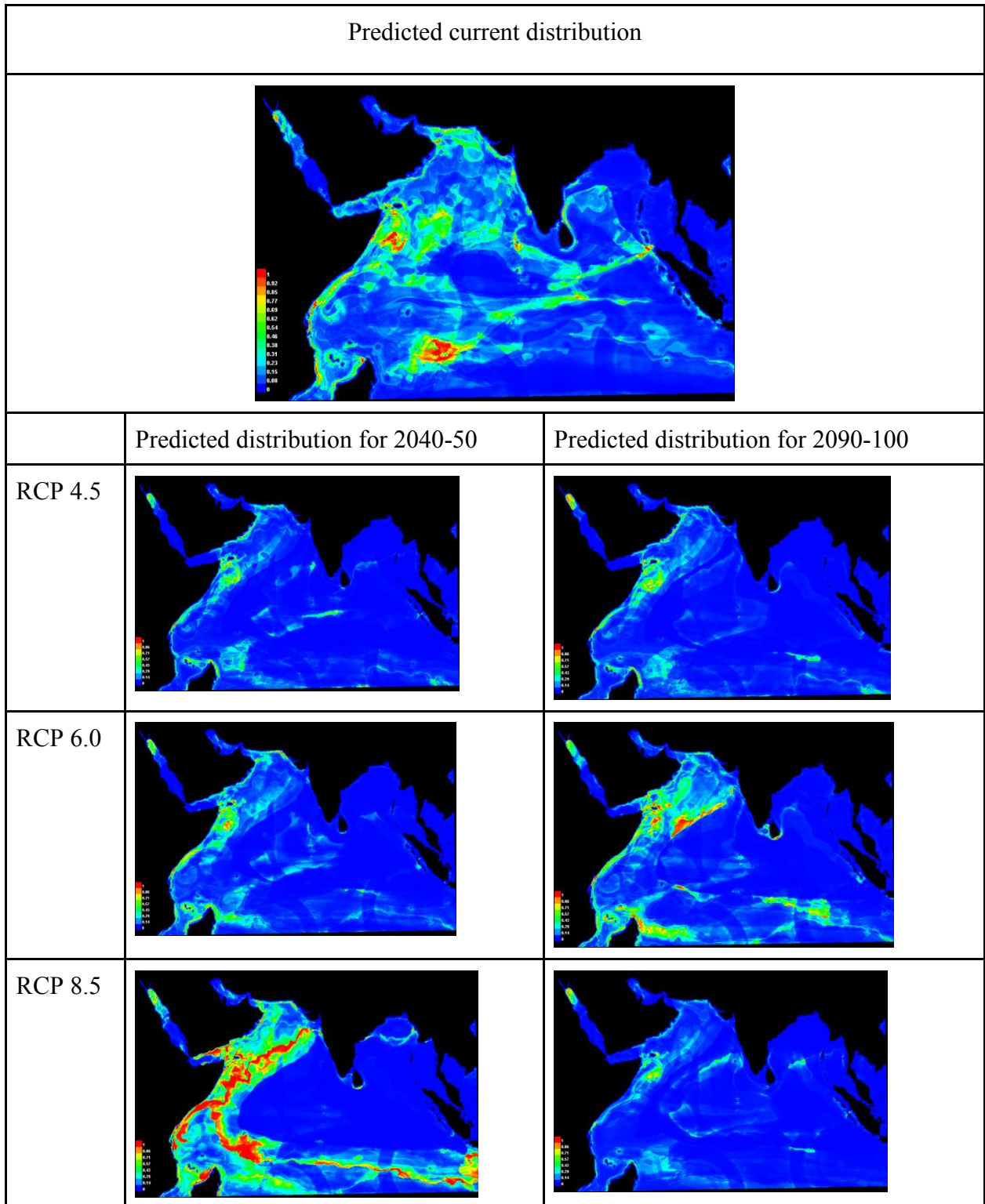


Fig. 100 Map showing the predicted current and future distributions of *Alopias vulpinus*

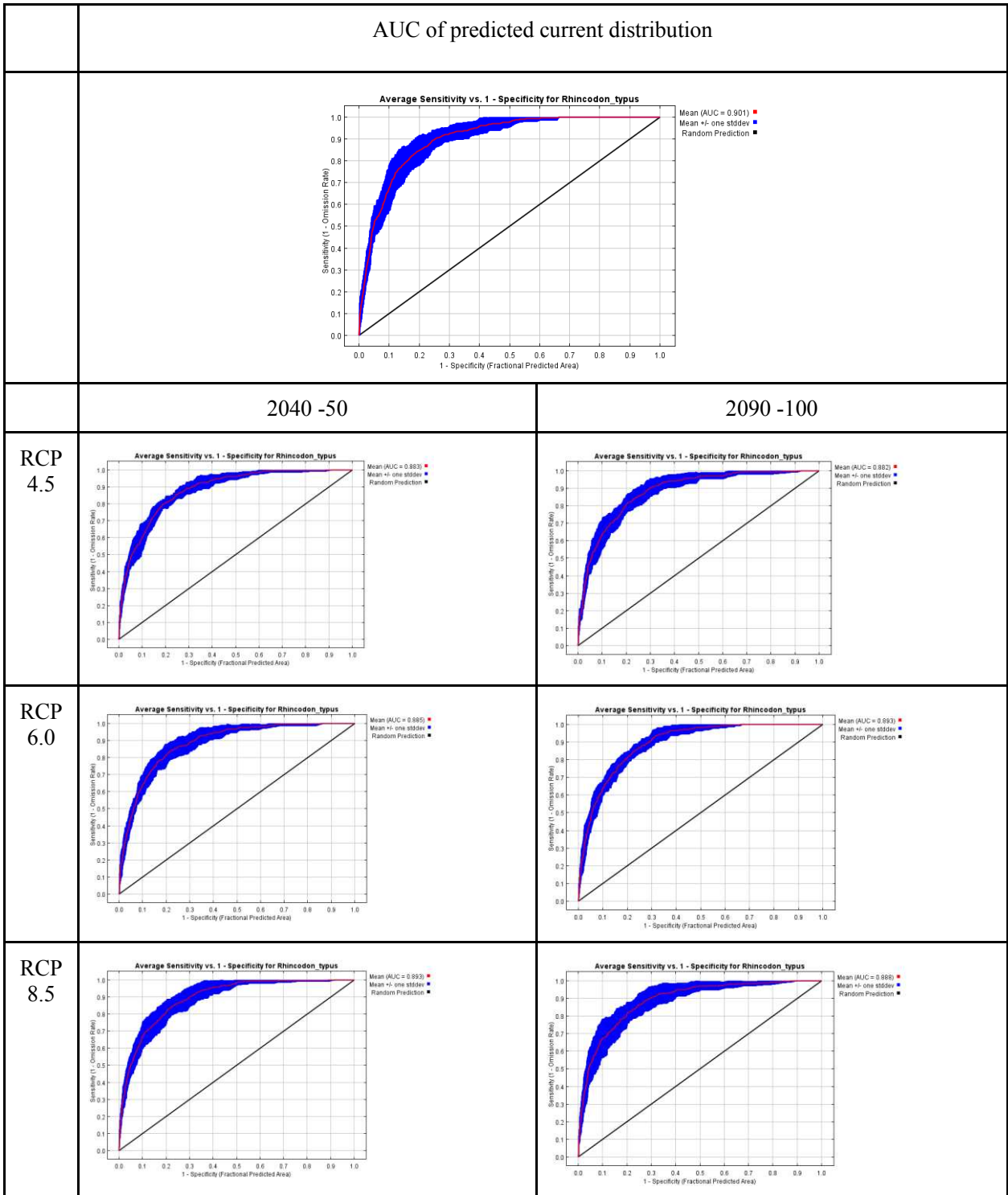


Fig. 101 The average sensitivity vs. 1- specificity graph for *Rhincodon typus* showing the mean Area Under the Curve (AUC) and standard deviation for the predicted current distribution the predicted future distributions

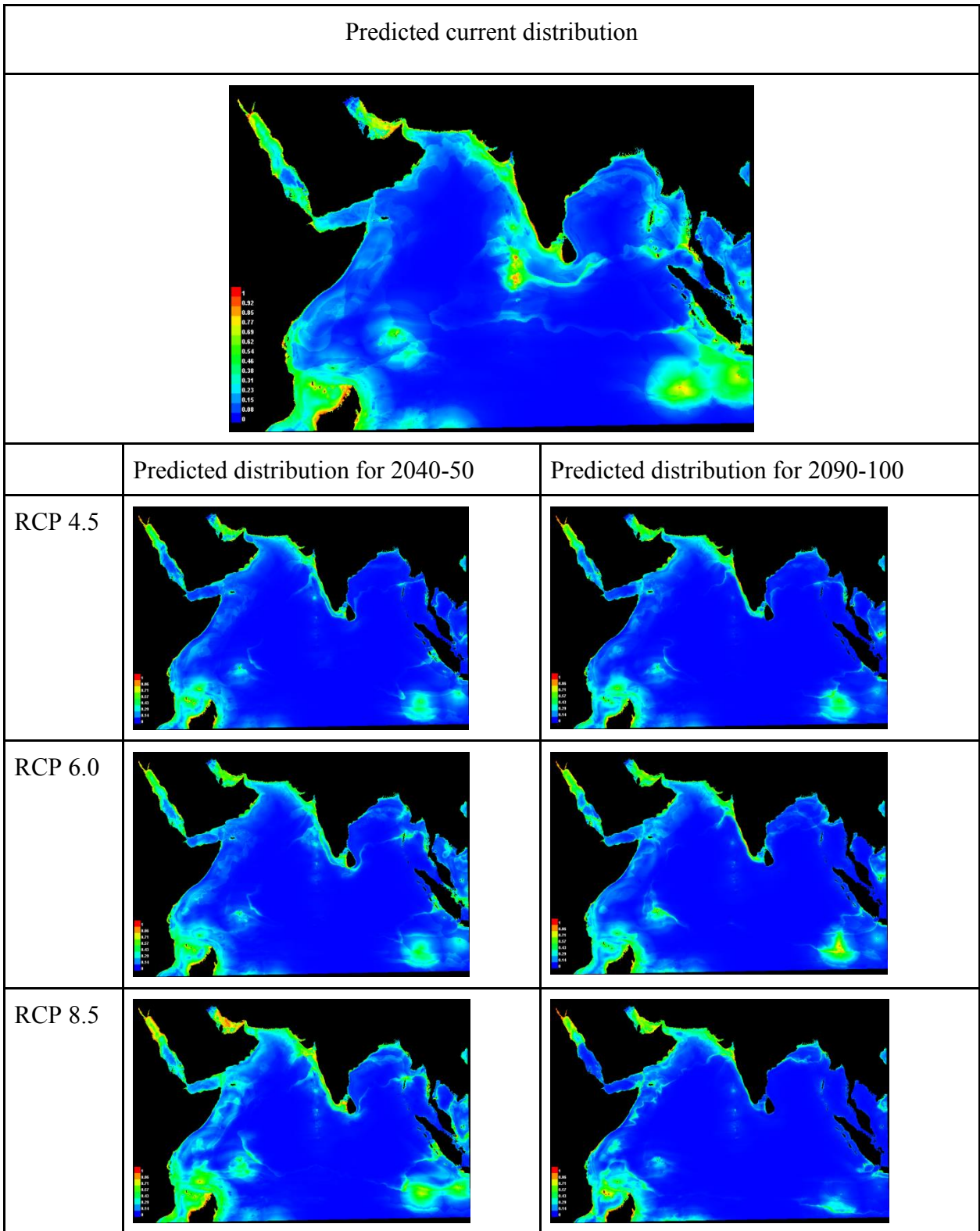


Fig. 102 Map showing the predicted current and future distributions of *Rhincodon typus*

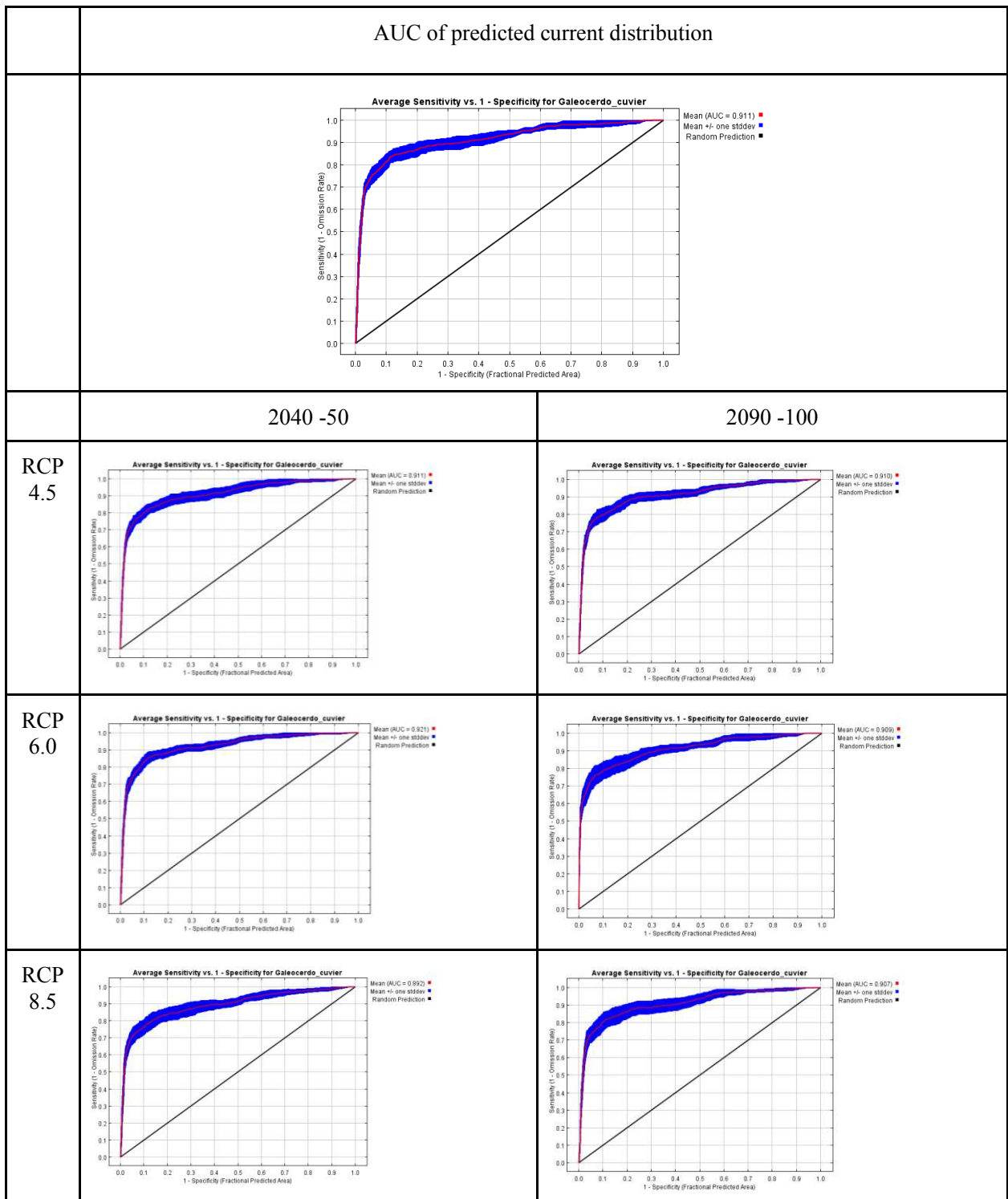


Fig. 103 The average sensitivity vs. 1- specificity graph for Galeocerdo_cuvier showing the mean Area Under the Curve (AUC) and standard deviation for the predicted current distribution the predicted future distributions.

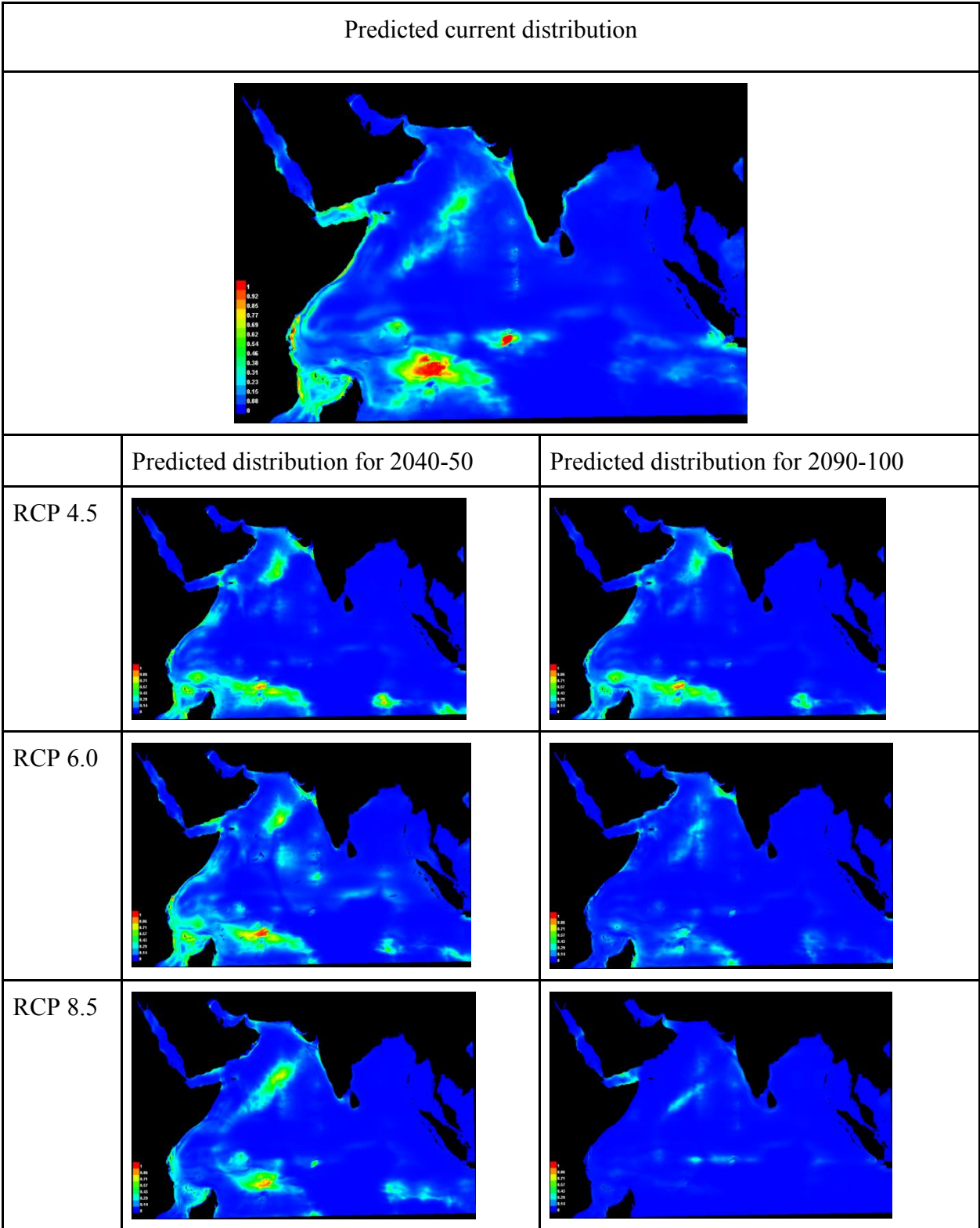


Fig. 104 Map showing the predicted current and future distributions of *Galeocerdo cuvier*

CHAPTER 5

DISCUSSION

Global oceans are warming at the rate of 0.11 °C per decade (Rhein *et al.*, 2013) and the Northern Indian Ocean has the maximum rate of increase in sea surface temperature (Roxy *et al.*, 2020). Such warming has immense effects on the pelagic fishes than the demersal ones (Johnson, 2018). Pelagic fishes may make poleward shifts in their distribution as a response to an increase in the ambient temperature (Poloczanska *et al.*, 2013). Currently, such distributional shifts of many of the pelagic species including the Clupeids which forms some of the major fisheries in the region are not known. Species distribution modelling of such species under different climate change scenarios can throw light to the future ranges of fish distribution and can help fishery managers immensely to make informed decisions to keep the fisheries sustainable.

India is one of the biggest maritime nations in the world. Pelagic fishes form the major commercially important fishes in Indian Ocean. The northern Indian Ocean belongs to the 17 major hotspots among the world oceans and is supposed to warm 90% faster than the world oceans (Zacharia *et al.*, 2016). Clupeidae, Scombridae, Carangidae, Trichiuridae *etc.* are some of the prominent families contributing to pelagic fisheries. Temperature differentiation in the ocean causes most marine species to shift their distributional range (Poloczanska *et al.*, 2014). Even a rise in 1°C can cause distributional change or even mortality in marine species (Vivekanadan *et al.*, 2009). Changes in ocean current pattern are more likely to affect the pelagic species than the demersal (Zacharia *et al.*, 2016). Ocean currents are one of the major biophysical factors, which influence productivity patterns (Rahmstorf *et al.*, 2015). The food and nutrient availability and the larvae dispersion are affected by the warm water intrusion due to changes in current velocity (Zacharia *et al.*, 2016).

The species distribution modelling has an important role in tackling the problem during scenarios where shifts in marine fishes had led to the lack of knowledge on the existing distribution of marine fisheries (Marshall *et al.*, 2014). It is a potential tool for estimating the impact of climate change on range shifts (Beaumont, 2008). In the past three decades, there have

been many developments in the field of species distribution modelling, and multiple methods are now available. Most of them require systematic abundance data produced by formal surveys. However, when such data is sparse, such as in the case of *N. nasus* from our study region, Maxent will be an excellent option which can model presence-only data (Phillips *et al.*, 2006; Phillips & Dudi'k, 2008).

Clupeiformes occupy a wide variety of habitats ranging from Open Ocean to freshwater lakes and rivers (Bloom, 2018). Major Species of clupeids include *Sardinella longiceps*, *Sardinella fimbriata*, *Stolephorus indicus* etc. According to Vivekanadan (2009), as sea surface temperature increases in the predicted line, the distribution of oil sardine may shift to the northern latitudes especially to Gujarat and west Bengal. This can be clearly visible from our prediction. In the predicted current distribution, the areas of western coast of India experience the greatest oil sardine distribution. But as in the case of the year 2040-50 and 2090-100, there is a tremendous decrease in the oil sardine distribution in the Kerala coast and then the Gujarat coast showing the highest probability of distribution. Current velocity is the one of the most contributing variables for *Sardinella longiceps*. (Jufaili *et al.*, 2020) suggest that the geostrophic current velocity, wind speed, SST, cyclone eddies; ENSO and IOD have significant influence on the interannual variability of Sardinella catch in the Omani shelf. According to Kripa *et al.* (2015) overexploitation accompanied by alterations in environmental parameters like SST, wind speed, upwelling, food availability and geostrophic wind driven by large scale oscillations, affect the catch of Sardinella in Kerala coast. According to CMFRI (2017), the south west coast of India and the Malabar upwelling zones are the major regions supporting Anchovy fisheries in India. The Indian anchovy, *Stolephorus indicus* is also distributed in the south west coast of Indian and is one of the best examples showing northward shift. From present distribution to 2050 and 2100, the distribution in the western coast of India gradually decreases and shifts northward to the Gujarat coast. Small pelagics such as sardine and anchovies are susceptible to even small climate variability and they counteract these responses by re-establishing their environments or by extinction (Checkley *et al.*, 2017).

Carangids are the most economically important pelagic fish species in the world (Mukherjee *et al.*, 2017). Some of the major fish species belonging to carangids are *Uraspis secunda*, *Elagatis bipinnulata*, *Seriola rivoliana*. Among these *Uraspis secunda* shows

distribution in the southern part of Arabian Sea, just above Madagascar. As in years 2040-50 and 2090-100, the probability of distribution decreases. Bethoux *et al.*, 1990 recorded the presence of *S. rivoliana* in the Mediterranean Sea and is reported due to the thermal increase in the ocean resulting from climate change. So as there is a decreased predicted distribution of *S. rivoliana* in the Indian Ocean in future years, there are chances that the species may shift to newer environments. Salinity mean is also one of the most contributing factors for *S. rivoliana*. Bohórquez-Cruz *et al.*, 2019 found that *S. rivoliana* larvae can only tolerate a salinity range of 35 and 40g/L. Torpedo scad or *Megalaspis cordyla* is one of the most important pelagic fish in the Indian Ocean (Kasim, 2003). Due to the impact of climate change the predicted current distribution of *M. cordyla* is predicted to decrease in the future.

The Indo-pacific sailfish *Istiophorus platypterus*, is one of the most emerging billfish fisheries in the Indian coast (Ganga *et al.*, 2008). Research on the distribution of sailfishes are very less when compared with other fishes like tunas (Ramalingam *et al.*, 2011). The predicted distribution shows a decline in distribution in the RCPs in 2050 but in 2100, the pattern of distribution is more or less similar in all RCPs but its extent decreased when compared to the predicted present distribution. The decline in extent can be attributed to the effects of climate change. Blue marlin, *Makaira nigricans* show a decreased distribution in all RCPs in both the years. Since it spends most of its time in the surface waters, increase in sea surface temperature will have a huge impact on the abundance of *M. nigricans* (Block *et al.*, 1992)

Increase in ocean temperature also drove the spawning grounds of *Thunnus obesus* in the western Pacific Ocean to switch from tropics to subtropical regions (Lehodey *et al.*, 2010). Rise in ocean temperature adversely affects the larval development of *Thunnus albacare* (Dell'Apa, A *et al.*, 2018). But contradictorily the predicted distribution of *Thunnus albacares* and *Thunnus obesus* shows an increased distribution in the future. There is a lack of sufficient studies regarding the increase in abundance of these till 2050 and is then predicted to decrease (Lehodey *et al.*, 2013). It also shows that spawning becomes more suitable at northern latitudes. Our predicted distribution shows a decreased distribution. Two species. *Thunnus alalunga* shows a decreased extent in range from predicted current distribution to 2100. Studies conducted by Sund *et al.*, 1981 found that the temperature change has most effect in the spawning and

survival of larvae of *T. alalunga*. The future distribution modelling in the Pacific Ocean suggests that there is increase in biomass of skipjack tuna, *Katsuwonus pelamis* in western central Pacific

The predicted distribution of Blue shark, *Prionace glauca* shows an increasing extent from present to 2100. Current velocity mean is one of the most contributing factors for *P. glauca*. This highly migratory fish is a generalist feeder which consumes a wide range of prey species (Corte's, 1999), and due to this it is predicted to expand its environment regardless of any variations in the prey in the climate changing scenario (Taguchi *et al.*, 2015). *Carcharhinus plumbeus* distribution shows a decrease in extent from predicted current distribution to future RCPs. Soufi-Kechaou *et al.* (2018) also found that climate change can also drive *C. plumbeus* northward. *Carcharhinus limbatus* distribution shows a decreasing trend in distribution until 2050 in all RCPs but then the distribution goes on increasing till 2100. This may be due to the change in environmental variables accordingly in all RCPs. But climate change also has an influence on the distribution of *C. limbatus*. Baitfish availability and temperature are some of the major factors determining the distribution (Kajiura and Tellman, 2016)

The predicted distribution for epipelagic whale sharks shows a range contraction in the future. In Indian Ocean, the environmental suitability is primarily correlated with the spatial variation in the SST and the whale shark can only tolerate a narrow range of temperature from 26.5°C to 30°C (Sequeira *et al.*, 2012). Studies conducted by Sequeira *et al.* (2014) from the period 1980 to 2010 suggests that in Indian ocean and Atlantic, due to predicted rise in sea surface temperature, the whale shark population faced a poleward shift together with range reduction. So, climate change adversely affects the distribution and abundance of whale shark (Gutierrez *et al.*, 2008). Distance from the shore is the most contributing factor for the distribution of *Rhincodon typus*. McKinney *et al.* (2012) found that distance from the continental shelf edge is one of the favouring factors for whale shark spotting as it is highly related with food availability. The Sea surface current has a little effect in the distribution of whale shark (Sleeman *et al.*, 2010)

Empirical orthogonal function analysis has been done to find the spatial and temporal variability in sea surface temperature in the Indian Ocean using SST datasets from 1993 to 2018. EOF 1 to 4 with spatial variability and its corresponding principle components showing

temporal variability has been obtained. The EOF1 shows a greater warming over the western Indian Ocean with 32.25% eigenvalue. The warming trend is predicted to be 0.0165°C per year and 0.4134°C per 25 years. (Rhein *et al.*, 2013) found that the global oceans are warming at the rate of 0.11°C per decade. The Indian Ocean has warmed more rapidly than other global tropical oceans (Dhame, *et al.*, 2020). According to Kulkarni et al, 2007 strong warming was reported in both eastern and western Indian Ocean after 1950. The EOF2 and 3 shows a dipole pattern over the Indian Ocean. This can be due to the internal mode of climatic variability over Indian ocean- the Indian Ocean dipole. This was first found by Saji et al, 1999. He used the 40-year GISST datasets from 1958 to 1998. Our predicted EOF shows a negative IOD over the Indian Ocean. The studies on the negative IOD are uncommon and some of them mainly focus on the extreme negative IOD in 2016 which caused severe drought in the East African region (Lu *et al.*, 2018, Lim *et al.*, 2017)

CHAPTER 6

SUMMARY

Earth's climate system is being subjected to constant changes. The term climate change itself implies the long-term alterations in the climate system. But the anthropogenic climate changes are causing unprecedented transformations in the planet. Increasing global average temperature, increased frequency of extreme events etc. are some of the effects of climate change. Global oceans are also being affected by this. The marine species counteract these changes by reallocating their distributional boundaries. Among the marine fish species, pelagic are mainly affected by the impact of climate change. It also pushes some species to higher latitude. As Indian Ocean is landlocked, the northward shift of the species will be further hindered. This can even cause local extinctions. The study mainly focused on investigating the changes in climatic parameters as well as the spatial distribution of marine fish species in the northern Indian Ocean. Predicting the shift in spatial distribution can enable proper prediction of future habitat suitability of the marine species and it also helps to take proper management actions.

Empirical orthogonal function analysis has been done to find the spatial and temporal variability of sea surface temperature. The SST data was taken from CMEMS Copernicus. Species distribution modelling using maximum entropy model (Maxent) has done to the major families of pelagic fish species in the northern Indian Ocean such as Clupeidea, Carangidae, Istiophoridae, Scombridae, Carcharhinidae etc. The major environmental parameters affecting the species have been taken. Pearson's rank correlation has been done to avoid multicollinearity. The environmental parameters selected are sea surface temperature Maximum, SST Mean, SST minimum, Sea surface salinity Mean, Current velocity mean, current velocity minimum and distance from the shore. Environmental layers of RCP 4.5, 6.0 and 8.5 for predicting the present, 2040-2050 and 2090-2100 have been taken from Bio-oracle with 9.2km resolution. The species data were taken from GBIF and OBIS open source databases.

EOF analysis on the sea surface temperature showed that there is an increased trend in sea surface temperature over the major parts of the northern Indian Ocean. The warming trend is predicted to be 0.0165°C per year and 0.4134°C per 25 years. Maximum entropy modelling

for the species predicted a changing in distribution pattern in almost all species. The predicted distribution of species such as *Sardinella longiceps* shows reduced extent of distribution over the Indian Ocean in the future RCPs. *Sphyrna zygaena*, *Rastrelliger kanagurta* etc shows a northward extent. This can be a clear indication of the impact climate change has on the species. But contradictorily some species such as *Thunnus albacare* , *Thunnus obesus* shows a tremendous increase in future years. This can be due to the food availability and habitat suitability.

CHAPTER 7

REFERENCES

- Al Jufaili, S.M. and Piontkovski, S.A. 2020. Seasonal and Interannual Variations of Sardine Catches along the Omani Coast. *Int. J. of Oceans and Oceanogr.* 14(1), pp.77-99.
- Al Sakaff, H. and Esseen, M. 1999. Occurrence and distribution of fish species off Yemen (Gulf of Aden and Arabian Sea). *Naga ICLARM Q.* 22(1):43-47.
- Alexander, R.E. 2016. *A comparison of GLM, GAM, and GWR modeling of fish distribution and abundance in Lake Ontario*. Doctoral dissertation, MSc Thesis. University of Southern California, Los Angeles, California, USA.
- Allen, G.R. and Erdmann, M.V. 2012. Reef fishes of the East Indies. Perth, Australia: University of Hawai'i Press. Volumes I-III. *Trop. Reef Res.*
- Allen, G.R., Erdmann, M.V. and Cahyani, D. 2012. Description of *Ptereleotris caerulea marginata* new species (Pisces: Ptereleotridae). In: Allen, G.R., Erdmann, M.V. (Eds.), Reef fishes of the East Indies, volume III, *Trop. Reef Res.*, Perth, Australia, pp. 1190–1193.
- Anderson, R.P., Lew, D. and Peterson, A.T. 2003. Evaluating predictive models of species' distributions: criteria for selecting optimal models. *Ecological Modelling* 162, 211–232.
- Azhar Ehsan, M., Nicoli, D., Kucharski, F., Almazroui, M., Tippet, M., Bellucci, A., Ruggieri, P. and Kang, I.S. 2020. May. Atlantic Ocean Influence on Middle East Summer Surface Air Temperature. In EGU General Assembly Conference Abstracts (p. 10459).
- Baasch, D.M., Tyre, A.J., Millspaugh, J.J., Hygnstrom, S.E., and Vercauteren, K.C. 2010. An evaluation of three statistical methods used to model resource selection. *Ecol. Model.* 221(4), pp.565-574.
- Bailey, H., and Thompson, P. M. 2009. Using marine mammal habitat modelling to identify priority conservation zones within a marine protected area. *Mar. Ecol. Prog. Ser.* 378. 279-287.
- Baldwin, R.A., and Bender, L.C. 2008. Den-Site Characteristics of Black Bears in Rocky Mountain National Park, Colorado. *J. Wildl. Manag.* 72(8). pp.1717-1724.

- Barlow, J. 1999. Trackline detection probability for long-diving whales. *Mar. mammals surv. & assess. methods*. 1, 209.
- Barve, N., Barve, V., Jiménez-Valverde, A., Lira-Noriega, A., Maher, S.P., Peterson, A.T., Soberón, J., and Villalobos, F. 2011. The crucial role of the accessible area in ecological niche modeling and species distribution modeling. *Ecol. Model.* 222(11). pp.1810-1819.
- Beaumont, L. J., L. Hughes and A. J. Pitman. 2008. Why is the choice of future climate scenarios for species distribution modelling important? *Ecol. lett.*, 11(11): 1135-1146.
- Berry, P.M., Dawson, T.P., Harrison, P.A., and Pearson, R.G. 2002. Modelling potential impacts of climate change on the bioclimatic envelope of species in Britain and Ireland. *Global. Ecol. Biogeogr.* 11(6). pp.453-462.
- Bertrand, A., Segura, M., Gutiérrez, M. and Vásquez, L. 2004. From small-scale habitat loopholes to decadal cycles: a habitat-based hypothesis explaining fluctuation in pelagic fish populations off Peru. *Fish and fish.* 5(4). pp.296-316.
- Bertrand, A., Lengaigne, M., Takahashi, K., Avadí, A., Poulain, F. and Harrod, C. 2020. El Niño Southern Oscillation (ENSO) Effects on Fisheries and Aquaculture.
- Bethoux J.P., Gentili B., Raunet J. & D. Tailliez, 1990. - Warming trend in the western Mediterranean deep water. *Nature*, 347: 660-662.
- Bigg, G.R., Cunningham, C.W., Ottersen, G., Pogson, G.H., Wadley, M.R. and Williamson, P. 2008. Ice-age survival of Atlantic cod: agreement between palaeoecology models and genetics. *Proceedings of the Royal Soc. B: Biol. l Sci.*, 275(1631). pp.163-173.
- Bineesh, K. K., Akhilesh, K. V., Abdussamad, E. M. and Pillai, N. G. K. 2013. *Chelidoperca maculicauda*, a new species of perchlet (Teleostei: Serranidae) from the Arabian Sea. *Aqua. Int. J. Ichthyology.* 19 (2), 71–78.
- Block, B. A., Booth, D. T., & Carey, F. G. 1992. Depth and temperature of the blue marlin, *Makaira nigricans*. observed by acoustic telemetry. *Mar. Biol.* 114(2), 175–183. doi:10.1007/bf00349517 <https://academic.oup.com/icesjms/article/68/6/1072/701442>
- Bloom, D.D. and Egan, J.P. 2018. Systematics of Clupeiformes and testing for ecological limits on species richness in a trans-marine/freshwater clade. *Neotropical Ichthyology*, 16(3).

- Bohórquez-Cruz M, Sonneholzer S, Argüello-Guevara W. 2019. Effect of water salinity on embryonic development of longfin yellowtail *Seriola rivoliana* larvae. *Aquac Res.* <https://doi.org/10.1111/are.14468>
- Bouchard, C. and Crumplin, W. 2010. Neglected no longer: the Indian Ocean at the forefront of world geopolitics and global geostrategy. *J. of the Indian Ocean Region*, 6(1), pp.26-51.
- Carpenter, K.E., Abrar, M., Aeby, G., Aronson, R.B., Banks, S., Bruckner, A., Chiriboga, A., Cortés, J., Delbeek, J.C., DeVantier, L., and Edgar, G.J. 2008. One-third of reef-building corals face elevated extinction risk from climate change and local impacts. *Science*, 321(5888), pp.560-563.
- Carpenter, K.E., F. Krupp, D.A. Jones and U. Zajonz, 1997. Living marine resources of Kuwait, eastern Saudi Arabia, Bahrain, Qatar, and the United Arab Emirates. FAO species identification field guide for fishery purposes. 293p + 17 col. plates. Rome, FAO.
- Caswell, H. 2001. Matrix Population Models: Construction, Analysis and Interpretation (Sinauer, Sunderland, MA).
- Cervigón, F. 1993. Los peces marinos de Venezuela. Volume 2. Fundación Científica Los Roques. Caracas, Venezuela. 497 p.
- Chatterjee, T.K. and Mishra, S.S. 2013. A new genus and new species of Gobioid fish (Gobiidae: Gobionellinae) from Sunderbans, India. *Rec. Zool. Surv. India* 112 (4), 85–88.
- Checkley DM Jr, Asch RG, Rykaczewski RR 2017 Climate, anchovy, and sardine. *Annu Rev. Mar. Sci.* 9:469–493
- Chen, I.C., Hill, J.K., Ohlemüller, R., Roy, D.B., and Thomas, C.D. 2011. Rapid range shifts of species associated with high levels of climate warming. *Science*, 333(6045). pp.1024-1026.
- Chen, I.C., Shiu, H. J., Benedick, S., Holloway, J.D., Chey, V.K., Barlow, H.S., Hill, J.K., and Thomas, C.D. 2009. Elevation increases in moth assemblages over 42 years on a tropical mountain. *Proc. Natl. Acad. Sci.* 106(5), pp.1479-1483.
- Cheung, W. W., Jones, M. C., Reygondeau, G., Stock, C. A., Lam, V. W., and Frölicher, T. L. 2016. Structural uncertainty in projecting global fisheries catches under climate change. *Ecol. Model.* 325, 57-66.

- Cheung, W.W., Lam, V.W., Sarmiento, J.L., Kearney, K., Watson, R. and Pauly, D. 2009. Projecting global marine biodiversity impacts under climate change scenarios. *Fish and fish*. 10(3), pp.235-251.
- CITES, UNEP-WCMC, 2017. The Checklist of CITES Species Website. Appendices I, II and III valid from 04 October 2017. CITES Secretariat, Geneva, Switzerland. Compiled by UNEP-WCMC, Cambridge, UK. <https://www.cites.org/eng/app/appendices.php> [Accessed 08/17/2017].
- Clark, C.O., Cole, J.E. and Webster, P.J. 2000. Indian Ocean SST and Indian summer rainfall: Predictive relationships and their decadal variability. *J. of Clim.* 13(14), pp.2503-2519.
- Close, C., Cheung, W., Hodgson, S., Lam, V., Watson, R. and Pauly, D. 2006. Distribution ranges of commercial fishes and invertebrates. p. In *Fishes in Databases and Ecosyst. Fish. Centre Res. Rep. 14 (4)*. University of British.
- CMFRI (2017) CMFRI annual report 2016–2017. Central Marine Fisheries Research Institute, Kochi
- Collette, B.B. and C.E. Nauen, 1983. FAO Species Catalogue. Vol. 2. Scombrids of the world. An annotated and illustrated catalogue of tunas, mackerels, bonitos and related species known to date. Rome: FAO. FAO Fish. Synop. 125(2):137 p.
- Collette, B.B. 2001. Scombridae. Tunas (also, albacore, bonitos, mackerels, seerfishes, and wahoo). p. 3721-3756. In K.E. Carpenter and V. Niem (eds.) FAO species identification guide for fishery purposes. The living marine resources of the Western Central Pacific. Vol. 6. Bony fish part 4 (Labridae to Latimeriidae), estuarine crocodiles. FAO, Rome.
- Compagno, L.J.V., D.A. Ebert and M.J. Smale, 1989. Guide to the sharks and rays of southern Africa. New Holland (Publ.) Ltd. London. 158 p.x
- Corbet, S.A., Saville, N.M., Fussell, M., Prÿs-Jones, O.E., and Unwin, D.M. 1995. The competition box: a graphical aid to forecasting pollinator performance. *J. Appl. Ecol.*, pp.707-719.
- Corte's, E. 1999. Standardized diet compositions and trophic levels of sharks. *ICES J. of Mar. Sci.* 56, 707–717. doi:10.1006/ JMSC.1999.0489

- Craig, R. 2010 “Stationarity is dead”-long live transformation: Five principles for climate change adaptation law. *Harvard Environ. Law* 34:9-75.
- Crouse, D.T., Crowder, L.B., and Caswell, H. 1987. A stage-based population model for loggerhead sea turtles and implications for conservation. *Ecol.* 68:1412-1423.
- Crowder, L.B., Crouse, D.T., Heppell, S.S., and Martin, T.H. 1994. Predicting the impact of turtle excluder devices on loggerhead sea-turtle populations. *Ecol. Appl.* 4:437-445.
- Cushing DH. Plankton production and year-class strength in fish populations: an update of the match/mismatch hypothesis. *Adv. Mar. Biol.* 1990, 26: 249–293.
- De Sylva, D.P. 1990. Sphyraenidae. p. 860-864. In J.C. Quero, J.C. Hureau, C. Karrer, A. Post and L. Saldanha (eds.) Check-list of the fishes of the eastern tropical Atlantic (clofeta). jnict, Lisbon; SEI, Paris; and UNESCO, Paris. Vol. 2.
- Degraer, S., Verfaillie, E., Willems, W., Adriaens, E., Vincx, M., and Van Lancker, V. 2008. Habitat suitability modelling as a mapping tool for macrobenthic communities: an example from the Belgian part of the North Sea. *Continental Shelf Res.* 28(3), 369-379.
- Dell’Apa, A., Carney, K., Davenport, T., & Vernon Carle, M. 2018. Potential medium-term impacts of climate change on tuna and billfish in the Gulf of Mexico: A qualitative framework for management and conservation. *Mar. Environmen. Res.* 141, 1– 11. <https://doi.org/10.1016/j.marenvres.2018.07.017>
- DeVaney, S.C. 2016. Species distribution modeling of deep pelagic eels. *Integrative & comp. biol.* 56(4), pp.524-530.
- DeVantier, L., Hodgson, G., Huang, D., Johan, O., Licuanan, A., Obura, D.O., Sheppard, C., Syahrir, M. and Turak, E. 2014. *Favia pallida*. The IUCN Red List of Threatened Species 2014:e.T132936A54163337.
- Dhame, S., Taschetto, A.S., and Santoso, A. 2020. Indian Ocean warming modulates global atmospheric circulation trends. *Clim. Dyn.* 55, 2053–2073
- Dulvy, N.K., Rogers, S.I., Jennings, S., Stelzenmüller, V., Dye, S.R., and Skjoldal. H.R. 2008. Climate change and deepening of the North Sea fish assemblage: a biotic indicator of warming seas. *J. Appl. Ecol.* 45(4), pp.1029-1039.

- Elith, J., Graham, H. C., Anderson, P., Dudík, Ferrier, R., Guisan, S., Hijmans, A., Huettmann, J.R., Leathwick, F.R., Lehmann, J., A. and Li, J. 2006. Novel methods improve prediction of species' distributions from occurrence data. *Ecography*, 29(2), pp.129-151.
- Elith, J., Graham, H. C., Anderson, P., Dudík, Ferrier, R., Guisan, S., Hijmans, A., Huettmann, J.R., Leathwick, F.R., Lehmann, J., A. and Li, J. 2006. Novel methods improve prediction of species' distributions from occurrence data. *Ecography*, 29(2), pp.129-151.
- Elith, J., Graham, H. C., Anderson, P., Dudík, Ferrier, R., Guisan, S., Hijmans, A., Huettmann, J.R., Leathwick, F.R., Lehmann, J., A. and Li, J. 2006. Novel methods improve prediction of species' distributions from occurrence data. *Ecography*, 29(2), pp.129-151.
- Ersts, P. J., and Rosenbaum, H. C. 2003. Habitat preference reflects social organization of humpback whales (*Megaptera novaeangliae*) on a wintering ground. *J. of Zool.* 260(4). 337-345.
- Eschmeyer, W.N., and Fong, J.D. 2014. Species By Family/Subfamily. Electronic version accessed 01 April 2014.
- Esselman, P. C., and Allan, J. D. 2011. Application of species distribution models and conservation planning software to the design of a reserve network for the riverine fishes of northeastern Mesoamerica. *Freshw. Biol.* 56(1), 71-88.
- FAO, Fisheries Department, 1994. World review of highly migratory species and straddling stocks. FAO Fish. Tech. Pap. No. 337. Rome, FAO. 70 p.
- FAO, I. and UNICEF, 2018. WFP and WHO: The State of Food Security and Nutrition in the World 2018. *Building climate resilience for food security and nutrition*, 200.
- Fatima, Q., and Jamshed, A. 2015. The Political and Economic Significance of Indian Ocean: An Analysis. *South Asian Studies*, 30(2), p.73.
- Ferrier, S. 2002. Mapping spatial pattern in biodiversity for regional conservation planning: where to from here. *Syst. Biol.* 51(2), pp.331-363.
- Ferrier, S., Drielsma, M., Manion, G., and Watson, G. 2002. Extended statistical approaches to modelling spatial patterns in biodiversity in northeast New South Wales. II. Community-level modelling. *Biodivers. Conserv.* 11(12), pp.2309-2338.
- Fielding, A.H., and Bell, J.F. 1997. A review of methods for the assessment of prediction errors in conservation presence/absence models. *Environ. Conserv.* 24(1), pp.38-49.

- Florida Museum of Natural History, 2005. Biological profiles: great barracuda. Retrieved on 26 August 2005. Ichthyology at the Florida Museum of Natural History: Education-Biological Profiles. FLMNH, University of Florida.
- Fly, E. K., Hilbish, T. J., Wetthey, D. S., and Rognstad, R. L. 2015. Physiology and biogeography: the response of European mussels (*Mytilus* spp.) to climate change. *Am. Malacological Bull.* 33(1), 136-149.
- Fly, E.K., Hilbish, T.J., Wetthey, D.S. and Rognstad, R.L. 2015. Physiology and biogeography: the response of European mussels (*Mytilus* spp.) to climate change. American Malacological Bulletin, 33(1), pp.136-149.
- Froese, R., Pauly, D. 2007. FishBase. World Wide Web electronic publication. Version 01/2007.
- Ganga U, NGK Pillai, M.N.K. Elayathu, 2008. Billfish fishery along the Indian coast with special reference to the Indo-Pacific sailfish *Istiophorus platypterus* (Shaw and Nodder 1792) *J Mar. Biol. Ass. India*, 50(2): 166-171.
- Giovanelli, J.G., de Siqueira, M.F., Haddad, C.F., and Alexandrino, J. 2010. Modeling a spatially restricted distribution in the Neotropics: How the size of calibration area affects the performance of five presence-only methods. *Ecol. Model.* 221(2), pp.215-224.
- Gormley, K. S., Hull, A. D., Porter, J. S., Bell, M. C., and Sanderson, W. G. 2015. Adaptive management, international co-operation and planning for marine conservation hotspots in a changing climate. *Mar. Policy*, 53, 54-66.
- Gotelli, N.J., and Ellison, A.M. 2006. Forecasting extinction risk with nonstationary matrix models. *Ecol. Appl.* 16(1), pp.51-61.
- Govindarajulu, P., Altwegg, R., and Anholt. B.R. 2005. Matrix model investigation of invasive species control: Bullfrog on Vancouver Island. *Ecol. Appl.* 15:2161-2170.
- Guisan, A. & Zimmerman, N.E. 2000. Predictive habitat distribution models in ecology. *Ecol. Model.* Vol.135,pp.147-186
- Guisan, A., and Thuiller, W. 2005. Predicting species distribution: offering more than simple habitat models. *Ecol. Lett.* 8(9), pp.993-1009.
- Gutierrez, A.P., Ponti, L., d'Oultremont, T. and Ellis, C.K. 2008. Climate change effects on poikilotherm tritrophic interactions. *Clim. change*, 87(1), pp.167-192.

- Halas, D. and Winterbottom, R. 2009. A phylogenetic test of multiple proposals for the origins of the East Indies coral reef biota. *J. Biogeogr.* 36, 1847–1860.
- Hannah, L., Midgley, G.F., and Millar, D. 2002. Climate change-integrated conservation strategies. *Glob. Ecol. Biogeogr.* 11(6), pp.485-495.
- Hare, J.A., Alexander, M.A., Fogarty, M.J., Williams, E.H., and Scott, J.D. 2010. Forecasting the dynamics of a coastal fishery species using a coupled climate–population model. *Ecol. Appl.* 20(2), pp.452-464.
- Hegerl, G.C. and Bindoff, N.L. 2005. Warming the world's oceans. *Science*, 309(5732), pp.254-255.
- Hernandez, P.A., Graham, C.H., Master, L.L., and Albert, D.L. 2006. The effect of sample size and species characteristics on performance of different species distribution modeling methods. *Ecography*, 29(5), pp.773-785.
- Hjort J. 1914. Fluctuations in the great fisheries of northern Europe, viewed in the light of biological research. *Rap. Proces.* 20: 1–228.
- Hoegh-Guldberg, O. and Bruno, J.F. 2010. The impact of climate change on the world’s marine ecosystems. *Science*, 328(5985), pp.1523-1528.
- Hongo, C., and Kayanne, H. 2011. Key species of hermatypic coral for reef formation in the northwest Pacific during Holocene sea-level change. *Mar. Geol.* 279(1-4), pp.162-177.
- Hunter, C.M., Caswell, H., Runge, M.C., Regehr, E.V., Amstrup, S.C., and Stirling, I. 2010. Climate change threatens polar bear populations: A stochastic demographic analysis. *Ecol.* 91:2883-2897.
- IPCC, 2018. Summary for Policymakers. In: Global warming of 1.5°C. An IPCC Special Report on the impacts of global warming of 1.5°C above pre-industrial levels and related global greenhouse gas emission pathways, in the context of strengthening the global response to the threat of climate change, sustainable development, and efforts to eradicate poverty [V. Masson-Delmotte, P. Zhai, H. O. Pörtner, D. Roberts, J. Skea, P. R. Shukla, A. Pirani, W. Moufouma-Okia, C. Péan, R. Pidcock, S. Connors, J. B. R. Matthews, Y. Chen, X. Zhou, M. I. Gomis, E. Lonnoy, T. Maycock, M. Tignor, T. Waterfield (eds.)]. World Meteorological Organization, Geneva, Switzerland, 32 pp

- IUCN, 2019. The IUCN Red List of Threatened Species. Version 2019-2. . Downloaded on 23 July 2019.
- Johnston, M. W., and Purkis, S. J. 2012. Invasion soft: a web-enabled tool for invasive species colonization predictions. *Aquatic Invasions*, 7(3), 405.
- Jones, M.C. and Cheung, W.W. 2015. Multi-model ensemble projections of climate change effects on global marine biodiversity. *ICES J. of Mar. Sci.* 72(3), pp.741-752.
- Jones, M.C., Dye, S.R., Pinnegar, J.K., Warren, R. and Cheung, W.W. 2012. Modelling commercial fish distributions: Prediction and assessment using different approaches. *Ecol. Model.* 225, pp.133-145.
- Jowett, I.G., Parkyn, S.M., and Richardson, J. 2008. Habitat characteristics of crayfish (*Paraneohaps planifrons*) in New Zealand streams using generalised additive models (GAMs). *Hydrobiologia*, 596(1), pp.353-365.
- Kailola, P.J., M.J. Williams, P.C. Stewart, R.E. Reichelt, A. McNee and C. Grieve, 1993. Australian fisheries resources. Bureau of Resource Sciences, Canberra, Australia. 422 p.
- Kajiura S.M., and Tellman, S.L. 2016. Quantification of Massive Seasonal Aggregations of Blacktip Sharks (*Carcharhinus limbatus*) in Southeast Florida. *PLoS ONE* 11(3): e0150911. <https://doi.org/10.1371/journal.pone.0150911>
- Kaschner, K., Watson, R., Trites, A. W., and Pauly, D. 2006. Mapping world-wide distributions of marine mammal species using a relative environmental suitability (RES) model. *Mar. Ecol. Progress Ser.* 316, 285-310.
- Kasim, H. M. 2003. Carangids. In J. M. Mohan & A. A. Jayaprakash (Eds.), Status of exploited marine fishery resources of India (pp. 66–75). Cochin: Central Marine Fisheries Research Institute.
- Kearney, Michael and P. Warren, 2009. "Mechanistic niche modelling: combining physiological and spatial data to predict species' ranges". *Ecol. Lett.* 12 (4): 334–350.
- Keeling, R.F., Körtzinger, A. and Gruber, N. 2009. Ocean deoxygenation in a warming world.
- Kripa, V., Prema, D., Jeyabaskaran, R., Khambadkar, L.R., Nandakumar, A., Anilkumar, P.S., Ambrose, T.V., Bose, J., Nair, P.G. and Pillai, V.N. 2015. Inter-annual variations of

- selected oceanographic parameters and its relation to fishery of small pelagics off Kochi, southwest coast of India. *J. of the Mar. Biol. Assoc. of India*, 57(2), pp.52-57.
- Krishnan, S. and Mishra, S. S.1993. On a collection of fish from Kakinada-Gopalpur sector of the east coast of India. *Rec. Zool. Surv. India*. 93 (1-2), 201–240.
- Kulkarni, A., S. S.Sabade, and R. H.Kripalani, 2007: Association between extreme monsoons and the dipole mode over the Indian subcontinent.*Meteor. Atmos. Phys.*, 95, 255–268
- Laevastu, T. 1963. Distribution and relative abundance of tunas in relation to their environment. FAO Fish. Rep., 6, pp.1835-1851.
- Lan, K.W., Evans, K. and Lee, M.A. 2013. Effects of climate variability on the distribution and fishing conditions of yellowfin tuna (*Thunnus albacares*) in the western Indian Ocean. *Clim. change*, 119(1), pp.63-77.
- Last, P. R., White, W. T., Gledhill, D. C., Hobday, A. J., Brown, R., and Edgar, G. J. 2011. Long-term shifts in abundance and distribution of a temperate fish fauna: a response to climate change and fishing practices. *Glob. Ecol. Biogeogr.*, 20, 58–72.
- Leathwick, J.R., Rowe, D., Richardson, J., Elith, J., and Hastie, T. 2005. Using multivariate adaptive regression splines to predict the distribution of New Zealand's freshwater diadromous fish. *Freshw. Biol.* 50(12), pp.2034-2052.
- Lee, S.K., Park, W., Baringer, M.O., Gordon, A.L., Huber, B. and Liu, Y. 2015. Pacific origin of the abrupt increase in Indian Ocean heat content during the warming hiatus. *Nature Geoscience*, 8(6), pp.445-449.
- Lehodey, P., Senina, I., Sibert, J., Bopp, L., Calmettes, B., Hampton, J. & Murtugudde, R. 2010 Preliminary forecasts of Pacific bigeye tuna population trends under the A2 IPCC scenario. *Progress in Oceanogr.* 86, 302–315.
- Lehodey, P., Senina, I., Calmettes, B., Hampton, J., & Nicol, S. 2013. Modelling the impact of climate change on Pacific skipjack tuna population and fisheries. *Clim.Change*, 119, 95– 109. <https://doi.org/10.1007/s10584-012-0595-1>
- Levine, J.M., and D'Antonio, C.M. 2003. Forecasting biological invasions with increasing international trade. *Conserv. Biol.* 17(1), pp.322-326.

- Lieske, E. and R. Myers, 1994. Collins Pocket Guide. Coral reef fishes. Indo-Pacific & Caribbean including the Red Sea. Harpercollins Publishers, 400 p.
- Lim, E., Hendon, H.H. 2017. Causes and Predictability of the Negative Indian Ocean Dipole and Its Impact on La Niña During 2016. *Sci. Rep.* 7
- Lima, F. P., Ribeiro, P. A., Queiroz, N., Xavier, R., Tarroso, P., Hawkins, S. J., and Santos, A. M. 2007. Modelling past and present geographical distribution of the marine gastropod *Patella rustica* as a tool for exploring responses to environmental change. *Glob. Change Biol.* 13(10), 2065-2077.
- Lindsey, R. and Dahlman, L. 2020. Climate Change: Global Temperature. NOAA Climate. gov.
- Lowe, D.G. 1995. Similarity metric learning for a variable-kernel classifier. *Neural computation*, 7(1), pp.72-85.
- Lu, B., Ren, H., and Scaife, 2018. A.A. An extreme negative Indian Ocean Dipole event in 2016: dynamics and predictability. *Clim. Dyn.* 51, 89–100
- Luo, Z., Vora, P.M., Mele, E.J., Johnson, A.C. and Kikkawa, J.M. 2009. Photoluminescence and band gap modulation in graphene oxide. *Appl. phys. lett.* 94(11), p.111909.
- Maigret, J. and B. Ly, 1986. Les poissons de mer de Mauritanie. *Sci. Nat.* Compiègne. 213 p.
- Maravelias, C.D. and Reid, D.G. 1997. Identifying the effects of oceanographic features and zooplankton on pre spawning herring abundance using generalized additive models. *Mar.Ecol.Progress Ser.* 147, pp.1-9.
- Marshall, C. E., G. A. Glegg and K. L. Howell. 2014. Species distribution modelling to support marine conservation planning: The next steps. *Mar. Policy*, 45: 330-332.
- Matsuura, K. 2001. Ostraciidae. Boxfishes. p. 3948-3951. In K.E. Carpenter and V. Niem (eds.) FAO species identification guide for fishery purposes. The living marine resources of the Western Central Pacific. Vol. 6. Bony fishes part 4 (Labridae to Latimeriidae), estuarine crocodiles. FAO, Rome.
- Maxwell, D.L., Stelzenmüller, V., Eastwood, P.D. and Rogers, S.I. 2009. Modelling the spatial distribution of plaice (*Pleuronectes platessa*), sole (*Solea solea*) and thornback ray (*Raja clavata*) in UK waters for marine management and planning. *J. of Sea Res.* 61(4), pp.258-267.

- McKinney, J.A., Hoffmayer, E.R., Wu, W., Fulford, R. and Hendon, J.M. 2012. Feeding habitat of the whale shark *Rhincodon typus* in the northern Gulf of Mexico determined using species distribution modelling. *Mar. Ecol. Progress Ser.* 458, pp.199-211.
- McMillan, P.J., M.P. Francis, G.D. James, L.J. Paul, P.J. Marriott, E. Mackay, B.A. Wood, L.H. Griggs, H. Sui and F. Wei, 2011. New Zealand fishes. Volume 1: A field guide to common species caught by bottom and midwater fishing. New Zealand Aquatic Environment and Biodiversity Report No. 68. 329 p.
- Mennesson-Boisneau, C., Aprahamian, M.W., Sabatié, M.R., and Cassou-Leins, J.J. 2000. Remontée migratoire des adultes. *Les aloses*, pp.55-72.
- Menon, A. G. K. 1961. A collection of fish from the Coromandel Coast of India including Pondicherry and Karaikal areas. *Rec. Indian Mus.* 59 (4), 369–404.
- Merow, C., Smith, M.J., and Silander Jr, J.A. 2013. A practical guide to MaxEnt for modeling species' distributions: what it does, and why inputs and settings matter. *Ecography*, 36(10), pp.1058-1069.
- Merow, C., Smith, M.J., and Silander Jr, J.A. 2013. A practical guide to MaxEnt for modeling species' distributions: what it does, and why inputs and settings matter. *Ecography*, 36(10), pp.1058-1069.
- Midgley, G.F., Hannah, L., Millar, D., Rutherford, M.C., and Powrie, L.W. 2002. Assessing the vulnerability of species richness to anthropogenic climate change in a biodiversity hotspot. *Glob. Ecol. Biogeogr.* 11(6), pp.445-451.
- Mills, K.E., Pershing, A.J., Brown, C.J., Chen, Y., Chiang, F.S., Holland, D.S., Lehuta, S., Nye, J.A., Sun, J.C., Thomas, A.C. and Wahle, R.A. 2013. Fisheries management in a changing climate: lessons from the 2012 ocean heat wave in the Northwest Atlantic. *Oceanogr.* 26(2), pp.191-195.
- Milly, P.C., Betancourt, J., Falkenmark, M., Hirsch, R.M., Kundzewicz, Z.W., Lettenmaier, D.P., and Stouffer, R.J. 2008. Climate change. Stationarity is dead: Whither water management. *Science*, 319(5863), pp.573-574.
- Mishra, S.S. 2013. Coastal Marine Fish Fauna of East Coast of India. In: Venkataraman, K., Sivaperuman, C., Raghunathan, C., (Eds.), Ecology and conservation of tropical marine faunal communities, *Springer-Verlag*, Berlin, Heidelberg. 245–260.

- Mishra, S.S., Kosygin, L. Rajan, P.T. and Gopi, K.C. 2013. Pisces. In: Venkataraman, K., Chattopadhyay, A., Subramanian, K.A., (Eds.), Endemic animals of India (Vertebrates). *Zool. Surv. India*, Kolkata. 7–107.
- Mohapatra, A., Ray, D. and Kumar, V. 2013. A new fish species of the genus *Hapalogenys* (Perciformes: Hapalogenyidae) from the Bay of Bengal. *India. Zootaxa* 3718 (4), 367–377.
- Moilanen, A., and Wintle B.A. 2007 Quantitative reserve network aggregation via the boundary quality penalty. *Conserv. Biol.* 21, 355–364.
- Monk, J., Ierodiaconou, D., Harvey, E., Rattray, A. and Versace, V.L. 2012. Are we predicting the actual or apparent distribution of temperate marine fishes? *PLoS One*, 7(4).
- Moore, C.H., Harvey, E.S. and Van Niel, K.P. 2009. Spatial prediction of demersal fish distributions: enhancing our understanding of species–environment relationships. *ICES J. of Mar. Sci.* 66(9), pp.2068-2075.
- Mukherjee, M., Karna, S.K., Suresh, V.R., Manna, R.K., Panda, D. and Apurba, R.A.U.T. 2018. New records of Carangids (Perciformes: Carangidae) from Chilika Lagoon, east coast of India. *FishTaxa*, 2(4), pp.226-231.
- Mundy, B.C. 2005. Checklist of the fishes of the Hawaiian Archipelago. Bishop Mus. Bull. Zool. (6):1-704.
- Nakamura, I. and N.V. Parin, 1993. FAO Species Catalogue. Vol. 15. Snake mackerels and cutlass fishes of the world (families Gempylidae and Trichiuridae). An annotated and illustrated catalogue of the snake mackerels, snoeks, escolars, gemfishes, sackfishes, domine, oilfish, cutlass fishes, scabbard fishes, hairtails, and frostfishes known to date. FAO Fish. Synop. 125(15):136 p.
- Nakamura, I. 1985. FAO species catalogue. Vol. 5. Billfishes of the world. An annotated and illustrated catalogue of marlins, sailfishes, spearfishers and swordfishes known to date. FAO Fish. Synop. 125(5):65p. Rome: FAO.
- Nelson, J.S. 2006. Fishes of the world. John Wiley & Sons, Inc, Hoboken, New Jersey, p. 601.
- New, M., Liverman, D., Schroder, H., & Anderson, K. 2011. Four degrees and beyond: The potential for a global temperature increase of four degrees and its implications.

- Philosophical Transactions of the Royal Society A: *Mathematical, Phy. and Eng. Sci.* 369(1934),619
- Ñiquen, M. and Bouchon, M. 2004. Impact of El Niño events on pelagic fisheries in Peruvian waters. *Deep sea res. part II: trop. studies in oceanogr.* 51(6-9), pp.563-574.
- Nix H. A. 1986. A biogeographic analysis of Australian elapid snakes. pp. 4-15 In Atlas of Elapid Snakes of Australia: Australian Flora and Fauna Series 7 (ed R. Longmore), Bureau of Flora and Fauna, Canberra.
- NOAA National Centers for Environmental Information, State of the Climate: Global Climate Report for Annual 2019, published online January 2020, retrieved on September 30, 2020 from <https://www.ncdc.noaa.gov/sotc/global/201913>.
- Nye, J.A., Link, J.S., Hare, J.A. and Overholtz, W.J. 2009. Changing spatial distribution of fish stocks in relation to climate and population size on the Northeast United States continental shelf. *Mr. Ecol. Prog. Ser.*, 393, 111–129.
- Ollerenshaw, C.B., and Smith, LP. 1969. Meteorological factors and forecasts of helminthic disease. *Adv. Parasitol.* (Vol.7, pp.283–323).
- Orlov, A.M. and V.A. Ul'chenko, 2002. A hypothesis to explain onshore records of long-nose lancetfish *Alepisaurus ferox* (Alepisauridae, Teleostei) in the North Pacific Ocean. *Mar. Freshw. Res.* 53:303-306.
- Palko, B.J., G.L. Beardsley and W.J. Richards, 1982. Synopsis of the biological data on dolphin-fishes, *Coryphaena hippurus* Linnaeus and *Coryphaena equiselis* Linnaeus. FAO Fish. Synop. (130); NOAA Tech. Rep. NMFS Circ. (443).
- Panigada, S., Zanardelli, M., MacKenzie, M., Donovan, C., Mélin, F., and Hammond, P. S. 2008. Modelling habitat preferences for fin whales and striped dolphins in the Pelagos Sanctuary (Western Mediterranean Sea) with physiographic and remote sensing variables. *Remote Sensing of Environ.* 112(8), 3400-3412.
- Pauly, D., A. Cabanban and F.S.B. Torres Jr. 1996. Fishery biology of 40 trawl-caught teleosts of western Indonesia. p. 135-216. In D. Pauly and P. Martosubroto (eds.) Baseline studies of biodiversity:the fish resource of western Indonesia. ICLARM Studies and Reviews 23.

- Pearson, R.G., Raxworthy, C.J., Nakamura, M., and Townsend Peterson, A. 2007. Predicting species distributions from small numbers of occurrence records: a test case using cryptic geckos in Madagascar. *J. Biogeogr.* 34(1), pp.102-117.
- Peeters, E. T. H. M. & J. J. P. Gardeniers, 1998. Logistic regression as a tool for defining habitat requirements of two common gammarids. *Freshw. Biol.* 39: 605–615.
- Peterson, A.T., Sánchez-Cordero, V., Soberón, J., Bartley, J., Buddemeier, R.W., and Navarro-Sigüenza, A.G. 2001. Effects of global climate change on geographic distributions of Mexican Cracidae. *Ecol. model.* 144(1), pp.21-30.
- Peterson, D.L., Millar, C.I., Joyce, L.A., Furniss, M.J., Halofsky, J.E., Neilson, R.P. and Morelli, T.L. 2011. Responding to climate change in national forests: a guidebook for developing adaptation options. *Gen. Tech. Rep. PNW-GTR-855. Portland, OR: US Department of Agric. For. Serv. Pacific Northwest Res. stn. 109 p., 855.*
- Philander, S. G. H. 1983. El Niño southern oscillation phenomena. *Nature* 302:295-301
- Philander, S.G. and Rasmusson, E.M. 1985. The southern oscillation and El Niño. In *Advances in Geophysics* (Vol. 28, pp. 197-215). *Elsevier*.
- Phillips, S. J., Anderson, R. P., and Schapire, R. E. 2006. Maximum entropy modeling of species geographic distributions. *Ecol. model.* 190(3-4), 231-259.
- Phillips, S.J., Dudík, M., Elith, J., Graham, C.H., Lehmann, A., Leathwick, J. and Ferrier, S. 2009. Sample selection bias and presence-only distribution models: implications for background and pseudo-absence data. *Ecol. appl.* 19(1), pp.181-197.
- Pinkerton, M.H., Smith, A.N., Raymond, B., Hosie, G.W., Sharp, B., Leathwick, J.R., and Bradford-Grieve, J.M. 2010. Spatial and seasonal distribution of adult *Oithona similis* in the Southern Ocean: predictions using boosted regression trees. *Deep Sea Research Part I: Oceanogr. Res. Papers*, 57(4), pp.469-485.
- Pinkerton, M.H., Smith, A.N., Raymond, B., Hosie, G.W., Sharp, B., Leathwick, J.R., and Bradford-Grieve, J.M. 2010. Spatial and seasonal distribution of adult *Oithona similis* in the Southern Ocean: predictions using boosted regression trees. *Deep Sea Res. Part I: Oceanogr. Res. Papers*, 57(4), pp.469-485.

- Pinsky, M.L., Worm, B., Fogarty, M.J., Sarmiento, J.L. and Levin, S.A. 2013. Marine taxa track local climate velocities. *Science*. 341, 1239–1242.
- Poloczanska, E. S., C. J. Brown, W. J. Sydeman, W. Kiessling, D. S. Schoeman, P. J. Moore, K. Brander, J. F. Bruno, L. B. Buckley, M. T. Burrows and C. M. Duarte. 2013. Global imprint of climate change on marine life. *Nat. Clim. Change*, 3(10): 919-925.
- Porter, W.P., Sabo, J.L., Tracy, C.R., Reichman, O.J., Ramankutty, N. 2002. Physiology on a landscape scale: plant-animal interactions. *Integr. Comp. Biol.* 42, 431– 453.
- Radosavljevic, A., and Anderson, R.P. 2014. Making better Maxent models of species distributions: complexity, overfitting and evaluation. *J. Biogeogr.* 41(4), pp.629-643.
- Rahmstorf, S., Feulner, G., Mann, M.E., Robinson, A., Rutherford, S. & Schaffernicht, E.J. 2015 Exceptional twentieth-century slowdown in Atlantic Ocean overturning circulation. *Nature Clim. Change*, 5, 475–480.
- Rajan, P.T., Sreeraj, C.R. and Immanuel, T. 2013. Fishes of Andaman and Nicobar Islands: A Checklist. *J. Andaman Sci. Assoc.*, 17 (1), 47–87.
- Ramalingam, L., Kar, A.B. and Blair, P. 2011. Distribution, abundance and biology of Indo Pacific sailfish, *Istiophorus platypterus* (Shaw and Nodder, 1792) in the Indian EEZ around Andaman and Nicobar.
- Randall, J.E. 1998. Zoogeography of shore fishes of the Indo-Pacific region. *Zool. Stud.* 37, 227–268.
- Rao, G.C. 1991. Lakshadweep: General features, Fauna of Lakshadweep, State Fauna Series. *Zool. Surv. India.* 2, 5–40.
- Raven, J.A. and Falkowski, P.G. 1999. Oceanic sinks for atmospheric CO₂. *Plant, Cell & Environment*, 22(6), pp.741-755.
- Ready, J., Kaschner, K., South, A.B., Eastwood, P.D., Rees, T., Rius, J., Agbayani, E., Kullander, S. and Froese, R. 2010. Predicting the distributions of marine organisms at the global scale. *Ecol. Model.* 221(3), pp.467-478.
- Redfern, J. V., Ferguson, M. C., Becker, E. A., Hyrenbach, K. D., Good, C., Barlow, J., and Fauchald, P. 2006. Techniques for cetacean–habitat modeling. *Mar. Ecol. Progress Ser.* 310, 271-295.

- Reiss, H., Birchenough, S., Borja, A., Buhl-Mortensen, L., Craeymeersch, J., Dannheim, J., Darr, A., Galparsoro, I., Gogina, M., Neumann, H. and Populus, J. 2015. Benthos distribution modelling and its relevance for marine ecosystem management. *ICES J. of Mar.Sci.* 72(2), pp.297-315.
- Rezaei, R., and Sengül, H. 2018. Development of Generalized Additive Models (GAMs) for *Salmo rizeensis* Endemic to North-Eastern Streams of Turkey. *Turk. J. Fish. Aquat. Sci.* 19(1), pp.29-39.
- Rhein, M., S. R. Rintoul, S. Aoki, E. Campos, D. Chambers, R. A. Feely, S. Gulev, G. C. Johnson, S. A. Josey, A. Kostianoy, C. Mauritzen, D. Roemmich, L. D. Talley and F. Wang. 2013. Observations: Ocean. In: *Climate Change 2013: The Physical Science Basis. Contribution of Working Group I to the Fifth Assessment Report of the Intergovernmental Panel on Climate Change* [Stocker, T.F., D. Qin, G.-K. Plattner, M. Tignor, S.K. Allen, J. Boschung, A. Nauels, Y. Xia, V. Bex and P.M. Midgley (eds.)]. Cambridge University Press, Cambridge, United Kingdom and New York, NY, USA.
- Riede, K. 2004. Global register of migratory species - from global to regional scales. Final Report of the R&D-Projekt 808 05 081. Federal Agency for Nature Conservation, Bonn, Germany. 329 p.
- Robinson, L.M., Elith, J., Hobday, A.J., Pearson, R.G., Kendall, B.E., Possingham, H.P. and Richardson, A.J. 2011. Pushing the limits in marine species distribution modelling: lessons from the land present challenges and opportunities. *Glob. Ecol. & Biogeogr.* 20(6), pp.789-802.
- Robinson, N.M., Nelson, W.A., Costello, M.J., Sutherland, J.E., and Lundquist, C.J. 2017. A systematic review of marine-based Species Distribution Models (SDMs) with recommendations for best practice. *Front. Mar. Sci.* 4, p.421.
- Roxy M. K. and C. Gnanaseelan. 2020. Indian Ocean Warming. In: Raghavan, K., Jayanarayanan, S., Gnanaseelan, C., Mujumdar, M., Kulkarni, A., Chakraborty, S. (eds) *Assessment of Climate Change over the Indian Region. Springer*, Singapore.
- Russell, B.C. and W. Houston, 1989. Offshore fishes of the Arafura Sea. *Beagle* 6(1):69-84.

- Schmiing, M., Afonso, P., Tempera, F. and Santos, R.S. 2013. Predictive habitat modelling of reef fishes with contrasting trophic ecologies. *Mar.Ecol. Progress Ser.* 474, pp.201-216.
- Seneviratne, S.I., Nicholls, D., Easterling, C.M. Goodess, S. Kanae, J. Kossin, Y. Luo, J. Marengo, K. McInnes, M. Rahimi, M. Reichstein, A. Sorteberg, C. Vera, and X. Zhang, 2012. Changes in climate extremes and their impacts on the natural physical environment. In: *Managing the Risks of Extreme Events and Disasters to Advance Climate Change Adaptation* [Field, C.B., V. Barros, T.F. Stocker, D. Qin, D.J. Dokken, K.L. Ebi, M.D. Mastrandrea, K.J. Mach, G.-K. Plattner, S.K. Allen, M. Tignor, and P.M. Midgley (eds.)]. A Special Report of Working Groups I and II of the Intergovernmental Panel on Climate Change (IPCC). Cambridge University Press, Cambridge, UK, and New York, NY, USA, pp. 109-230.
- Sequeira, A., Mellin, C., Rowat, D., Meekan, M. G., Bradshaw, C.J.A. 2012. Ocean-scale prediction of whale shark distribution. *Divers. Distrib.* 18: 504–518
- Sequeira, A. M. M., Mellin, C., Fordham, D. A., Meekan, M. G., & Bradshaw, C. J. A. 2014. Predicting current and future global distributions of whale sharks. *Glob. Change Biol.* 20(3), 778–789. doi:10.1111/gcb.12343
- Sheppard, A., Fenner, D., Edwards, A., Abrar, M., and Ochavillo, D. 2014. *Porites lutea*. The IUCN Red List of Threatened Species 2014: e.T133082A54191180.
- Šiaulys, A., and Bučas, M. 2012. Species distribution modelling of benthic invertebrates in the south-eastern Baltic Sea. *Baltica*, 25(2), 163-170.
- Sleeman, J.C., Meekan, M.G., Wilson, S.G., Polovina, J.J., Stevens, J.D., Boggs, G.S. and Bradshaw, C.J. 2010. To go or not to go with the flow: Environmental influences on whale shark movement patterns. *J. Exp. Mar. Biol. and Ecol.* 390(2), pp.84-98.
- Smith, M.D., Knapp, A.K., Collins, S.L. 2009. A framework for assessing ecosystem dynamics in response to chronic resource alterations induced by global change. *Ecology*, 90:3279–3289.
- Smith, M.M. and P.C. Heemstra, 1986. Balistidae. p. 876-882. In M.M. Smith and P.C. Heemstra (eds.) *Smiths' sea fishes*. Springer-Verlag, Berlin.

- Smith-Vaniz, W.F. 1984. Carangidae. In W. Fischer and G. Bianchi (eds.) FAO species identification sheets for fishery purposes. Western Indian Ocean fishing area 51. Vol. 1. [pag. var.]. FAO, Rome.
- Soufi-Kechaou, E., Amor, K.O.B., Souissi, J.B., Amor, M.M.B. and Capapé, C. 2018. The capture of a large predatory shark, *Carcharhinus plumbeus* (Chondrichthyes: Carcharhinidae), off the Tunisian coast (Central Mediterranean). In *Annales: Ser.Historia Naturalis* (Vol. 28, No. 1, pp. 23-28). Scientific and Research Center of the Republic of Slovenia.
- Stockwell, D. 1999. The GARP modelling system: problems and solutions to automated spatial prediction. *Int. J. Geogr. Inf. Sci.* 13(2), pp.143-158.
- Stockwell, D.R., and Noble, I.R. 1992. Induction of sets of rules from animal distribution data: a robust and informative method of data analysis. *Math. Comput. Simul.* 33(5-6), pp.385-390.
- Stoner, A.W., Spencer, M.L. and Ryer, C.H. 2007. Flatfish-habitat associations in Alaska nursery grounds: Use of continuous video records for multi-scale spatial analysis. *J. Sea Res.* 57(2-3), pp.137-150.
- Sund, P.N., Blackburn, M. and Williams, F. 1981. Tunas and their environment in the Pacific Ocean: a review. *Oceanogr. Mar. Biol. Ann. Rev.* 19, pp.443-512.
- Swain, D.P., Benoît, H.P. and Hammill, M.O. 2015. Spatial distribution of fishes in a Northwest Atlantic ecosystem in relation to risk of predation by a marine mammal. *J. Animal Ecol.* 84(5), pp.1286-1298.
- Taguchi, M., King, J. R., Wetklo, M., Withler, R. E., & Yokawa, K. 2015. Population genetic structure and demographic history of Pacific blue sharks (*Prionace glauca*) inferred from mitochondrial DNA analysis. *M. & Freshw. Res.* 66(3), 267. doi:10.1071/mf14075
- Tao, W., Huang, G., Hu, K., Qu, X., Wen, G. and Gong, H. 2015. Interdecadal modulation of ENSO teleconnections to the Indian Ocean Basin Mode and their relationship under global warming in CMIP5 models. *Int. J.Clim.* 35(3), pp.391-407.

- Thomas, C.D., Cameron, A., Green, R.E., Bakkenes, M., Beaumont, L.J., Collingham, Y.C., Erasmus, B.F., De Siqueira, M.F., Grainger, A., Hannah, L., and Hughes, L. 2004. Extinction risk from climate change. *Nature*, 427(6970), p.145.
- Thorn, J.S., Nijman, V., Smith, D., and Nekaris, K.A.I. 2009. Ecological niche modelling as a technique for assessing threats and setting conservation priorities for Asian slow lorises (Primates: Nycticebus). *Divers. Distrib.* 15(2), pp.289-298.
- Thuiller, W., Lavorel, S., Sykes, M.T. and Araújo, M.B. 2006. Using niche-based modelling to assess the impact of climate change on tree functional diversity in Europe. *Divers. & Distributions*, 12(1), pp.49-60.
- Torres, A.F., and Ravago-Gotanco, R. 2018. Rarity of the “common” coral *Pocillopora damicornis* in the western Philippine archipelago. *Coral Reefs*, 37(4), pp.1209-1216.
- Torres, Leigh G., Patricia E. Rosel, Caterina D'Agrosa, and Andrew J. Read. "Improving the management of overlapping bottlenose dolphin ecotypes through spatial analysis and genetics." *Mar. Mammal Sci.* 19, no. 3 (2003): 502-514.
- Vierod, A. D., Guinotte, J. M., & Davies, A. J. 2014. Predicting the distribution of vulnerable marine ecosystems in the deep-sea using presence-background models. *Deep Sea Research Part II: Topical Stud. in Oceanogr.* 99, 6-18.
- Vivekanandan, E., Rajagopalan, M. and Pillai, N. G. K. 2009. Recent trends in sea surface temperature and its impact on oil sardine. In: Aggarwal, P. K. (Ed.), *Global climate change and Indian agriculture*. Indian Council of Agricultural Research, New Delhi, p. 89-92.
- Wang, L., Kerr, L.A., Record, N.R., Bridger, E., Tupper, B., Mills, K.E., Armstrong, E.M. and Pershing, A.J. 2018. Modeling marine pelagic fish species spatiotemporal distributions utilizing a maximum entropy approach. *Fish. Oceanogr.* 27(6), pp.571-586.
- Ward, E.J., Holmes, E.E., Thorson, J.T., and Collen, B. 2014. Complexity is costly: a meta-analysis of parametric and non-parametric methods for short-term population forecasting. *Oikos*. 23:652–661.
- Wei, C. L., Rowe, G. T., Escobar-Briones, E., Boetius, A., Soltwedel, T., Caley, M. J., and Pitcher, C. R. 2010. Global patterns and predictions of seafloor biomass using random forests. *PloS one*, 5(12), e15323.

- Whitehead, P.J.P. 1985. FAO Species Catalogue. Vol. 7. Clupeoid fishes of the world (suborder Clupeoidei). An annotated and illustrated catalogue of the herrings, sardines, pilchards, sprats, shads, anchovies and wolf-herrings. FAO Fish. Synop. 125(7/1):1-303. Rome: FAO.
- Wiley, E.O., McNyset, K.M., Peterson, A.T., Robins, C.R. and Stewart, A.M. 2003. Niche modeling perspective on geographic range predictions in the marine environment using a machine-learning algorithm.
- Worm B. et al. 2006. Impacts of biodiversity loss on ocean ecosystem services. *Science* 314: 787– 790.
- Yamano, H., Sugihara, K., and Nomura, K. 2011. Rapid poleward range expansion of tropical reef corals in response to rising sea surface temperatures. *Geophys. Res. Lett.* 38(4).
- Yan, X.H., Boyer, T., Trenberth, K., Karl, T.R., Xie, S.P., Nieves, V., Tung, K.K. and Roemmich, D. 2016. The global warming hiatus: Slowdown or redistribution? *Earth's Future*, 4(11), pp.472-482.
- Yee, T.W., and Mitchell, N.D. 1991. Generalized additive models in plant ecology. *J. Veg. Sci.* 2(5), pp.587-602.
- Young, M. and Carr, M.H. 2015. Application of species distribution models to explain and predict the distribution, abundance and assemblage structure of nearshore temperate reef fishes. *Divers. & Distributions*, 21(12), pp.1428-1440.
- Zacharia P.U, A.P. Dineshbabu, Sujitha Thomas, Shoba Joe Kizhakudan, E. Vivekanandan, S. Lakshmi Pillai, M. Sivadas, Shubhadeep Ghosh, U. Ganga, K.M. Rajesh, Rekha J. Nair. T.M. Najmudeen, Mohammed Koya, Anulekshmi Chellappan, Gyanranjan Dash, Indira Divipala, K.V. Akhilesh, M. Muktha, Swathi Priyanka Sen Dash, 2016. Relative vulnerability assessment of Indian marine fishes to climate change using impact and adaptation attributes. CMFRI Special Publication No. 125, (CMFRI-NICRA Publication no. 5), Central Marine Fisheries Research Institute, Kochi, India pp. 192.

**INVESTIGATIONS ON THE CLIMATIC TRENDS AND SHIFTS IN
THE SPATIAL DISTRIBUTION OF MARINE FISH SPECIES OF
NORTHERN INDIAN OCEAN**

by

**SWATHY S.
(2015 - 20 - 021)**

THESIS ABSTRACT

**Submitted in partial fulfillment of the requirements for the
degree of**

B.Sc. – M.Sc. (Integrated) Climate Change Adaptation

Faculty of Agriculture

Kerala Agricultural University



ACADEMY OF CLIMATE CHANGE EDUCATION AND RESEARCH

VELLANIKKARA, THRISSUR – 680 656 KERALA,

INDIA

2020

ABSTRACT

Climate change exacerbates massive changes in the global oceans. Increasing ocean temperature, reduced oxygen content, sea level rise, ocean acidification, storm activities *etc.* reduces the capability of the ocean to provide the ecosystem services, which adversely affect marine ecosystems. The Northern Indian Ocean being a major hotspot among world oceans, its rate of warming is extremely alarming. Marine species counteract these changes by reallocating their distributional range. It steers the shift of species towards the poles. But the landlocked nature of the northern Indian Ocean hinders the further movement which finally leads to local extinctions. This study focuses on investigating the pattern of trend in remotely sensed variables and the shift in the spatial distribution of 34 marine pelagic fish species of the northern Indian Ocean in the future climatic scenarios. The species data have been taken from open-source databases such as OBIS, GBIF and various published literatures. The environmental data for the future years 2040- 2050 and 2090- 2100 for RCPs 4.5, 6.0 and 8.5 are taken from Bio-oracle with 9.2 km resolution. Empirical orthogonal function analysis explains the warming of Indian Ocean with a rate of 0.016°C per year. The predicted distribution of species such as *Sardinella longiceps* shows reduced extent of distribution over the Indian Ocean in the future RCPs. *Sphyrna zygaena*, *Rastrelliger kanagurta* *etc.* shows a northward extent. But contradictorily tuna species such as *Thunnus obesus* and *T. albacare* shows an increased distribution in future scenarios. Fish species respond differently to changing climatic conditions. Sustainable and productive fisheries protect the environment and natural resources. The knowledge of the spatial distribution of fish species in the specified area needs to be examined for the effective utilization of fishery resources and for planning conservation policies and management activities.